

Description of two new species of Paraonidae (Annelida) from the Gulf of Thailand, Western Pacific

Jintana Plathong^{1,2}, Pablo Hernández-Alcántara³, Leslie Harris⁴, Sakanan Plathong²

1 Marine Ecosearch Management Co., Ltd., 4/31 Moo 1, Namnoi, Hatyai, Songkhla, Thailand **2** Marine Science Learning Center, Department of Biology, Faculty of Science, Prince of Songkla University, Hatyai, Songkhla, Thailand **3** Unidad Académica de Ecología y Biodiversidad Acuática, Instituto de Ciencias del Mar y Limnología, Universidad Nacional Autónoma de México. Circuito Exterior S/N, Cd. Universitaria, Cd. México, México **4** Natural History Museum of Los Angeles County, 900 Exposition Blvd. Los Angeles CA, USA

Corresponding author: Sakanan Plathong (sakanan2004@yahoo.com)

Academic editor: C. Glasby | Received 3 March 2020 | Accepted 7 May 2020 | Published 22 July 2020

<http://zoobank.org/923C9D0D-E386-4AB8-BFFD-2022949D1564>

Citation: Plathong J, Hernández-Alcántara P, Harris L, Plathong S (2020) Description of two new species of Paraonidae (Annelida) from the Gulf of Thailand, Western Pacific. ZooKeys 951: 1–20. <https://doi.org/10.3897/zookeys.951.51686>

Abstract

Two new species of *Aricidea* Webster, 1879 (Paraonidae), *Aricidea* (*Acmira*) *anusakdii* **sp. nov.** and *Aricidea* (*Aricidea*) *thammapinanae* **sp. nov.** were collected from 10–26.5 m depth, in soft bottoms with mud mixed with sand and shells at Songkhla Sea, the Gulf of Thailand between 2011–2018. *Aricidea* (*Acmira*) *anusakdii* **sp. nov.** is clearly distinguished from other species of the subgenus *Acmira* by having a rounded bilobed prostomium divided by a slight notch on the anterior margin; red pigments on the subdistal to the tip of each branchia (new character); two prebranchial chaetigers; 48–68 pairs of branchiae; and modified neurochaetae as strong curved spines with blunt shafts surrounded by pubescence from chaetigers 19–44. On the other hand, *Aricidea* (*Aricidea*) *thammapinanae* **sp. nov.** can be separated from other members of the subgenus *Aricidea* by the presence of a biarticulated median antenna; distinctive notopodial lobes as broad triangular with short distal protuberances on chaetiger 3, 4–8 pairs of branchiae; and modified neurochaetae as bidentate neurochaetae with a long pubescent subterminal arista on the concave side. All data have been archived and are freely available from the Dryad Digital Repository (<https://doi.org/10.5061/dryad.hqbzkh1cn>).

Keywords

Aricidea, paraonids, polychaetes, Songkhla Sea, taxonomy

Introduction

Polychaetes in the seas around Thailand are poorly known, especially those belonging to Paraonidae, a family of small burrowing polychaetes usually found in soft sediments (Rouse and Pleijel 2001). Until now, the only study of Thai paraonid species was published by Lovell (2002), who reported 19 taxa of paraonids from the Andaman Sea around Phuket Island, of which three species were newly described. The present study is the result of a monitoring program carried out between 2011 and 2018 entitled “Status of Coastal and Marine Resources and Ecosystem in Songkhla’s Sea and Monitoring projects of Petroleum Production Area in Songkhla Sea”. The family Paraonidae was one of the most species-rich families in the study area with over 20 undescribed taxa. The genus *Aricidea* is the most diverse in the Paraonidae, with more than 75 known species (Blake 2019). Strelzov (1973) divided the genus into four subgenera: *Aricidea* sensu stricto, *Aedicira* Hartman, 1957, *Allia* Strelzov, 1973 (= *Strelzovia* Aguirrezabalaga, 2012), and *Acesta* Strelzov, 1973 (= *Acmira* Hartley, 1981), which were separated based on the nature of the modified neurochaetae. Hartley (1981) pointed out that the chaetal differences are unclear to justify the generic status for the four subgenera (Blake 2019), and these subgenera have largely been accepted by taxonomists (Blake 1996, 2019; Lovell 2002; Arriaga-Hernández et al. 2013, among others). During the identification process, we observed several specimens from the genus *Aricidea* Webster, 1879 that had a combination of taxonomic characters not found in the previously described species.

At present, 19 species of the subgenus *Aricidea* (*Acmira*) have been described (Read and Fauchald 2020), but *Aricidea* (*Acmira*) *simonae* Laubier & Ramos, 1974 is the only species that has two prebranchial chaetigers. From the Andaman Sea around Phuket, Lovell (2002) reported five species of *Aricidea* (*Acmira*), all with three prebranchial chaetigers: *Aricidea* (*Acmira*) *assimilis* Tebble, 1959, *A. (Acmira) catherinae* Laubier, 1967 and *A. (Acmira) simplex* Day, 1963 and two taxa that have not yet been formally named.

Another subgenus, *Aricidea* (*Aricidea*), is characterized by the presence of cirri-form prostomial antennae, usually articulated, and modified neurochaetae either pseudocompound or hooked with subterminal spines on the concave side (Blake 1996). Fifteen species have been described from various localities around the world (Table 1), but in the seas around Thailand only *Aricidea* (*Aricidea*) *fragilis* Webster, 1879, *A. (Aricidea) multiantennata* Lovell, 2002 and *A. (Aricidea) thailandica* Lovell, 2002 have been reported. The specimens examined in the present study were characterized by the shape of the median antenna, the structure of the modified chaetae, and particularly by the shape of the third notopodial lobe. The latter was broadly triangular with a short round distal protuberance; this feature suggested that these paraonids could belong to an undescribed species.

The aim of this study is to examine in detail the morphological characteristics of these specimens using scanning electron microscope (SEM) images and light microscope photographs to verify differences from previously described species, and to confirm them as new species or not. Comparative tables of the diagnostic features of the new species and of those observed in closely similar taxa are included.

Table 1. Comparative morphological characteristics of species belonging to the subgenus *Aricidea* (*Aricidea*) Webster, 1879.

Species	Prostomium	Eyes	Antenna (end at chaetiger)	Branchiae from chaetiger	Notopodial postchaetal lobes (at body region)	Modified neurochaetae	Modified chaetae from chaetiger	Type locality
<i>Aricidea</i> (<i>Aricidea</i>) <i>capensis</i> Day, 1961	Elongate cone, tapered anteriorly	Absent	Long, faintly annulated; to chaetiger 2	4 to 17	Prebranchial: small. Branchial: enlarged. Posterior: very slender, threadlike	Bidentate hooked, with enlarged long spine on concave side of stem	Posterior chaetigers	South Africa
<i>Aricidea</i> (<i>Aricidea</i>) <i>capensis bansei</i> Laubier & Ramos, 1974	Elongate, longer than wide	When present, one pair (red)	Long, annulated, moniliform; to chaetiger 2	4 to 12–13	Chaetigers 1–2 rudimentary; well developed from chaetiger 3. Posterior: very long	Hooked, with 1–3 secondary teeth on principal tooth; with a subterminal spine on concave side of stem	22–27	Northwestern Mediterranean Sea; Adriatic Sea
<i>Aricidea</i> (<i>Aricidea</i>) <i>curviseta</i> Day, 1963	Blunted triangular	Absent	Short, not reaching the tip of prostomium	4 to 40	Prebranchial and branchial: short, conical; slender. Posterior: as slender filament	Thick stem directly transferring into slender spine	Postbranchial chaetigers	South Africa
<i>Aricidea</i> (<i>Aricidea</i>) <i>fragilis</i> Webster, 1879	Triangular, rounded anteriorly	One pair, small (usually not visible when preserved)	Short, subulate; to chaetiger 2	4 to 53–63	Chaetiger 1–2: short, digitiform. Chaetiger 3 and branchial: longer, wider basally. Posterior: digitiform to filiform	Pseudoarticulate, stouter basally, partially or completely fracturing at the midpoint	4–5 post-branchial chaetigers	Chesapeake Bay, off Eastern shore, Virginia
<i>Aricidea</i> (<i>Aricidea</i>) <i>longicirrata</i> Hartmann-Schröder, 1965	Pin shaped, tapered anteriorly	Absent	Short; to chaetiger 1	4 up to 17	Chaetiger 1–2: short, tuberculate. Chaetiger 3: digitate. Branchial: threadlike. Posterior: shorter	Acicular, hooked, with slender subterminal spine on concave side of stem	13	Chile
<i>Aricidea</i> (<i>Aricidea</i>) <i>longobranchiata</i> Day, 1961	Roughly cordate, bluntly rounded anteriorly	Absent	Very long; to chaetiger 5	4 to 21	Prebranchial and branchial: cirriform with basal enlargement. Posterior: very short, slender	Acicular, hooked, with enlarged long spine on concave side of stem	Posterior chaetigers	South Africa
<i>Aricidea</i> (<i>Aricidea</i>) <i>minima</i> Strelzov, 1973	Elongated, conical, tapered anteriorly	Absent	Thickened; to chaetiger 2	4 to 19	Chaetigers 1–2: tuberculate. Chaetiger 3 and branchial: long with asymmetrical enlargement. Posterior: thin, longer.	Pseudoarticulate	Last branchial chaetiger	Patagonia, South America
<i>Aricidea</i> (<i>Aricidea</i>) <i>minuta</i> Southward, 1956	Conical	Absent	Short, bi- or triarticulate; to chaetiger 1	4 to 16	Chaetiger 1–2: very short, tuberculate. Chaetiger 3: digitiform, slender. Branchial digitiform. Posterior: thinner	Pseudoarticulate	Unknown	Irish Sea and Baltic Sea

Species	Prostomium	Eyes	Antenna (end at chaetiger)	Branchiae from chaetiger	Notopodial postchaetal lobes (at body region)	Modified neurochaetae	Modified chaetae from chaetiger	Type locality
<i>Aricidea (Aricidea) multiantennata</i> Lovell, 2002	Triangular, bulbous end	Faded eyespot present	Five short tapering digitate branches	4 to 27–28	Prebranchial: digitate. Branchial and posterior: filiform	Pseudoarticulate, with a fringe on the convex side	37–39	Phuket, Andaman Sea, Thailand
<i>Aricidea (Aricidea) petaculcoensis</i> de León-González et al., 2006	Conical, rounded anteriorly	Absent	Short, bifurcate; to chaetiger 1	4 to 13–14	Chaetiger 1–2: absent. Chaetiger 3 and branchial: digitate. Posterior: increasing in size	Distally curved, with a subterminal spine on concave side of shaft	21	Western Mexico
<i>Aricidea (Aricidea) pseudoarticulata</i> Hobson, 1972	Triangular	Absent	Short, clavate with terminal papilla (bottle-shaped); chaetiger 1	4 to 14–16	Prebranchial: short. Branchial: longer, broad at base. Posterior: longer, cirriform	1) pseudoarticulate, long appendage; 2) tapered to hairlike tip; 3) hooked with hairlike tip; 4) hooked without hairlike tip	28–35	Southern California
<i>Aricidea (Aricidea) rosea</i> Reish, 1968	Triangular, rounded anteriorly	Absent	Slender; to chaetiger 2	4 to 14–15	Cirriform	Curved acicular with a subterminal spine on the concave side and pointed hood	Around 20–25	Los Angeles Bay, Gulf of California
<i>Aricidea (Aricidea) sanmartini</i> Aguado & López, 2003	Triangular, rounded anteriorly	Two pairs	Very long; to chaetiger 9	4 to 20	Chaetiger 1–2: very short. From chaetiger 3: strong, longer. Posterior: short, slender	Thick, hooked, with a very long subterminal spine	20–21	Coiba Island, Panama
<i>Aricidea (Aricidea) thailandica</i> Lovell, 2002	Triangular	One pair	With 2–3 pseudoarticulate branches, each with subdistal swelling tapering to filiform tip	4 to 18–24	Prebranchial: papillary, longer at chaetiger 3. Branchial: digitate. Posterior: filiform	Acicular, recurved tip, with terminal arista and hood emerging from concave side	34	Phuket, Andaman Sea, Thailand
<i>Aricidea (Aricidea) wassi</i> Pettibone, 1965	Conical, elongated	Absent	Long, articulate (12 articles); to chaetiger 4	4 to 13–21	Prebranchial: tuberculate. Branchial: cirriform. Posterior: very slender, threadlike	Acicular, hooked, with enlarged subterminal spine on concave side of stem	22–40	Northwestern Atlantic Ocean
<i>Aricidea (Aricidea) thammapiñanae</i> sp. nov.	Conical, distally rounded	One pair	Short, biarticulate; to chaetiger 1	4 to 7–11	First two short, third larger, broadly triangular, with a short round distal protuberance; digitiform in branchial region; slender posteriorly	Bidentate hooked, with distal pubescence, with a very long subterminal spine on concave side of shaft	10–19	Songkhla Sea, Gulf of Thailand

Materials and methods

Specimens were collected between 2011 and 2018 in the southern Gulf of Thailand ($7^{\circ}14'21''$ – $7^{\circ}49'21''$ N, $100^{\circ}24'42''$ – $100^{\circ}49'00''$ E) (Fig. 1), with a Van Veen grab (0.1 m^2) at depths ranging from 10 to 26.5 m. The collected samples were sieved with 2.0 mm, 1.0 mm and 0.5 mm mesh screens in the field. Later, water and sediment from the sieved grab samples were passed through a $300 \mu\text{m}$ filter bag. Specimens retained by both separation methods were separately fixed with a 4% formaldehyde in seawater solution. In the laboratory, samples were washed with fresh water and transferred to 70% ethanol. The polychaetes were sorted into taxonomic groups using a stereomicroscope and those belonging to the proposed new species were examined under dissection and compound light microscopes. SEM images were produced with a JEOL JSM-5800LV microscope and Apreo-Field Emission Scanning Electron Microscope (FESEM) at the Office of Scientific Instrument and Testing (OSIT), Prince of Songkla University, Hatyai, Thailand. Light microscope photographs were taken with a Leica digital camera in the OSIT, Prince of Songkla University and Olympus SZX16 with DP74 digital camera at MEM. The morphological measurements of the holotype are indicated in the taxonomic description. Information on character variability found in the paratypes is included in parentheses. The confirmation of the taxonomic status of the new species was based on the excellent revision and compilation of the diagnostic characteristics of all recognized species of the subgenera *Aricidea* (*Acmira*) and *Aricidea* (*Aricidea*) by Blake (1996), Lovell (2002) and Arriaga-Hernández et al. (2013). For comparative purposes, a table with the main diagnostic characters of the new species and closely related species was also included.

The type material was deposited in the Princess Maha Chakri Sirindhorn Natural History Museum, Prince of Songkla University (PSUZC), Thailand and the Australian Museum (AM), Sydney, Australia. Additional material is maintained in the personal collections of Jintana and Sakanan Plathong at MEM (Marine Ecoscience Management Co., Ltd.).

Systematics

Class Polychaeta

Subclass Sedentaria

Infraclass Scolecida

Family Paraonidae Cerruti, 1909

Genus *Aricidea* Webster, 1879

Subgenus *Aricidea* (*Acmira*) Hartley, 1981

Aricidea (*Acmira*) *anusakdii* sp. nov.

<http://zoobank.org/5D4169E8-76CF-4638-8E77-70D681CCCF3B>

Figures 1A, 2–4

Material examined. 178 specimens, incomplete, collected from Songkhla Sea, the Gulf of Thailand, Western Pacific. Coll. MEM (Marine Ecoscience Management Co., Ltd.),

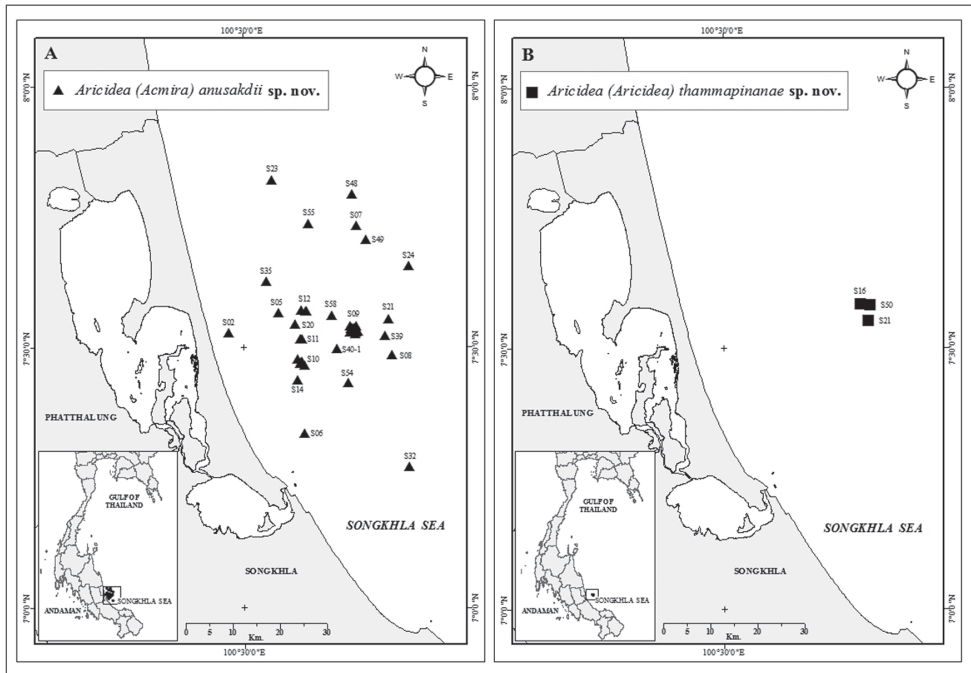


Figure 1. Sampling sites in the Songkhla Sea, Gulf of Thailand, showing stations where *Aricidea (Acmira) anusakdii* sp. nov. (A) and *Aricidea (Aricidea) thammapinanae* sp. nov. (B), were collected between 2011 and 2018.

mud mixed with sand and shells. Details of geographic positions and environmental characteristics of sampling stations are in Table 2. **Holotype.** PSUZC-POL-0047, Sta. S09-24, 21 Mar. 2017. **Paratypes.** PSUZC-POL-0048 (1 spec.), Sta. S09-6, 4 Mar. 2011; PSUZC-POL-0049 (1 spec.), Sta. S07, 4 Jun. 2014; PSUZC-POL-0050 (1 spec.), Sta. S08, 4 Jun. 2014; PSUZC-POL-0051 (1 spec.), Sta. S10-3, 5 May 2018; PSUZC-POL-0052 (1 spec.), Sta. S07, 22 Sep. 2016; PSUZC-POL-0053 (1 spec., coated with gold for SEM), Sta. S05, 23 Mar. 2012; PSUZC-POL-0054 (2 specs., coated with gold for SEM), Sta. S07, 1 Jun. 2013; PSUZC-POL-0055 (1 spec.), Sta. S08, 14 Oct. 2015; PSUZC-POL-0056 (1 spec., coated with gold for SEM), Sta. S07, 16 Mar. 2016; PSUZC-POL-0058 (1 spec.), Sta. S07, 22 Sep. 2016; PSUZC-POL-0059 (1 spec.), Sta. S10-9, 6 May 2018; PSUZC-POL-0060 (1 spec.), Sta. S09-3, 16 Aug. 2018; AM W.52894 (1 spec.), Sta. S12-3, 9 Feb. 2012; AM W.52895 (1 spec.), Sta. S10-9, 6 May 2018.

Description. Holotype incomplete with 123 chaetigers, 25 mm long, 1.2 mm wide. Paratypes incomplete with 19–81 chaetigers, 3–13 mm long, 0.51–0.77 mm wide. Body robust, widest anteriorly, dorsoventrally flattened in branchial region (Fig. 2A), thinner with cylindrical segments in postbranchial region. Cilia scattered on dorsum along the body. Opaque white in alcohol, with red pigments on the distal and subdistal regions of each branchia (Fig. 2C). Prostomium wider than long (0.36 mm wide; 0.26 mm long); anterior margin of prostomium bilobed divided by a shallow notch which dorsally extends to the antenna (Figs 2B, 4A). Two large nuchal grooves

Table 2. Stations, geographic positions, depths and sediment types where *Aricidea (Acmira) anusakdii* sp. nov. and *Aricidea (Aricidea) thammapiñanae* sp. nov. were collected in the Songkhla Sea, Gulf of Thailand. (* = specimen used for SEM image and italic = *A. (A.) thammapiñanae*).

Station	Sampling Date/ Number of individuals	Latitude / Longitude	Depth (m)	Sediment type
S02	11/10/2013 (1)	7°31'44"N, 100°28'15"E	10	Muddy with sand
S05	23/5/ 2012 (1*), 21/5/2015 (2)	7°34'03"N, 100°33'57"E	16.5	Muddy with sand and shells; upper sediment brown, lower sticky and dark
S06	17/10/2013 (1)	7°20'09"N, 100°36'58"E	15.5	Upper sediment muddy with sand, lower sticky mud with shells
S07	24/5/2012 (2), 10/10/2012 (1), 21/2/2013 (1), 1/6/2013 (5*), 16/10/2013 (3), 5/2/2014 (2), 4/6/2014 (3), 8/10/2014 (5), 26/2/2015 (1), 20/5/2015 (4), 20/5/2015 (2), 16/3/2016 (1*), 18/5/2016 (3), 22/9/2016 (5)	7°44'01"N, 100°43'02"E	26.5	Muddy with shells; upper sediment brown, lower sticky and green
S08	30/1/2012 (1), 24/5/2012 (2), 10/10/2012 (1), 1/6/2013 (1), 16/10/2013 (1), 5/2/2014 (4), 4/6/2014 (1), 8/10/2014 (1), 14/10/2015 (1*)	7°29'10"N, 100°47'06"E	25.0	Muddy with shells; lower sediment sticky mud
S09-1	7/2/2012 (1), 24/3/2017 (2), 17/8/2018 (2)	7°32'13"N, 100°42'41"E	24	Muddy with sand and shells
S09-3	7/3/2011 (1), 8/3/2014 (1), 16/8/2018 (2)	7°32'1"N, 100°42'41"E	24	Muddy with sand and shells
S09-5	17/8/2018 (2)	7°32'1"N, 100°42'30"E	24	Muddy with sand and shells
S09-6	4/3/2011 (1)	7°32'13"N, 100°42'21"E	23.6	Muddy with sand and shells
S09-7	7/2/2012 (1)	7°32'18"N, 100°42'24"E	23.7	Muddy with sand and shells
S09-10	7/3/2014 (1), 25/3/2017 (1)	7°31'55"N, 100°42'47"E	24.3	Muddy with sand and shells
S09-11	8/3/2014 (2), 25/3/2017 (1)	7°31'52"N, 100°42'42"E	23	Muddy with sand and shells
S09-12	6/2/2012 (1), 8/3/2014 (1), 25/3/2017 (2)	7°31'55"N, 100°42'24"E	23.8	Muddy with sand and shells
S09-14	1/3/2011 (2), 7/3/2014 (2), 1/3/2016 (2)	7°32'30"N, 100°42'12"E	24	Muddy with sand and shells
S09-16	1/3/2016 (2), 23/3/2017 (2)	7°32'30"N, 100°42'59"E	24	Muddy with sand and shells
S09-17	17/3/2013 (1), 7/3/2014 (2)	7°31'54"N, 100°43'5"E	24	Muddy with sand and shells
S09-18	6/2/2012 (1), 7/3/2014 (1)	7°31'44"N, 100°42'58"E	24	Muddy with sand and shells
S09-19	6/2/2012 (2), 7/3/2014 (1)	7°31'37"N, 100°42'48"E	24	Muddy with sand and shells
S09-20	6/2/2012 (2)	7°31'44"N, 100°42'12"E	24	Muddy with sand and shells
S09-22	16/8/2018 (1)	7°32'13"N, 100°42'30"E	24	Muddy with sand and shells
S09-24	7/2/2012 (1), 7/3/2014 (1), 21/3/2017 (1)	7°32'18"N, 100°42'47"E	24.5	Muddy with sand and shells
S10	2/3/2011 (1)	7°28'20"N, 100°36'33"E	19	Muddy with shells

Station	Sampling Date/ Number of individuals	Latitude / Longitude	Depth (m)	Sediment type
S10-3	16/2/2015 (2), 5/5/2018 (2)	7°28'22"N, 100°36'41"E	19	Muddy with shells
S10-4	6/2/2012 (1), 15/2/2015 (3), 5/5/2018 (2)	7°28'14"N, 100°36'39"E	19	Muddy with shells
S10-5	6/2/2012 (4), 6/5/2018 (1)	7°28'12"N, 100°36'31"E	18.5	Muddy with shells
S10-8	5/2/2012 (3), 6/5/2018 (1)	7°28'43"N, 100°36'10"E	18.5	Muddy with shells
S10-9	16/2/2015 (2), 6/5/2018 (2)	7°27'57"N, 100°36'56"E	19	Muddy with shells
S11-2	27/3/2017 (1)	7°31'01"N, 100°36'39"E	18.9	Muddy with shells
S11-3	15/3/2013 (1), 27/3/2017 (1)	7°31'01"N, 100°36'27"E	18.8	Muddy with shells
S12	16/3/2013 (1)	7°34'18"N, 100°36'34"E	20	Muddy with sand and shells
S12-2	26/3/2017 (1)	7°34'12"N, 100°37'15"E	20	Muddy with sand and shells
S12-3	9/2/2012 (1)	7°34'13"N, 100°37'4"E	19.8	Muddy with sand and shells
S14	14/3/2013 (1), 5/3/2014 (1), 19/2/2015 (1)	7°26'13"N, 100°36'12"E	15.5	Muddy with sand and shells
S16	21/08/2012 (1*)	7°35'11"N, 100°45'47"E	22	Muddy with sand and shells
S20	20/8/2012 (2)	7°32'41"N, 100°35'54"E	21	Muddy with shells
S21	21/8/2012 (2), 23/3/2017 (4), 16/8/2018 (1), 21/08/2012 (1), 15/03/2013 (3, 1*), 3/06/2013 (1), 23/03/2017 (1), 23/09/2017 (1*), 16/08/2018 (4)	7°33'16"N, 100°46'43"E	24	Muddy with sand and shells
S23	29/2/2016 (1)	7°49'20"N, 100°33'17"E	20.5	Muddy with sand and shells
S24	30/10/2014 (1), 16/9/2014 (3), 30/10/2014 (1), 15/7/2015 (1)	7°39'22"N, 100°49'1"E	27	Fine mud with shells
S32	26/9/2011 (5)	7°16'18"N, 100°49'0"E	20	Muddy with shells
S35	29/9/2011 (1)	7°37'35"N, 100°32'35"E	24	Muddy with sand and shells
S39	27/9/2011 (2)	7°31'22"N, 100°46'15"E	22	Muddy sand
S40-1	20/8/2012 (1)	7°29'51"N, 100°40'41"E	20	Muddy sand
S48	22/2/2015 (1)	7°47'37"N, 100°42'29"E	24.6	Slightly muddy soil
S49	21/2/2015 (2)	7°42'25"N, 100°44'6"E	24.7	Slightly muddy soil
S50	27/02/2015 (1)	7°35'00"N, 100°46'57"E	24	Muddy with sand and shells, greenish brown
S54	21/2/2015 (2)	7°25'57"N, 100°42'2"E	15	Muddy with shells
S55	14/7/2015 (1)	7°44'16"N, 100°37'30"E	21	Muddy with shells
S58	30/9/2011 (2)	7°33'43"N, 100°40'10"E	20	Muddy with sand and shells

on posterior half of prostomium; two ciliated bands on middle prostomium, and a ciliary band border on the inferior mid-region (Figs 2A, B, 4A). Short median antenna, proximally inflated, tapering to a short, blunt end, extending to posterior margin of prostomium (Figs 2A, B, 4A). No eyes. Anterior region of the mouth with a middle lobe and a ciliary row on its middle-anterior margin; posterior buccal lip with 12–14 small longitudinal folds, extending to chaetiger 2 (Figs 2D, 4B).

Two prebranchial chaetigers (Figs 2A, B, 4A). Branchiae start from chaetiger 3, 53 pairs (48–68 pairs in paratypes), bearing numerous long and slender cilia on dorsal mid-line (Fig. 3A); last pair of branchiae shorter. Parapodia large and thick with numerous simple chaetae on noto- and neuropodia. Notopodial postchaetal lobes from chaetiger

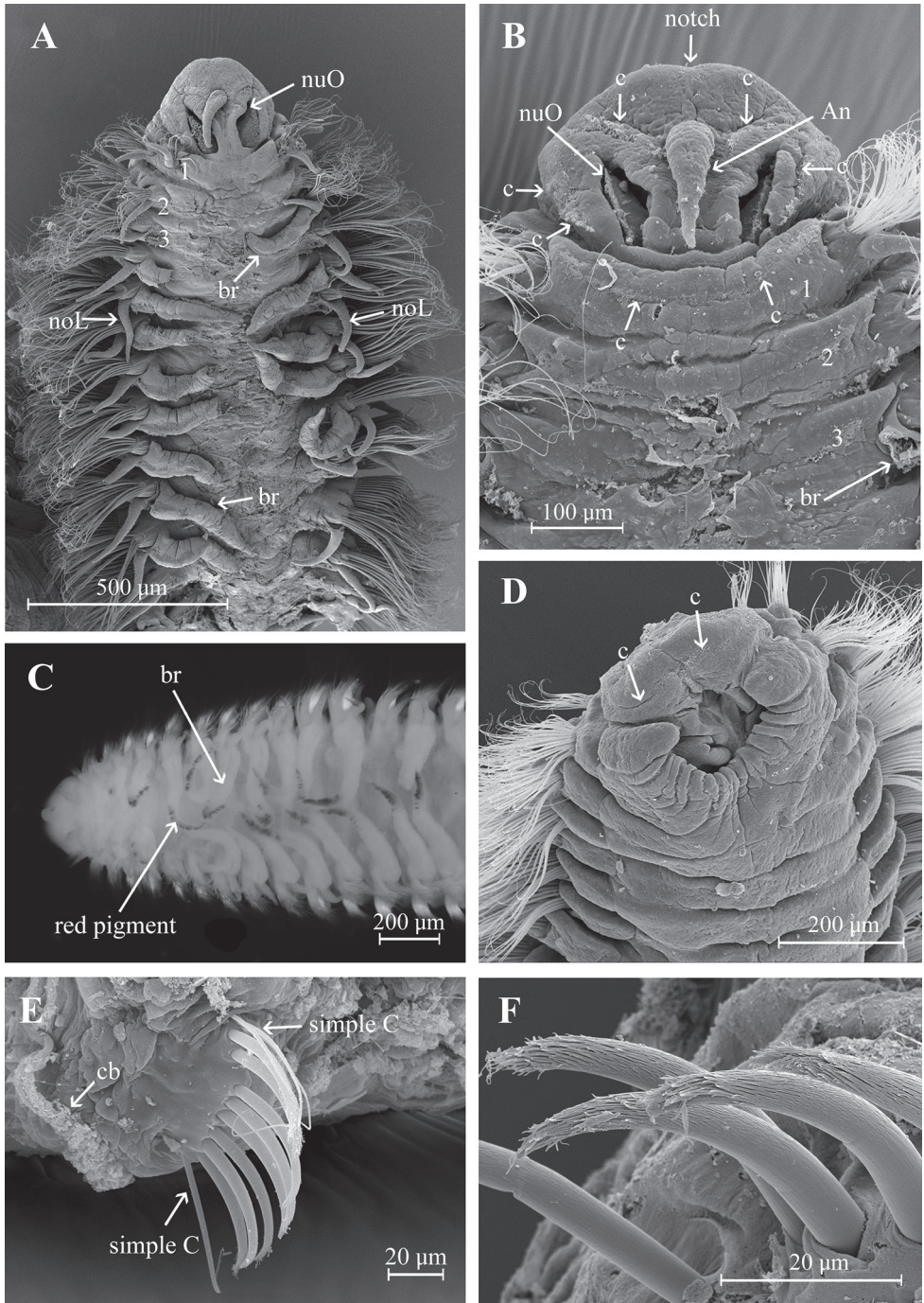


Figure 2. *Aricidea (Acmira) anusakdii* sp. nov. **A, B** anterior region, dorsal view **C** mouth, ventral view **D** branchial region, dorsal view **E** modified neurochaetae from posterior chaetiger **F** modified hooks. Abbreviations: An: antennae, br: branchia, c: cilia, cb: cilia band, noL: notopodial postchaetal lobe, nuO: nuchal organ, simple C: simple chaetae.

1 long, digitiform; cirriform in branchial and postbranchial chaetigers (Fig. 3B, E, F). Neuropodial postchaetal lobes shorter than notopodial postchaetal lobes (Fig. 3A, C, F).

Modified neurochaetae from chaetiger 37 (from 18–44 in paratypes) to posterior body region; up to nine modified chaetae per fascicle, each a curved spine with blunt shaft surrounded by pubescence (Fig. 2F), accompanied by about four simple chaetae on the superior and inferior parts of bundle (Figs 2E, 4C). All other chaetae long and slender capillaries (Figs 2C, 3D); notochaetae longer than neurochaetae (Fig. 3B, C). Pygidium unknown.

Reproduction. Holotype and paratypes of *A. (Acmira) anusakdii* sp. nov. collected in March, May, June, and August had eggs in their branchial chaetigers. Eggs were also found in October in non-type material.

Etymology. The species was named in honor of, and to remember, Mr Anusakdi Plathong, Sakanan's deceased father.

Habitat. At 10–26.5 m depth, in mud mixed with sand and shells substrates.

Distribution. Songkhla Sea, Gulf of Thailand, Western Pacific.

Remarks. Currently, the subgenus *Aricidea (Acmira)* Hartley, 1981 is represented by 20 species, including the new species described in the present study. The species that make up this subgenus can be separated by the features of modified neurochaetae (teeth, hood, distal arista, and pubescence), the length and shape of the median antenna, the number of prebranchial chaetigers and the number of branchiae (Arriaga-Hernández et al. 2013). Previously, only one species, *A. (Acmira) simonae* Laubier & Ramos, 1974, had been described with two prebranchial chaetigers. However, this taxon, originally described from Marseille, France, and common in Mediterranean and Black Sea is entirely different from the new species collected in Thailand. *Aricidea (Acmira) simonae* has smooth neuropodial spines, without pubescence, a very short antenna on the insertion area, bears only 20–32 pairs of branchiae and lacks neuropodial lobes. *Aricidea (Acmira) anusakdii* sp. nov. has curved spines with blunt shafts surrounded by pubescence, an antenna that reaches the posterior margin of the prostomium, has neuropodial lobes and bears a significantly higher number of branchial pairs (48–68 pairs).

Apart from *A. (Acmira) simonae* and *A. (Acmira) anusakdii* sp. nov., eight species of this genus also have smooth modified spines, lacking hood and distal arista, of which only *A. (Acmira) hirsuta* Arriaga-Hernández, Hernández-Alcántara & Solís-Weiss, 2013 from the southern Gulf of Mexico, *A. (Acmira) horikoshi* Imajima, 1973 from Japan and *A. (Acmira) flava* Zhou & Reuscher, 2013 from China, and probably *A. (Acmira) simplex* from South Africa and *A. (Acmira) strelzovi* from Antarctica, have modified spines with distal or subdistal pubescence. However, in these first three species the branchiae initially appear in chaetiger 4, bearing 7–15, 27 and 5 branchial pairs respectively. Clearly, these characteristics distinguish these species from *A. (A.) anusakdii* sp. nov., which, has two prebranchial chaetigers and a much greater number of branchiae (48–68 pairs). *Aricidea (Acmira) anusakdii* sp. nov. can also be separated from *A. (Acmira) hirsuta* because the new species has neuropodial lobes, which are absent in *A. (Acmira) hirsuta* (Table 3).

Although the modified spines in *A. (Acmira) mirifica* and *A. (Acmira) fnitima* have no hood and do not bear distal or subdistal pubescence, in the first species the spines

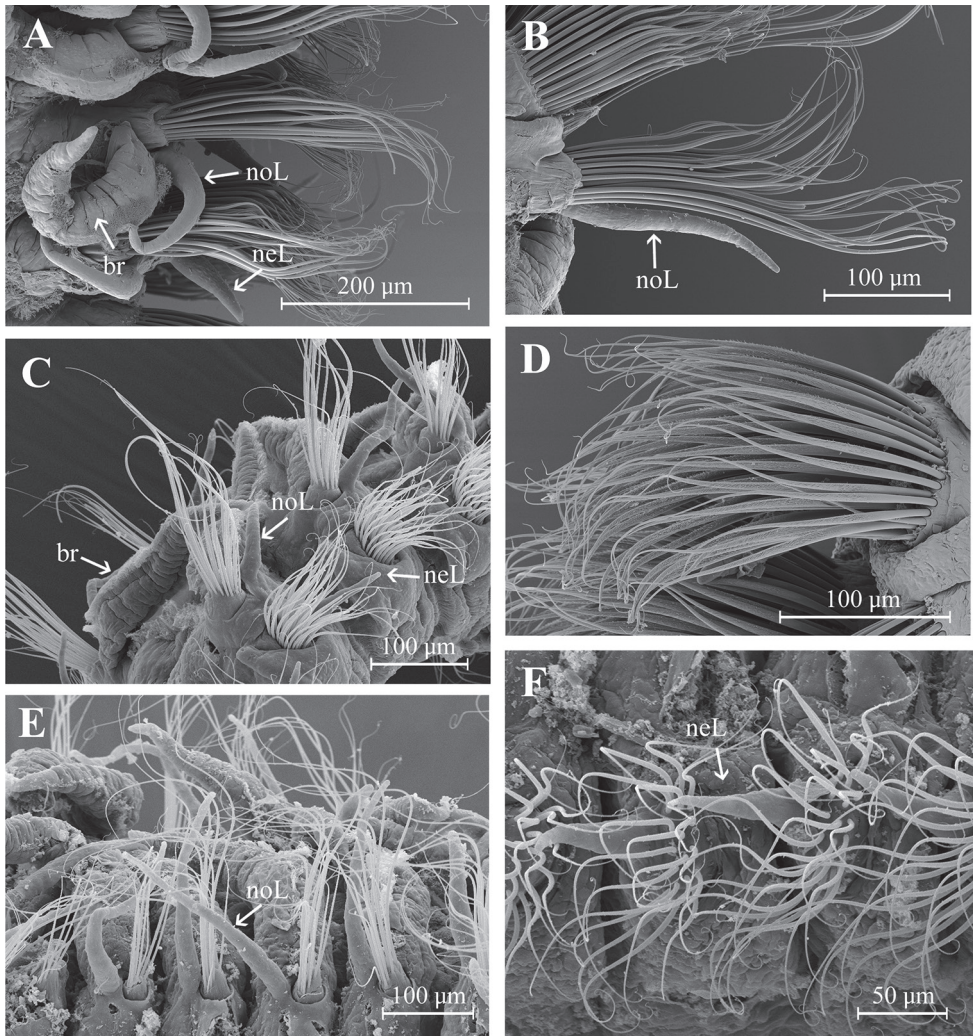


Figure 3. *Aricidea (Acmira) anusakdii* sp. nov. **A** branchiae at chaetiger 7 **B** notochaetae and notopodial postchaetal lobes (chaetiger 6) **C** noto- and neuropodial postchaetal lobes from chaetigers 13–14 **D** neurochaetae at chaetiger 14 **E** notopodial postchaetal lobes from midbranchial chaetiger **F** neuropodial postchaetal lobes and neurochaetae from midbranchial chaetiger. Abbreviations: br: branchia, neL: neuropodial postchaetal lobe, noL: notopodial postchaetal lobe).

sometimes bear a short distal arista and in the second they almost always bear arista. Nonetheless, both these species can also be separated from the new species because they have three prebranchial chaetigers, their antennae are longer (reaching chaetiger 1–3 or 6), and they bear fewer branchiae, 12 and 14–27 pairs, respectively.

It is important to note that previously, the presence of lobes and notches on the anterior margin of the prostomium had only been reported in two species: *A. (Acmira) simonae*, which has three lobes in ventral view (Laubier and Ramos

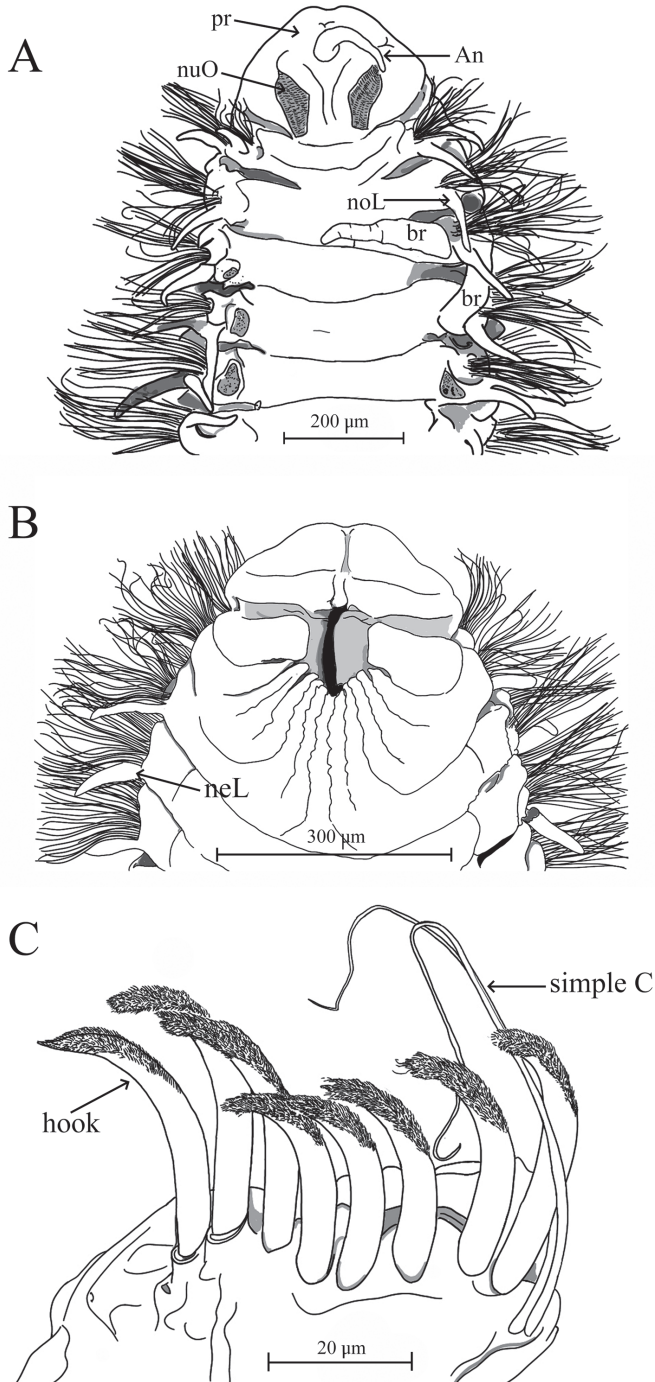


Figure 4. *Aricidea (Acmira) anusakdii* sp. nov. **A** anterior region, dorsal view **B** the buccal lip; ventral view **C** posterior modified neurochaetae. Abbreviations: An: antenna, br: branchia, neL: neuropodial postchaetal lobe, noL: notopodial postchaetal lobe, nuO: nuchal organ, pr: prostomium, simple C: simple chaetae).

Table 3. Comparison of *Aricidea (Acmira)* species with modified spines lacking distal aristae and hood (modified from Arriaga-Hernández et al. 2013).

Character	<i>Aricidea (Acmira) flava</i> Zhou & Reuscher, 2013	<i>Aricidea (Acmira) hirsuta</i> Arriaga-Hernández et al., 2013	<i>Aricidea (Acmira) horikoshi</i> Imajima, 1973	<i>Aricidea (Acmira) simonae</i> Laubier & Ramos, 1974	<i>Aricidea (Acmira) anusakdii</i> sp. nov.
Antenna (end at chaetiger)	3	Posterior margin of prostomium	4 to 5	Very short, on insertion area	Posterior margin of prostomium
Branchiae from chaetiger	4 to 21	4 to 10–18	4 to 33	3 to 20–32	3 to 48–68
Spines	Unidentate	Unidentate	Unidentate	Unidentate	Unidentate
Hood on spine	Absent	Absent	Absent (a narrow sheath on convex side)	Absent	Absent
Distal arista on spines	Absent	Absent	Absent	Absent	Absent
Pubescence on spines	Distal	Distal and subdistal	Distal	Absent	Distal and subdistal
Notopodial lobes	Present	Present	Present	Present	Present
Neuropodial lobes	Present (inconspicuous, low tubercles)	Absent	Present	Absent	Present
Type locality	Northern coast of China	Términos Lagoon, southern Gulf of Mexico	Japan, North Pacific Ocean	Famagusta Bay, Marseille, France	Songkhla Sea, Gulf of Thailand

1973) and other differences, smooth neuropodial spines, a very short antenna on the insertion area, bears only 20–32 pairs of branchiae and lacks neuropodial lobes, with the new species has been previously argued; and *Aricidea (Acmira) trilobata* Imajima, 1973, distributed on the continental shelves of Japan and California (Blake, 1996), which also bears three lobes on the anterior edge of the prostomium and the branchiae start from chaetiger 4. However, unlike the new species, this last species also bears three lobes on the anterior edge of the prostomium, the branchiae start from chaetiger 4, the median antenna extending to chaetiger 2 and only bears 18 to 20 branchial pairs.

Genus *Aricidea* (Webster, 1879)

Subgenus *Aricidea (Aricidea)* [Webster, 1879, *sensu stricto*]

Aricidea (Aricidea) thammapiñanae sp. nov.

<http://zoobank.org/6B8798D3-662C-4097-8DC9-83A5640E332C>

Figures 1B, 5–9

Material examined. 13 specimens, collected from Songkhla Sea, Gulf of Thailand, 24 m depth. Coll. MEM (Marine Ecosoearch Management Co., Ltd.), in mud mixed with sand and shells. Details of geographic positions and environmental character-

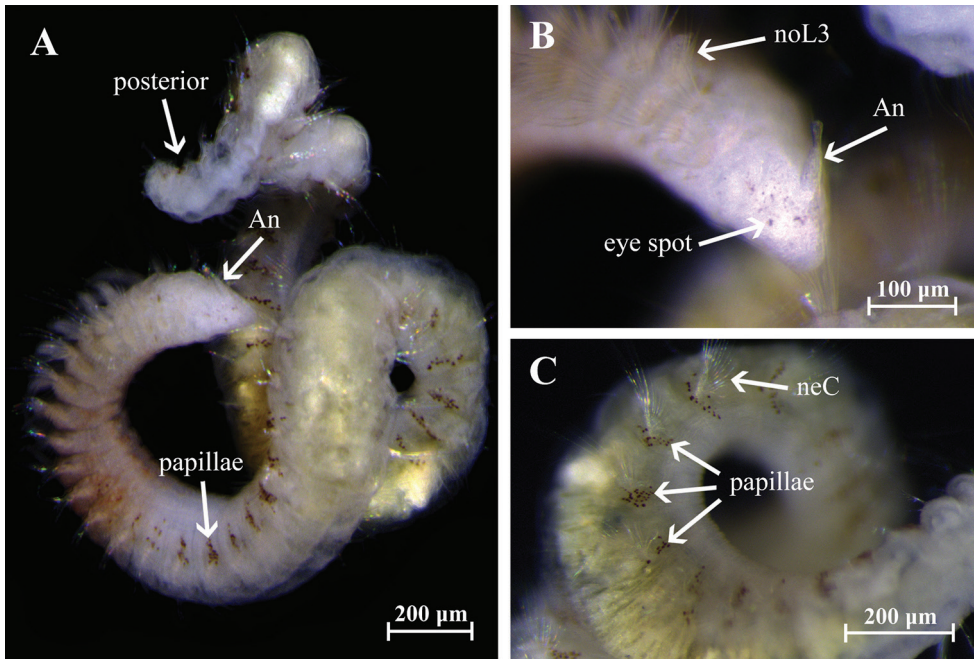


Figure 5. *Aricidea (Aricidea) thammapiñanae* sp. nov. PSUZC 0047, holotype. **A** complete specimen, ventral view **B** prostomium, lateral view **C** red-brown papillae and neurochaetae, lateral view. Abbreviations: An: median antenna, neC: neurochaetae, noL3: notopodial postchaetal lobe chaetiger 3.

istics of sampling stations are in Table 2. **Holotype.** PSUZC-POL-00021 (1 spec., complete), Sta. S21, 16 Aug. 2018. **Paratypes.** PSUZC-POL-00022 (1 spec.), Sta. S21, 21 Aug. 2012; PSUZC-POL-00023, (1 spec., coated with gold for SEM), Sta. S21, 15 Mar. 2013; PSUZC-POL-00024 (1 spec.), Sta. S21, 3 Jun. 2013; PSUZC-POL-00025 (1 spec.), 23 Mar. 2017; PSUZC-POL-00026, (1 spec., coated with gold for SEM), Sta. S21, 23 Sep. 2017; PSUZC-POL-0027, (1 spec., coated with gold for SEM), Sta. S16, 21 Aug. 2012; PSUZC-POL-0062 (2 specs.), Sta. S21, 16 Aug. 2018; AM W.52904 (1 spec.), Sta. S50, 27 Feb. 2015.

Description. Holotype complete with approximately 50 chaetigers (posterior region coiled, difficult to count segments), 5.47 mm long, 0.3 mm wide (Fig. 5A–C); two complete paratypes with 29 and 45 chaetigers, others incomplete with 21 to 32 chaetigers, 1.8–4.5 mm long and 0.01–0.23 mm wide. Body small, new preserved specimens reddish-orange in prebranchial and branchial regions (Fig. 5A); dorsal ciliary bands present on the prebranchial and branchial chaetigers. Prostomium conical, distally rounded, longer than wide; one pair of small black or brown eyes present; two pairs of long ciliary bands, one pair located above nuchal grooves and other at lateral margins of prostomium. Median antenna biarticulated, basal portion clavate, distal portion triangular, ciliated on distal end; basal portion of median antenna about two times longer than distal portion, extending to chaetiger 1 (Figs 6B, D, 9A). Nuchal

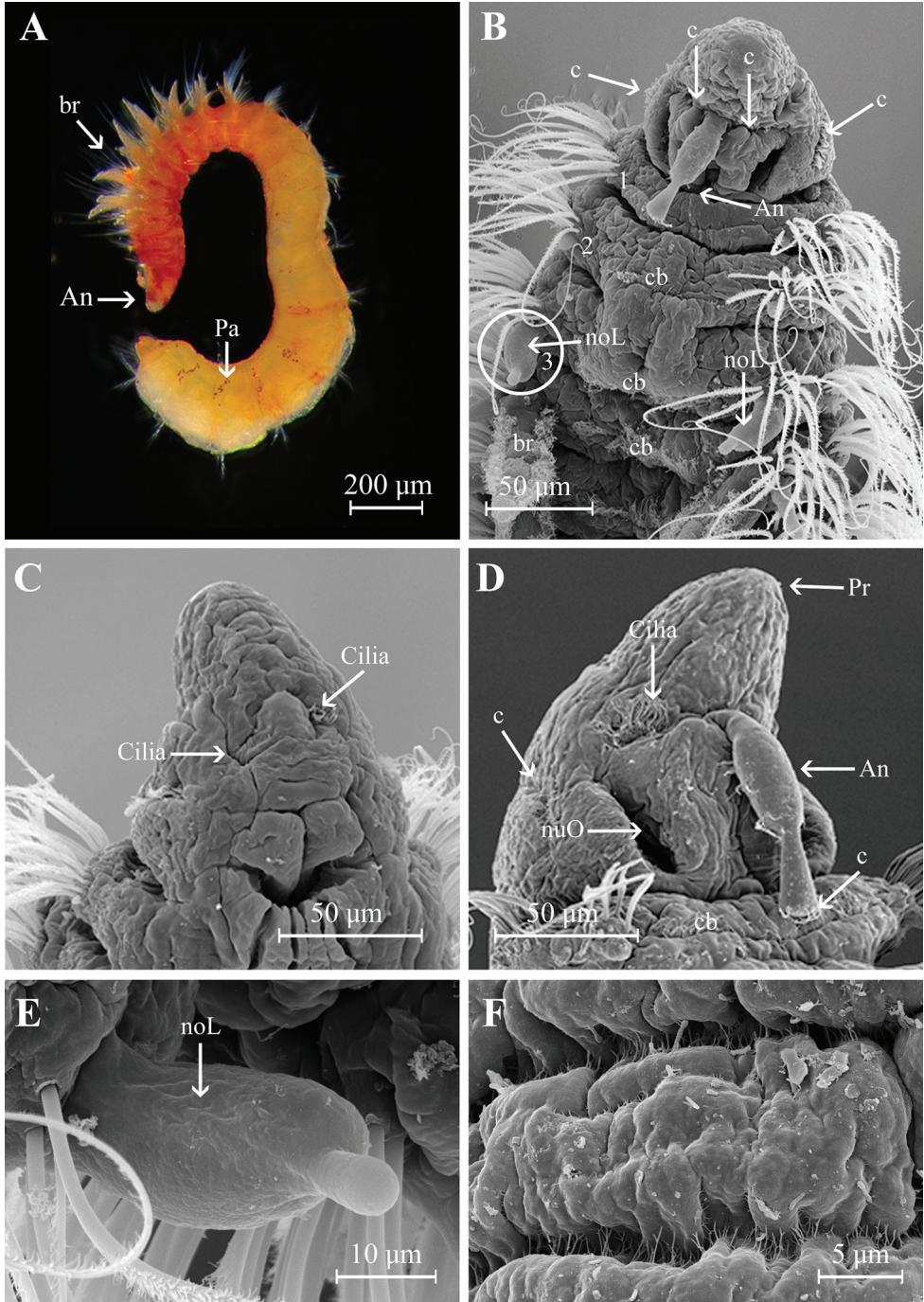


Figure 6. *Aricidea (Aricidea) thammapiñanae* sp. nov. **A** body color in alcohol, lateral view **B** anterior region, dorsal view **C** mouth, arrows show cilia **D** prostomium, dorso-lateral view **E** notopodial lobe from chaetiger 3 **F** close up of posterior chaetiger, showing the cilia. Abbreviations: An: antenna, br: branchiae, c: cilia, cb: cilia band, noL: notopodial postchaetal lobe, nuO: nuchal organ, Pr: prostomium.

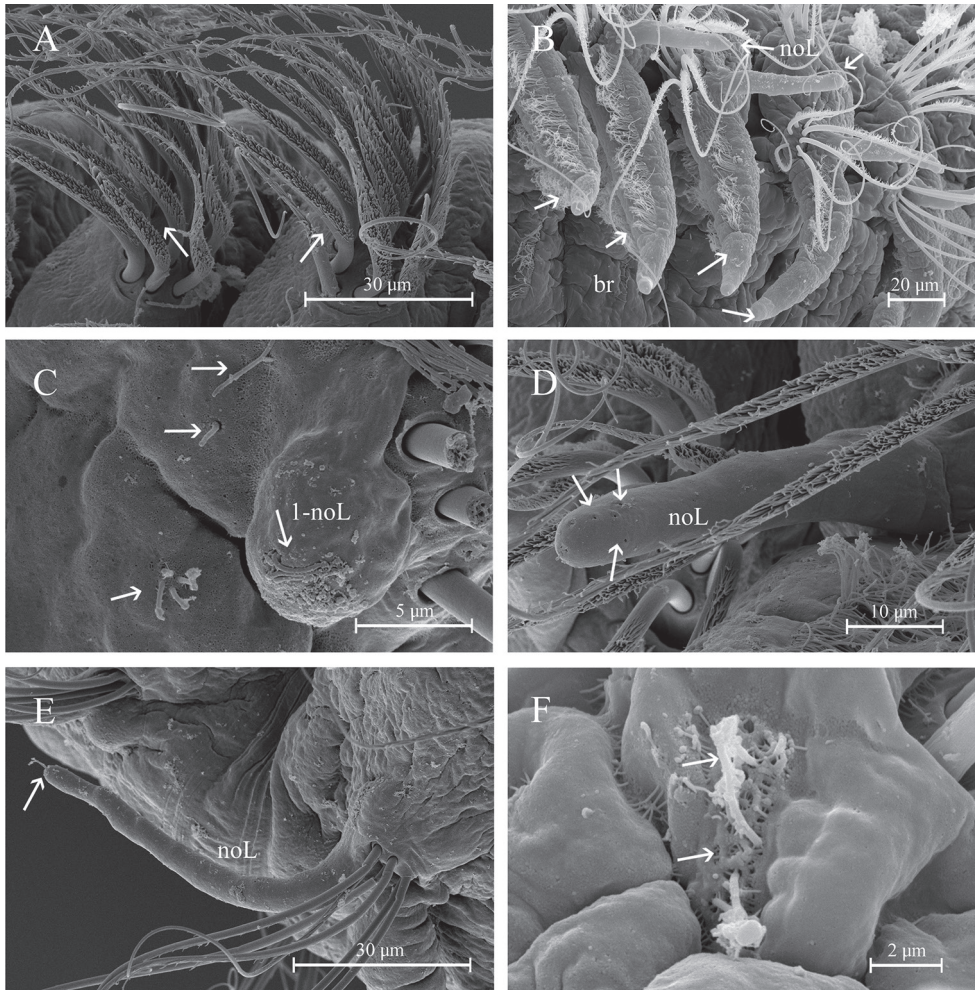


Figure 7. *Aricidea (Aricidea) thammapiñanae* sp. nov. **A** three rows of neurochaetae in prebranchial area, ventral view **B** branchiae with long cilia **C** first notopodial lobe **D, E** pores on the distal area of notopodial lobe **E** notopodial lobe from chaetiger 3 **F** filaments or cilia in notopodial pores.

organs as pair of oblique, deep slits. Posterior buccal lip with six longitudinal folds, extending to chaetiger 1, with one pair of ciliary patches above the buccal region (Figs 6C, 9B). Numerous small filaments along body, and thin papillae present on the body (Fig. 6F) and notopodial pores (Fig. 7F).

Postbranchial region presents numerous dark red or brown pigmented papillae adjacent to neurochaetal rami on all chaetigers (Fig. 5A, C). First two notopodial postchaetal lobes very short, usually hidden by chaetae; those of chaetiger 3 much larger, broadly triangular, with a short, rounded distal protuberance. Notopodial postchaetal lobes digitate on branchial segments, filiform on following segments. Neuropodial postchaetal lobes small, inconspicuous (Figs 6B, E, 9A).

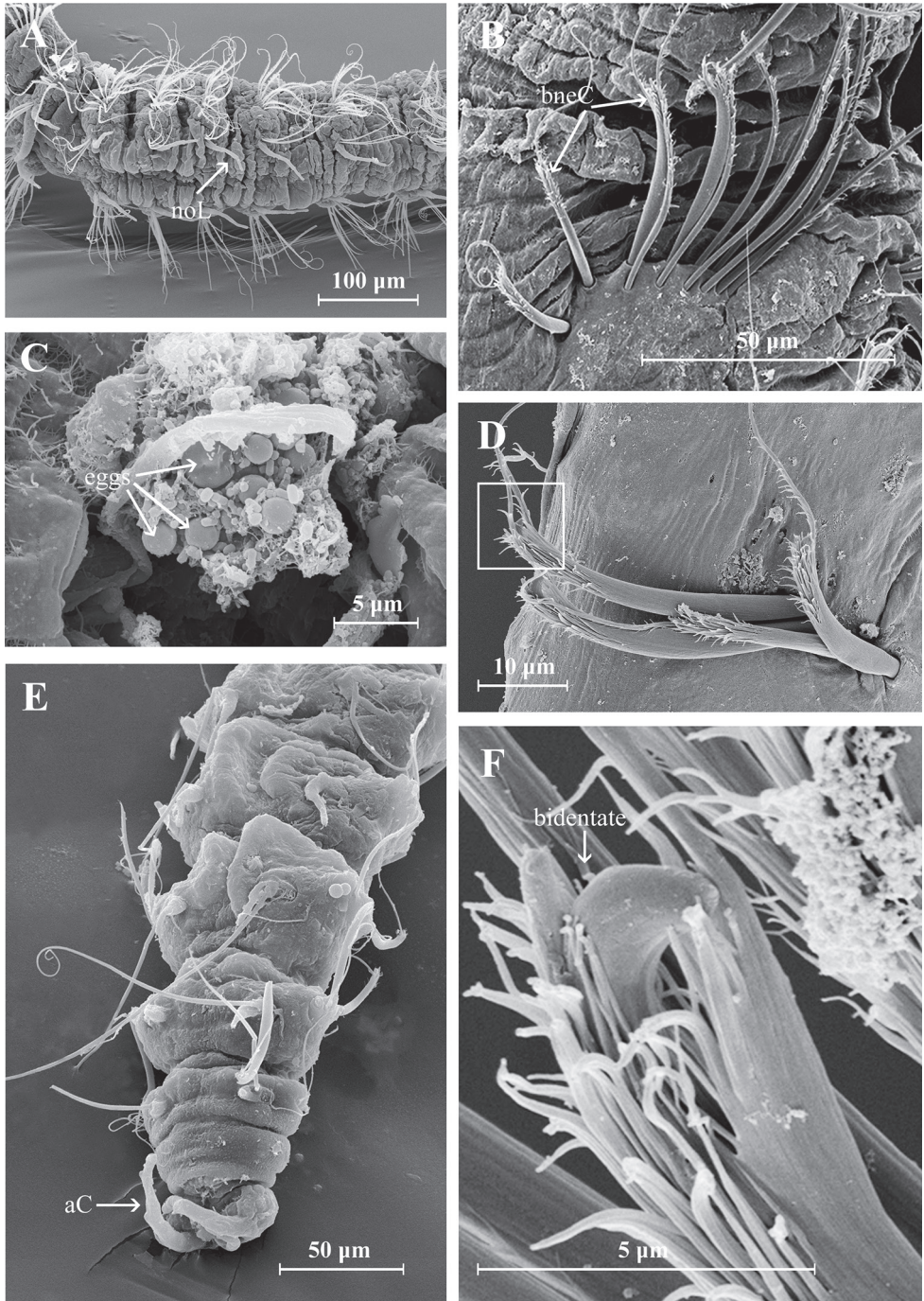


Figure 8. *Aricidea (Aricidea) thammapiñanae* sp. nov. **A** postbranchial region, arrow shows the notopodial postchaetal lobe **B, D, F** modified neurochaetae **C** eggs in postbranchial region **E** posterior region, pygidium with two anal cirri. Abbreviations: aC: anal cirri, bneC: bidentate neurochaetae, noL: notopodial postchaetal lobe.

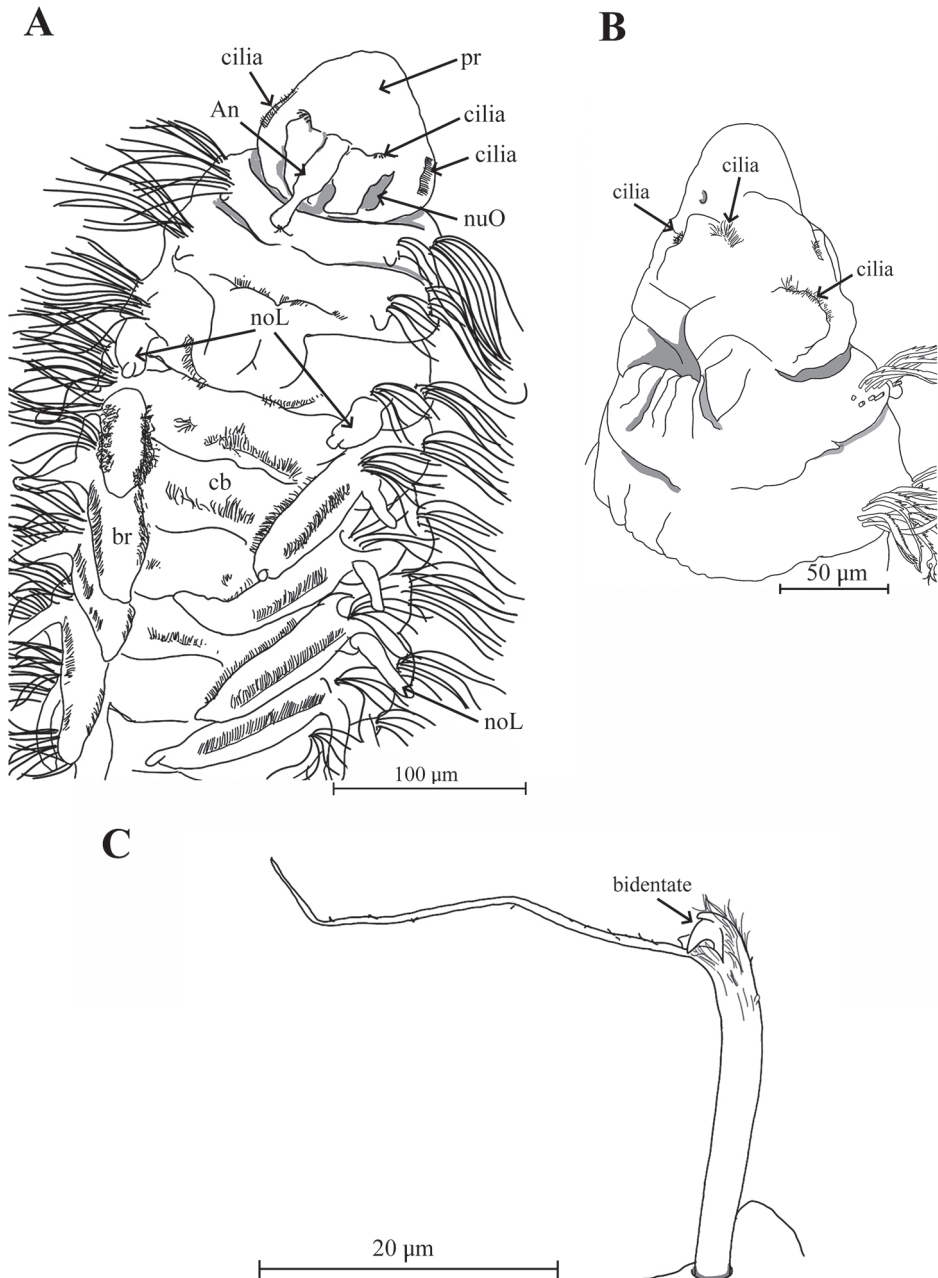


Figure 9. *Aricidea (Aricidea) thammapiñanae* sp. nov. **A** anterior region, dorsal view **B** the buccal lip; lateral view **C** posterior modified neurochaetae, lateral view. Abbreviations: An: antenna, br: branchiae, cb: cilia band, noL: notopodial postchaetal lobe, nuO: nuchal organ, pr: prostomium.

Three prebranchial chaetigers; 8 pairs of branchiae (4 to 8 in paratypes) present on chaetigers 4 to 11, robust, conical, with lateral margins markedly ciliated; last pair smaller. Anterior noto- and neurochaetae fringed with capillaries (Fig. 6A, B); notochaetae longer than neurochaetae, decreasing in number from anterior to posterior segments. Modified neurochaetae bidentate (Fig. 8B, E, F), beginning in chaetiger 17 (10–19 in paratypes), superior tooth small, inferior tooth large, surrounded by pubescence on distal region of shaft, with very long subterminal spine arising from concave side of shaft; spine almost twice as long as shaft, with pubescence throughout, starting from chaetiger 10–19. Posterior neurochaetae arranged in two rows, first row with both simple and modified bidentate chaetae, and second row with only simple chaetae; up to 5 bidentate chaetae per fascicle per row, accompanied by 10–12 long capillary chaetae (Fig. 8B). Pygidium with three anal cirri, two lateral and one triangular, short mid-ventral (Fig. 8E).

Reproduction. Holotype and paratypes of *Aricidea (Aricidea) thammapihanae* sp. nov. collected in March, August, and September had eggs in the coelomic cavities of postbranchial chaetigers.

Etymology. The species epithet *thammapihanae*, is after the family name of Ms Vorramaz Thammapihan. This species is named in honor of her initiation, coordination, and assistance to the research project in Songkhla Sea.

Habitat. At 20–24 m depth, mud with sand and shells.

Distribution. Songkhla Sea, Gulf of Thailand, Western Pacific.

Remarks. This is a small species of the subgenus *Aricidea (Aricidea)* having a maximum length of 5.47 mm (holotype) and with only 4–8 pairs of branchiae. The presence of eggs (Fig. 7C) in individuals collected during several sampling months implies that the small size of this new taxon is a specific characteristic. The presence of bidentate chaetae is unusual in species belonging to the subgenus *Aricidea (Aricidea)*. Until now, 15 species have been described in this subgenus but only *Aricidea (Aricidea) capensis* Day, 1961 from South Africa (Day 1961) has bidentate modified chaetae (Table 1). However, the species presents clearly different characteristics from those observed in *A. (Aricidea) thammapihanae* sp. nov., since the bidentate modified chaetae of *A. (Aricidea) capensis* Day, 1961 are smooth, without pubescence along the shaft or on the subterminal spine. Besides the antenna, extending to chaetiger 2, is faintly annulated, eyes are lacking, 14 branchial pairs are present, and all prebranchial notopodial lobes are small and slender (Table 1). In contrast, the proposed new species has bidentate modified neurochaetae with pubescence on the distal shaft and along the subterminal spine, a biarticulated antenna that extends to chaetiger 1, and a pair of eyes. Only 4–8 branchial pairs are present, and on chaetiger 3, distinctive broad triangular notopodial lobes with short distal protuberances.

Acknowledgements

We would like to thank Winai Theppunpon, Werayut Sripoka, and all MEM (Marine Ecoscience and Management Co., Ltd.) staff for field and laboratory work. Special thanks to CEC International, Ltd. (Thailand Branch) for project grants. Thanks are

due Ratchakorn Sirijarukul and Monrach Intarasiri for assisting with photographs. Thanks also to Mrs Apinya Sukolra, Ms Benjaporn Nooklay, and all staff at the SEM section at the Office of Scientific Instrument and Testing (OSIT), Prince of Songkla University. Special thanks to Mr Pacharadon Plathong for drawing the illustrations. Finally, special thanks to Larry Lovell for checking and commenting on the *Aricidea* (*Aricidea*) species list. We are grateful to editor, Dr. Christopher J. Glasby and reviewer, Dr. Melih Ertan Çinar for provided comments and suggestions that helped us to improve the quality of the manuscript.

References

- Arriaga-Hernández S, Hernández-Alcántara P, Solís-Weiss V (2013) Description and distribution of two new species of Paraonidae (Annelida: Polychaeta) from a lagoon-estuarine ecosystem in the Southern Gulf of Mexico. *Zootaxa* 3686(1): 51–64. <https://doi.org/10.11646/zootaxa.3686.1.2>
- Blake JA (1996) Family Paraonidae Cerruti, 1909. In: Blake JA, Hilbig B, Scott PH (Eds) Taxonomic Atlas of the Benthic Fauna of the Santa Maria Basin and the Western SantaBarbara Channel. Santa Barbara Museum of Natural History. Volume 6. Santa Barbara, 27–70.
- Blake JA (2019) Paraonidae Cerruti, 1909. In: Westheide W, Purschke G, Böggeman M (Eds) Annelida: Basal groups and Pleistoannelida, Sedentaria I. A natural history of the phyla of the Animal Kingdom. Handbook of Zoology Online.
- Day JH (1961) The Polychaete Fauna of South Africa. Part 6. Sedentary species dredged off Cape coasts with a few new records from the shore. *Journal of the Linnean Society of London* 44(299): 463–560. <https://doi.org/10.1111/j.1096-3642.1961.tb01623.x>
- Lovell LL (2002) Paraonidae (Annelida: Polychaeta) of the Andaman Sea, Thailand. In: Danny EJ (Ed.) Proceedings of the International Workshop on the Polychaete of the Andaman Sea June–August 1997: Phuket Marine Biological Center Special Publication No. 24, Phuket, 33–56.
- Hartley JP (1981) The family Paraonidae (Polychaeta) in British waters: a new species and new records with a key to species. *Journal of the Marine Biological Association of the United Kingdom* 61: 133–149. <https://doi.org/10.1017/S0025315400045975>
- Laubier L, Ramos J (1974) Paraonidae (Polychètes sédentaires) de Méditerranée. *Bulletin du Muséum National D’Histoire Naturelle* 3, 113: 1097–1148. [dated 1973, but printed 30 March 1974]
- Read G, Fauchald K (2020) World Polychaeta database. *Aricidea* Webster, 1879. World Register of Marine Species. <http://www.marinespecies.org/aphia.php?p=taxdetails&id=129430> [Accessed 2020-04-14]
- Rouse GW, Pleijel F (2001) *Polychaetes*. Oxford, 354 pp.
- Strelzov VE (1973) Polychaete worms of the Family Paraonidae Cerruti, 1909 (Polychaeta, Sedentaria). *Akademiya Nauk SSSR, Leningrad*, 212 pp.

New genus and species of calanoid copepods (Crustacea) belonging to the group of Bradfordian families collected from the hyperbenthic layers off Japan

Sota Komeda¹, Susumu Ohtsuka¹

¹ Takehara Station, Setouchi Field Science Center, Graduate School of Integrated Sciences for Life, Hiroshima University, 5–8–1 Minato-machi, Takehara, Hiroshima, 725–0024, Japan

Corresponding author: Sota Komeda (d196208@hiroshima-u.ac.jp)

Academic editor: Danielle Defaye | Received 10 January 2020 | Accepted 29 April 2020 | Published 22 July 2020

<http://zoobank.org/D6B82671-C4A8-4846-AA72-E59B17C19E0C>

Citation: Komeda S, Ohtsuka S (2020) New genus and species of calanoid copepods (Crustacea) belonging to the group of Bradfordian families collected from the hyperbenthic layers off Japan. ZooKeys 951: 21–35. <https://doi.org/10.3897/zookeys.951.49990>

Abstract

A new genus and species of calanoid copepods belonging to the group of Bradfordian families, *Pogonura rugosa* **gen. et sp. nov.**, is described from the deep-sea hyperbenthic layers off Nagannu Island, Okinawa Prefecture, southwestern Japan. *Pogonura* **gen. nov.** is similar to another Bradfordian genus *Proconognatha* in sharing the following characteristics: (1) segmentation of the antennule, fused segments II–IV, X–XI, XXVII–XXVIII in females and II–IV, X–XII, XXVII–XXVIII, right XXII–XXIII in males; (2) retained setae on the ancestral segments I–IV of the antennary exopod; (3) setules on the mandibular gnathobase; (4) 3 sclerotized setae on the maxillary endopod; (5) absence of sensory seta on the maxilliped; (6) large spinules on the posterior surface of the rami of legs 2 and 3; and (7) setation and segmentation of female leg 5. *Pogonura* **gen. nov.** is distinctly distinguished from *Proconognatha* by the following features: (1) reduction of a seta on the ancestral segment IX of the antennary exopod, (2) 8 setae (7 in *Proconognatha*) on the maxillular exopod, (3) 5 brush-like setae (6 in *Proconognatha*) on the maxillary endopod, and (4) reduction of right endopod of male leg 5. The systematic position of *Pogonura* **gen. nov.** in the Bradfordian families is also discussed. Although this new genus shares synapomorphies with some diaixid genera, an assignment of this genus to any Bradfordian family should be pending until the taxonomy of this family group is clearly settled.

Keywords

Bradfordian families, Clausocalanoidea, Diaixidae, hyperbenthos, Tharybidae

Introduction

Some clausocalanoidean families of calanoid copepods are characterized by the presence of chemosensory setae on the maxillary endopods, and in some taxa, on the maxillules and maxillipeds (Bradford 1973; Nishida and Ohtsuka 1997) and are called the Bradfordian families (Ferrari and Steinberg 1993). These groups are distributed in various marine habitats including both the pelagic realm and the hyperbenthic layers of the oceans (Bradford-Grieve 2004). Recently, many new families and genera collected from deep-sea hyperbenthic layers were established in the Bradfordian group (Ferrari and Markhaseva 1996; Ohtsuka et al. 2002, 2003; Markhaseva et al. 2008; Markhaseva and Schulz 2009). So far, seven families of the Bradfordian group have been recognized: Diaixidae Sars, 1902; Kyphocalanidae Markhaseva & Schulz, 2009, Parkiidae Ferrari & Markhaseva, 1996; Phaennidae Sars, 1902; Rostrocalanidae Markhaseva, Schulz & Martinez Arbizu, 2008; Scolecitrichidae Giesbrecht, 1892; and Tharybidae Sars, 1902.

According to Bradford (1973), the Scolecitrichidae and Phaennidae are families that are well defined by the armature of sensory elements on the maxillae, whereas the Diaixidae and Tharybidae are not as clearly diagnosed. Markhaseva et al. (2014) considered only *Tharybis* as a member of Tharybidae based on an autapomorphic character, an enlarged and vaulted arthrite of the maxillulary praecoxa which can differentiate between Tharybidae and Diaixidae. *Undinella* and *Brodskius* were conventionally included in Tharybidae (e.g., Markhaseva et al. 2014). Recently, analyses of relationships among the Bradfordian genera were performed by Markhaseva and Ferrari (2005) and Laakmann et al. (2019). Laakmann et al. (2019) also conducted a molecular-based phylogenetic analysis of these families but concluded that relationships between these seven families or 15 genera were not supported, except for the closeness between *Procegnatha* (conventionally assigned to Diaixidae) and *Tharybis* (Tharybidae).

The present paper deals with a description of a new genus and species of calanoid copepods belonging to the Bradfordian family collected from the deep-sea hyperbenthic layers off Nagannu Island, Okinawa Prefecture, southwestern Japan. The systematic position of this new genus is also discussed.

Materials and methods

Copepods were collected from the deep-sea hyperbenthic layer off Nagannu Island, west of Okinawa Prefecture, southwestern Japan (26°19.23'N, 127°26.35'E, depths of 595–627 m) on May 21, 2011, using a sledge net (mouth area of 1450 × 326 mm, mesh size of 0.33 mm; see Ohtsuka et al. 1992) towed along the sea bottom for 30 minutes at 2 knots. Samples were fixed with 10% neutralized formalin seawater immediately after capture. Type specimens are deposited at the National Museum of Nature and Science, Tsukuba, Japan (NMST-Cr 27413–27415). The morphological terminology follows Huys and Boxshall (1991).

Taxonomy

Order Calanoida Sars, 1901

Superfamily Clausocalanoidea Giesbrecht, 1893

Genus *Pogonura* gen. nov.

<http://zoobank.org/FC4F858B-9AC7-4D82-B5A7-FD861A8DF4A1>

Diagnosis. Female. Body compact. Cephalosome incompletely fused to first pediger with suture line dorsally and laterally visible. Fourth and fifth pedigers completely fused, weakly produced posteriorly into round lobes. Rostrum produced ventrally, with pair of filaments. Genital double-somite symmetrical, with pair of seminal copulatory pores and seminal receptacles; seminal copulatory pores ovaliform; genital operculum ventrally located midway; two spiniform setae located ventrolaterally, as long as genital double-somite. Antennule 24-segmented, with ancestral segments II–IV, X–XI, and XXVII–XXVIII fused; II–IV, VII, X–XI, XIV, XVI, XXI and XXVII–XXVIII with aesthetasc. Setal formula of antennary exopod as follows: 1, 1-1-1, 1, 1-1, 1, 0, 3. Mandible with gnathobase having 1 triangular ventral tooth, 5 chitinized teeth, 16 long setules, and 1 dorsal seta. Maxillulary exopod with 8 setae. Maxillary endopod with 5 brush-like setae and 3 sclerotized setae. Maxilliped with syncoxa having 1, 2, 3, 3 sclerotized setae. Legs 1–4 of typical clausocalanoidean segmentation and setation. Posterior surface of legs 2 and 3 with an exopodal spinule and 3 endopodal spinules. Leg 5 uniramous, 2-segmented, distal segment with 3 lateral process and 1 articulated spine.

Male. Body similar to that of female. Fusion between cephalosome and first pediger and between fourth and fifth pedigers resembling those of female. Genital somite with gonopore on left side. Rostrum as in female. Right antennule 22-segmented, with ancestral segments II–IV, X–XII, XXII–XXIII, and XXVII–XXVIII fused. Left antennule 23-segmented, with ancestral segments II–IV, X–XII, and XXVII–XXVIII fused. Antenna, mandible, maxillule, maxilla, maxilliped and legs 1–4 similar to those of female. Leg 5 complex in structure. Right leg uniramous, endopod absent; exopod 2-segmented. Left leg biramous with 1-segmented endopod; exopods 2-segmented, decorated by various armatures; distal part of exopod with rugose plate.

Remarks. Because *Pogonura* gen. nov. has brush-like sensory setae on the maxillary endopod, it can be assigned to one of the Bradfordian families. The new genus can be tentatively included in Diaixidae because it fits the familial diagnosis proposed by Markhaseva et al. (2014), except for the proximal basal endite of the maxillule with 3 setae (vs. 4 setae typical for the Diaixidae) and 2-segmented exopods of both legs 5 of the male.

The present new genus also shares the following characteristics with the diaixid genus *Procenognatha* (Markhaseva and Schulz 2010): the maxilliped carries no specialized sensory setae; legs 2 and 3 carry 3 large spinules on the posterior surface; and leg 5 of the female is uniramous, 2-segmented, with the distal segment having 3 processes and 1 articulated spine.

The male of the present new species has complex structures on leg 5, which can be seen in other diaixid genera such as *Anawekia* and *Diaixis*. These three genera have rows of setules and/or spinules on the left exopod of leg 5 [cf. figs 7 and 9 in Othman and Greenwood (1994); figs 11 and 12 in Andronov (1979)], and these setulae and/or spinules seem to be homologues in position and shape. However, *Anawekia* and *Diaixis* have some derivative characteristics: (1) the posterior corner of the prosome, leg 4, and the urosome of both sexes are asymmetrical; (2) female leg 5 is totally reduced; and (3) the left endopod of male leg 5 is reduced.

According to Markhaseva et al. (2014), the family Diaixidae has hitherto accommodated 15 genera. *Pogonura* gen. nov. is differentiated from these diaixid genera by the following features (morphological data from Markhaseva et al. 2014): (1) the genital double-somite of the female has a symmetrical pair of long spiniform setae (only *Pogonura* gen. nov.), (2) the distal part of the left exopod on male leg 5 has a rugose plate (only *Pogonura* gen. nov.), (3) the ancestral segments XI–XII of the male antennule are fused (shared by *Pogonura* gen. nov., *Byrathis*, *Diaixis*, *Paraxantharus*, *Procenognatha* and *Xantharus*), (4) the setal formula of the antennary exopod is 1, 1-1-1, 1, 1-1, 1, 0, 3 (only *Pogonura* gen. nov.), (5) the mandibular gnathobase has long setules (*Pogonura* gen. nov., *Cenognatha*, *Neoscolecithrix*, *Paraxantharus* and *Procenognatha*), and (6) the maxillary endopod has 3 sclerotized setae (*Pogonura* gen. nov. and *Procenognatha*).

Etymology. The new generic name is derived from two Greek words *pogon*, meaning “beard”, and *oura*, meaning “tail”, to denote the paired setae like moustache on the genital double-somite of the female. Gender feminine.

Type species. *Pogonura rugosa* sp. nov. (original designation).

***Pogonura rugosa* gen. et sp. nov.**

<http://zoobank.org/6C0D4F63-BDD0-41A7-88D3-8D7D2EC9BB3C>

Figs 1–8

Material examined. Holotype. One ♀; whole body in vial (NSMT-Cr 27413). **Allotype.** One ♂, dissected and appendages mounted on glass slide, body in vial (NSMT-Cr 27414). **Paratype.** One ♀, dissected and appendages mounted on glass slide, body in vial (NSMT-Cr 27415). Body length. Adult female: 1.69 mm (holotype), 1.73 mm (paratype). Adult male: 1.71 mm (allotype).

Description of adult female. Body (Fig. 1A, B) weakly sclerotized; cephalosome incompletely fused to first pediger with future line dorsally and laterally visible; fourth and fifth pedigers completely fused; posterolateral corners of prosome extending posteriorly, rounded and covering one-third of genital double-somite. Rostrum (Fig. 1C) produced ventrally, with pair of frontal filaments distally. Urosome (Fig. 1D, E) 4-segmented; genital double-somite symmetrical with pair of seminal copulatory pores and seminal receptacles (Figs 1D, E, 8); seminal copulatory pores ovaliform; seminal receptacles narrow near the seminal copulatory pores and becoming semicircular in the inner part; genital operculum semicircular, ventrally located midway; two spiniform

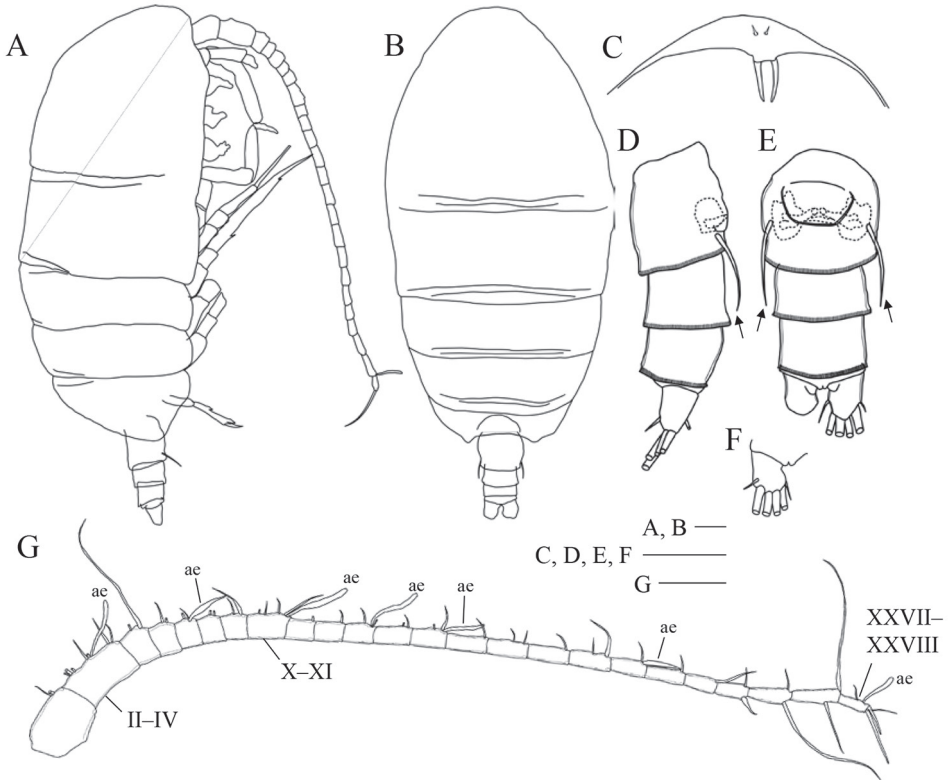


Figure 1. *Pogonura rugosa* gen. et sp. nov., adult female, paratype **A** lateral habitus **B** dorsal habitus **C** rostrum **D** urosome, lateral view **E** urosome, ventral view **F** caudal rami, dorsal view **G** right antennule; ae, aesthetascs. Arrows on **D** and **E** indicate twin spiniform setae on genital double-somite. Scale bars: 0.1 mm.

setae located ventrolaterally, as long as genital double-somite (Figs 1D, E, 8, indicated by arrows). Caudal rami (Fig. 1D–F) symmetrical, about 1.2 times as long as wide; seta I reduced, short seta II dorsally, seta III–VI long, short seta VII ventrally.

Antennule (Fig. 1F) 24-segmented, exceeding posterior border of third pediger; ancestral segments II–IV, X–XI and XXVII–XXVIII fused; armature as follows: I–2, II–3 (2+1ae?), III–2+1ae, IV–2, V–2, VI–2, VII–2+1ae, VIII–2, IX–2, X–2, XI–2+1ae, XII–1, XIII–1, XIV–2+1ae, XV–2, XVI–2+1ae, XVII–1, XVIII–2, XIX–1, XX–2, XXI–1+1ae, XXII–1, XXIII–1, XXIV–1+1, XXV–1+1, XXVI–1+1, XXVII–2, and XXVIII–2+1ae.

Antenna (Fig. 2A, B) with 1 seta and row of long setules on coxa; basis with 2 setae at inner distal corner; exopod 7-segmented; ancestral segments II–IV fused and VI–VII incompletely fused without suture line, setal formula of 1, 1-1-1, 1, 1-1, 1, 0, 3; fused segments II–IV having row of fine setules along outer distal margin; endopod 2-segmented, proximal segment with 2 setae, distal segment bilobed, bearing 8 setae on inner lobe and 6 setae and short setules on outer lobe.

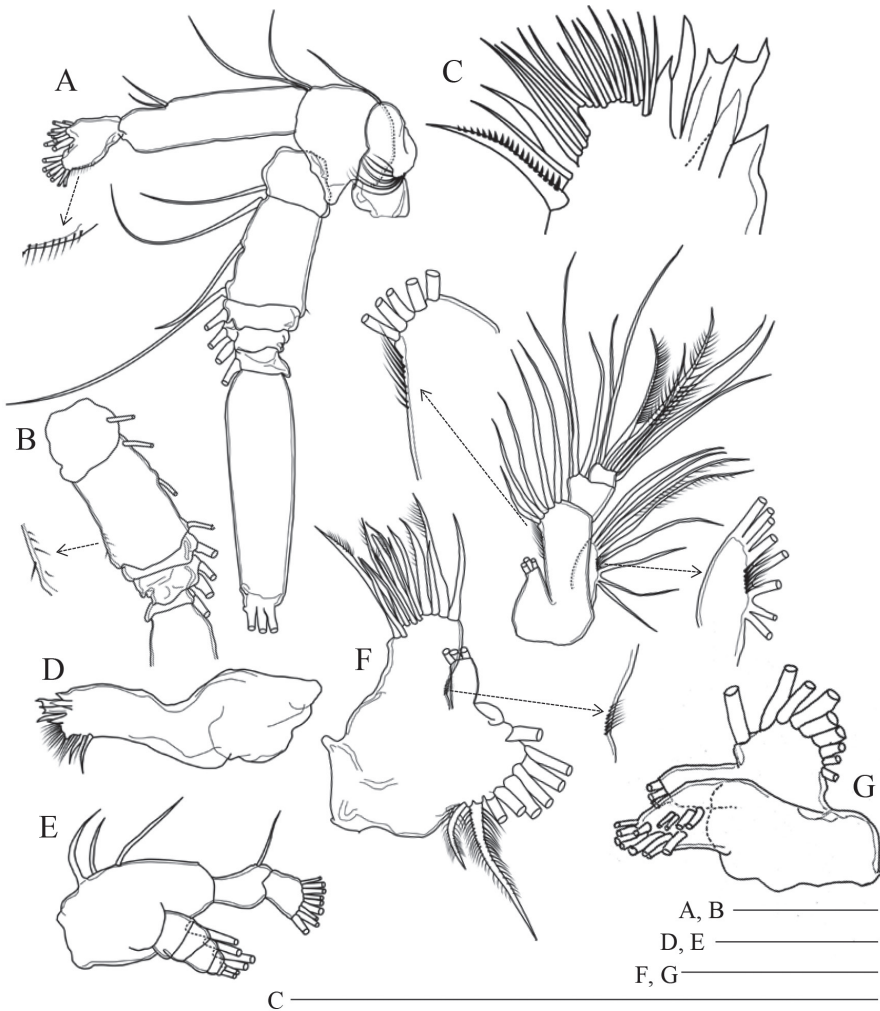


Figure 2. *Pogonura rugosa* gen. et sp. nov., adult female, paratype **A** right antenna **B** exopod of right antenna, other side **C** gnathobase on right mandible **D, E** right mandible **F, G** praecoxa and coxa of left maxillule **H** basis, endopod, and exopod of left maxillule. Scale bars: 0.1 mm.

Mandible (Fig. 2C–E) having gnathobase with triangular ventralmost tooth, 5 chitinized teeth, 16 long setules and dorsal seta; palp with basis having 3 inner setae; endopod 2-segmented; proximal endopodal segment bearing 1 seta, distal segment with 9 setae; exopod 5-segmented, with setal formula of 1, 1, 1, 1, 2.

Maxillule (Fig. 2F–H) with 9 terminal and 4 posterior setae on praecoxal arthrite; coxal endite with 3 setae; coxal epipodite with 9 setae; proximal and distal basal endites having 3 and 5 setae, respectively; proximal and distal segments of endopod with 3 and 8 setae, respectively; exopod with 8 setae; rows of setules on arthrite, basis and exopod.

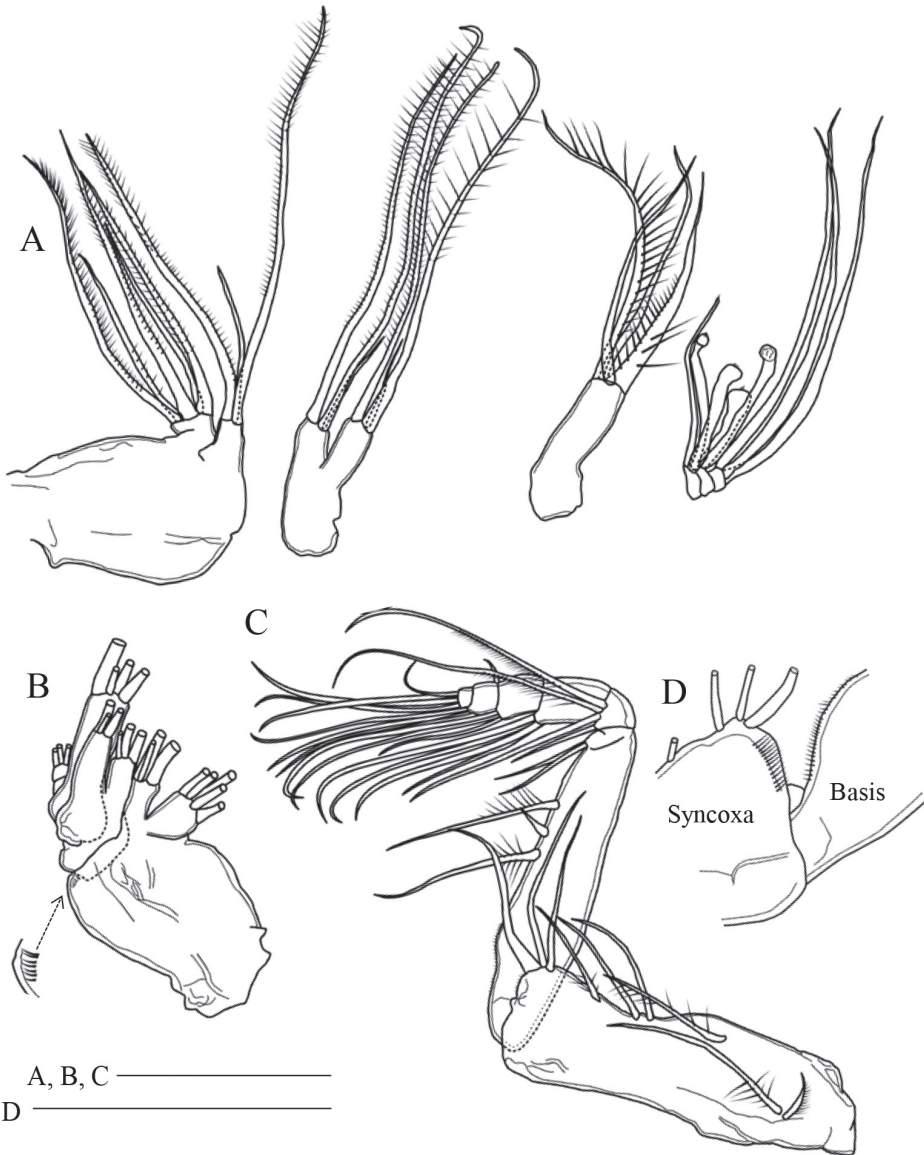


Figure 3. *Pogonura rugosa* gen. et sp. nov., adult female, paratype **A** right maxilla **B** right maxilla, other side **C** right maxilliped **D** rows of setulae on right maxilliped. Scale bars: 0.1 mm.

Maxilla (Fig. 3A, B) with 2 praecoxal and 2 coxal endites having 5, 3, 3, and 3 setae, respectively; basis with 1 well-chitinized and 3 slender setae; endopod 3-segmented, with 3 sclerotized and 5 brush-like setae of various length, proximal segment with 3 brush-like setae (1 slender, 1 short and stout, 1 moderate), middle segment with 2 brush-like setae (1 short and stout, 1 moderate), distal segment with 3 sclerotized setae.

Maxilliped (Fig. 3C, D) with syncoxal endites having 1, 2, 3 and 3 setae; row of fine setules at syncoxal distal corner and along basal inner margin; basis with 3 setae midway; first endopodal segment almost incorporated into basis; first to sixth endopodal segments with 2, 4, 4, 3, 3+1, and 4 setae, respectively.

Seta and spine formulae of legs 1–4 are shown in Table 1. Leg 1 (Fig. 4A) with medial long setules on coxa and basis; von Vaupel Klein organ (Vaupel Klein 1972) distinct on anterior surface of endopod; distal seta of basis twice as long as endopod;

Table 1. Setal formula of legs 1–4 of *Pogonura rugosa* gen. et sp. nov. Roman numeral: spine, Arabic numeral: seta.

	Coxa	Basis	Exopod			Endopod		
			1	2	3	1	2	3
Leg 1	0-0	0-1	I-0;	I-1;	I, 1, 3	0, 2, 3		
Leg 2	0-1	0-0	I-1;	I-1;	III, I, 4	0-1;	1, 2, 2	
Leg 3	0-1	0-0	I-1;	I-1;	III, I, 4	0-1;	0-1;	1, 2, 2
Leg 4	0-1	0-0	I-1;	I-1;	III, I, 4	0-1;	0-1;	1, 2, 2

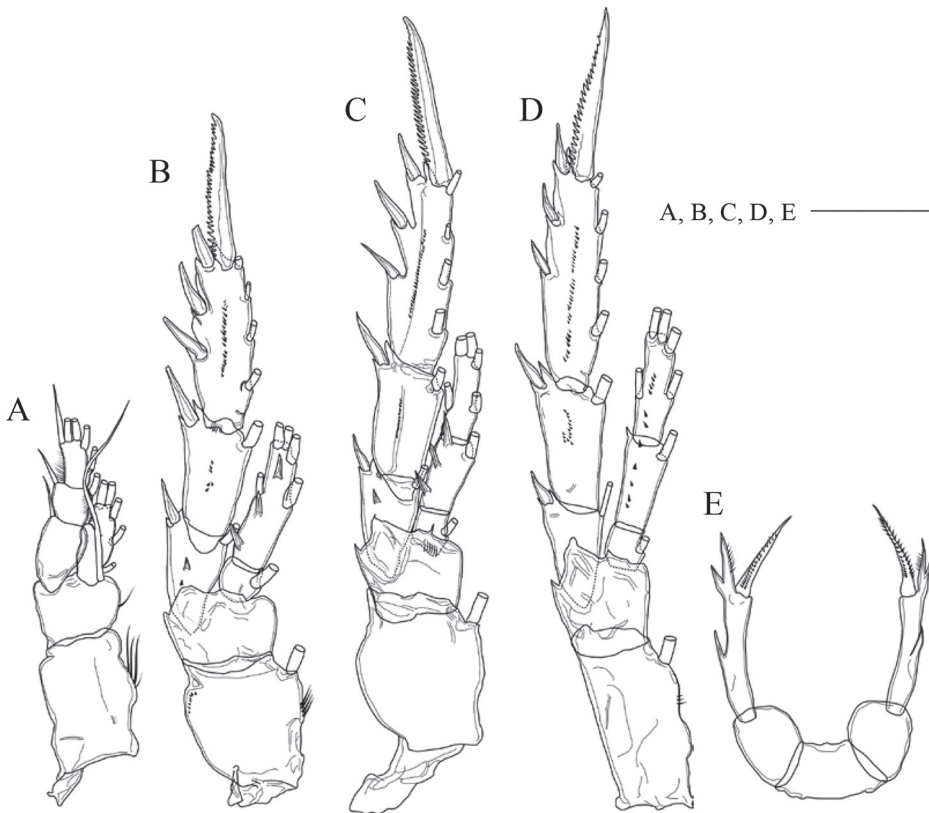


Figure 4. *Pogonura rugosa* gen. et sp. nov., adult female, paratype **A** leg 1, anterior side **B** leg 2, posterior side **C** leg 3, posterior side **D** leg 4, posterior side **E** leg 5. Scale bar: 0.1 mm.

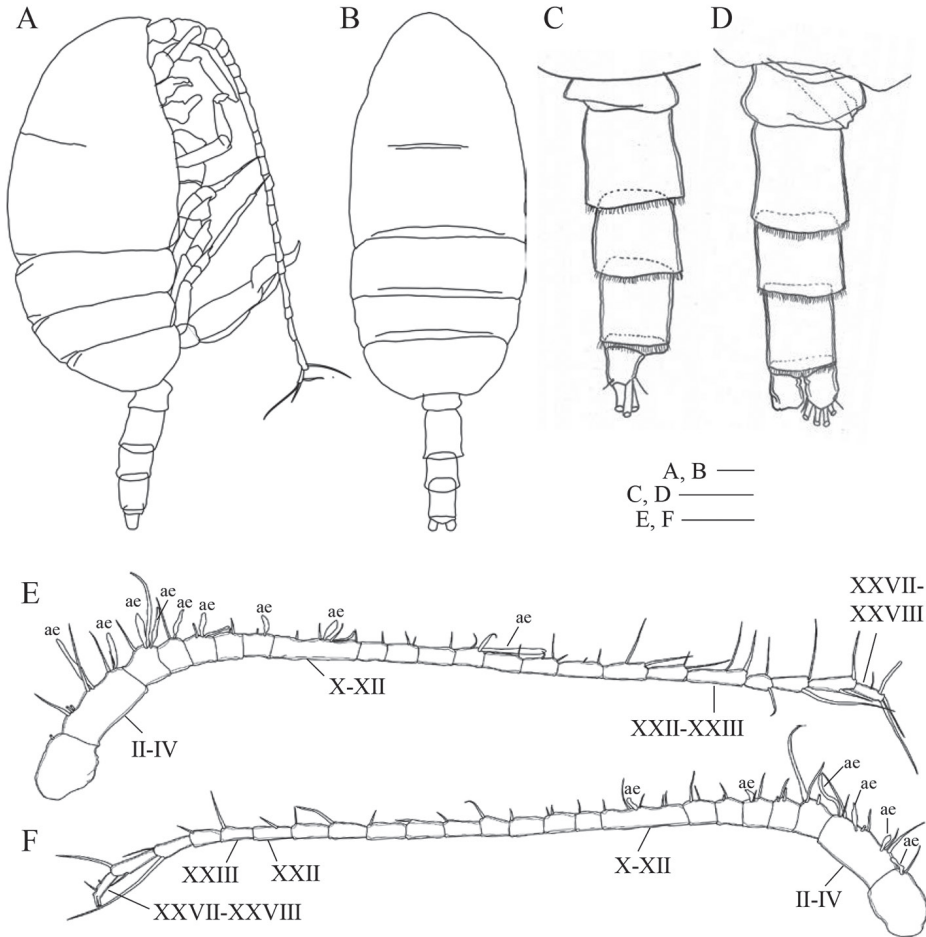


Figure 5. *Pogonura rugosa* gen. et sp. nov., adult male, allotype **A** lateral habitus **B** dorsal habitus **C** urosome, lateral view, left side **D** urosome, ventral view **E** right antennule **F** left antennule; ae, aesthetascs. Scale bars: 0.1 mm.

distal segment of exopod with outer row of setules. Leg 2 (Fig. 4B) with coxa having row of fine setules midway and row of fine spinules at distal outer corner; first exopodal segment with 1 large and 1 minute prominence on posterior surface; distal endopodal segment having 3 large prominences on posterior surface. Leg 3 (Fig. 4C) with basis having row of minute setules at base of endopod on posterior surface; second endopodal segment having 3 large prominences on posterior surface. Leg 4 (Fig. 4D) with first and second segments of both rami having small prominences on posterior surface.

Leg 5 (Fig. 4E) uniramous; coxae and intercoxal sclerite fused to form common base; basis broad, about 1.3 times as long as wide; exopod 1-segmented, ca. 4.4 times as long as wide, with 3 lateral processes and 1 terminal bipinnate spine.

Description of adult male. Body (Fig. 5A, B) weakly sclerotized like the female; fusion between cephalosome and first pediger and between fourth and fifth pedigers

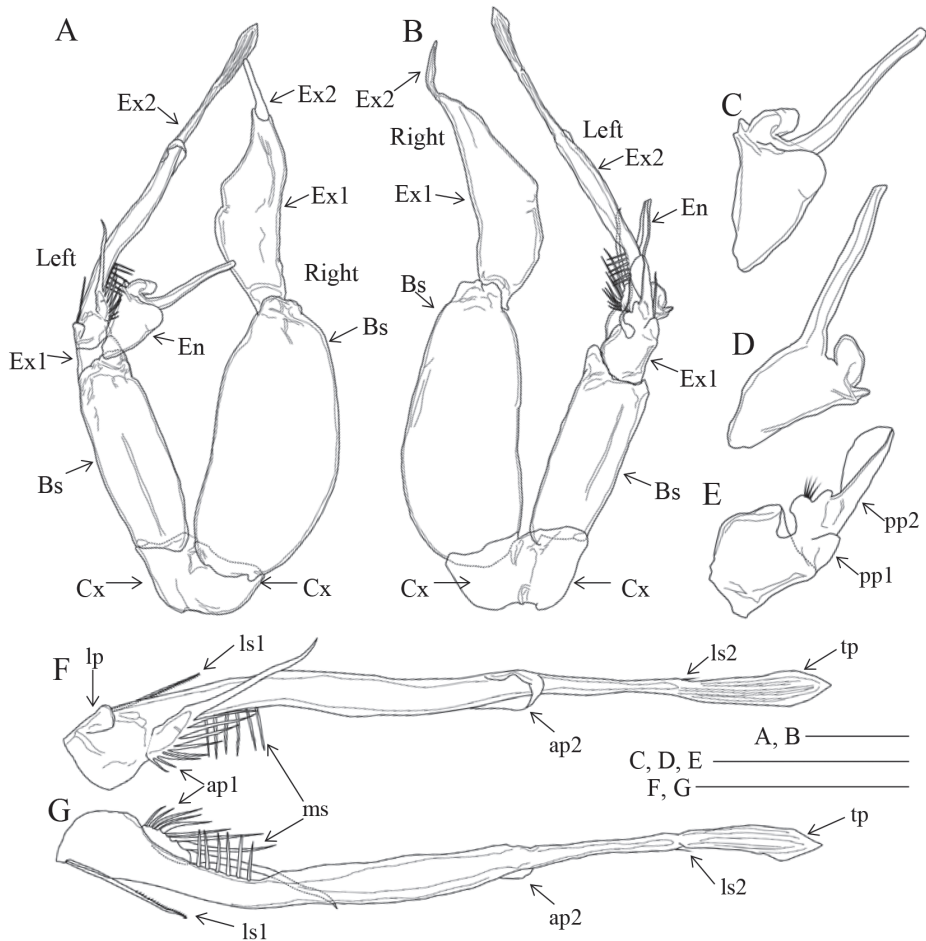


Figure 6. *Pogonura rugosa* gen. et sp. nov., leg 5 of adult male, allotype **A** anterior side **B** posterior side **C** left endopod, anterior side **D** left endopod, posterior side **E** proximal segment of left exopod, posterior side **F** distal segment of left exopod, anterior side **G** distal segment of left exopod, posterior side. Bs: basis, En: endopod, Ex1: proximal segment of exopod, Ex2: distal segment of exopod, pp1: proximal posterior plate, pp2: distal posterior plate, lp: lateral plate, ls1: proximal lateral spinule, ls2: distal lateral spinule, ap1: proximal anterior plate, ap2: distal anterior plate, ms: medial spinules, tp: terminal plate. Scale bars: 0.1 mm.

similar to those of female; posterolateral corners of prosome rounded, not extending posteriorly. Rostrum similar to that of female. Urosome (Fig. 5C, D) 5-segmented; gonopore located on the left side; small plate covering around gonopore; caudal rami similar to those of female.

Antennule asymmetrical in fusion patterns. Right antennule (Fig. 5E) 22-segmented; ancestral segments II–IV, X–XII, XXII–XXIII and XXVII–XXVIII fused; armature elements as follows: I–1, II–3 (2+1ae?), III–1+1ae, IV–2+1ae, V–2+2ae, VI–1+ae, VII–

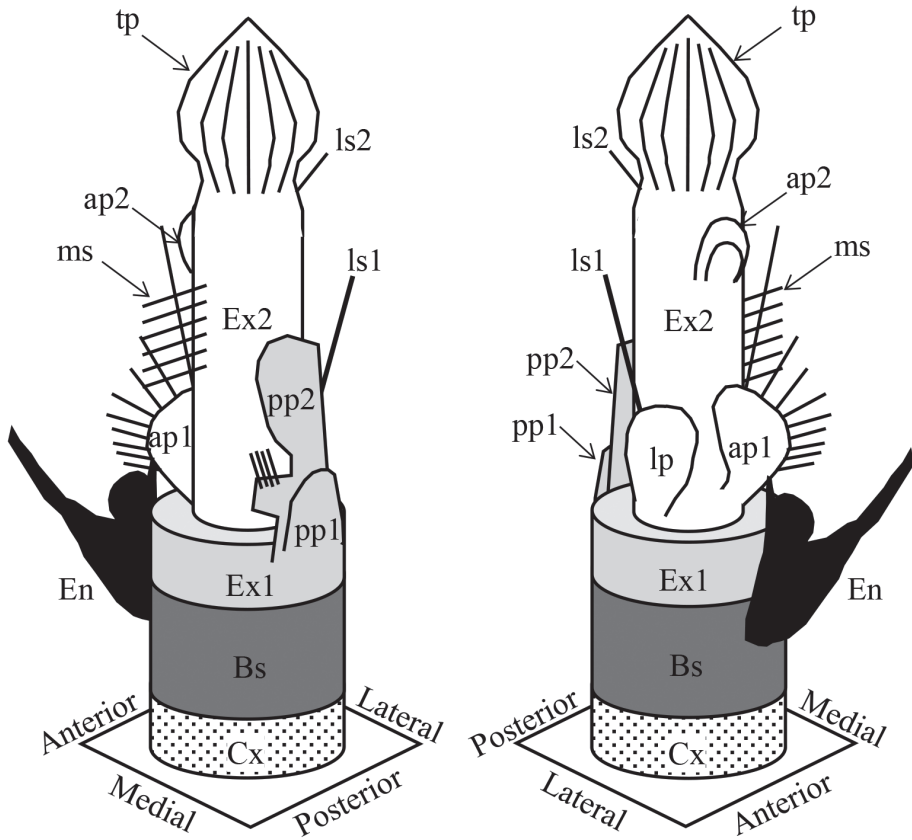


Figure 7. Schematic diagram of armatures on left leg 5 of male *Pogonura rugosa* gen. et sp. nov. Cx: coxa (with dots), Bs: basis (dark gray), En: endopod (black), Ex1: proximal segment of exopod (light gray), Ex2: distal segment of exopod (white), pp1: proximal posterior plate, pp2: distal posterior plate, lp: lateral plate, ls1: proximal lateral spinule, ls2: distal lateral spinule, ap1: proximal anterior plate, ap2: distal anterior plate, ms: medial spinules, tp: terminal plate.

2+1ae, VIII-2, IX-1+1ae, X-1, XI-2+1ae, XII-2, XIII-1, XIV-2, XV-1, XVI-2+1ae, XVII-1, XVIII-3, XIX-2, XX-2, XXI-2, XXII-1, XXIII-1, XXIV-1+1, XXV-1+1, XXVI-1+1, and XXVII-1, and XXVIII-2+1ae. Left antennule (Fig. 5F): 23-segmented; ancestral segments II-IV, X-XII and XXVII-XXVIII fused; armature elements as follows: I-1+1ae, II-2+1ae, III-2+ae, IV-2+1ae, V-3, VI-3, VII-2+1ae, VIII-2, IX-2, X-2, XI-2+1ae, XII-1, XIII-1, XIV-2, XV-1, XVI-1, XVII-1, XVIII-1, XIX-1, XX-1, XXI-1, XXII-1, XXIII-1, XXIV-1, XXV-1+1, XXVI-1+1, XXVII-2, and XXVIII-2.

Other appendages similar to those of the female, except leg 5.

Right leg 5 (Fig. 6A, B) uniramous; endopod absent; coxa small; basis robust, 2.2 times as long as wide; exopod 2-segmented, proximal segment plate-like, distal segment spiniform. Left leg 5 (Figs 6A-G, 7) biramous; coxa small; basis smaller than

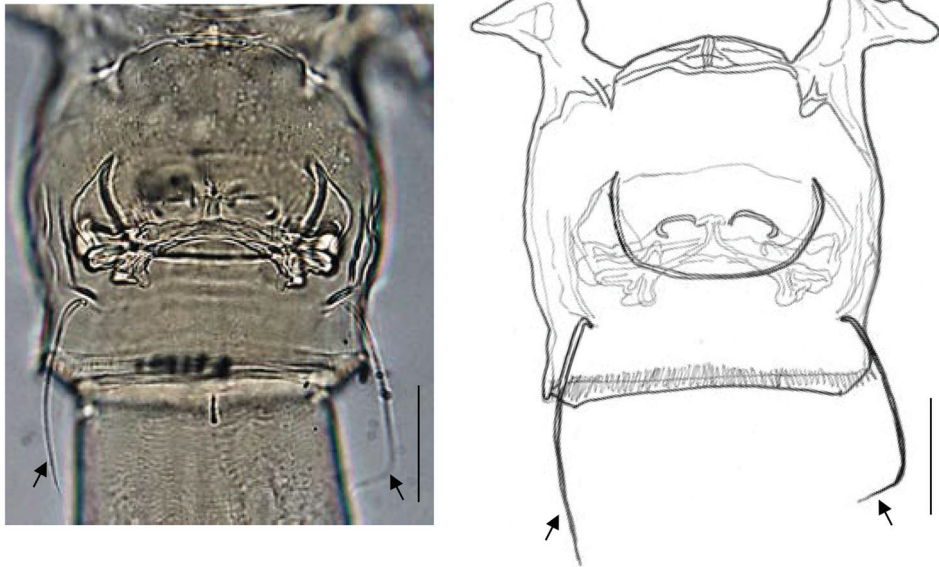


Figure 8. Ventral views of genital double-somite of female *Pogonura rugosa* gen. et sp. nov., paratype. Arrows indicate twin spiniform setae. Scale bar: 50 μ m.

right basis and slender, 2.5 times as long as wide; endopod 1-segmented, plate-like, and having baculiform plate and semicircular plate; exopod 2-segmented and highly complex in structure; proximal segment of exopod having proximal plate without armament (“pp1” in Figs 6, 7) and distal plate, larger, semicircular plate with 4 setules (“pp2” in Figs 6, 7); distal segment of exopod elongate, 9.0 times as long as proximal segment; proximal part of distal segment having 6 medial spinules (“ms” in Figs 6, 7), lateral spinule (“ls1” in Figs 6, 7) and anterior plate with 9 spinules (“ap1” in Figs 6, 7), midpoint of segment having thin, curved plate (“ap2” in Figs 6, 7) anteriorly, and distal part having spinule (“ls2” in Figs 6, 7) and thin plate with crest (“tp” in Figs 6, 7).

Remarks. *Pogonura rugosa* gen. et sp. nov. has a symmetrical pair of spiniform setae on the genital double-somite of the female (Figs 1E, 8). *Diaixis centrura* Connell, 1981, *D. gambiensis* Andronov, 1979, and *D. trunovi* Andronov, 1979 also have armatures on the counterparts [figs 39 and 94 in Andronov (1979); fig. 4 in Connell (1981)]; however, those of *Diaixis* are asymmetrical and consist of fine spinules.

Etymology. The specific name of the new species is derived from a Latin word *rugosa*, meaning “rugose”, to denote leg 5 of the adult male with many foliaceous armatures.

Discussion

The females of *Pogonura rugosa* gen. et sp. nov. have a ventrolateral pair of spiniform setae on their genital double-somite (Figs 1, 8). These armatures are similar to leg 6 possessed by females of podoplean copepods in the position (symmetrical armatures

on the ventrolateral of the genital double-somite) (cf. Huys and Boxshall 1991). However, these spiniform setae do not seem to be a homologue of leg 6. Generally, leg 6 comprises a symmetrical pair of basal processes with a few elements at the tip (at most 3 setae or spines on each process) and is connected to the inner muscles at the base (Boxshall 1982; Huys and Boxshall 1991). However, the spiniform setae of *P. rugosa* gen. et sp. nov. lack basal processes and are not connected with inner muscles like the podoplean's leg 6. Some groups of calanoids generally have the genital operculum on their genital double-somite of adult females, which is considered a homologue of leg 6 (Bradford-Grieve et al. 2010).

Pogonura gen. nov. has 3 setae on the terminal exopodal segment of the maxilla, although almost all copepods have at most 2 setae on this segment (Ferrari and Ivanenko 2008). In the Clausocalanoidea, however, some genera of the family Aetideidae have 3 setae on their counterparts (cf. *Pseudeuchaeta vulgaris* Markhaseva, Mohrbeck & Renz, 2017; *Paracomantenna profunda* Markhaseva & Renz, 2019). This retention in setae can be considered as an ancestral state in the clausocalanoideans.

Markhaseva and Ferrari (2005) and Laakmann et al. (2019) attempted to morphologically classify the Bradfordian genera into three main groups by considering the setations of the maxillary endopods, the antennary exopods and the maxillipedal praecoxal endites [=syncoxal endites sensu Huys and Boxshall (1991)], viz., Group A (Diaixidae and Tharybidae), Group B (Phaennidae and Parkiidae), and Group C (Scolecitrichidae). Laakmann et al. (2019) simultaneously conducted a molecular phylogenetic analysis of the Bradfordian genera but failed to assign different families or genera into any robust group except for *Procenognatha* and *Tharybis*. *Pogonura* gen. nov. shares some plesiomorphies with Group A sensu Markhaseva and Ferrari (2005) in the setation of the maxillipedal syncoxa. In addition, members of Group A have the following other plesiomorphies: all setae on the ancestral segments I–IV of the antennary exopod are retained and no specialized chemosensory seta is observed on the maxillipedal syncoxa. As mentioned in Remarks, *Pogonura* gen. nov. shares the following synapomorphies with some diaxid genera: with *Procenognatha*, posterior spinules are present on legs 2 and 3 (Markhaseva and Schulz 2010) and with *Anawekia* and *Diaixis*, a row of spinules is found on the left exopod of male leg 5 (Andronov 1979; Connell 1981; Othman and Greenwood 1994). These synapomorphies of *Pogonura* gen. nov. imply their close relationships with these diaixids. According to Laakmann et al.'s (2019) molecular analysis, *Procenognatha* comprises a robust clade with *Tharybis* (Tharybidae). In the present study, an assignment of *Pogonura* gen. nov. to any Bradfordian family should be pending until the taxonomy of this family group is clearly settled.

Acknowledgements

We would like to express our sincere thanks to the captain and crew of TRV TOY-OSHIO-MARU for their help in field samplings. We are also grateful to two reviewers, Dr. F.D. Ferrari and Dr. E.L. Markhaseva, for their careful and constructive comments.

Parts of this study were supported by a Sasakawa Scientific Research Grant 2019-4074 from the Japan Science Society (awarded to SK) and a grant-in-aid from the Japan Society of the Promotion of Science (KAKEN no, 19H03032, awarded to SO).

References

- Andronov VN (1979) Diaixidae (Copepoda, Calanoida) of the western coast of Africa (Russian with English summary). *Byulleten' Moskovskogo Obshchestva Ispytatelei Prirody, Otdel Biologicheskii* 84: 90–102.
- Boxshall GA (1982) On the anatomy of the misophrioid copepods, with special reference to *Benthomisophria palliata* Sars. *Philosophical Transactions of the Royal Society of London* 297: 125–181. <https://doi.org/10.1098/rstb.1982.0036>
- Bradford J (1973) Revision of family and some generic definitions in the Phaennidae and Scolecithricidae (Copepoda: Calanoida). *New Zealand Journal of Marine and Freshwater Research* 7: 133–152. <https://doi.org/10.1080/00288330.1973.9515460>
- Bradford-Grieve JM (2004) Deep-sea benthopelagic calanoid copepods and their colonization of the near-bottom environment. *Zoological Studies* 43: 276–291.
- Bradford-Grieve JM, Boxshall GA, Ahyong ST, Ohtsuka S (2010) Cladistic analysis of the calanoid Copepoda. *Invertebrate Systematics* 24: 291–321. <https://doi.org/10.1071/IS10007>
- Connell AD (1981) The taxonomy and distribution of some calanoid copepods in South African east coast estuaries. *Annals of the Natal Museum* 24: 489–500.
- Ferrari FD, Steinberg DK (1993) *Scopalatum vorax* (Esterly, 1991) and *Scolecithricella lobophora* Park, 1970, calanoid copepods (Scolecithricidae) associated with a pelagic tunicate in Monterey Bay. *Proceedings of the Biological Society of Washington* 106: 467–489.
- Ferrari FD, Markhaseva EL (1996) *Parkius karenwishnerae*, a new genus and species of calanoid copepod (Parkiidae, new family) from benthopelagic waters of the eastern tropical Pacific Ocean. *Proceedings of the Biological Society of Washington* 109: 264–285.
- Ferrari FD, Ivanenko VN (2008) The identity of protopodal segments and the ramus of maxilla 2 of copepods (Copepoda). *Crustaceana* 81: 823–835. <https://doi.org/10.1163/156854008784771702>
- Huys R, Boxshall GA (1991) Copepod evolution. The Ray Society, London, 468 pp.
- Laakmann S, Markhaseva EL, Renz J (2019) Do molecular phylogenies unravel the relationships among the evolutionary young “Bradfordian” families (Copepoda; Calanoida)? *Molecular Phylogenetics and Evolution* 130: 330–345. <https://doi.org/10.1016/j.ympev.2018.10.028>
- Markhaseva EL, Ferrari FD (2005) New benthopelagic bradfordian calanoids (Crustacea: Copepoda) from the Pacific Ocean with comments on generic relationships. *Invertebrate Zoology* 2: 111–168. <https://doi.org/10.15298/invertzool.02.2.01>
- Markhaseva EL, Schulz K, Arbizu PM (2008) New family and genus *Rostrocalanus* gen. nov. (Crustacea: Calanoida: Rostrocalanidae fam. nov.) from deep Atlantic waters. *Journal of Natural History* 42: 2417–2441. <https://doi.org/10.1080/00222930802254771>

- Markhaseva EL, Schulz K (2009) A new family and genus of calanoid copepods (Crustacea) from the abyss of the Atlantic Ocean. *Zootaxa* 2304: 21–40. <https://doi.org/10.11646/zootaxa.2304.1.2>
- Markhaseva EL, Schulz K (2010) New benthopelagic calanoids (Crustacea: Copepoda) from deep Atlantic waters. *Proceedings of the Zoological Institute RAS* 314: 3–23.
- Markhaseva EL, Laakmann S, Renz J (2014) An interim synopsis of the Bradfordian families with a description of *Thoxancalanus spinatus* (Copepoda: Calanoida), a new diaixid genus and species from the deep Atlantic Ocean. *Marine Biodiversity* 44: 63–88. <https://doi.org/10.1007/s12526-013-0185-0>
- Markhaseva EL, Mohrbeck I, Renz J (2017) Description of *Pseudeuchaeta vulgaris* n. sp. (Copepoda: Calanoida), a new aetideid species from the deep Pacific Ocean with notes on the biogeography of benthopelagic aetideid calanoids. *Marine Biodiversity* 47: 289–297. <https://doi.org/10.1007/s12526-016-0527-9>
- Markhaseva EL, Renz J (2019) Two new calanoids (Copepoda: Aetideidae) from the abyss of the World Ocean. *Arthropoda Selecta* 28: 213–224. <https://doi.org/10.15298/arthsel.28.2.04>
- Nishida S, Ohtsuka S (1997) Ultrastructure of the mouthpart sensory setae in mesopelagic copepods of the family Scolecitrichidae. *Plankton biology and ecology* 44: 81–90.
- Ohtsuka S, Huys R, Boxshall GA, Ito T (1992) *Misophriopsis okinawensis* sp. nov. (Crustacea: Copepoda) from hyperbenthic waters off Okinawa, South Japan, with definitions of related genera *Misophria* Boeck, 1864 and *Stygomisophria* gen. nov. *Zoological Science* 9: 859–859.
- Ohtsuka S, Nishida S, Nakaguchi K (2002) Three new species of the genus *Macandrewella* (Copepoda: Calanoida: Scolecitrichidae) from the Pacific Ocean, with notes on distribution and feeding habits. *Journal of Natural History* 36: 531–564. <https://doi.org/10.1080/00222930010015861>
- Ohtsuka S, Boxshall GA, Fosshagen A (2003) A New Species of *Neoscolecithrix* (Crustacea; Copepoda; Calanoida) from off Okinawa, Southwestern Japan, with Comments on the Generic Position in the Superfamily Clausocalanoidea. *Bulletin of the National Science Museum of Tokyo, Series A (Zoology)* 29: 53–63.
- Othman BHR, Greenwood JG (1994) A new genus with three new species of copepods from the family Diaixidae (Crustacea: Calanoida), and a redefinition of the family. *Journal of Natural History* 28: 987–1005. <https://doi.org/10.1080/00222939400770531>
- Vaupel-Klein JC von (1972) A new character with systematic value in *Euchirella* (Copepoda, Calanoida). *Zoologische Mededelingen* 47: 497–512.

Ash-free dry mass values for northcentral USA caddisflies (Insecta, Trichoptera)

David C. Houghton¹, Ryan Lardner¹

¹ Department of Biology, Hillsdale College, 33 East College Street, Hillsdale, MI 49242, USA

Corresponding author: David C. Houghton (david.houghton@hillsdale.edu)

Academic editor: R. Holzenthal | Received 1 January 2020 | Accepted 20 April 2020 | Published 22 July 2020

<http://zoobank.org/8BEB5FC3-09E6-4A4D-A1C1-7047C885A2F8>

Citation: Houghton DC, Lardner R (2020) Ash-free dry mass values for northcentral USA caddisflies (Insecta, Trichoptera). ZooKeys 951: 37–46. <https://doi.org/10.3897/zookeys.951.49790>

Abstract

Ash-free dry mass (AFDM) values are presented for the adult stage of 63 caddisfly species commonly found throughout the northcentral US. Weights ranged from 0.01 mg for the smallest species to 7.22 mg for the largest. These values represent the first published data on the AFDM of the adult stage of Trichoptera, and can be used in other studies for more precise assessments of stream conditions without destruction of specimens. This increased precision is demonstrated herein by re-analyzing a previously published data set.

Keywords

ash-free dry mass, biomass, caddisfly, Great Lakes, organic, Trichoptera

Introduction

The organic biomass of organisms is one of the most important quantifiable variables in ecological studies. Measurements of biomass are informative about ecosystem production, metabolism, food web ecology, and the overall health and biotic integrity of the community (Enquist and Niklas 2001; Gruner et al. 2008; Eklöf et al. 2017). For aquatic ecosystems, biomass measurements are also indicative of the relative contribution of different functional feeding groups (FFGs), which can be used to assess ecosystem continuity, types and availability of organic carbon, and anthropogenic disturbance (Vannote et al. 1980; Barbour et al. 1999).

There are several measurements used to express the biomass of organisms, including wet mass, dry mass, and ash-free dry mass (AFDM). To determine AFDM, specimens are incinerated at temperatures high enough to volatilize organic tissue but not inorganic tissue. The difference between pre-incineration and post-incineration weights reflects the mass of the organic tissue volatilized. AFDM is considered the most accurate measurement of biomass since it encompasses the biologically active tissue (Eklöf et al. 2017).

Various parameters of immature aquatic insect assemblages, including their AFDM, have been used for many years to assess the functioning and biotic integrity of aquatic ecosystems. Some challenges to using the immature stage, such as the difficulty of sampling all aquatic microhabitats representatively and identifying specimens to the species level, can be alleviated by using the winged adult stage, particularly that of taxonomically and ecologically diverse groups such as the caddisflies (Trichoptera) (Gerth and Herily 2006; Chessman et al. 2007; Cao and Hawkins 2011; Houghton et al. 2011). Assemblages of caddisfly adults, particularly the relative abundance of specimens within different FFGs, have been shown in several studies to be indicative of stream conditions (Dohet 2002; Houghton 2007; Blinn and Ruiter 2013; Houghton et al. 2018). Such studies, however, treated all specimens equally and did not reflect the differences in biomass between different species. Since the largest caddisfly species are >100× heavier than the smallest species, not accounting for this difference results in a loss of precision. Because measurements of FFG biomass directly relate to the biomass of available carbon sources and, thus, habitat differences, increasing precision in these FFG biomass measurements is of substantial importance.

Due to the necessity of maintaining museum collections of the taxonomically important caddisfly adults, most researchers are understandably reluctant to destroy them in order to obtain AFDM values. Indeed, while many studies have published data on caddisfly larvae (Johnston and Cunjak 1999), we have been unable to find a single one measuring the AFDM of the adult stage, although several have reported dry mass (Svensson 1975; Peterson 1989; Wagner 2002; Wagner 2005; Jannot et al. 2007) or wet mass (Wallace and Howard 1992). The purpose of this study, therefore, was to determine and publish AFDM values of common and abundant caddisfly species in our collection for future ecological studies using adult caddisflies.

Materials and methods

We have been collecting caddisfly adults in the northcentral US since 2000, mostly utilizing an 8-watt ultraviolet light placed over a white pan filled with 80% EtOH. Such devices can capture 1000s of specimens during a single evening of heavy flight activity. Collected specimens are preserved in 80% EtOH for long-term storage, which limits decomposition and loss of organic biomass over time (Wetzel et al. 2005).

Species were chosen for biomass determination largely due to practical considerations. The weight of single specimens of most species is lower than the detection limit of most standard balances. Thus, specimens needed to be weighed in groups of

5 to 500 depending on the size of the species. This limitation meant that we could only determine biomass for abundant species for which we had ample extra specimens. Likewise, the specimen collecting localities that we chose were simply the ones with the most available specimens. Most of these specimens were from Michigan, with some from Indiana, Minnesota, and Wisconsin (Figure 1). Each determined species was from a single collection of a single locality. We generally determined only male specimens, except for some species (e.g., *Psychomyia flavida* Hagen) where females were highly abundant and males were rare. All females were carefully dissected before weighing to confirm they had already oviposited. In no case were both sexes weighed.

To determine organic biomass, specimens of each tested species were taken from their vials of EtOH and placed into pre-dried porcelain crucibles. Crucibles containing the specimens were dried at low heat over a hot plate for several h until all of the EtOH had evaporated and the specimens appeared completely dry. The crucibles and specimens were then further dried for 2 h at 60 °C in a drying oven and then slowly cooled to room temperature before weighing. Crucibles and specimens were then transferred to a muffle furnace and incinerated at 500 °C for 3 h. After cooling to room temperature in the muffle furnace, the resulting material was transferred back to the drying oven, dried for 1 h at 60 °C, cooled to back room temperature, and weighed. AFDM was calculated as the final mass of material remaining after incineration subtracted from the mass of specimens before entering the muffle furnace. Total AFDM per sample divided by the number of specimens in that sample calculated the mean AFDM per specimen. This procedure was repeated 2–5× for each species, depending on how many specimens were available for incineration. Global mean AFDM ± SE for each species was then determined from these data.

Results

Resultant AFDM values are in Table 1. We determined the organic biomass of 63 common caddisfly adults. This total represented 17% (63 of 366) of the known caddisfly species of Indiana, Michigan, Minnesota, and Wisconsin, 58% (47 of 81) of known genera, and all 20 known families. Determined species represented 78% (448589 of 574928) of all caddisfly specimens from the four states in our collection. AFDM values ranged from 7.217 mg for *Prilostomis semifasciata* (Say) (Phryganeidae) to 0.011 mg for *Orthotrichia aegerfasciella* (Chambers) (Hydroptilidae). Mean familial weight was highest in the Phryganeidae, followed by the Limnephilidae and the Rhyacophilidae. Glososomatidae, Psychomyiidae, and Hydroptilidae were the lightest families (Figure 2).

Discussion

The lack of previous research on the AFDM weights of adult caddisflies renders direct comparisons to other results impossible. Even indirect comparisons are difficult.

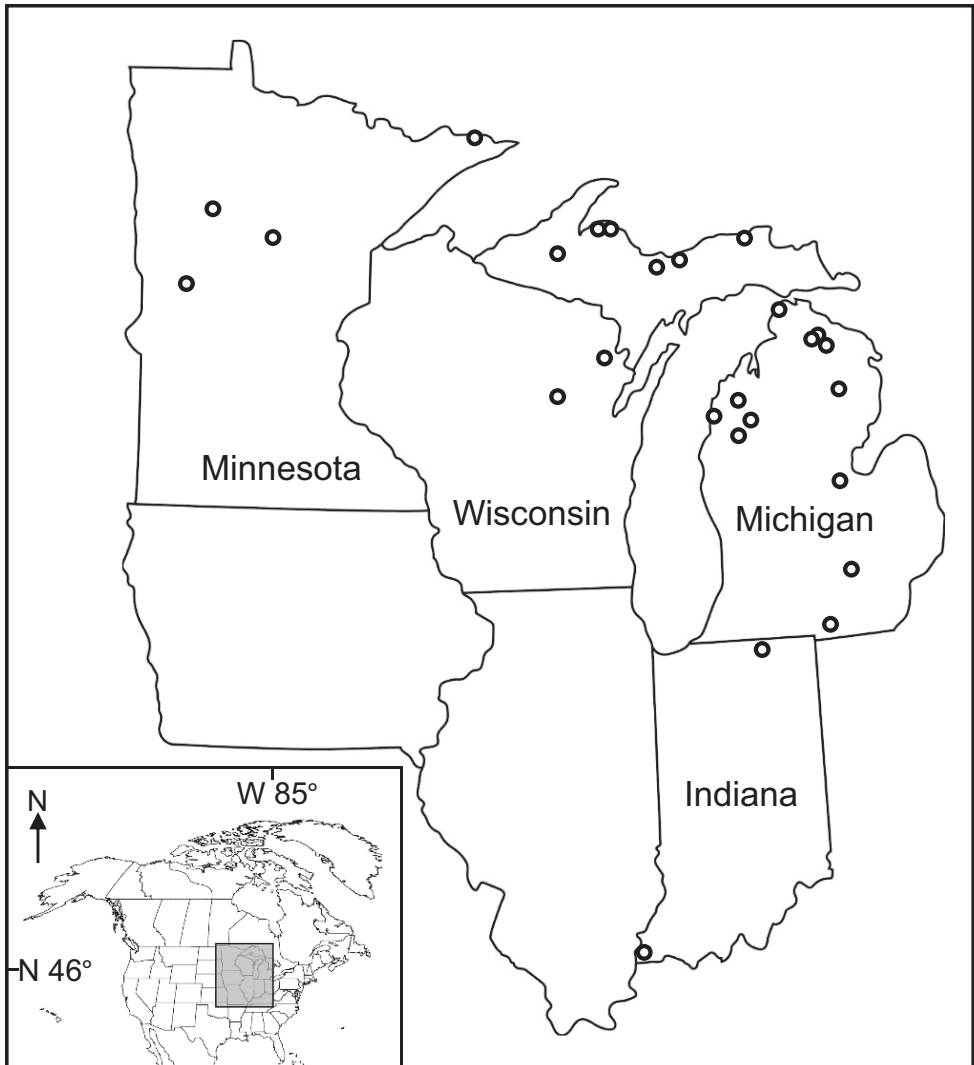


Figure 1. The northcentral US, showing localities from where our AFDM-determined specimens were collected.

Of the caddisflies previously weighed via dry mass calculation, none are of the same species that we weighed. Four species: *Agrypnia deflata* (Milne) (Jannot et al. 2007), *Apatania fimbriata* (Pictet) (Wagner 2005), *Mystacides azureus* (L) (Peterson 1989), and *Rhyacophila fasciata* Hagen (Wagner 2005), are within a genus that includes a species that we tested. The four species were 1.3–3.3× heavier than their congeners in our study. Some of that difference is attributable to the different method—dry mass will always be heavier than AFDM because it also includes inorganic matter. Some difference may be due to inherent size difference between congeneric species. Subtle differences in experimental procedure or storage medium may also have led to differences in

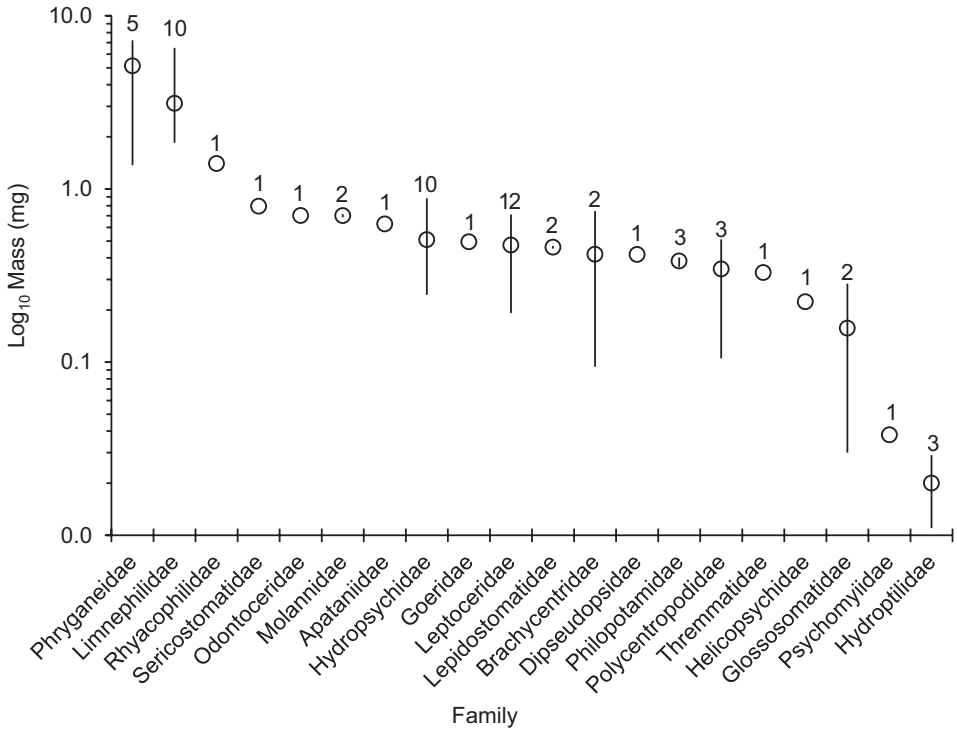


Figure 2. The Log₁₀ high, low, and mean biomass values for each of the 20 different caddisfly families measured. Number of species measured within each family above each bar.

measured weight. Such differences have frequently been noted in studies of immature aquatic insects (Johnston and Cunjak 1999).

Some weight differences between our specimens and those of other studies may also be due to actual variation between specimens. Several studies have reported 2–5× differences in dry mass between conspecific specimens in the same study due to differences in environmental conditions, larval food quality, or emergence timing (Svensson 1975; Wagner 2002; Wagner 2005). We did not address these topics in our study, instead choosing our specimens based on practical considerations only. Further, our procedure included weighing only one sex per species, weighing specimens of a single collection for each species, and weighing specimens in groups and then calculating standard error based on global means of tested groups. All of these aspects intentionally homogenized biomass variability between specimens. Also, the age of our specimens ranged <1–19 years (Table 1), so some unknown level of decomposition and biomass loss could have taken place in some of the specimens. Thus, our AFDM values should still be considered fairly coarse. Even so, the >500× difference in biomass between the largest and smallest species measured emphasized the increased precision in utilizing AFDM values in ecological calculations instead of simple specimen counting.

Table 1. The 63 species of caddisfly adults for which ash-free dry mass (AFDM) (\pm SE) was determined. Key: Year, year collected. #, number of specimens tested per incineration. *N*, the number of incinerations per species. M/F, whether male or female specimens were measured.

Taxon	Site	Year	#	<i>N</i>	M/F	AFDM (mg)	\pm SE
APATANIIDAE							
<i>Apatania zonella</i> (Zetterstedt, 1840)	MI: Lk. Superior, 46.9083, -87.9225	2019	50	3	M	0.628	0.149
BRACHYCENTRIDAE							
<i>Brachycentrus americanus</i> (Banks, 1899)	MI: Fairbanks Cr., 44.0481, -85.6586	2014	50	3	M	0.745	0.104
<i>Micrasema wataga</i> Ross, 1938	MN: Straight R., 46.8745, -95.0586	2000	300	3	F	0.094	0.026
DIPSEUDOPSIDAE							
<i>Phlyocentropus placidus</i> (Banks, 1905)	MI: Nunn's Cr., 46.0572, -84.5639	2010	35	3	M	0.418	0.064
GLOSSOSOMATIDAE							
<i>Glossosoma nigrilor</i> Banks, 1911	MI: Fairbanks Cr., 44.0481, -85.6586	2011	100	3	F	0.284	0.140
<i>Protoptila maculata</i> (Hagen, 1861)	MI: Manistee R., 44.2836, -85.8614	2010	500	3	F	0.030	0.008
GOERIDAE							
<i>Goera stylata</i> Ross, 1938	MI: Fairbanks Cr., 44.0481, -85.6586	2011	100	6	M	0.495	0.074
HELICOPSYCHIDAE							
<i>Helicopsyche borealis</i> (Hagen, 1861)	MI: Black R., 45.1664, -84.3264	2015	250	6	M	0.223	0.042
HYDROPSYCHIDAE							
<i>Cheumatopsyche campyla</i> Ross, 1938	MI: Tittabawase R., 43.4811, -84.0931	2011	150	6	M	0.346	0.062
<i>C. speciosa</i> (Banks, 1904)	MN: Pine R., 46.5717, -94.0281	2000	150	3	F	0.245	0.054
<i>Diplectrona modesta</i> Banks, 1908	MI: Fairbanks Cr., 44.0481, -85.6586	2014	50	3	M	0.502	0.071
<i>Hydropsyche betteni</i> Ross, 1938	MI: Fairbanks Cr., 44.0481, -85.6586	2014	75	6	M	0.685	0.123
<i>H. morosa</i> (Hagen, 1861)	MI: Au Sable R., 44.6599, -84.1292	2011	100	3	M	0.392	0.110
<i>H. simulans</i> Ross, 1938	MN: Chippewa R., 45.9408, -95.7383	2000	50	3	M	0.712	0.104
<i>H. sparna</i> Ross, 1938	MI: Mountain St., 46.8692, -87.8933	2019	100	3	M	0.452	0.099
<i>Macrostemum zebratum</i> (Hagen, 1861)	WI: Peshtigo R., 45.2325, -88.0136	2015	50	3	M	0.884	0.159
<i>Parapsyche apicalis</i> (Banks, 1908)	MI: Fairbanks Cr., 44.0481, -85.6586	2011	50	3	M	0.472	0.066
<i>Potamyia flava</i> (Hagen, 1861)	IN: Ohio R., 37.7783, -87.9468	2018	200	6	M	0.399	0.072
HYDROPTILIDAE							
<i>Agraylea multipunctata</i> Curtis, 1834	IN: Ohio R., 37.7783, -87.9468	2018	500	3	F	0.029	0.004
<i>Hydroptila xera</i> Ross, 1938	MI: Two-hearted R., 46.6419, -85.4792	2011	500	3	M	0.017	0.003
<i>Orthotrichia aegerfasciella</i> (Chambers, 1873)	MI: Manistee R., 44.2836, -85.8614	2010	500	4	M	0.011	0.003
LEPIDOSTOMATIDAE							
<i>Lepidostoma bryanti</i> (Banks, 1908)	MI: Fairbanks Cr., 44.0481, -85.6586	2011	50	6	M	0.452	0.115
<i>L. togatum</i> (Hagen, 1861)	MI: Black R., 45.1664, -84.3264	2015	50	6	M	0.469	0.108
LEPTOCERIDAE							
<i>Ceraclea arielles</i> (Denning, 1942)	MI: Pine R., 44.1339, -85.6956	2010	150	3	M	0.318	0.054
<i>C. resurgens</i> (Walker, 1852)	MI: Mountain St., 46.8692, -87.8933	2019	75	3	M	0.712	0.459
<i>C. tarsipunctata</i> (Vorhies, 1909)	MI: Manistee R., 44.2836, -85.8614	2010	100	6	M	0.681	0.409
<i>C. transversa</i> (Hagen, 1861)	MN: North Brule R., 48.0076, -90.4169	2001	100	3	M	0.695	0.140
<i>Leptocerus americanus</i> (Banks, 1899)	MI: Saint Joseph R., 41.8361, -84.4772	2015	100	6	M	0.235	0.035
<i>Mystacides interjecta</i> (Banks, 1914)	MI: Benton Lk., 43.6718, -85.8916	2011	100	3	M	0.321	0.055
<i>Nectopsyche candida</i> (Hagen, 1861)	MI: Manistee R., 44.2836, -85.8614	2010	100	3	M	0.594	0.107
<i>N. pavidata</i> (Hagen, 1861)	IN: Elkhart R., 41.5815, -85.8439	2018	100	3	F	0.254	0.116
<i>Oecetis avara</i> (Banks, 1895)	MI: Sturgeon R., 46.5689, -88.6564	2011	100	6	M	0.418	0.135
<i>O. inconspicua</i> (Walker, 1852)	MI: Bush Lk., 45.1919, -84.3177	2015	100	6	M	0.453	0.145
<i>Setodes incertus</i> (Walker, 1852)	MI: Big Sable R., 44.1176, -86.2010	2014	150	3	M	0.192	0.035
<i>Trienodes tardus</i> Milne, 1934	MN: Bush Lk., 45.1919, -84.3177	2015	50	3	M	0.595	0.166
LIMNIPHILIDAE							
<i>Anabolia bimaculata</i> (Walker, 1852)	MI: Silver Lk., 45.2042, -84.3117	2015	15	3	M	2.413	0.531
<i>A. consocia</i> (Walker, 1852)	MI: Fairbanks Cr., 44.0481, -85.6586	2011	15	3	M	1.849	0.407
<i>Hydatophylax argus</i> (Harris, 1869)	MI: Fairbanks Cr., 44.0481, -85.6586	2010	5	6	F	6.521	1.655
<i>Limnephilus indivisus</i> Walker, 1852	MI: Fairbanks Cr., 44.0481, -85.6586	2012	10	3	M	2.295	0.487
<i>Nemotaulis hostilis</i> (Hagen, 1873)	MI: Fairbanks Cr., 44.0481, -85.6586	2012	7	3	F	5.515	0.827
<i>Onocosmoecus unicolor</i> (Banks, 1897)	MI: Salmon Trout R., 46.8485, -87.7989	2019	25	3	M	2.357	0.604
<i>Platycentropus radiatus</i> (Say, 1824)	MI: Fairbanks Cr., 44.0481, -85.6586	2013	8	3	M	3.973	0.596
<i>Pycnopsyche antica</i> (Walker, 1852)	MI: Fairbanks Cr., 44.0481, -85.6586	2013	25	6	M	2.263	0.354

Taxon	Site	Year	#	N	M/F	AFDM (mg)	± SE
<i>P. guttifera</i> (Walker, 1852)	MI: Fairbanks Cr., 44.0481, -85.6586	2012	25	6	M	2.199	0.396
<i>P. lepida</i> (Hagen, 1861)	MI: Mountain St., 46.8692, -87.8933	2019	25	3	M	2.095	0.342
MOLANNIDAE							
<i>Molanna blenda</i> Sibley, 1926	MI: Fairbanks Cr., 44.0481, -85.6586	2011	50	3	M	0.686	0.099
<i>M. uniophila</i> Vorhies, 1909	MI: Howe Lk. 46.8932, -87.9436	2019	50	3	M	0.715	0.122
ODONTOCERIDAE							
<i>Psilotreta indecisa</i> (Walker, 1852)	MI: Mountain St., 46.8692, -87.8933	2019	50	3	M	0.702	0.179
PHILOPOTAMIDAE							
<i>Chimarra obscura</i> (Walker, 1852)	MI: Livermore Cr., 42.4457, -84.0420	2009	200	6	M	0.354	0.026
<i>C. socia</i> (Hagen, 1861)	MI: Sturgeon R., 46.5689, -88.6564	2011	200	6	M	0.402	0.082
<i>Dolophilodes distinctus</i> (Walker, 1852)	MI: Fairbanks Cr., 44.0481, -85.6586	2013	100	3	M	0.394	0.067
PHRYGANEIDAE							
<i>Agrypnia improba</i> (Hagen, 1873)	MI: Goose Pond, 45.7434, -84.8975	2011	7	3	M	3.059	0.551
<i>Banksiola crotchii</i> Banks, 1844	MI: Fairbanks Cr., 44.0481, -85.6586	2013	25	6	M	1.371	0.412
<i>Phryganea cinerea</i> Walker, 1852	MI: Fairbanks Cr., 44.0481, -85.6586	2011	5	6	M	6.846	1.504
<i>Pilostomis ocellifera</i> (Walker, 1852)	MI: Fairbanks Cr., 44.0481, -85.6586	2011	5	6	M	7.169	1.367
<i>P. semifasciata</i> (Say, 1828)	MI: Slapneck Cr., 46.3331, -86.9369	2011	5	6	M	7.217	2.073
POLYCENTROPODIDAE							
<i>Holocentropus interruptus</i> Banks, 1914	MI: Rockwell Lk., 44.0445, -85.6476	2011	50	3	M	0.511	0.982
<i>Nyctiophylax affinis</i> (Banks, 1897)	MI: Benton Lk., 43.6718, -85.8916	2011	200	3	M	0.105	0.018
<i>Polycentropus pentus</i> Ross, 1941	MI: Fairbanks Cr., 44.0481, -85.6586	2014	75	3	M	0.418	0.092
PSYCHOMYIIDAE							
<i>Psychomyia flavida</i> Hagen, 1861	WI: Red R., 44.8022, -88.6711	2015	500	6	F	0.038	0.005
RHYACOPHILIDAE							
<i>Rhyacophila fuscula</i> (Walker, 1852)	MI: Miners R., 46.4747, -86.5314	2011	75	6	M	1.402	0.355
SERICOSTOMATIDAE							
<i>Agarodes distinctus</i> (Ulmer, 1905)	MI: Howe Lk. 46.8932, -87.9436	2019	25	6	M	0.795	0.127
THREMMATIDAE							
<i>Neophylax concinnus</i> MacLachlan, 1871	MI: Miners R., 46.4747, -86.5314	2019	75	3	M	0.329	0.071

This increased precision of using AFDM instead of specimen counting in ecological calculations can be observed when analyzing a previously published data set (Houghton and Wasson 2013). In this study, 13 sets of blacklight samples of adult caddisflies were collected from June to August 2012 at five sites along the continuum of a first order stream in Michigan (USA). The local habitat at the majority of these sites was dense forest, except for a single ~500m stretch of open meadow. The purpose of the study was to assess differences in FFG composition between the forest sites and the meadow site. Based on specimen counting, the authors observed shredders as the dominant FFG at the forested sites, filtering collectors as the dominant FFG at the meadow site, and no change in scrapers throughout the continuum (Figure 3). When substituting the AFDM values per specimen reported herein, biomass of shredders, scrapers, and filtering collectors were approximately equal at the meadow site. This difference is due to the larger body weight of shredders relative to the other FFGs, and the change in dominant scraper taxa along the continuum from the relatively small *Glossosoma nigrior* Banks to the larger *Molanna blenda* Sibley. While not a stark difference from the original conclusions of the study, utilizing AFDM values does allow for a more precise analysis of stream conditions.

These data allow, for the first time, the use of biomass data when assessing stream conditions using adult Trichoptera. Further research will be needed on intra- and inter-population biomass variation within a region. Further, the weights of the fairly

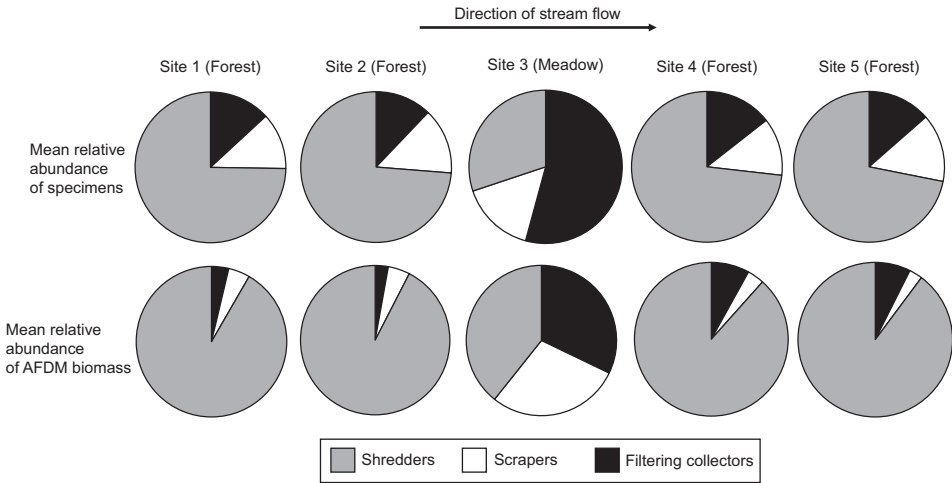


Figure 3. Comparison of mean specimen abundance (% of total specimens) and AFDM biomass (% of total biomass) for the caddisfly FFGs of a Michigan first order stream, based on 13 blacklight samples from each of 5 sites collected weekly from June to August 2012 (Houghton and Wasson 2013). AFDM biomass determined by multiplying determined AFDM values reported herein for each species by the number of specimens of that species in each sample.

high-latitude populations measured in our region may be different than lower latitude populations of the same species. It is our hope that similar studies are conducted in other areas of the US and elsewhere to further increase the value of the adult caddisflies as a biological monitoring taxon.

Acknowledgements

Collection of specimens utilized in this study was supported by a US Environmental Protection Agency Science to Achieve Results Fellowship, grants from the Minnesota Nongame Research Program and the Huron Mountains Wildlife Foundation, and funds from the Hillsdale College biology department. We thank Tony Swinehart for use of his laboratory and equipment. We thank Ralph Holzenthal and the University of Minnesota Insect Museum for donating specimens of several species. The valuable comments of Desi Robertson and Andy Rasmussen improved earlier versions of the manuscript. This is paper #22 of the GH Gordon Biological Station Research Series.

References

Barbour MT, Gerritsen J, Snyder BD, Stribling JB (1999) Rapid bioassessment protocols for use in streams and rivers: periphyton, benthic macroinvertebrates, and fish (2nd ed.). EPA 841-B-99-002. Office of Water, U.S. Environmental Protection Agency, Washington.

- Blinn DW, Ruitter DE (2013) Tolerance values and effects of selected environmental determinants on caddisfly (Trichoptera) distribution in northwest and north central Washington, USA. *Western North American Naturalist* 73: 270–294. <https://doi.org/10.3398/064.073.0302>
- Cao Y, Hawkins CP (2011) The comparability of bioassessments: a review of conceptual and methodological issues. *Journal of the North American Benthological Society* 30: 680–701. <https://doi.org/10.1899/10-067.1>
- Chessman B, Williams S, Besley C (2007) Bioassessment of streams with macroinvertebrates: effect of sampled habitat and taxonomic resolution. *Journal of the North American Benthological Society* 26: 546–565. <https://doi.org/10.1899/06-074.1>
- Dohet A (2002) Are caddisflies an ideal group for the assessment of water quality in streams? In: W Mey (Ed.) *Proceedings of the 10th international symposium on Trichoptera*, 30 July–05 August, Potsdam, Germany. *Nova Supplementa Entomologica*, Keltern, Germany, 507–520.
- Enquist BJ, Niklas KJ (2001) Invariant scaling relations across tree-dominated communities. *Nature* 410: 655–660. <https://doi.org/10.1038/35070500>
- Eklöf J, Austin Å, Bergström U, Donadi S, Ericksson B, Hansen J, Sundblad G (2017) Size matters: relationship between body size and body mass of common coastal, aquatic invertebrates in the Baltic Sea. *PeerJ* 5: e2906. <https://doi.org/10.7717/peerj.2906>
- Gerth W, Herily AT (2006) Effect of sampling different habitat types in regional macroinvertebrate bioassessment surveys. *Journal of the North American Benthological Society* 25: 501–512. [https://doi.org/10.1899/0887-3593\(2006\)25\[501:EOSDHT\]2.0.CO;2](https://doi.org/10.1899/0887-3593(2006)25[501:EOSDHT]2.0.CO;2)
- Gruner DS, Smith JE, Seabloom EW, Sandin SA, Ngai JT, Hillebrand H, Harpole WS, Elser JJ, Cleland EE, Bracken MES, Borer ET, Bolker BM (2008) A cross-system synthesis of consumer and nutrient resource control on producer biomass. *Ecology Letters* 11: 740–755. <https://doi.org/10.1111/j.1461-0248.2008.01192.x>
- Houghton DC (2007) The effects of landscape-level disturbance on the composition of Minnesota caddisfly (Insecta: Trichoptera) trophic functional groups: evidence for ecosystem homogenization. *Environmental Monitoring and Assessment* 135: 253–264. <https://doi.org/10.1007/s10661-007-9647-9>
- Houghton DC, Wasson JL (2013) Abrupt biological discontinuity in a small Michigan stream due to historical riparian canopy loss. *Journal of Freshwater Ecology* 28: 293–306. <https://doi.org/10.1080/02705060.2013.774298>
- Houghton DC, Berry EA, Gilchrist A, Thompson J, Nussbaum M (2011) Biological changes along the continuum of an agricultural stream: Influence of a small terrestrial preserve and use of adult caddisflies in biomonitoring. *Journal of Freshwater Ecology* 26: 381–397. <https://doi.org/10.1080/02705060.2011.563513>
- Houghton DC, Albers BA, Fitch WF, Smith EG, Smith MC, Steger EM (2018) Serial discontinuity in naturally alternating forest and floodplain habitats of a Michigan (USA) stream based on physicochemistry, benthic metabolism, and organismal assemblages. *Journal of Freshwater Ecology* 33: 139–155. <https://doi.org/10.1080/02705060.2018.1431967>
- Jannot JE, Bruneau E, Wissinger SA (2007) Effects of larval energetic resources on life history and adult allocation patterns in a caddisfly (Trichoptera: Phryganeidae). *Ecological Entomology* 32: 376–383. <https://doi.org/10.1111/j.1365-2311.2007.00876.x>

- Johnston TA, Cunjak RA (1999) Dry mass-length relationships for benthic insects: a review with new data from Catamaran Brook, New Brunswick, Canada. *Freshwater Biology* 41: 653–674. <https://doi.org/10.1046/j.1365-2427.1999.00400.x>
- Peterson E (1989) Age-associated male mating success in three swarming caddisfly species (Trichoptera: Leptoceridae). *Ecological Entomology* 14: 335–340. <https://doi.org/10.1111/j.1365-2311.1989.tb00962.x>
- Svensson BW (1975) Morphometric variation of adult *Potamophylax cingulatus* (Trichoptera) reflecting environmental heterogeneity in a south Swedish stream. *Oikos* 26: 365–377. <https://doi.org/10.2307/3543509>
- Vannote RL, Minshall GW, Cummins KW, Sedell JR, Cushing CE (1980) The river continuum concept. *Canadian Journal of Fisheries and Aquatic Sciences*. 37: 130–137. <https://doi.org/10.1139/f80-017>
- Wagner R (2002) The influence of temperature and food on size and weight of adult *Chaetopteryx vilosa* (Fabricius) (Insecta: Trichoptera). *Archiv für Hydrobiologie* 154: 393–411. <https://doi.org/10.1127/archiv-hydrobiol/154/2002/393>
- Wagner R (2005) The influence of stream water temperature on size and weight of caddisflies (Insecta, Trichoptera) along the Breitenbach 1983–1991. *Archiv für Hydrobiologie* 163: 65–79. <https://doi.org/10.1127/0003-9136/2005/0163-0065>
- Wallace J, Howard F (1992) The growth and natural history of the caddisfly *Pycnopsyche luculenta* (Betten) (Trichoptera: Limnephilidae). *Journal of Freshwater Ecology* 7: 399–405. <https://doi.org/10.1080/02705060.1992.9664709>
- Wetzel MA, Leuchs H, Koop JHE (2005) Preservation effects on wet weight, dry weight, and ash-free dry weight biomass estimates of four common estuarine macro-invertebrates: no difference between ethanol and formalin. *Helgoland Marine Research* 59: 206–213. <https://doi.org/10.1007/s10152-005-0220-z>

Revision of the Afrotropical genus *Leiodontocercus* (Orthoptera, Tettigoniidae, Phaneropterinae) with a description of four new species

Bruno Massa¹

¹ Department of Agriculture, Food and Forest Sciences, University of Palermo, Italy

Corresponding author: Bruno Massa (bruno.massa@unipa.it)

Academic editor: Tony Robillard | Received 30 April 2020 | Accepted 9 June 2020 | Published 22 July 2020

<http://zoobank.org/96D4ECCD-ECAB-4942-9FE5-FB55D6D1C7B3>

Citation: Massa B (2020) Revision of the Afrotropical genus *Leiodontocercus* (Orthoptera, Tettigoniidae, Phaneropterinae) with a description of four new species. *ZooKeys* 951: 47–65. <https://doi.org/10.3897/zookeys.951.53814>

Abstract

Specimens belonging to the genus *Leiodontocercus* are rare or even absent in natural history museum collections; this is likely due to at least two reasons, notably, their relatively small size, and, the sheer difficulty in finding them in dense Afrotropical forests. Until recently, three species from less than fifteen specimens were known from this genus, whose identification relied on a singular diagnostic character, that is, the shape of the male cerci. The present contribution is based on the examination of thirty specimens collected from various countries, ranging from central to west Africa; apart from the male cerci, a second diagnostic character – the stridulatory file – is used to distinguish species, even though it is difficult to examine in mounted specimens. As a result, four new species were detected, namely, *L. vicii* **sp. nov.**, *L. spinicercatus* **sp. nov.** (from the Central African Republic), *L. muticus* **sp. nov.** (from Gabon and Cameroon) and *L. philipporum* **sp. nov.** (from Côte d’Ivoire). Moreover, *L. condylus* is recorded from the Central African Republic, the only country where three species of this genus co-occur. It is suggested that population isolation during fluctuating humid and dry periods, consequent to the influence of Ice Age impact during the Pleistocene in tropical central Africa, is the best explanation for the adaptive radiation of the group.

Keywords

Central and West Africa, leaf katydids, new species, speciation, taxonomy

Introduction

The genus *Leiodontocercus* was described by Chopard (1954) together with its type-species *L. angustipennis* from Mt. Nimba (Guinea, tropical Africa). Ragge (1962), subsequently revised the genera of the tribe Phlaurocentrini Karsch, 1889, describing two new species within this genus, *L. condylus* from the Democratic Republic of Congo and *L. malleus* from Ghana; Ragge's new descriptions were based on the shape of the male cerci. Since these initial works, very few specimens were studied: Chopard (1954) examined only one specimen, Ragge (1962) studied a further 12 specimens, while Massa (2013) examined another seven specimens, recorded from the Central African Republic; finally, Massa et al. (2020) listed 21 specimens. The present author studied a total of 30 specimens for this revision, most of which were collected during different entomological expeditions to the Côte d'Ivoire, Central African Republic, Cameroon and Gabon, respectively.

Material and methods

The species currently grouped in *Leiodontocercus* were, until recently, recognized only by the shape of the male cerci; no other characters have hitherto been known or proposed to separate the species. In this paper, the stridulatory file under the male's left forewing and the associated number and arrangement of teeth have been used as diagnostic characters. They are useful characters that determine whether species are bio-acoustically separated from another one (Ragge 1980, Heller 2006).

Specimens studied for this contribution were collected at night time, attracted to a light trap (UV) that was set up both on the ground and in the canopy (35 to 55 meters high) in central-western countries of tropical Africa (Côte d'Ivoire, Gabon, Cameroon and the Central African Republic). Before mounting the specimens, the left wing of every male characterized by different cerci was spread in a manner that allowed a clear examination of the stridulatory file under the fore wing. Some specimens were dissected to inspect organs as well as to extract eggs from female specimens. Characters of specimens, stridulatory area, stridulatory file, cerci in frontal and lateral views were photographed with a Nikon Coolpix 4500 digital camera, mounted on a Wild M3 Stereomicroscope. Photographs were integrated using the freeware CombineZP (Hadley 2008). Mounted specimens were measured with a digital caliper (precision 0.01 mm); the following measurements were taken (in mm): body length; dorsal length from the head to the apex of the abdomen; pronotum length and height; tegmina: length and maximum width; hind femora length.

In view of the difficulty to distinguish between females of different species, in the present paper they are listed together with male specimens that were collected in the same locality and on the same date. For the same reason, no females are listed within the paratypes of new species, but merely as material examined. Thus, the description of female characters is reported within that of the genus.

Abbreviations used in this paper

ANHRT	African Natural History Research Trust, Hereford, UK;
BMPC	Bruno Massa Private Collection, Palermo, Italy;
MNHN	Muséum National d'Histoire Naturelle, Paris, France;
MSNP	Museo di Storia Naturale, University of Pavia, Italy;
NHW	Naturhistorisches Museum Wien, Vienna, Austria;
PAPC	Philippe Annoyer Private Collection, Sainte Croix Volvestre, France.

Results

Characters of *Leiodontocercus* Chopard, 1954 (species-type: *L. angustipennis* Chopard, 1954)

The word *Leiodontocercus* derives from the Greek and means “cercus with a smooth tooth” (λείος = smooth, ὀδόντος genitive of ὀδούς = tooth). *Leiodontocercus* is characterized by a strongly compressed fastigium of vertex which slopes to the frons and is sulcate above; tegmina are very narrow, obliquely truncate apically; male last sternite without styli, and cerci stout and enlarged apically. Like in the other Phlaurocentrini, the 10th abdominal tergite of the female is hood-like and conceals the supra-anal plate; the ovipositor is very similar to that of *Buettneria* Karsch, 1889, it is much reduced and with smooth and short valves. Ventral valves are short, upward and apically pointed, dorsal valves longer than ventral ones, straight like two short fingers; the subgenital plate of the female lacks diagnostic characters, in all specimens examined it is triangular with a central fine keel (Figs 1–3). Thus, like in the other genera of the tribe Phlaurocentrini the valves of the ovipositor are not flattened laterally. This indicates that the eggs are not inserted between the layers of the leaf epidermis, as in most Phaneropterinae, but possibly they are laid between cracks of tree bark. The eggs of *Leiodontocercus* species are not flat, like most species of Phaneropterinae, but nearly round and thick, similarly to species of *Phlaurocentrum* Karsch, 1889. Very likely this shape conveys a high resistance to desiccation (very thick chorionic layers that reduce the rate of water loss). The number of eggs found within the female oviduct was low (between 10 and 15).

Annotated list of species

Leiodontocercus angustipennis Chopard, 1954

Figs 14, 16, 16a

Leiodontocercus angustipennis Chopard 1954. Mem. Inst. franc. Afr. Noire 40(2): 84; type locality: Mt. Nimba, Guinea (MNHN).

Material examined. Guinea, Mt. Nimba (♂ holotypus) (MNHN)

Distribution. After the description by Chopard (1954), Ragge (1962) recorded another specimen from Sierra Leone. Massa (2013) recorded *L. angustipennis* also from

the Central African Republic, but later Massa et al. (2020) stated that the specimens were erroneously identified and actually they belong to *L. condylus*; in addition, they wrote that other specimens belong to another two undescribed species, described below.

***Leiodontocercus philipporum* sp. nov.**

<http://zoobank.org/18E7A412-0C64-44B7-808C-C250EA4479BF>

Figs 1, 7, 12, 19, 20

Material examined. Côte d'Ivoire, Lamto Nature Scientific Reserve, Bandama River, 4.IX.1982 (♂ holotypus) (BMPC); Côte d'Ivoire, Taï National Park, Research Station, 22.III–4.IV.2017, P. Moretto & P. Annoyer (3♀) (BMPC).

Description. Male. General habitus and colour. Predominantly green-brown, two lateral black spots on fore margin of pronotum and corresponding hind margin of head, black stripe interrupted on the hind margin of pronotum, abdomen yellow, last abdominal tergite orange, antennal segments reddish, legs yellowish, hind tibiae yellowish with black rings. **Head and antennae.** Eyes oval-roundish, prominent, antennae long and thin. **Thorax.** Anterior margin of pronotum slightly concave, posterior margin straight. Lower margin of pronotal lobes rounded. Tegmina very narrow. Central part of the stridulatory file consists of ca 60 teeth (Fig. 7). The stridulatory area of the left tegmen wider than the rest of tegmen (Fig. 12). Right tegmen without mirror. **Legs.** Fore coxae armed. Tympana on fore tibiae open on outer, closed on inner side. Fore femora with 8 inner ventral spines, fore tibiae with 4 inner and outer ventral spines. Mid femora armed with 7 outer ventral spines, mid tibiae dorsally with 2 inner spines, 7 spines on outer and inner ventral margins. Hind femora with 8–9 outer and inner ventral spines, hind tibiae straight with many ventral spines. Two pairs of small spines on the outer and inner knees of hind femora. **Abdomen.** Cerci stout and hairy, in frontal view apically triangular with serrated margins; ventrally they have a long-tipped appendage (Figs 19, 20). Hind margin of the subgenital plate nearly straight, styli absent.

Measurements (mm). Body length: 19.4; length of pronotum: 3.0; depth of pronotum: 3.2; length of hind femora: 20.0; length of tegmina: 24.4; width of tegmina: 3.3.

Etymology. *Leiodontocercus philipporum* sp. nov. is named after Philippe Annoyer and Philippe Moretto, who organized a one-month entomological mission to Taï National Park and Mt. Tonkoui of the Côte d'Ivoire, helping me in the night trapping and generously providing all Orthoptera collected there.

***Leiodontocercus spinicercatus* sp. nov.**

<http://zoobank.org/F34AB84D-BFF9-4505-8CCE-C35AAB07FCCE>

Figs 2, 3, 5, 10, 23, 24

Material examined. Central African Republic, Dzanga-Sangha Special Reserve, Camp 5, 15–16.II.2005, P. Annoyer (♂ holotypus); Dzanga-Sangha Special Reserve, Camp 5,



Figures 1–3. Female ovipositor of *Leiodontocercus*: **1** 10th abdominal tergite concealing the supra-anal plate in the female of *L. muticus* sp. nov. from Gabon **2** ventral view of the ovipositor of *L. spinicercatus* sp. nov. from Central African Republic **3** lateral view of the ovipositor of *L. spinicercatus* sp. nov. from Central African Republic.

7–8.II.2005 (light), P. Annoyer (1♀); Dzanga-Sangha Special Reserve, 15–16.X.2008 (light), P. Annoyer (1♀) (BMPC).

Description. Male. General habitus and colour. Predominantly green-brown, two lateral black spots on fore margin of pronotum and corresponding hind margin of head, black stripe interrupted on the hind margin of pronotum, abdomen yellow, last abdominal tergite orange, antennal segments reddish, legs yellowish, hind tibiae yellowish with black rings. **Head and antennae.** Eyes oval-roundish, prominent, antennae long and thin. **Thorax.** Anterior margin of pronotum slightly concave, posterior margin straight. Lower margin of pronotal lobes rounded. **Tegmina** very narrow. Central part of the stridulatory file consists of ca 55 teeth (Fig. 5). The stridulatory area of the left tegmen wider than the rest of tegmen (Fig. 10). Right tegmen without mirror. **Legs.** Fore coxae armed. Tympana on fore tibiae open on outer, closed on inner side. Fore femora with 7 inner ventral spines, fore tibiae with 4 inner and outer ventral spines. Mid femora armed with 9 outer ventral spines, mid tibiae dorsally with 2 inner spines, 7 spines on outer and inner ventral margins. Hind femora with 8–9 outer and inner ventral spines, hind tibiae straight with many ventral spines. 2 pairs of small spines on the outer and inner knees of hind femora. **Abdomen.** Cerci stout and apically incurved, with an apical ventral pointed tip (Figs 23, 24). Hind margin of the subgenital plate nearly straight, styli absent.

Measurements (mm). Body length: 14.2; length of pronotum: 2.9; depth of pronotum: 2.5; length of hind femora: 19.7; length of tegmina: 23.4; width of tegmina: 3.2.

Etymology. *Leiodontocercus spinicercatus* sp. nov. is named after the ventral spine on the male cerci.

Distribution. It is known from the Dzanga-Sangha Special Reserve (Central African Republic).

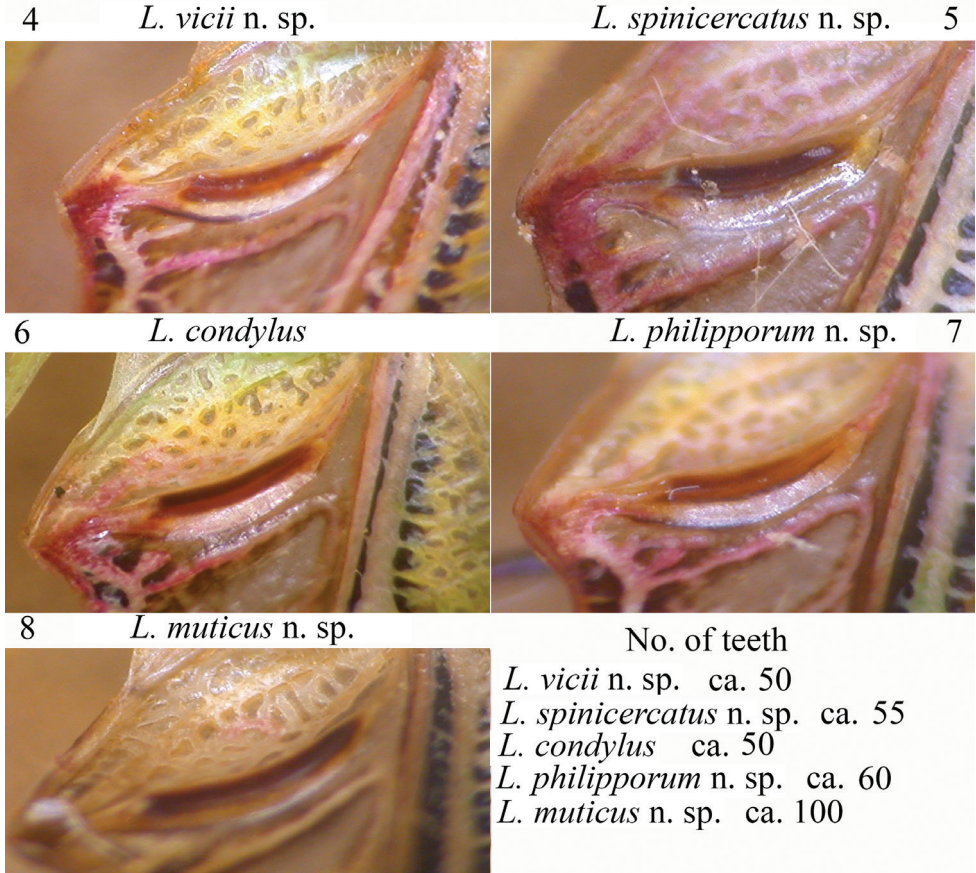
Leiodontocercus vicii sp. nov.

<http://zoobank.org/6F371136-432D-4F01-B6AD-4FDDC631CB2C>

Figs 4, 9, 21, 22

Material examined. Central African Republic, Dzanga-Ndoki NP, Lake 1, 8–10. II.2012, SANGHA2012 Team (♂ holotypus) (BMPC); Dzanga-Ndoki NP, Lake 1, 20–23.II.2012 (hand catching and light), SANGHA2012 Team (1♂ paratypus) (BMPC).

Description. Male. General habitus and colour. Predominantly green-brown, two lateral black spots on anterior margin of pronotum and corresponding hind margin of head, black stripe interrupted on the posterior margin of pronotum, abdomen yellow, last abdominal tergite orange, antennal segments reddish, legs yellowish, hind tibiae yellowish with black rings. **Head and antennae.** Eyes oval-roundish, prominent, antennae long and thin. **Thorax.** Anterior margin of pronotum slightly concave, posterior margin straight. Lower margin of pronotal lobes rounded. **Tegmina** very narrow. Central part of the stridulatory file consists of ca 50 teeth (Fig. 4). The stridulatory area of the left tegmen less protruding backwards than in the other species (Fig. 9).



Figures 4–8. Stridulatory file and detail of teeth in the following species of *Leiodontocercus*: **4** *L. vicii* sp. nov. **5** *L. spinicercatus* sp. nov. **6** *L. condylus* **7** *L. philipporum* sp. nov. **8** *L. muticus* sp. nov.

Right tegmen without mirror. **Legs.** Fore coxae armed. Tympana on fore tibiae open on outer, closed on inner side. Fore femora with 8 inner ventral spines, fore tibiae with 4 inner and outer ventral spines. Mid femora armed with 7 outer ventral spines, mid tibiae dorsally with 2 inner spines, 7 spines on outer and inner ventral margins. Hind femora with 7–8 outer and inner ventral spines, hind tibiae straight with many ventral spines. 2 pairs of small spines on the outer and inner knees of hind femora. **Abdomen.** Cerci stout and apically swollen, with the apex down curved and its margins serrated (Figs 21, 22). Posterior margin of the subgenital plate nearly straight, styli absent.

Female. Unknown.

Measurements (mm). Body length: 13.5–15.5; length of pronotum: 3.1–3.2; depth of pronotum: 2.8–2.9; length of hind femora: 20.0–20.1; length of tegmina: 24.7–24.8; width of tegmina: 2.3–2.4.

Etymology. *Leiodontocercus vicii* sp. nov. is named after the nickname of my son-in-law Vincenzo Cigna, as sign of his esteem and sincere friendship.

Distribution. Presently it is only known from the Dzanga-Ndoki National Park (Central African Republic).

***Leiodontocercus condylus* Ragge, 1962**

Figs 6, 13, 15, 15a, 16, 27

Leiodontocercus condylus Ragge. 1962. Bull. Br. Mus. (Nat. Hist.) Ent. 13: 15; type locality: Kibali-Ituri, Yindi (Democratic Republic of Congo) (NHM).

Material examined. Central African Republic, Dzanga-Ndoki National Park, Dieké 25.XI.2010, P. Annoyer (1♂, 1♀); Dzanga-Ndoki National Park, Lake 1, 31.I–2.II.2012 (1♀), 12–13.II.2012 (1♂), 13–14.II.2012 (3♂), 17.II.2012 (1♀); 20–23.II.2012 (1♀), 22–23.II.2012 (1♀); 28–29.II.2012 (1♂) (hand catching and light), SANGHA2012 Team; Lake 3, 25–26.II.2012 (light), P. Annoyer (1♀) (BMPC & PAPC); Central African Republic, La Maboké, M’Baiki II.1964, M. Pavan (1♂) (MSNP).

Remarks. *Leiodontocercus condylus* has the central part of the stridulatory file with ca 50 thick teeth, that appear just deeper than in the other species (Fig. 6). The stridulatory area of the left tegmen is a little backwards protruding, more than in the other species (Fig. 13). This species is characterized by cerci stout with an apical swelling with the outer margin serrated and the inner part with two pointed black tipped teeth (Figs 15, 16).

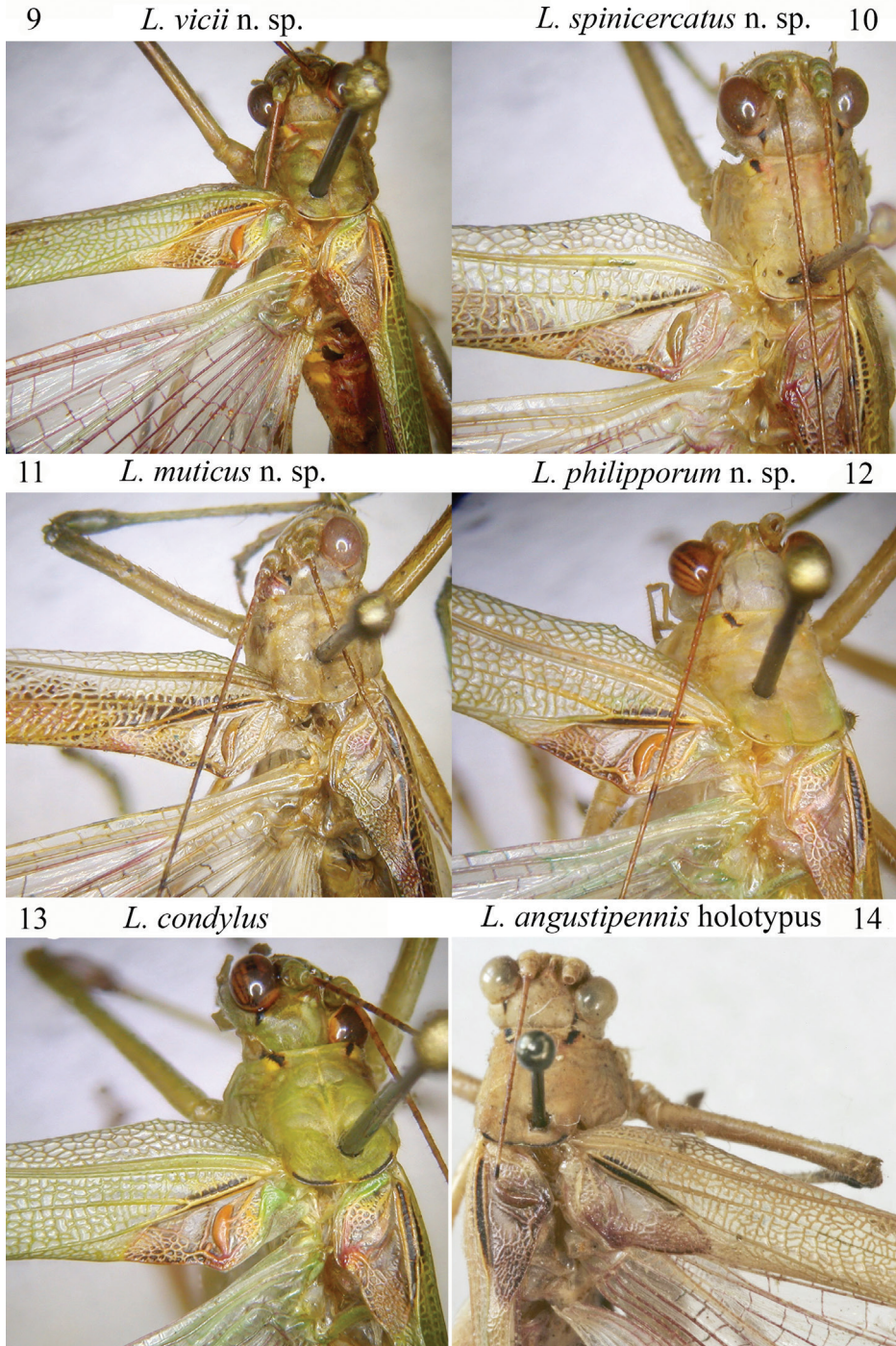
Distribution. *Leiodontocercus condylus* has been described from Zaire (= Democratic Republic of Congo) and has been reported from Central African Republic (Dzanga-Ndoki National Park) by Massa et al. (2020); it is here recorded also from the M’Baiki forest in Central African Republic. Presently females are not recognized at species level and were identified as *L. condylus* because they were collected together with the males of this species.

***Leiodontocercus muticus* sp. nov.**

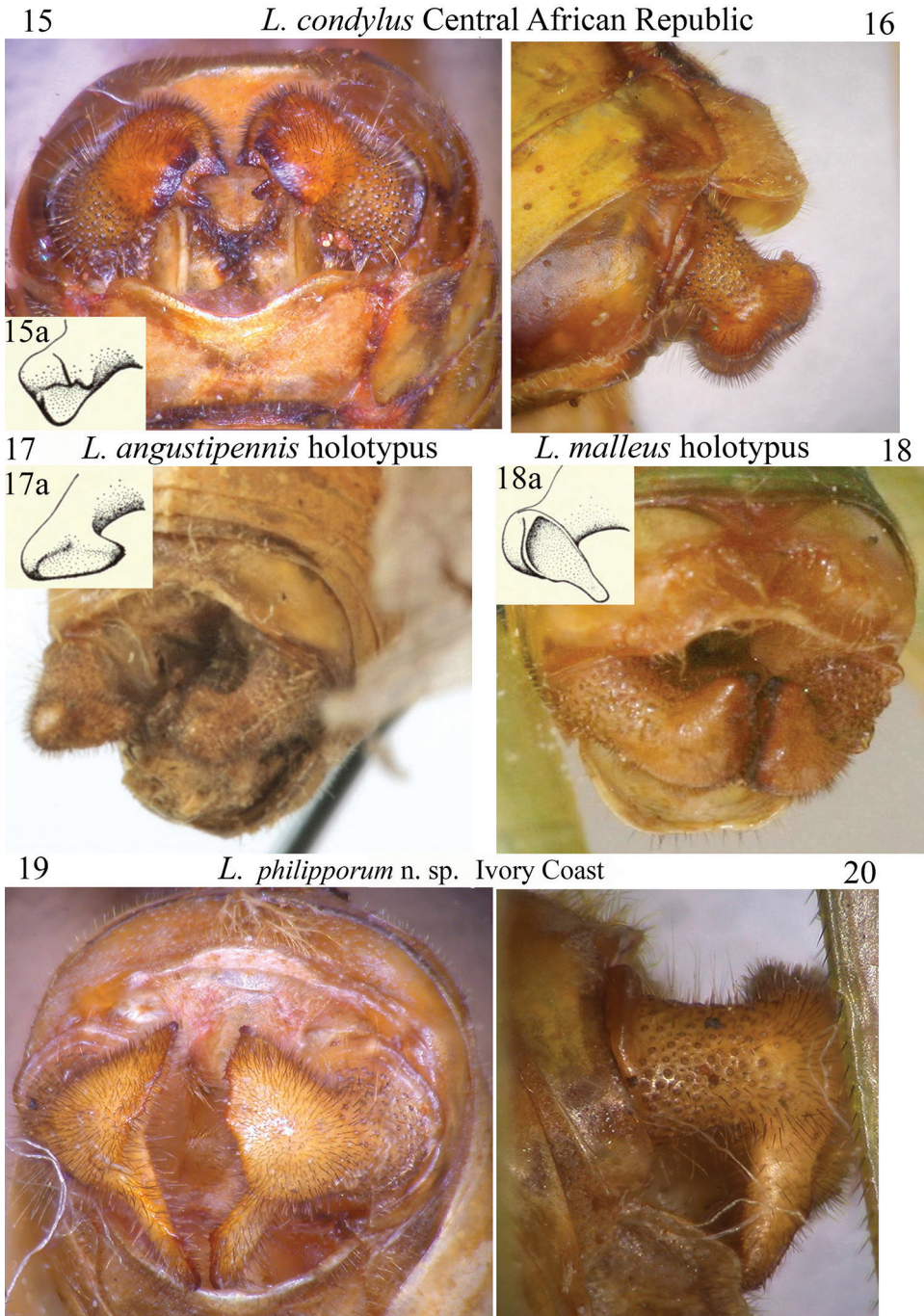
<http://zoobank.org/10E50D8E-F830-4D8D-B231-A74919255CB5>

Figs 8, 11, 25, 26

Material examined. Gabon, Mikongo (Rougier), Mts de Cristal (secondary forest) (430 m) 0°29'47"N, 11°10'42"E, 28.VII–12.VIII.2019 (MV Light Trap), Albert, Aristophanous, Bie Mba, Dérozier, Moretto (♂ holotypus, 1♂ paratypus) (ANHRT); Gabon, Mikongo (Rougier), Mts de Cristal (secondary forest) (430 m) 0°29'47"N, 11°10'42"E, 28.VII–12.VIII.2019 (Actinic Light Trap), Albert, Aristophanous, Bie Mba, Dérozier, Moretto (1♀) (ANHRT); Gabon, Nyonié (lowland forest) 0°2'22"S, 9°20'25"E (10 m) 23–28.VIII.2019 (LepiLED Light Trap), Albert, Aristophanous, Bie Mba, Dérozier, Moretto (1♂ paratypus) (BMPC); Gabon, Lope National Park



Figures 9–14. Dorsal view of the head, pronotum and the stridulatory area of the following species of *Leiodontocercus*: **9** *L. vicii* sp. nov. **10** *L. spinicercatus* sp. nov. **11** *L. muticus* sp. nov. **12** *L. philipporum* sp. nov. **13** *L. condylus* **14** *L. angustipennis* (holotypus).



Figures 15–20. Frontal and lateral view of cerci of the following species of *Leiodontocercus*: **15, 16** *L. condylus* (inset 15a: cercus after Ragge 1962), **17** *L. angustipennis* (holotypus; inset **17a** cercus after Ragge 1962) **18** *L. malleus* (holotypus; inset **18a** cercus after Ragge 1962) **19, 20** *L. philipporum* sp. nov. **17** and **18** after OSFonline (<http://orthoptera.speciesfile.org/Common/basic/Taxa.aspx?TaxonNameID=1136208>).

21 *L. vicii* n. sp. Central African Republic

22

23 *L. spinicercatus* n. sp. Central African Republic

24

25 *L. muticus* n. sp. Gabon

26



Figures 21–26. Frontal and lateral view of cerci of the following species of *Leiodontocercus*: **21, 22** *L. vicii* sp. nov. **23, 24** *L. spinicercatus* sp. nov. **25, 26** *L. muticus* sp. nov.



Figure 27. Multi-stratified canopy of the forest of the Dzanga-Ndoki National Park (Central African Republic), where *Leiodontocercus* species may occur exploiting different ecological niches (Photo by P. Annoyer).

4.IV.2014 (light), N. Moulin (1♀) (BMPC); Cameroon, Campo Ma'an National Park (lowland rainforest) (950 m) 10–22.III.2018 (MV Light Trap), Fotsing, Ishmael, Miles, Safian (1♂ paratypus, 1♀) (ANHRT); Cameroon, Mundame (1♀) (NHW).

Description. Male. General habitus and colour. Green-brown, tegmina brownish, abdomen yellow, last abdominal tergite brown, cerci brown, antennal segments reddish, legs yellowish. **Head and antennae.** Eyes oval-roundish, prominent, antennae long and thin. **Thorax.** Anterior margin of pronotum slightly concave, posterior margin rounded. Lower margin of pronotal lobes rounded. **Tegmina** very narrow. Central part of the stridulatory file consists of ca 100 teeth (Fig. 8). The stridulatory area of the left tegmen wider than the rest of tegmen (Fig. 11). Mirror absent on the right tegmen. **Legs.** Fore coxae armed. Tympana on fore tibiae open on outer, closed on inner side. Fore femora with 9 inner ventral spines, fore tibiae with 6 inner and outer ventral spines. Mid femora armed with 8 outer ventral spines, mid tibiae dorsally with 2 inner spines, 6 spines on outer and inner ventral margins. Hind femora with 9–10 outer and inner ventral spines, hind tibiae straight with many ventral spines. 2 pairs of small spines on the outer and inner knees of hind femora. **Abdomen.** Cerci stout and hairy, in frontal view slightly incurved with an apical bulge just serrated on inner margin (Figs 25, 26). Posterior margin of the subgenital plate nearly straight, styli absent.

Female. Interestingly, the females collected with males of *L. muticus* sp. nov. have black spots on the pronotum and black rings on the hind legs, like the other species of the genus. In addition, an alive female specimen photographed by P. Moretto (Fig. 29) shows alternate black and white abdominal sternites. In the males of *L. muticus* sp. nov. these black markings are absent. The female from Mundame (Cameroon) at NHW is tentatively identified, in absence of males.

Measurements (mm). Body length: 12.9–14.9; length of pronotum: 2.9–3.2; depth of pronotum: 3.0–3.2; length of hind femora: 19.6–19.7; length of tegmina: 24.4–24.6; width of tegmina: 3.4–3.5.

Etymology. *Leiodontocercus muticus* sp. nov. is named after the complete absence of any spine or appendage on the male cerci.

Distribution. This species is known from some forested areas in Gabon and in Cameroon, situated about 300 km apart.

Leiodontocercus malleus Ragge, 1962

Fig. 18, 18a

Leiodontocercus malleus Ragge. 1962. Bull. Br. Mus. (Nat. Hist.) Ent. 13: 14; type locality: Western Region, near Wiawso (Ghana) (NHM).

Notes. This species is presently known only from the male holotype, another male paratype from Tafo (Ghana) and one female paratype from Ashanti (Ghana), localities not far to the north-east of Wiawso. Cerci are shown in Fig. 18 and 18a.

Discussion

The structure of the stridulatory file

The song produced by species of this genus is, to date, still unknown. Nonetheless, the stridulatory file (the structure that allows most Orthoptera to produce a song) was examined in detail for any discernable morphological differences. All the species of *Leiodontocercus* have a very short stridulatory file under the male's left forewing, no longer than 0.5 mm (Figs 4–8). At first glance, even at very high magnification, it appears identical in all the males. However, a closer and more detailed examination revealed differences in the number of teeth, but not in their arrangement. The stridulatory file consists of very thick central teeth, that vary in number in the different species; in addition, the distal and the proximal parts of the stridulatory file have a small number of evenly-spaced small teeth. Evidently, the difference in the number of teeth (even though their structural arrangement is similar) and their different depth will produce a different song, which permits the male to attract a female of the same species. Among the examined species, the highest number of teeth in the central part of the stridula-

tory file (ca 100) has been found in *L. muticus* sp. nov., while a lowest number (ca 50) has been found in *L. condylus*, *L. spinicercatus* sp. nov. and *L. vicii* sp. nov., and an intermediate number (ca 60) was noted in *L. philipporum* sp. nov. Very likely, the song is produced using both central, distal and proximal teeth. It is remarkable to note that the three species with similar stridulatory files co-occur in the same areas of Central African Republic.

The stridulatory area

The left and right tegmina of males bear the stridulatory area; this body portion is generally well characterized for each species. However, species of *Leiodontocercus* do not show great differences: the right forewing lacks the characteristic mirror, while the left forewing has an evident arched bulge that corresponds to the stridulatory file under the wing (Figs 9–14). Small diagnostic characters are recognizable in the different taxa: *L. vicii* sp. nov. has the left tegmen particularly narrow also in the stridulatory area, while the other species described in the present work have a deeper stridulatory area compared with the rest of the wing. In addition, *L. muticus* sp. nov., the species with the highest number of teeth in the stridulatory file, has a matching area on the dorsal left tegmen that is longer compared to other species. Furthermore, *L. condylus* has a stridulatory area that protrudes further backwards than that of the other species, while *L. malleus* has a brownish stridulatory area, sharply contrasting with the rest of the green-coloured tegmina (Ragge 1962); this brownish stridulatory area may also be observed in *L. condylus*.

The shape of male cerci

The shape of the male cerci is the best diagnostic character of this genus; currently three different species have been described on the basis of the different cerci, and further, four new species are here described, mainly based on the shape of the cerci. The best way to observe cerci is through frontal and lateral views (Figs 15–26); this allows visibility of a possible ventral appendage, not otherwise visible through a dorsal view. Cerci are used by males during mating; many species of Tettigoniidae have been observed to use their cerci as a pincer that immobilizes the female's ovipositor or abdomen (e.g., Vahed et al. 2014). It is highly likely that the shape of the male cerci and mating modality are congruent and that a female would recognize the male of the same species by the song it emits. Thus, we may presume that the female reacts to the stimulus originating from the song of a male of the same species and, subsequently, the male cerci could act as a second stimulus during mating.

Habitat and habits of *Leiodontocercus* species

The Guineo-Congolian region, the tropical forest region of Central and West Africa, covers about 90% of the total forest surface in central Africa, but merely 6% in West

Africa (Malhi et al. 2013). Most species of tropical African Tettigoniidae live in the multi-stratified canopy, and are nocturnal. All the species of *Leiodontocercus* have been found (generally single individuals) in multi-stratified and well-preserved primary forests (Fig. 27), and, in some cases, in secondary forests.

One live male specimen of *L. condylus* was photographed by Samuel Danflous in the Central African Republic (Dzanga-Ndoki National Park) in 2010 and one female of *L. muticus* sp. nov. was photographed by Philippe Moretto in Gabon (Figs 28, 29). They show a peculiar leg posture, with the femora more or less vertically positioned in respect to the body, similar to the posture of a spider or some grasshoppers of the Eumastacidae (C. Hemp, pers. comm.). The dark rings on hind tibiae, when exposed (as in these cases), and dark spots and markings on the body (including the abdomen of the female), may function in disruptive mimicry. Dark markings on the wings or on the legs are common within those species occurring inside the canopy (e.g., *Enochletica ostentatrix* Karsch, 1896, *Mylocentrum* species, some *Arantia* and *Eurycorypha* species, among others); it is very likely an adaptation to minimise predation by birds or other forest vertebrates, as well as invertebrates through mimicry.

Speciation in *Leiodontocercus*

Leiodontocercus specimens are scarce in museums and collections, and this is probably the reason why their diversity has not been appreciated earlier. In addition, the species belonging to this genus are very small and delicate, with a body length that does not exceed 20 mm (15 mm on average) and a stridulatory file of no more than 0.5 mm; this makes it all the more difficult to study the very few existing, previously mounted specimens, accurately. Figure 30 shows the distribution of the currently known seven species of *Leiodontocercus*; interestingly, only the Central African Republic (protected areas Dzanga-Ndoki and Dzanga-Sangha) holds three species, which very likely occur syntopically. This finding probably results from more intensive research carried out in those areas, mainly through the use of light traps (UV), both on the forest floor and in the canopy (35 to 55 meters high) (cf. Massa 2013, Massa et al. 2020). The co-occurrence of different species distinguished by their different songs, different courtship behaviour, and small morphological differences including male cerci indicates the existence of reproductive barriers between them.

The high local biodiversity in central-western tropical African forests is shown by the high number of species of insects, Orthoptera being a case point. Generally, African Phaneropterinae are considered a taxonomic group with a great propensity to speciate; probably it is the forest ecosystem that facilitated speciation of most African Phaneropterinae. *Leiodontocercus* species, under a selective regime, may have acquired advantageous traits, that have increased local differentiation rate (cf. Simões et al. 2016). The case of speciation in *Leiodontocercus* is similar to that of *Tetraconcha* Karsch, 1890 (Phaneropterinae, Otiaphysini) (Massa 2017). Both genera show multiple speciation within tropical forest ecosystems of central and western Africa. Concerning *Leiodontocercus*, the small morphological disparity is very likely the effect of an evolutionary



Figures 28, 29. Mimicry of *Leiodontocercus condylus* Ragge, 1962, Central African Republic, Dzanga-Ndoki National Park, 25th November 2010 (Photo by S. Danflous) (above) and of *L. muticus* sp. nov., Gabon, Mikongo, 12th August 2019 (Photo by P. Moretto) (below).

radiation, which may depend on local isolation. In the case of *Tetraconcha*, the morphological character observed to distinguish species is the stridulatory system, and in the case of *Leiodontocercus*, the main differences lie in the shape of the male cerci. Both the stridulatory system and cerci shape are linked to courtship and mating.



Figure 30. Updated distribution of the seven currently known species of the genus *Leiodontocercus*.

Climatic radiation is a type of geographic radiation in which allopatric speciation in the region is driven by changes in climate (Simões et al. 2016). In accordance with Maley (1996), African rainforests retreated during dry periods after the Ice Age, and climate fluctuations would have favored the dispersion of species. The climate of tropical Africa following the Ice Age was warmer and wetter than present (African humid period; Willis et al. 2013); in most Central African areas it shifted to a drier regime between 4000 and 2000 years BP, when the forest cover retreated (Willis et al. 2013). This may have allowed local isolation of populations that evolved in the absence of gene flow. Speciation events are often correlated with humid and dry periods; forest expansion during humid periods and retraction during dry periods are considered the best explanation for the patterns of geographical species distribution found on East African mountains (Schultz et al. 2007, Hemp et al. 2015); this climatic episode has also been proposed for *Tetraconcha* by Massa (2017) and is here proposed also for *Leiodontocercus*.

Acknowledgements

I wish to thank Philippe Moretto and Philippe Annoyer, Organizer of the expedition Sangha 2012 and President of the Association Insectes du Monde (www.insectesdu-monde.org), respectively, who kindly let me study the material collected during the 2005–2012 Sangha entomological missions (Central African Republic), as well as to Samuel Danflous and Matias Loubes for their collaboration and help during the collecting nights at light in the Taï National Park (Côte d'Ivoire) in March 2017, both at ground level and in the canopy. I am grateful to Samuel Danflous for providing an interesting photograph of a species of *Leiodontocercus* taken in Central African Republic, to Philippe Moretto for a photograph of a female of *Leiodontocercus* from Gabon and to Philippe Annoyer for a photograph of the forest habitat of the Dzanga-Ndoki National Park (Central African Republic). I am indebted to Richard Smith, Chairman

of the African Natural History Research Trust (ANHRT) (Hereford, UK), who loaned specimens collected in Gabon and Cameroon, to Hitoshi Takano, researcher and curator of ANHRT and to the collectors and collaborators of the Cameroon and Gabon entomological expeditions, which were carried out by ANHRT and the Association Catharsius (in Gabon: Philippe Moretto, Marios Aristophanous, Violette Dérozier and Jean-Louis Albert; in Cameroon: Ernest Fotsing, Kobe Ishmael, William Miles, Szabolcs Safian and Gábor Simonics). ANHRT and I would very much like to extend our thanks to the following: Ministre des Eaux et Forêts of Gabon, Prof. Lee White; Monsieur l'Administrateur Général of Centre National de la Recherche Scientifique for the research authorizations; the Rector of the Université des Sciences et Techniques of Masuku, Prof. Ella Missang Crépin; the director of the Département de Biologie, Prof. Nicaise Lepengue and Dr Stefan Ntie. Finally, I thank Nicolas Moulin for providing one female specimen from Lope National Park, in Gabon.

I am indebted with Claudia Hemp, who revised the first manuscript, and to Louis Cassar for the English revision. This research received support from the Synthesys Project, which was financed by European Community Research Infrastructure Action under the FP7 “Capacities” Programme at the Museo Nacional de Ciencias Naturales, Madrid (CSIC) (2013: ES-TAF-2438), the Museum für Naturkunde, Berlin (2014: DE-TAF-4109), the Naturhistorisches Museum, Vienna (2016: AT-TAF-5324), the National Museum, Prague (2016: CZ-TAF-5559) and the Royal Belgian Institute of Natural Sciences, Bruxelles (2017: BE-TAF-6319). I am especially indebted to Mercedes Paris (Museo Nacional de Ciencias Naturales of Madrid), Michael Ohl (Museum für Naturkunde of Berlin), Suzanne Randolph and Harald Bruckner (Naturhistorisches Museum, Vienna), Jérôme Constant (Royal Belgian Institute of Natural Sciences, Bruxelles), Martin Fikáček (National Museum Natural History, Prague), Laure Desutter (Muséum National d'Histoire Naturelle, Paris), Stefano Maretti and Jessica Maffei (Museo Storia Naturale University of Pavia), who facilitated the examination of specimens preserved in their museums.

Collecting authorizations and research permits were obtained as follows: 019/UB/DSV2012 of 16.I.2012 from Bangui University, Central African Republic; 021/MESRS/DGRI of 15.II.2017 from the Ministère de l'Enseignement Supérieur e de la Recherche Scientifique of Côte d'Ivoire; AR0029/19/MESRSTT/CENAREST/CG/CST/CSAR of 11.VII.2019, issued by the Commission Scientifique d'Examen des Demandes d'Autorisations de Recherche of the Ministère de l'Enseignement Supérieur, de la Recherche Scientifique et du Transfert des technologies du Gabon.

References

- Chopard L (1954) La réserve naturelle intégrale du Mont Nimba. II. Orthoptères Ensifères. Mémoires Institut français Afrique noire 40:25–97. <https://doi.org/10.1111/j.1365-2311.1954.tb00767.x>
- Hadley A (2008) Combine Z. www.hadleyweb.pwp.blueyonder.co.uk [downloaded on February 2009]

- Heller K-G (2006) Song Evolution and Speciation in Bushcrickets. In: Drosopoulos S, Claridge MF (Eds) *Insect Sounds and Communication*. Taylor & Francis, Boca Raton, London, New York, 137–151. <https://doi.org/10.1201/9781420039337.ch9>
- Hemp C, Kehl S, Schultz O, Wägele JW, Hemp A (2015) Climatic fluctuations and orogenesis as motors for speciation in East Africa: case study on *Parepistaurus* Karsch, 1896 (Orthoptera). *Systematic Entomology* 40: 17–34. <https://doi.org/10.1111/syen.12092>
- Maley J (1996) The African rain forest – main characteristics of changes in vegetation and climate from Upper Cretaceous to the Quaternary. *Proceedings of the Royal Society of Edinburgh* 104: 31–73. <https://doi.org/10.1017/S0269727000006114>
- Malhi Y, Adu-Bredu S, Asare RA, Lewis SL, Mayaux P (2013) African rainforests: past, present and future. *Philosophical Transactions of the Royal Society B* 368 (1625). <https://doi.org/10.1098/rstb.2012.0312>
- Massa B (2013) Diversity of leaf katydids (Orthoptera: Tettigoniidae: Phaneropterinae) of Dzanga-Ndoki National Park, Central African Republic, with selected records from other African countries. *Journal of Orthoptera Research* 22(2): 125–152. <https://doi.org/10.1665/034.022.0201>
- Massa B (2017) Revision of the tropical African genus *Tetraconcha* (Orthoptera: Tettigoniidae: Phaneropterinae) with the description of ten new species. *Journal of Orthoptera Research* 26: 211–232. <https://doi.org/10.3897/jor.26.21469>
- Massa B, Annoyer P, Perez C, Danfloss S, Duvot G (2020) Orthoptera Tettigoniidae (Conocephalinae, Hexacentrinae, Phaneropterinae, Mecopodinae, Hetrodinae) from some protected areas of Central African Republic. *Zootaxa* 4780(3): 401–447. <https://doi.org/10.11646/zootaxa.4780.3.1>
- Ragge DR (1962) A revision of the genera *Phlaurocentrum* Karsch, *Buettneria* Karsch and *Leiodontocercus* Chopard (Orthoptera: Tettigoniidae). *Bulletin British Museum (Natural History) Entomology* 13: 1–17. <http://www.biodiversitylibrary.org/item/102952#page/8/mode/1up>
- Ragge DR (1980) A review of the African Phaneropterinae with open tympana (Orthoptera: Tettigoniidae). *Bulletin British Museum (Natural History) Entomology* 40: 1–192. <http://www.archive.org/details/bulletinofbritis40entolond>
- Schultz O, Hemp C, Hemp A, Wägele JW (2007) Molecular phylogeny of the endemic East African flightless grasshoppers *Altiusambilla* Jago, *Usambilla* (Sjöstedt) and *Rhainopomma* Jago (Orthoptera: Acridoidea: Lentulidae). *Systematic Entomology* 32: 1–8. <https://doi.org/10.1111/j.1365-3113.2007.00395.x>
- Simões M, Breikreuz L, Alvarado M, Baca S, Cooper JC, Heins L, Herzog K, Lieberman BS (2016) The evolving theory of Evolutionary Radiations. *Trends in Ecology and Evolution* 31: 27–34. <https://doi.org/10.1016/j.tree.2015.10.007>
- Vahed K, Gilbert JDJ, Weissman DB, Barrientos-Lozano L (2014) Functional equivalence of grasping cerci and nuptial food gifts in promoting ejaculate transfer in katydids. *Evolution* 68(7): 2052–2065. <https://doi.org/10.1111/evo.12421>
- Willis KJ, Bennett KD, Burrough SL, Macias-Fauria M, Tovar C (2013) Determining the response of African biota to climate change: using the past to model the future. *Philosophical Transactions of the Royal Society B* 368(1625). <https://doi.org/10.1098/rstb.2012.0491>

Geographical distribution of the giant honey bee *Apis laboriosa* Smith, 1871 (Hymenoptera, Apidae)

Nyaton Kitnya¹, M.V. Prabhudev^{2,3}, Chet Prasad Bhatta^{4,5}, Thai Hong Pham⁶,
Tshering Nidup⁷, Karsing Megu², Jharna Chakravorty¹,
Axel Brockmann^{2*}, G.W. Otis^{8*}

1 Department of Zoology, Rajiv Gandhi University, University Road, Itanagar, Papum Pare, Arunachal Pradesh 791112, India **2** National Centre for Biological Sciences - Tata Institute of Fundamental Research, Bellary Road, Bangalore 560065, Karnataka, India **3** Department of Biosciences, University of Mysore, Krishnaraja Boulevard Road, K.G. Koppal, Mysore 570006, Karnataka, India **4** Department of Ecology and Evolutionary Biology, University of Kansas, 1200 Sunnyside Avenue, Lawrence, KS 66045, USA **5** Department of Biology, Radford University Carilion, 101 Elm Avenue SE, Roanoke, VA 24013, USA **6** Research Center for Tropical Bees and Beekeeping, Vietnam National University of Agriculture, Trau Quy - Gia Lam - Ha Noi, Vietnam **7** Department of Environment & Life Sciences, Sherubtse College, Royal University of Bhutan, Kanglung, Trashigang, Bhutan **8** School of Environmental Sciences, University of Guelph, Guelph, Ontario N1G 2W1, Canada

Corresponding author: Nyaton Kitnya (nyatonkitnya@gmail.com)

Academic editor: Michael S. Engel | Received 6 January 2020 | Accepted 29 April 2020 | Published 22 July 2020

<http://zoobank.org/D34D5192-F7DA-46F8-A9F7-61EE3F6263E9>

Citation: Kitnya N, Prabhudev MV, Bhatta CP, Pham TH, Nidup T, Megu K, Chakravorty J, Brockmann A, Otis GW (2020) Geographical distribution of the giant honey bee *Apis laboriosa* Smith, 1871 (Hymenoptera, Apidae). ZooKeys 951: 67–81. <https://doi.org/10.3897/zookeys.951.49855>

Abstract

Worldwide pollinator declines have dramatically increased our need to survey and monitor pollinator distributions and abundances. The giant honey bee, *Apis laboriosa*, is one of the important pollinators at higher altitudes of the Himalayas. This species has a restricted distribution along the Himalayas and neighbouring mountain ranges of Asia. Previous assessments of its distribution, published more than 20 years ago, were based on museum specimens. Since then, 244 additional localities have been revealed through field trips by the authors, publications, and websites. We present a revised distribution for *A. laboriosa* that better defines its range and extends it eastward to the mountains of northern Vietnam,

* Co-senior authors

southward along the Arakan Mountains to west-central Myanmar, into the Shillong Hills of Meghalaya, India, and northwestward in Uttarakhand, India. This species is generally found at elevations between 1000–3000 m a.s.l.. In northeastern India *A. laboriosa* colonies occur during summer at sites as low as 850 m a.s.l. and some lower elevation colonies maintain their nests throughout the winter. Finally, we report three regions in Arunachal Pradesh, India, and nine locations in northern Vietnam, where we observed workers of *A. laboriosa* and *A. dorsata* foraging sympatrically; their co-occurrence supports the species status of *Apis laboriosa*.

Keywords

Apidae, *Apis dorsata*, conservation, Himalayas, pollinator, sympatry

Introduction

The Himalayan giant honey bee *A. laboriosa* is a spectacular but poorly understood species, in large part because it usually nests on inaccessible cliff faces in the Himalaya Mountains (Cronin 1979; Sakagami et al. 1980; Roubik et al. 1985; Underwood 1990a; Joshi et al. 2004; Gogoi et al. 2017). The first specimen was collected in the mountainous regions of western Yunnan and named by Frederick Smith (Moore et al. 1871), who noted several characteristics that he felt distinguish *A. laboriosa* from lowland *A. dorsata*. This taxon was subsequently ignored until Maa (1953) undertook his reassessment of honey bee taxonomy. He stated its distribution as “India (Sikkim; Assam); China (western Yunnan). Probably also occurring in N. Burma”. Sakagami et al. (1980) provided the first detailed descriptions of the morphology, biology, and geography of *A. laboriosa* and provided strong evidence that it should be recognized as a distinct species different from the lowland giant honey bee *A. dorsata*. They also presented a range map depicting 22 localities along several rivers that extend into the Himalayas of Nepal. They noted that records outside Nepal were “scarce” and provided just one locality in “Tibet” and four in Arunachal Pradesh (Sakagami et al. 1980: p. 63). Interestingly, Sakagami et al. (1980) mentioned one site (Denling Forest, Kameng Div., Arunachal Pradesh, 229 m a.s.l.) from which both *A. laboriosa* and *A. dorsata* had been collected, indicating that in some parts of Asia these two forms occur sympatrically.

The most recent range map of *A. laboriosa* (Otis 1996) was published more than 20 years ago. Although Otis (1996) compiled all locality data available at that time, there were obvious gaps (e.g., in Bhutan, northeastern India, northern Myanmar, Laos, and Vietnam). Since then, the number of verified reports has increased rapidly due to additional fieldwork, new publications and postings of photos and videos by naturalists on iNaturalist and other websites.

We present here an updated distribution map of *A. laboriosa* and present additional evidence that *A. laboriosa* and its sister species *A. dorsata* co-occur in several locations in Asia.

Materials and methods

Identification of *Apis laboriosa*

The Himalayan giant honey bee *A. laboriosa* differs significantly from the giant honey bee *A. dorsata* of mainland Asia in many characters noted by Sakagami et al. (1980). Sakagami et al. (1980) could always distinguish the two taxa on the basis of thoracic hair colour, which was “tawny yellow” in *laboriosa* and “mostly dark” in *dorsata*. Additionally, the first two gastral tergites of *laboriosa* are black (grey in callow adults); in *dorsata* of mainland Asia, they are orange-brown (pale yellow in callows; Fig. 1). Several genetic analyses indicate these two taxa have diverged sufficiently to consider *A. laboriosa* to be a distinct species (Arias and Sheppard 2005; Raffiudin and Crozier 2007; Lo et al. 2010; Chhakchhuak et al. 2016; Takahashi et al. 2018). Despite these many differences, Engel (1999), in the most recent reassessment of *Apis* taxonomy, considered *A. laboriosa* to be a subspecies of *A. dorsata* that may be deserving of species status. Because of substantive differences in drone morphology (NK and GWO, unpubl. data) and distinct morphometric differences (NK, unpublished data) between the two taxa collected sympatrically in northeastern India (this study), we are confident that *A. laboriosa* is a distinct species and refer to it as such below. For this study, we identified specimens and photos of the bees on the basis of thoracic hair and abdominal colour (Sakagami et al. 1980).

Data collection

The starting point for this project was the list of collection localities reported by Otis (1996) who summarized the 105 records available from museum specimens and literature up to that time (Maa 1953; Sakagami et al. 1980; Kuang and Li 1985; Roubik et al. 1985; Underwood 1990a; Batra 1996).

Subsequently, Trung et al. (1996) remarkably extended the distribution of *A. laboriosa* well into Vietnam. Additional localities in Vietnam have been detected in seven northern provinces by THP. Between 2001–2008 he sought information on cliff-nesting honey bees at high elevations (> 900 m a.s.l.) in northern Vietnam from beekeepers, honey-hunters, and others living in those regions. For those who responded positively, he visited the region and showed informants photos and specimens of *A. laboriosa* and *A. dorsata*. If the information suggested the bees were *A. laboriosa*, then he contacted them to visit the nesting cliff to observe the colonies and collect specimens, if possible, for verification.

CPB collected specimens from many parts of Nepal to analyze genetic variability within *A. laboriosa*; he contributed 17 additional localities in Nepal. Joshi et al. (2004) reported numerous localities ($N = 54$) in the Kaski District of Nepal.

TN contributed 29 new localities in Bhutan in addition to the two localities he and his colleague had reported earlier (Nidup and Dorji 2016).



Figure 1. *Apis laboriosa* and *Apis dorsata* worker bees. *A. laboriosa* (left) has a completely dark abdomen and long golden thoracic hairs. *A. dorsata* (right) has several orange or yellow anterior abdominal segments and dark thoracic hairs. Details for the specimens photographed: *A. laboriosa*, collected by BA Underwood, Kaski District, Nepal, 1860 m, 8 v 1984 (Nest 6–8); *A. dorsata*, collected by GW Otis, Serdang, Selangor, Malaysia, 3.00 N, 101.68 E, 8 ii 1989. Scale bar: 1 cm.

Within India, a team (NK, MVP, KM, JC, and AB), in their fieldwork on *A. laboriosa*, have added numerous localities from northern and northeastern India. Several authors have reported sites where this bee species occurs in Uttarakhand, India (Gupta 2004; Joshi et al. 2008; Joshi et al. 2016). Additional localities were reported from Arunachal Pradesh, India, by Gogoi and colleagues (Gogoi et al. 2017; Tayeng and Gogoi 2018). The Nagaland Beekeeping and Honey Mission (NBHM) has collated information on the “Rock bee” within the state of Nagaland (Team NBHM 2015). Similarly, Chhakchhuak et al. (2016) reported a nesting cliff in Murlen in Mizoram. Vivek Sarkar (pers. comm.) shared three localities in the highlands of Meghalaya.

Hliang Min Oo (pers. comm.) located cliffs inhabited by ~50 colonies of *A. laboriosa* in the mountains of western Myanmar. He shared photos that are clearly of that

species. Anne Schooffs (pers. comm.) and Kevin Kamp (pers. comm.) contributed their observations in Laos. Similarly, Xin Zhou and Li Fei Qui (pers. comm.) shared details of their 2019 collection locality in Yunnan, China. Cao and colleagues already reported two localities in Yunnan in 2012 (Cao et al. 2012).

We recognize that some records are stronger than others. Consequently, we have distinguished four categories of records:

1. Observations by the authors. These include observations of nests on rock cliffs and of foragers (many of which were collected for further study) at flowers and human urine.
2. Internet records. GWO searched the internet extensively for photographs of bees and bee nests that could be definitively identified as *A. laboriosa* based on abdominal and thoracic hair colour. This search included websites and images retrieved from Google searches of “*Apis laboriosa*”, “cliff bee”, “giant honey bee + (country name)”, and “honeyhunting + (country name)”, with the search including all mountainous countries in Asia from Pakistan east to Vietnam; records of *A. laboriosa* posted to iNaturalist (www.inaturalist.org), all of which were verified as *A. laboriosa* by John Ashcher, National University of Singapore; and the Nature Picture Library (www.naturepl.com). When details were lacking in the post (locality, date, etc.), the people who had posted the sightings were contacted directly.
3. Records from published reports. Scientists who mentioned *A. laboriosa* in their works were presumably aware of the differences between *A. laboriosa* and *A. dorsata*. We trusted their identifications, i.e., in most cases we did not attempt to contact them to verify their ability to distinguish *A. laboriosa*.
4. Personal observations of naturalists and honey-hunters that cannot be verified by other means. Honey-hunters, through their extensive experiences, generally distinguish between *A. laboriosa* (the “cliff bee” with a black abdomen) and *A. dorsata* (the “tree bee” with the orange abdomen). In cases where they differentiated these two forms, we included the localities they reported. We have used different coloured symbols for these different categories of information on our revised distribution map, with category 1 records being the uppermost layer on the map. Some lower category localities are obscured by stronger higher category records.

We obtained additional bee localities by searching for photos on the internet and literature about the yellow-rumped honeyguide (*Indicator xanthonotus*). The honeyguides (Indicatoridae) are one of the few taxa of animals known to be able to digest wax (Downs et al. 2002). Males of this Himalayan species defend empty combs of *A. laboriosa*, then mate with females that arrive to feed on beeswax (Cronin and Sherman 1976; Cronin 1979; Underwood 1992). The geographic and elevational distributions of the yellow-rumped honeyguide (Bird Life International; www.birdlife.org) closely match those of *A. laboriosa* (this study). We performed Google and iNaturalist searches for “yellow-rumped honeyguide” and “*Indicator xanthonotus*”. Localities for the honeyguide at elevations >1500 m a.s.l. that included depictions or descriptions of them associated with open-nesting honey bees have been included.

In our personal field work, we used global positioning system (GPS) instruments (i.e., eTrex 20, Garmin Ltd, Olathe, Kansas, USA) to document locations. When that was not possible or we had only a locality name (e.g., many of the localities reported in publications), we searched for them using Google Maps. Occasionally due to changes in names or spellings, we undertook lengthy web searches to find the current names. Not all records could be located (e.g., “Pamir, Arunachal Pradesh” reported by Sakagami et al. 1980). Latitude and longitude coordinates are presented in degrees and decimal degrees (Suppl. material 1: Table S1).

We plotted locality records using ArcGIS Desktop 10.3 of ESRI (Environmental System Research Institute, www.esri.com). The boundary maps of the region of interest were extracted from Google Earth Pro (v7.3) as a Keyhole Markup language Zipped (kmz) file and imported into ArcGIS.

Results

Revised distribution of *Apis laboriosa*

We have compiled a list of 349 localities of *Apis laboriosa* foragers or nests (Suppl. material 1), of which we were able to locate and map 345 (see Fig. 2). The mapped localities are as follows: Bhutan (57), China (48), India (92), Laos (3), Myanmar (4), Nepal (132), and Vietnam (13). The species is distributed almost continuously over a distance of >2500 km along the Pan-Himalaya region from Uttarakhand, India, eastward through Nepal, Sikkim and northern West Bengal (Darjeeling), Bhutan, northeastern India, Yunnan and southern Tibet in China, and the northern portions of Myanmar, Laos, and Vietnam. We report for the first time numerous records southward along the Arakan Mountains in eastern Arunachal Pradesh, Nagaland, Manipur, and Mizoram (India) to Matupi in west-central Myanmar. We have also verified that it occurs in the Shillong Hills of Meghalaya.

Elevational distribution of *Apis laboriosa*

Localities range in elevation from approximately 230–4270 m a.s.l. Nearly all records (94%) fall within the altitudinal range of 500–3500 m a.s.l., and 77.2% were between 1000–3000 m a.s.l. (Fig. 3). We confirmed the observation of Sakagami et al. (1980) that *A. laboriosa* occurs at lower elevations in Arunachal Pradesh than at sites further west in Bhutan, Nepal, and Uttarakhand, India. The lowest recorded elevation was reported by Sakagami et al. (1980), at 229 m a.s.l. in “Denling Forest”, western Arunachal Pradesh, India. We were unable to find that locality to map it. However, we (NK, KM, and GWO) observed foragers at a similar elevation (233 m a.s.l.) in central Arunachal Pradesh. Relatively few records are from sites higher than 3000 m a.s.l. and the records from Trubuking Kharka, Nepal (4100 m a.s.l.; Sakagami et al. 1980) and a specimen in the Natural History Museum, London (4267 m a.s.l.) are the only observations above 4000 m a.s.l.

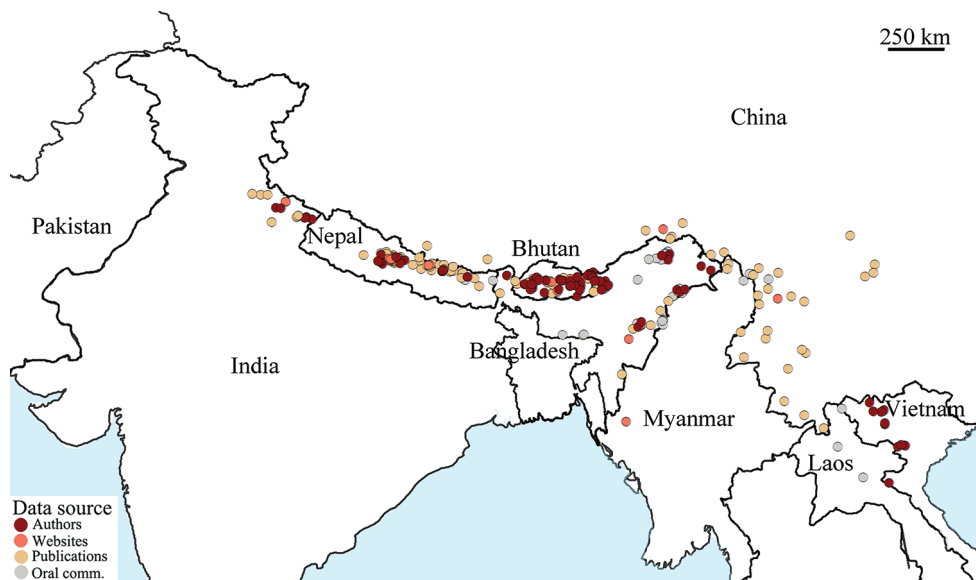


Figure 2. Geographical distribution of *Apis laboriosa*. Each circle indicates a locality at which a nest of *A. laboriosa* or workers foraging on flowers were found. The color indicates the source of information. Dark red: information collected by one or several of the authors; orange: photos published on websites; tan: information from published papers; and grey: oral reports by colleagues or local people. Scale bar: 250 km.

Sympatric occurrence of *Apis laboriosa* with *Apis dorsata*

In their field trips, the Indian team discovered five sites in three regions of Arunachal Pradesh in northeastern India where *A. laboriosa* foraged together with its sister species *A. dorsata*. The regions and sites were: (1) Western Arunachal: West Kameng District, Nag Mandir; (2) Central Arunachal: West Siang District, Tumbin and Siang District, Modi; and (3) Southeast Arunachal: Tirap District, Kala Pahar and Tutnyu (Fig. 4). Additionally, THP observed both species in close proximity at nine sites in northern Vietnam. These are located in five provinces: Hoa Binh, Lao Cai, Lai Chau, Son La, and Yen Bai. The details of these records are presented in Suppl. material 1.

Discussion

Apis laboriosa inhabits a 2500 km swath along the southern edge of the Pan-Himalaya region. We have added considerably to the distribution of this species as last presented by Otis (1996). First, we have added many additional localities for this species in Uttarakhand in northern India, the eastern portion of Nepal, all of Bhutan, and much of Arunachal Pradesh in northeastern India, demonstrating that this species is widespread over that region. More importantly, the records we have compiled show range extensions eastward to several provinces in northern Vietnam (first reported there by Trung

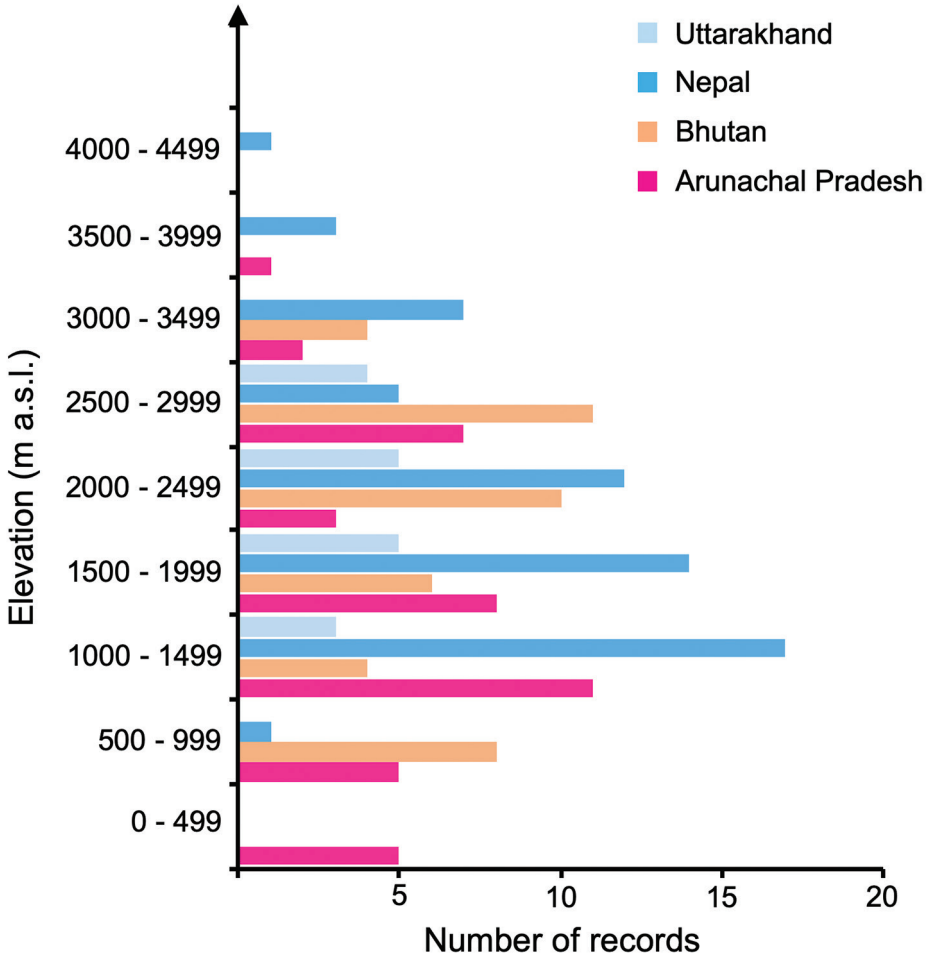


Figure 3. Elevational distribution of *A. laboriosa* records for Uttarakhand, Nepal, Bhutan and Arunachal Pradesh. 94% of all records were found between 500–3500 m a.s.l.. The lowest occurrence of *A. laboriosa* was observed in Arunachal Pradesh (229 m a.s.l.), and the highest in Nepal (4267 m a.s.l.). Uttarakhand ($N = 17$; range: 1008–2743 m a.s.l.; mean: 1927 ± 131 m), Nepal ($N = 60$; range: 800–4100 m a.s.l.; mean: 2036 ± 103 m), Bhutan ($N = 43$; range: 631–3399 m a.s.l.; mean: 2077 ± 124 m), Arunachal Pradesh ($N = 17$; range: 229–3649 m a.s.l.; mean: 1620 ± 143 m).

et al. 1996) and southward for 600 km in the Arakan Mountains (Patkai Range, Naga Hills, and Mizo Hills of Nagaland, Manipur, and Mizoram) to 21.7°N latitude in the Chin Hills of Myanmar. We also report for the first time *A. laboriosa* from the Shillong Plateau in Meghalaya, India.

Very few ($N = 10$; 6.2%) collections and observations have been made at locations situated at elevations below 500 m or above 3500 m a.s.l. (Fig. 3). Roubik et al. (1985) reported the mean elevations of their observations in central Nepal to be 3143 m a.s.l.

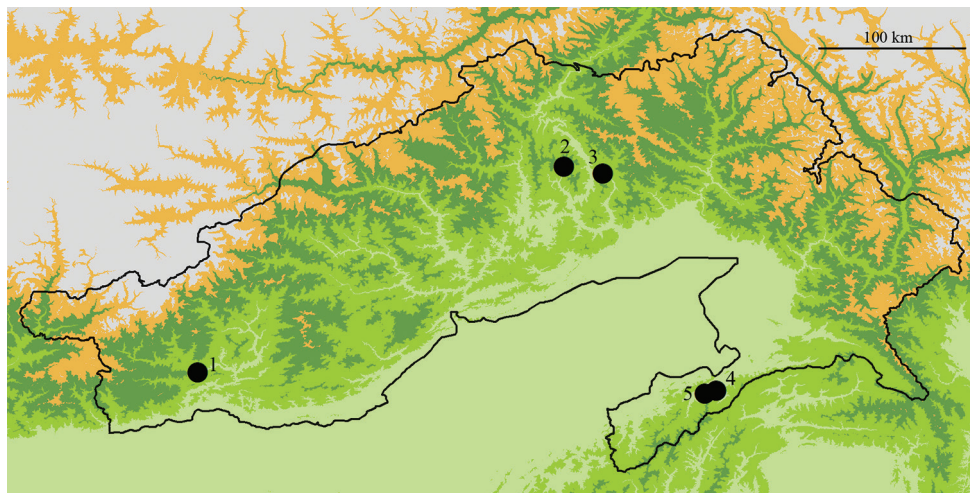


Figure 4. Sites of sympatric occurrence of *Apis laboriosa* and *Apis dorsata* in Arunachal Pradesh, India. All five localities (black dots) where we found *A. laboriosa* and *A. dorsata* foraging together were below 1500 m a.s.l. (1) West Kameng District, Nag Mandir, 27.203N, 92.561E, 1164 m a.s.l.; (2) West Siang District, Tumbin, 28.456N, 94.684E, 356 m a.s.l.; (3) Siang District, Modi, 28.487N, 95.087E, 534 m a.s.l.; (4) Tirap District, Kala Pahar, 26.934N, 95.576E, 1470 m a.s.l.; (5) Tutnyu, 26.962N, 95.631E, 1060 m a.s.l. Scale bar: 100 km.

(range from 1800–3800 m a.s.l.), which is much higher than the mean of 2036 m a.s.l. (range from 800–4100 m a.s.l.) determined from our more complete data set. Our new observations have confirmed the initial observation of Sakagami et al. (1980) that this species occurs at lower elevations in northeastern India than in Nepal (Fig. 3). However, simply mapping localities of nests and foraging bees is static and fails to recognize the dynamic elevational migrations of colonies. Underwood (1990a) reported that *A. laboriosa* colonies abandon most nesting cliffs in fall and spend the winter in combless swarms at lower elevations. By April they have generally recolonized lower elevation nesting cliffs. As the season progresses, colonies continue to move higher in elevations along river valleys during the summer, before they retreat downhill for the winter. The records we have reported (Suppl. material 1) lack sufficient elevational and temporal details to reconstruct patterns of seasonal migrations. However, preliminary observations by NK in Arunachal Pradesh suggest that both *A. laboriosa* and *A. dorsata* migrate considerable distances along river valleys leading into the mountains during summer months. Detailed observations throughout the seasons along elevational transects are warranted.

Earlier research reported that the altitudinal ranges of *A. laboriosa* and its sister species *A. dorsata* differ substantially (Sakagami et al. 1980; Roubik et al. 1985; Oldroyd and Wongsiri 2006; Hepburn and Radloff 2011). However, Sakagami et al. (1980) commented that these species were both collected at the Denling Forest in Kameng Division, West Arunachal, at an elevation 229 m a.s.l. on 5 May. This rela-

tively late date in spring suggests these bees were nesting near that site. We have confirmed the sympatric occurrence of these two species in five additional locations within three widely separated regions of Arunachal Pradesh (Fig. 3) and five provinces within northern Vietnam. All of these locations were at altitudes below 1500 m a.s.l. Interestingly, Joshi and colleagues (Joshi et al. 2008; Joshi et al. 2016) reported these two species as temporally occurring sympatrically at elevations of 2100–2800 m a.s.l. in Uttarakhand, India; and THP found them co-occurring in nine locations in northern Vietnam. Thus, depending on the environments, both species show variation in their altitudinal range (Underwood 1990a; Woyke et al. 2001; Joshi et al. 2008). More detailed collections and observations of *A. laboriosa* and *A. dorsata* at such sites will be required to verify whether these honey bees hybridize where they occur sympatrically (McEvoy and Underwood (1988). However, till today there is no evidence of intermediate forms where the two species co-occur (Sakagami et al. 1980; Roubik et al. 1985); rather, preliminary morphometric analyses of the specimens from the areas of sympatry in Arunachal Pradesh confirm their differences in size, shape, and colour (NK, unpublished data). If further collections confirm the preliminary conclusion that they maintain their distinctive species-specific characters in sympatry, that will provide additional support for the status of *A. laboriosa* as a distinct species.

Separate from its species status, *A. laboriosa* shows several unique characters that seem to be specific adaptations to living in mountainous habitats. Comparative studies of *A. laboriosa* and *A. dorsata* have shown that they differ in behaviour such as thermoregulation of thoracic temperature during flight (Underwood 1991); minimum temperature for foraging flight activity (Woyke et al. 2012); dorso-ventral abdomen flipping to stabilize body temperature (Woyke et al. 2008) and mating flight times, i.e., early afternoon in *A. laboriosa* (Underwood 1990b) compared to after sunset in *A. dorsata* (Tan et al. 1999; Otis et al. 2000). They also differ in other behaviours that may be related to living in high elevation, such as dance communication (Kirchner et al. 1996), pheromonal chemistry (Blum et al. 2000) and defensive body movements (Woyke et al. 2008).

Apis laboriosa is notably absent from the western third of Nepal, from 80.5N to 82.6E longitude. This may reflect the relatively dry climate of western Nepal, a lack of collections, or habitat degradation. Field work in several other mountainous portions of Asia may detect this species. These include:

1. northeastern Myanmar (Kumon Range and Gooligong Mountains), eastern Myanmar (much of Shan State), northern Laos (e.g., Annam Highlands and Xiangkhoang Plateau), and possibly extreme northern Thailand (e.g., Doi Pha Hom Pok National Park);
2. the valleys of the Mekong, Yangtze, Yalong, and Dadu rivers that extend into the southeastern edge of the Tibetan Plateau.
3. northeastern Punjab, Pakistan, and western Jammu, India.

Several lines of evidence point to the existence of *A. laboriosa* in Pakistan. Khan et al. (2014) reported several specimens of giant honey bees they collected in Murree, Pakistan

(33.92N, 73.40E) at an elevation of ~2300 m a.s.l. as “*A. dorsata*”, despite the general understanding that *A. dorsata* lives below 1200 m a.s.l. elevation in Pakistan (Muzaffar and Ahmed 1990). Unfortunately, the specimens from that study were not retained. Historically, the yellow-rumped honeyguide (*Indicator xanthonotus*), a bird with an intimate association with *A. laboriosa* combs (Cronin and Sherman 1976, Underwood 1992, Inskipp et al. 2008), has been observed in Murree (Magrath 1909). Just 60 km to the east of Murree, giant honey bees collected in Poonch, Jammu, India (33.82N, 74.12E), differed markedly in morphometric analyses from other *A. dorsata* specimens from Jammu and the rest of India (Mutharaman et al. 2013). Finding *Apis laboriosa* in this region would extend its distribution another 400–500 km northwestward.

Conclusion

Worldwide pollinator declines have increased the urgency to survey abundances of pollinators and to study their biology and ecology for their conservation. Asian honey bees and in particular species like *A. laboriosa*, with a restricted distribution in areas difficult to access, are dramatically understudied. Our study provides a revised description of the distribution of the Himalayan giant honey bee, *Apis laboriosa*. This is a necessary step to revitalize studies on this important pollinator species in the Himalayas (Batra 1996).

Numerous reports on *A. laboriosa* indicate that this honey bee shows specific adaptations to living in high elevation mountainous areas compared to other more tropical honey bee species. Detailed studies on its biology promise to provide interesting insights into the evolutionary history and plasticity of honey bee physiology and social behavior. Locations where *A. laboriosa* and *A. dorsata* co-occur temporally, like those we report in Arunachal Pradesh and Vietnam, are particularly suitable regions for future studies.

Acknowledgements

We thank M. Hliang (University of Veterinary Science, Yezin, Myanmar), A. Schooffs (Association for Sustainable Beekeeping, Laos), K. Kamp (Agro-Biodiversity Initiative, National Agricultural and Forestry Research Institute, Laos), V. Sarkar (Wildlife Institute of India, Dehradun, India), K. Tan (Xishuangbanna Tropical Botanical Garden, Chinese Academy of Sciences, Kunming, China), K.A. Khan (Unit of Bee Research and Honey Production, King Khalid University, Abha, Saudi Arabia, for information about Pakistan), and X. Zhou and L. Qui (Agricultural University, Beijing, China) for sharing information on locations of bees in the respective countries. M. Messar, J. Narah, N. Jamoh, D. Songthing and I. Haikam helped to collect data in Arunachal Pradesh and Nagaland, India. Numerous people who have posted photographs to iNaturalist and other websites (identified in Suppl. material 1) provided additional data related to their photos and the sites where they were taken. We also thank S. Paiero for helping with photographs of specimens using the Insect Systematics stacking camera system.

Research and field trips of researchers from RGU and NCBS were supported by funds from Department of Biotechnology Twinning R&D programme for the North-East NER to JC and AB (BT/PR16880/NER/95/333/2015); and institutional funding from National Centre for Biological Sciences (NCBS-TIFR; 12P4167) to AB. NCBS also provided funds for the open access fee. AB acknowledges support of the Department of Atomic Energy, Government of India, under 472 project no. 12-R&D-TFR-5.04-0800. Finally, we would like to thank the reviewers, D.R. Smith and N. Dahanukar, for their useful comments and suggestions.

References

- Arias MC, Sheppard WS (2005) Phylogenetic relationships of honey bees (Hymenoptera: Apinae: Apini) inferred from nuclear and mitochondrial DNA sequence data. *Molecular Phylogenetics and Evolution* 37: 25–35. <https://doi.org/10.1016/j.ympev.2005.02.017>
- Batra S (1996) Biology of *Apis laboriosa* Smith, a pollinator of apples at high altitude in the great Himalaya range of Garhwal, India. (Hymenoptera: Apidae). *Journal of the Kansas Entomological Society* 69: 177–181.
- Blum MS, Fales HM, Morse RA, Underwood BA (2000) Chemical characters of two related species of giant honeybees (*Apis dorsata* and *Apis laboriosa*): Possible ecological significance. *Journal of Chemical Ecology* 26(4): 801–807. <https://doi.org/10.1023/A:1005476405192>
- Cao LF, Zheng HQ, Chen X, Niu DF, Hu FL, Hepburn HR (2012) Multivariate morphometric analyses of the giant honey bees, *Apis dorsata* F. and *Apis laboriosa* F. in China. *Journal of Apicultural Research* 51: 245–251. <https://doi.org/10.3896/IBRA.1.51.3.05>
- Chhakchhuak L, De Mandal S, Gurusubramanian G, Sudalaimuthu N, Gopalakrishnan C, Mugasimangalam RC, Vanramliana, Kumar NS (2016) Complete mitochondrial genome of the Himalayan honey bee, *Apis laboriosa*. *Mitochondrial DNA* 27: 3755–3756. <https://doi.org/10.3109/19401736.2015.1079891>
- Cox Jr J (1999) Birds recorded on a west-central Nepal trek, 79 pp. Unpublished. www.digitalhimalaya.com/collections/birdsofnepal/bon.html [see Supplementary file 1: Collection Locality Information]
- Cronin Jr EW (1979) *The Arun: A Natural History of the World's Deepest Valley*. Houghton-Mifflin, Boston.
- Cronin Jr EW, Sherman PW (1976) A resource-based mating system: the orange-rumped honeyguide. *Living Bird* 15: 5–32. <https://eurekamag.com/research/004/619/004619312.php>
- Downs CT, van Dyk RJ, Iji P (2002) Wax digestion by the lesser honeyguide *Indicator minor*. *Comparative Biochemistry and Physiology Part A* 133: 125–134. [https://doi.org/10.1016/S1095-6433\(02\)00130-7](https://doi.org/10.1016/S1095-6433(02)00130-7)
- Engel MS (1999) The taxonomy of fossil and recent honey bees (Hymenoptera: Apidae; *Apis*). *Journal of Hymenoptera Research* 8: 165–196.
- Gogoi H, Tayeng M, Taba M (2017) Pan-Himalayan high altitude endemic cliff bee, *Apis laboriosa* Smith (Hymenoptera: Apidae): a review. *Proceedings of the Zoological Society* 72: 3–12. <https://doi.org/10.1007/s12595-017-0234-y>

- Gupta SK (2004) Insecta: Hymenoptera. In: Kumar A, Gupta SK, Padmanaban P (Eds) Some Selected Fauna of Gobind Pashu Vihar, Conservation Area Series 18, Zoological Survey of India, Kolkata, 21–28.
- Hepburn HR, Radloff SE (2011) Biogeography. In: Hepburn HR, Radloff SE (Eds) Honeybees of Asia. Springer Verlag, Berlin, 51–68. https://doi.org/10.1007/978-3-642-16422-4_3
- Inskipp C, Inskipp T, Winspear R, Collin P, Robbin A (2008) Bird survey of the Kanchenjunga Conservation Area, April 2008. Report to Critical Ecosystem Partnership Fund. Bird Conservation Nepal and Royal Society for the Protection of Birds. Bird Conservation Nepal, Kathmandu, and Royal Society for the Protection of Birds, Sandy, UK. http://himalaya.socanth.cam.ac.uk/collections/inskip/2008_005.pdf
- Joshi NC, Joshi PC, Kumar S, Nath P, Singh VK, Mansotra D (2016) Entomofaunal diversity in fruit orchards along the altitudinal gradients of district Nainital, Uttarakhand (India). International Journal of Fauna and Biological Studies 3: 113–120. <https://doi.org/10.22271/23940522>
- Joshi PC, Kumar K, Arya M (2008) Assessment of insect diversity along an altitudinal gradient in Pindari Forests of Western Himalayas, India. Journal of Asia-Pacific Entomology 11: 5–11. <https://doi.org/10.1016/j.aspen.2008.02.002>
- Joshi SR, Ahmad F, Gurung MB (2004) Status of *Apis laboriosa* populations in Kaski district, western Nepal. Journal of Apicultural Research 43: 176–180. <https://doi.org/10.1080/00218839.2004.11101133>
- Khan KA, Ansari MJ, Al-Ghamdi A, Sharma D, Ali H (2014) Biodiversity and relative abundance of different honeybee species (Hymenoptera: Apidae) in Murree-Punjab, Pakistan. Journal of Entomology and Zoology Studies 2(4): 324–327.
- Kirchner WH, Dreller C, Grasser A, Baidya D (1996) The silent dance of the Himalayan honeybee, *Apis laboriosa*. Apidologie 27: 331–339. <https://doi.org/10.1051/apido:19960501>
- Kuang BY, Li YC (1985) The genus *Apis* in China. Chinese Beekeeping 76: 7–9. [Chinese]
- Lo N, Gloag RS, Anderson DL, Oldroyd BP (2010) A molecular phylogeny of the genus *Apis* suggests that the giant honey bee of the Philippines, *A. breviligula* Maa, and the plains honey bee of southern India, *A. indica* Fabricius, are valid species. Systematic Entomology 35: 226–233. <https://doi.org/10.1111/j.1365-3113.2009.00504.x>
- Maa TC (1953) An inquiry into the systematics of the tribus Apidini or honeybees (Hym.) Treubia 21: 525–640.
- Magrath HAF (1909) Bird notes from Murree and the Galis. Journal of the Bombay Natural History Society 19: 142–156.
- McEvoy MV, Underwood BA (1988) The drone and species status of the Himalayan honey bee, *Apis laboriosa* (Hymenoptera). Journal of the Kansas Entomological Society 61: 246–249.
- Moore F, Walker F, Smith F (1871) Descriptions of some new insects collected by Dr. Anderson during the expedition to Yunnan. Proceedings of the Zoological Society of London 1871: 244–249.
- Mutharaman M, Raju AJS, Vijaykumar J, Devanesan S, Abrol DP, Viraktamath S (2013) Morphometry of rock bee, *Apis dorsata* Fabricius. In: Viraktamath S, Fakrudin B, Vas-trad AS, Mohankumar S (Eds) Monograph on the morphometry and phylogeography of honey bees and stingless bees in India, 5–13. Network Project on Honey bees and

- Stingless bees. Department of Agricultural Entomology. University of Agricultural Sciences Dharwad, India.
- Muzaffar N, Ahmed R (1990) *Apis* spp. (Hymenoptera: Apidae) and their distribution in Pakistan. *Pakistan Journal of Agricultural Research* 11: 65–69.
- Nidup T, Dorji P (2016) The honey bees (Hymenoptera: Apidae) of Bhutan with a key to the *Apis* species. *Biology Bulletin* 2(2): 01–07.
- Oldroyd BP, Wongsiri S (2006) *Asian Honey Bees. Biology, Conservation, and Human Interactions*. Harvard University Press, Boston, MA.
- Otis GW (1996) Distributions of recently recognized species of honey bees (Hymenoptera: Apidae; *Apis*) in Asia. *Journal of Kansas Entomological Society* 69: 311–333.
- Otis GW, Koeniger N, Rinderer TE, Hadisoeso S, Yoshida T, Tingek S, Wongsiri S, Mardan M (2000) Comparative mating flight times of Asian honeybees. In: (IBRA/AAA) Proceedings of the 7th International Conference on Tropical Bees: Management and Diversity. 5th Asian Apicultural Association Conference. 137–141.
- Raffiudin R, Crozier RH (2007) Phylogenetic analysis of honey bee behavioral evolution. *Molecular Phylogenetics and Evolution* 43: 543–552. <https://doi.org/10.1016/j.ympev.2006.10.013>
- Roubik WD, Sakagami SF, Kudo I (1985) A note on distribution and nesting of the Himalayan honey bee *Apis laboriosa* Smith (Hymenoptera: Apidae). *Journal of the Kansas Entomological Society* 58: 746–749.
- Sakagami S F, Matsumura T, Ito K (1980) *Apis laboriosa* in Himalaya, the little known world largest honeybee (Hymenoptera: Apidae). *Insecta Matsumurana* 19: 47–77.
- Takahashi JI, Rai J, Wakamiya T, Okuyama H (2018) Characterization of the complete mitochondrial genome of the giant black Himalayan honeybee (*Apis laboriosa*) from Nepal. *Conservation Genetics Resources* 10: 59–63. <https://doi.org/10.1007/s12686-017-0765-6>
- Tan NQ, Mardan M, Thai PH, Chinh PH (1999) Observations of multiple mating flights of *Apis dorsata* queens. *Apidologie* 30(4): 339–346. <https://doi.org/10.1051/apido:19990410>
- Tayeng M, Gogoi H (2018) Insect pollinators of crops and fruits in Arunachal Pradesh, eastern Himalaya: rich diversity in flowers with yellow anther. *Proceedings of the Zoological Society* 71: 56–62. <https://doi.org/10.1007/s12595-016-0185-8>
- Team NBHM (2015) In search of the giant honey bees & the honey hunters. Team NBHM travelogue to Khongjiri village Kiphire, Nagaland. *Apinews* 8: 16–19, Nagaland Beekeeping and Honey. <http://www.nbhm.in/apinews/>
- Trung LQ, Dung PX, Ngan TX (1996) A scientific note on first report of *Apis laboriosa* F Smith, 1871 in Vietnam. *Apidologie* 27: 487–488. <https://doi.org/10.1051/apido:19960608>
- Turin, R, Heegaard M, Priemé A (1987) Northern Part of the Indian Subcontinent 87: 30 pp, unpublished. (www.digitalhimalaya.com/collections/birdsofnepal/bon.html [see Supplementary file 1: Collection Locality Information])
- Underwood BA (1990a) Seasonal nesting cycle and migration patterns of the Himalayan honey bee *Apis laboriosa*. *National Geographic Research* 6: 276–290.
- Underwood BA (1990b) Time of drone flight of *Apis laboriosa* Smith in Nepal. *Apidologie* 21: 501–504. <https://doi.org/10.1051/apido:19900602>

- Underwood BA (1991) Thermoregulation and energetic decision-making by the honeybees *Apis cerana*, *Apis dorsata* and *Apis laboriosa*. *Journal of Experimental Biology* 157: 19–34. <https://doi.org/10.1016/j.jinsphys.2010.08.002>
- Underwood BA (1992) Notes on the orange-rumped honeyguide *Indicator xanthonotus* and its association with the Himalayan honey bee *Apis laboriosa*, *J. Bombay Nat. Hist. Soc.* 89: 290–295. <https://www.biodiversitylibrary.org/part/156573>.
- Woyke J, Wilde J, Wilde M (2001) A scientific note on *Apis laboriosa* winter nesting and brood rearing in the warm zone of Himalayas. *Apidologie* 32(6): 601–602. <https://doi.org/10.1051/apido:2001104>
- Woyke J, Wilde J, Wilde M (2012) Swarming and migration of *Apis dorsata* and *Apis laboriosa* honey bees in India, Nepal and Bhutan. *Journal of Apicultural Science* 56: 81–91. <https://doi.org/10.2478/v10289-012-0009-7>
- Woyke J, Wilde J, Wilde M, Sivaram V, Cervancia C, Nagaraja N, Reddy M (2008) Comparison of defense body movements of *Apis laboriosa*, *Apis dorsata dorsata* and *Apis dorsata breviligula* honey bees. *Journal of Insect Behavior* 21: 481–494. <https://doi.org/10.1007/s10905-008-9144-1>

Supplementary material I

Collection locality information

Authors: Nyaton Kitnya, M.V. Prabhudev, Chet Prasad Bhatta, Thai Hong Pham, Tshering Nidup, Karsing Megu, Jharna Chakravorty, Axel Brockmann, Gard Otis

Data type: Excel spreadsheet

Explanation note: Abbreviations as follows – Type of data: Author’s observation (1), Photo from website (2), Publications (3), Personal communication (4). Source of Information: Authors’ initials- Chet Prasad Bhatta (CPB), Gard Williams Otis (GWO), Karsing Megu (KM), Nyaton Kitnya (NK), M.V. Prabhudev (MVP), Thai Hong Pham (THP), Tsering Nidup (TN); Organizations and Museums: Nagaland Beekeeping and Honey Mission (NBHM), Natural History Museum United Kingdom (NHMUK), National Museum of Natural History, US (USNM), Rijksmuseum of Natural History, Leiden, the Netherlands (RNH). Sakagami et al. (1980) and Underwood (1990a) numbered localities in their papers. Asterisks (*) indicate sites where *A. laboriosa* and *A. dorsata* occurred sympatrically.

Copyright notice: This dataset is made available under the Open Database License (<http://opendatacommons.org/licenses/odbl/1.0/>). The Open Database License (ODbL) is a license agreement intended to allow users to freely share, modify, and use this Dataset while maintaining this same freedom for others, provided that the original source and author(s) are credited.

Link: <https://doi.org/10.3897/zookeys.951.49855.suppl1>

A new species of the genus *Caissa* Hering, 1931 from Yunnan, China (Lepidoptera, Limacodidae)

Jun Wu¹, Chun-Sheng Wu², Hui-Lin Han¹

1 School of Forestry, Northeast Forestry University, Harbin, 150040, China **2** Key Laboratory of Zoological Systematics and Evolution, Institute of Zoology, Chinese Academy of Sciences, Beijing 100101, China

Corresponding author: Hui-Lin Han (hanhuilin@aliyun.com)

Academic editor: J. Adams | Received 11 April 2020 | Accepted 23 June 2020 | Published 22 July 2020

<http://zoobank.org/2BE08BA2-B4B7-4711-B2F0-D6BF26899AF5>

Citation: Wu J, Wu C-S, Han H-L (2020) A new species of the genus *Caissa* Hering, 1931 from Yunnan, China (Lepidoptera, Limacodidae). ZooKeys 951: 83–89. <https://doi.org/10.3897/zookeys.951.53151>

Abstract

A new species, *Caissa yunnana* **sp. nov.** is described from Yunnan Prov., China. The new species is illustrated with images of the adult habitus and male genitalia, and compared with the similar species *C. caissa* Hering, 1931. A world checklist of the genus *Caissa* Hering, 1931 is provided

Keywords

Caissa, China, Lepidoptera, Limacodidae, new species

Introduction

The genus *Caissa* Hering, 1931, a member of the family Limacodidae, is based on the type species *C. caissa* Hering, 1931. Hering (1931) first established the genus *Caissa*, which included two newly described species, *C. caissa* and *C. gambita* from India. Later, Yoshimoto (1994) described another species, *C. medialis* from Nepal; Orhant (2000) described *C. parenti* from Myanmar; Solovyev and Witt (2009) described two

species, *C. aurea* and *C. bezverkhovi* from Vietnam; Solovyev and Saldaitis (2014) provided several images of adults and genitalia in their paper, including of the type species. The species *C. fasciatum* (Hampson, 1893) was originally described as *Ceratonema fasciatum* by Hampson (1892), then Solovyev (2009) moved it to the genus *Caissa*. Recently, Irungbam et al. (2017) reported the distribution of *C. fasciatum* in Bhutan. In China, the first recorded species of this genus was *C. gambita* (Cai 1981). Subsequently, three new species (*C. longisaccula* Wu & Fang, 2008, *C. caii* Wu & Fang, 2008 and *C. staurognotha* Wu, 2011) and one newly recorded species (*C. parenti* Orhant, 2000) were reported (Wu and Fang 2008; Wu 2011). In 2013, another species, *C. kangdinga* Solovyev & Saldaitis, 2013, was described from Kangding in Sichuan, China.

The features common to the genus are filiform male antennae, labial palpus somewhat appressed and upcurved, not quite reaching the vertex. The forewing has an obvious dark medial band, and the hindwing has a dark tornal spot. The species of the genus are diverse in external morphological characters, in wing venation, and in male genitalia. According to Solovyev and Witt (2009), three species groups can be distinguished within the genus by external characters and male genitalia. The first group contains the type species *C. caissa* and the new species *C. yunnana* sp. nov. This group is characterized by the following characters: forewing ground color is dark brown, with unequal-sized white patches; the tornus contains 2 to 4 whitish spots; the terminal area is white, forming a nearly right triangle; in the male genitalia, the bifurcation of the sacculus process is thin, and the terminal part of the juxta is strongly sclerotized, with dense black spurs; the phallus is slightly curved, and the coecum is very short.

The second group includes *C. fasciatum*, *C. gambita*, *C. longisaccula*, *C. aurea* and *C. bezverkhovi*. This group is characterized as follows: the forewing ground color is pale yellow, with an oblique pale medial line, which is embedded in the black-brown medial band, running from 1/2 costal margin to 1/3 inner margin; the postmedial line is very indistinct or almost absent; there are 1 or 2 small black spots near the apex of the terminal line and a dark spot near the base of vein CuP; in the male genitalia, the cucullus is round; the sacculus is significantly inflated, about half the length of the valva; the broad bifurcation of the sacculus process is triangular blade shaped or finger-like; the phallus is curved, and the coecum is short.

The third group includes *C. medialis*, *C. parenti*, *C. caii*, *C. staurognotha* and *C. kangdinga*. This group is characterized as follows: the forewing medial band is black or brown, without an embedded pale medial line; the inner border of the medial band runs from 1/3 the distance from the wing base on the costal margin, to 2/5 from the wing base on the inner margin, and the outer border runs from 2/5 from the wing base on the costal margin, to 3/5 from the wing base on the inner margin; the arcuate postmedial line is distinct; in the male genitalia, the gnathos is varied, well developed or reduced; the terminal part of the juxta has a distinct elongation; the inflated part of the sacculus is short, about 1/3 length of the valva; the sacculus process is not forked; the phallus is straight, and the coecum is rather longer than in the other two groups, over 1/3 length of the phallus.

Here we describe a new species from Yunnan Province in southwest China. Based on the features of the forewing with unequal-sized white patches, the white terminal

area forming a nearly right triangle, and the terminal part of juxta strongly sclerotized, U-like, with dense black spurs, it is assigned to the first group. The genus now includes 11 species, six of which are distributed in China.

Material and methods

The specimens were collected at 220 V/450 W mercury light and DC black light in Yunnan Province, China. Standard methods for dissection and preparing of the genitalia slides were used (described by Kononenko and Han 2007). Specimens were photographed using a Nikon D700 camera; the genitalia slides were photographed using an Olympus photo microscope aided by the Helicon Focus software, and further processed in Adobe Photoshop CS6. The type material of the new species is deposited in the collection of Northeast Forestry University, Harbin, China (NEFU).

Taxonomic account

Genus *Caissa* Hering, 1931

Caissa Hering, 1931, in Seitz, *Macrolep. World*, 10: 670, 700. Type species: *Caissa caissa* Hering, 1931 [India: Khasis Hills].

Caissa yunnana sp. nov.

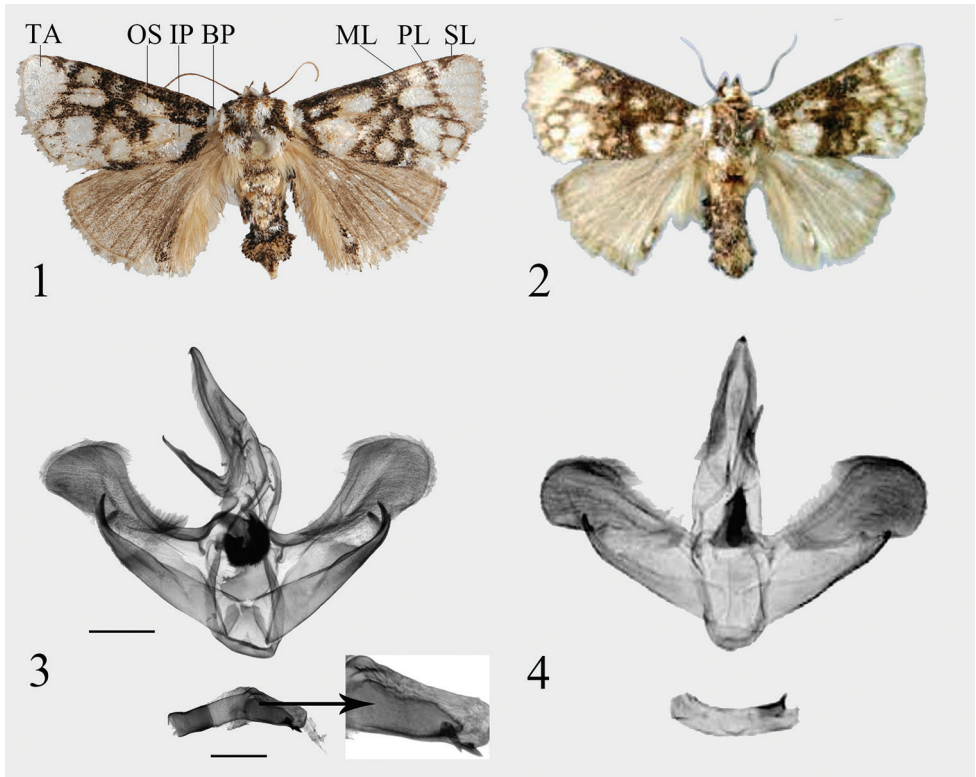
<http://zoobank.org/2BE08BA2-B4B7-4711-B2F0-D6BF26899AF5>

Figures 1, 3

Holotype. ♂, China, Yunnan Province, Lvchun County, Mt. Huanglian, 27–31. VII.2018, leg. HL. Han, J. Wu, MR. Li [NEFU], genit. prep. WuJ-069-1.

Paratypes. 3♂, same data as holotype [NEFU], genit. prep. for one dissected paratype WuJ-068-1.

Description. Adult (Fig. 1). Wingspan 29–31 mm in male. Head white, labial palpus and patagium brown. The male antennae filiform, brown; the thorax mixed white and brown, the tegula white with brown margin; dorsally abdomen yellowish brown to dark brown, ventrally white or yellowish brown. Forewing ground color dark brown, with unequal-sized white patches; light-colored basal patch small, not connected with inner patch; orbicular spot large, broadly connected to the larger inner patch; two medium-sized white patches lie in the middle of the forewing, near the inner margin, distal to the medial line which runs from the costal margin at 1/2 the distance from the wing base, to the inner margin at 1/3 from the wing base; arcuate postmedial line from the costal margin at 2/3 from the wing base to the tornus; postmedial area with 4 large whitish spots, the tornus with 2 whitish spots; subterminal line curved strongly



Figures 1–4. *Caissa* spp., adults: **1** *C. yunnana* sp. nov., male, holotype **2** *C. caissa* Hering, 1931, male, holotype (after Solovyev and Saldaitis 2014); male genitalia: **3** *C. yunnana* sp. nov., holotype **4** *C. caissa* Hering, 1931, holotype (after Solovyev and Saldaitis 2014). Scale bars: 1 mm. (BP: basal patch; IP: inner patch; ML: medial line; OS: orbicular spot; PL: postmedial line; SL: subterminal line; TA: terminal area).

inward, from apex to the outer margin at $3/5$ from the apex, combined with postmedial line on R_5 ; terminal area white, forming a nearly right triangle. Hindwing brown and mixed with a small amount of red, anal area light brown with oblong dark blotch with a white spot inside. The white spot is much smaller than the encircling brown.

Male genitalia (Fig. 3). Uncus slender, with a small subapical spur. Gnathos well developed, very straight rod-shaped terminal part with slightly curved apex. The base of valva wider than middle; the cucullus wide and round; costa simple, slightly shorter than valve; sacculus sclerotized and shorter than costa, sacculus process bifurcated, distinctly incurved and hook-shaped. Juxta asymmetrical, the right side of terminal part strongly sclerotized, U-like, with dense black spurs. Saccus inconspicuous. Phallosus curved, weakly sclerotized, bent into an obtuse angle in the middle; $1/2$ of the terminal part with a strongly sclerotized wedge-shaped area; the terminal part of carina sclerotized, short, cone-shaped; vesica with big cyst, surface covered with small spines, with a big, sclerotized cornutus.

Female genitalia. Unknown.

Diagnosis. The new species is similar in appearance to *C. caissa* (Fig. 2), but can be distinguished from the latter by the characters of the forewing and male genitalia, as follows. In *C. yunnana* the light-colored basal patch is small, not connected with the inner patch; orbicular spot large, connected with the inner patch (Fig. 1); in *C. caissa*, the basal patch is bigger than in *C. yunnana*, and it is broadly connected with the inner patch, but not connected with the small orbicular spot. Also, the tornus of *C. yunnana* contains only 2 whitish spots, but the same location in *C. caissa* contains 4 whitish spots. The color of the hindwing in *C. yunnana* is darker than in *C. caissa*.

In the male genitalia, the new species clearly differs from *C. caissa* (Fig. 4) by the sclerotized area of the sacculus being wider than the same area in *C. caissa*; in *C. yunnana* the sacculus process is bifurcate, distinctly incurved and hook-shaped, whereas in *C. caissa* it is short, and although bifurcate, barely hooked. The phallus of *C. yunnana* differs from that of *C. caissa* by the middle being bent into an obtuse angle, 1/2 of the terminal part with a strongly sclerotized wedge-shaped area, and the vesica with a big cyst and a big sclerotized cornutus. The phallus of *C. caissa* is smoothly curved, and the vesica is membranous, without a cyst or cornutus.

Distribution. China (Yunnan Province: Mt. Huanglian) (Fig. 5).

Etymology. The species is named for its type locality in Yunnan Province, China.

Bionomics. The moths fly in July. The specimens were collected with a light trap close to a broad-leaved forest with ferns and shrubs (Fig. 6).



Figures 5, 6. Map and habitat of *C. yunnana* sp. nov. **5** Collecting site of *C. yunnana* sp. nov.: Yunnan Prov., Mt. Huanglian (red dot) **6** Collecting site close to a broad-leaved forest with ferns and shrubs.

World checklist of the genus *Caissa*, with type localities

Group 1:

- C. caissa* Hering, 1931 (India: Khasis Hills)
C. yunnana Wu, Wu & Han, sp. nov. (China: Yunnan)

Group 2:

- C. fasciatum* (Hampson, 1893) (India: Nágas)
C. longisaccula Wu & Fang, 2008 (China: Fujian)
C. gambita Hering, 1931 (India: Travancore)
C. aurea Solovyev & Witt, 2009 (Vietnam: Lao Cai)
C. bezverkhovi Solovyev & Witt, 2009 (Vietnam: Nghe An)

Group 3:

- C. kangdinga* Solovyev & Saldaitis, 2013 (China: Sichuan)
C. caii Wu & Fang, 2008 (China: Shaanxi)
C. parenti Orhant, 2000 (Myanmar: Maymyo)
C. medialis Yoshimoto, 1994 (Nepal: Kathmandu)
C. staurognatha Wu, 2011 (China: Sichuan)

Acknowledgments

The present study was supported by the National Nature Science Foundation of China (No. 31872261, 31572294), and the Fundamental Research Funds for the Central Universities (No. 2572019CP11). We also thank the staff of Huanglianshan Nature Reserve in Yunnan for their support in our collection work.

References

- Cai RQ (1981) Limacodidae. Iconographia Heterocerorum Sinicorum 1. Science Press, Beijing, 97–104. [In Chinese]
- Hampson GF (1892) The Fauna of British India, including Ceylon and Burma. Vol. I. Taylor and Francis, London, 527 pp.
- Hering M (1931) Limacodidae. In: Seitz A (Ed.) Die Gross-Schmetterlinge der Erde, 10. Alfred Kernen Verlag, Stuttgart, 665–728.
- Irungbam JS, Chhib MS, Solovyev AV (2017) Moths of the family Limacodidae Duponchel, 1845 (Lepidoptera: Zygaenoidea) from Bhutan with six new generic and 12 new species records. Journal of Threatened Taxa 9(2): 9795–9813. <https://doi.org/10.11609/jott.2443.9.2.9795-9813>

- Kononenko VS, Han HL (2007) Atlas Genitalia of Noctuidae in Korea (Lepidoptera). In: Park K-T (Ed.) Insects of Korea (Series 11). Junhaeng-Sa, Seoul, 464 pp.
- Orhant GERJ (2000) New species of Limacodidae from Myanmar and Thailand (Lepidoptera, Limacodidae). *Lambillionea* 100(3): 471–474. [Tome 2]
- Solovyev AV, Witt ThJ (2009) The Limacodidae of Vietnam. *Entomofauna, Supplement*. No. 16: 33–229.
- Solovyev AV, Saldaitis A (2013) A new species of *Caissa* Hering, 1931 (Lepidoptera, Limacodidae) from China. *Zootaxa* 3693 (1): 97–100. <https://doi.org/10.11646/zootaxa.3693.1.8>
- Solovyev AV, Saldaitis A (2014) *Pseudohampsonella*: a new genus of Limacodidae (Lepidoptera: Zygaenoidea) from China, and three new species. *Journal of Insect Science* 14, 46. <https://doi.org/10.1673/031.014.46>
- Wu CS (2011) Six new species and twelve newly recorded species of Limacodidae from China (Lepidoptera, Zygaenoidea). *Acta Zootaxonomica Sinica* 36(2): 249–256.
- Wu CS, Fang CL (2008) A review of the genus *Caissa* Hering in China (Lepidoptera: Limacodidae). *Zootaxa* 1830(1): 63–68. <https://doi.org/10.11646/zootaxa.1830.1.6>
- Yoshimoto H (1994) Limacodidae. In: Haruta T (Ed.) *Moths of Nepal, Part 3. Tinea*, 14(Suppl. 1): 85–89.

Facultative amphidromy and pelagic larval duration plasticity of *Rhinogobius formosanus* (Teleostei, Gobioidaei)

Te-Yu Liao¹, Wen-Chien Huang^{2,3}, Yoshiyuki Iizuka⁴,
Ming-Tai Chou⁵, Jen-Chieh Shiao⁶

1 Department of Oceanography, National Sun Yat-sen University, Kaohsiung 804, Taiwan **2** Doctoral Degree Program in Marine Biotechnology, National Sun Yat-sen University, Kaohsiung 804, Taiwan **3** Doctoral Degree Program in Marine Biotechnology, Academia Sinica, Taipei 115, Taiwan **4** Institute of Earth Sciences, Academia Sinica, Taipei 115, Taiwan **5** Printech Electronics Corporation, New Taipei 235, Taiwan **6** Institute of Oceanography, National Taiwan University, Taipei 106, Taiwan

Corresponding author: Jen-Chieh Shiao (jcshiao@ntu.edu.tw)

Academic editor: N. Bogutskaya | Received 24 January 2020 | Accepted 6 April 2020 | Published 22 July 2020

<http://zoobank.org/4747CCE5-C044-48E5-A2FC-ACBE8F868899>

Citation: Liao T-Y, Huang W-C, Iizuka Y, Chou M-T, Shiao J-C (2020) Facultative amphidromy and pelagic larval duration plasticity of *Rhinogobius formosanus* (Teleostei, Gobioidaei). ZooKeys 951: 91–107. <https://doi.org/10.3897/zookeys.951.50429>

Abstract

Rhinogobius formosanus Oshima, 1919 has long been considered an amphidromous goby. However, a landlocked population recently found in the Jingtualiao Creek upstream of the Feitsui Reservoir in Taipei suggests that *R. formosanus* may complete its life in the river. This study aims to verify the habitat use of the landlocked population of *R. formosanus* collected from the Feitsui Reservoir and an amphidromous population collected in Malian Creek using otolith Sr:Ca ratio analysis. The hypothesis that early life history varies between the landlocked and migratory gobies was also tested. Genetic analyses show that the Feitsui Reservoir and Malian Creek populations are not genetically different. *Rhinogobius formosanus* from Malian Creek showed high-to-low otolith Sr:Ca ratios suggesting that these specimens spent a planktonic larval stage in the sea followed by a freshwater life at later stages. In contrast, *R. formosanus* from the Feitsui Reservoir showed constant lower otolith Sr:Ca ratios, implying a landlocked life history of fish in the creek upstream of the reservoir. In addition, the analysis of growth increments showed a longer pelagic larval duration for the fish in the Malian Creek (58.8 days) than those in the Feitsui Reservoir (38.8). Variation of pelagic larval duration in two genetically homogenous populations implies acclimatization to

the reservoir by the landlocked gobies. This study shows that *R. formosanus*, like some other congeners, is capable of adapting to a freshwater landlocked environment in its early developmental stage and supports the hypothesis that landlocked populations may have a shorter pelagic larval duration.

Keywords

COI sequences, diadromous, goby, landlocked, otolith

Introduction

Amphidromy is a diadromous behavior that applies to larvae living in the estuary or sea followed by the post-larvae return to a river where the fish are hatched (McDowall 2007). Amphidromous fishes are more common in the tropics and their planktonic larvae in the sea may facilitate distant dispersal (Lester and Ruttenberg 2005). Amphidromous gobies showed diverse life history traits, distribution ranges and genetic structure among populations. *Sicyopterus japonicus* Tanaka, 1909 and *S. lagocephalus* Pallas, 1770, for example, are two small amphidromous gobies with a long pelagic larval duration (PLD) of 133 to 266 days and distributed across ranges of c. 2400 and 18000 km, respectively (Shen and Tzeng 2002; Hoareau et al. 2007; McDowall 2007). The dispersal of the former is documented by genetic homogeneity across the distribution range (Watanabe et al. 2006; Ju et al. 2013), but the later shows high population structure across the Indo-Pacific Barrier (Lord et al. 2012). Narrowly endemic species, such as *Sicyopterus aiensis* Keith, Watson & Marquet, 2004 and *S. sarasini* Weber & de Beaufort, 1915 have relatively shorter PLD's of c. 80 days and do not display genetic structure across their distribution areas in Vanuatu and New Caledonia, respectively (Lord et al. 2010, 2012).

The reconstruction of ontogenetic life stages of fish at different habitats usually relies on the analysis of otolith microstructure and chemical compositions. Fish otolith is a biomineralized structure that accretes with time by adding a growth increment on the surface (Campana and Neilson 1985; Rogers et al. 2019). Counting otolith daily growth increments can reconstruct ontogenetic stages, such as PLD and demersal life stage. In addition, otolith strontium:calcium (Sr:Ca) ratios are extensively applied to study the migration between the sea and rivers for various fishes (Tzeng et al. 2002; Shiao et al. 2016; Lozys et al. 2017; Tran et al. 2019). This is because the higher Sr concentration in sea water than in fresh water allows marine fish to deposit relatively higher Sr contents in the otolith (Campana 1999; Brown and Severin 2009).

The genus *Rhinogobius* Gill, 1859 is a group of small fishes distributed in East Asia. Species of this genus are splendid and colorful and becoming popular in the aquarium trade. Various life histories are observed in *Rhinogobius*, including amphidromous and landlocked forms (Tsunagawa and Arai 2008; Shiao et al. 2015; Yamasaki et al. 2015), while some species, such as *R. candidianus* (Regan, 1908) and three undescribed species from Japan were considered facultatively amphidromous, and either migratory or landlocked depending on whether passage to the sea is possible (Tsunagawa and

Arai 2008). *Rhinogobius formosanus* Oshima, 1919 (Fig. 1) is a colorful goby easily distinguished from its syntopic congeners by numerous irregular stripes on the cheek. This species is sexually dimorphic with an extended first dorsal fin, longer snout, and intensive coloration in adult males while gravid females have a bluish abdomen (Chen and Fang 1999). *Rhinogobius formosanus* is distributed in northern Taiwan and Fujian, China (Chen and Fang 1999; Yuan et al. 2012) and has long been considered an amphidromous fish (Chen and Fang 1999), inhabiting running water close to the tidal reach of small tributaries and creeks directly connected to the sea. Chen and Fang (1999) stated that *R. formosanus* could be landlocked, but detailed information was not provided. Recently, a population of *R. formosanus* was found upstream of the Feitsui Reservoir (FR) in Taipei. This population may be landlocked, since the dam of 122.5 m height completely blocks upstream migration of aquatic life. Even if the fish larvae survive the downstream passage from the reservoir, the juvenile and adult fish cannot return upstream of the dam (Chang et al. 1999). The Feitsui Reservoir was built at the upper reaches of Tamsui River in 1987, so the FR population has probably been landlocked since then if this species was native to that area, or afterwards if it was artificially released.

Based on the above facts, this study aims to test two hypotheses. First, *R. formosanus* upstream of FR reside in the river for their whole life while conspecifics not blocked by dams are amphidromous. Secondly, we hypothesize that the landlocked goby will have a shorter larval planktonic stage than amphidromous conspecifics since the later may spend more time drifting to the sea during the early larval stage, dispersing away from the coasts, then returning to the estuary at the post-larval stage. To test the hypotheses, the early life history of the fish was reconstructed by reading daily growth increments and analyzing otolith Sr:Ca ratios. In addition, mitochondrial cytochrome oxidase subunit I (*COI*) fragments were sequenced to provide molecular data of genetic differentiation between landlocked and amphidromous populations in order to infer the landlocked life history, if any, as a consequence of acclimation or adaptation.

Material and methods

Samplings

A total of 20 specimens of *R. formosanus* were collected from two creeks in northern Taiwan: Jingualiao Creek, which flows into the upstream area of FR, representing a landlocked population with syntopic congeners *R. candidianus* and *R. similis* Gill, 1859; and Malian Creek (MLC), representing an amphidromous population with syntopic congener *R. similis*, directly connected to the sea (Fig. 2; Table 1). The FR dam is approximately 50 km away from the Tamsui River mouth and the sampling site at the Jingualiao Creek was approximately 20 km upstream of the reservoir dam. Sampling sites for MLC were approximately 1 km away from stagnant water and 2 km away



Figure 1. *Rhinogobius formosanus*. Male; approximately 7 cm TL, specimen not preserved.

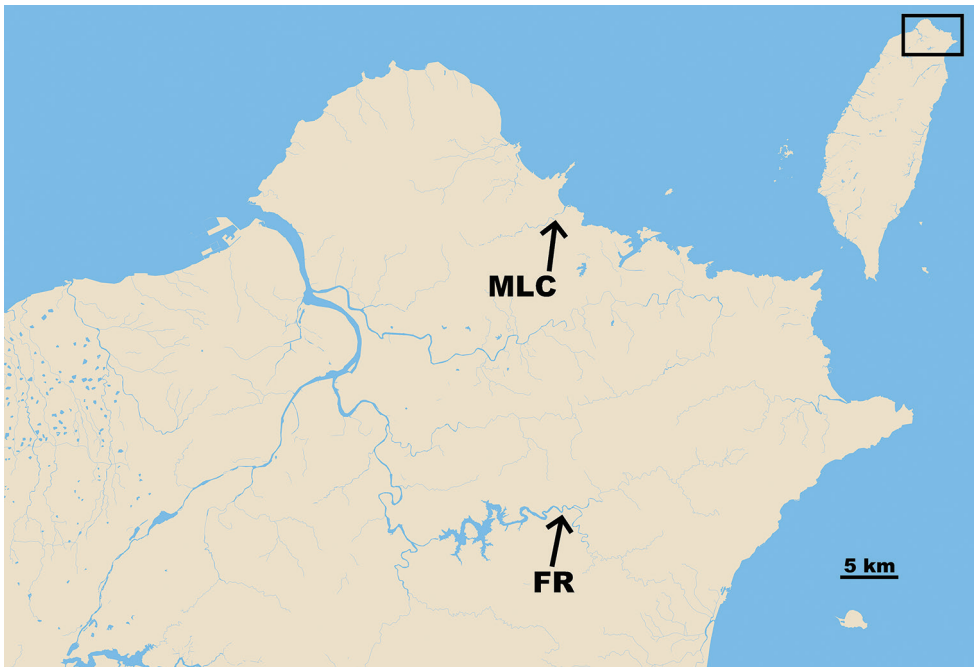


Figure 2. Sampling localities of *Rhinogobius formosanus* in Taiwan. Location codes are given in Table 1. FR, Feitsui Reservoir (GPS: 24°55'46.8"N, 121°41'29.6"E), representing a landlocked population; MLC, Malian Creek (GPS: 25°10'17.2"N, 121°40'47.7"E), representing an amphidromous population.

Table 1. Sampling locations and diversity indices of *COI* fragment of *Rhinogobius formosanus*. *N* for sample size of molecular analyses; *n* for sample size of otolith study; *h* for haplotype diversity; π for nucleotide diversity.

Locality	Abb.	<i>N</i>	<i>n</i>	<i>COI</i> sequence/ haplotypes	<i>h</i> ± SD	π ± SD
Feitsui Reservoir	FR	10	8	10/2	0.200 ± 0.154	0.00036 ± 0.00028
Malian Creek	MLC	10	5	10/5	0.800 ± 0.100	0.00244 ± 0.00064
	Total	20	13	20/6	0.574 ± 0.122	0.00161 ± 0.00046

from the river mouth while sampling site for FR was 10–20 m away from the lentic reservoir. Both sampling sites were lotic. All specimens were collected using a hand net and anesthetized immediately after capture. They were brought back to the lab for further molecular and otolith analyses. All specimens were preserved in 95% ethanol, cataloged and deposited in the collection of the Department of Oceanography, National Sun Yat-sen University (DOS), Kaohsiung. The voucher numbers of specimens are as follow: FR, DOS 03534–2, –11, –14, –15, –16, –19, –33, –35, –36, –37; MLC, DOS 02416–1, –2, –5, –6, –7, –12, –13, –15, –20, –22. All the procedures in this study were approved by the “Institutional Animal Care and Use Committee of National Taiwan University”.

Molecular analyses

DNA was extracted from fin clips using GeneMark DNA Purification Kit (GMbiolab, Taichung, Taiwan). The mitochondrial *COI* gene was amplified by polymerase chain reaction (PCR) with universal primers designated by Ward et al (2005): FishF1 (5'-TCAACCAACCACAAAGACATTGGCAC-3') and FishR1 (5'-TAGACTTCTGGGTGGCCAAAGAATCA-3'). The total reaction volume of the PCR was 25 μ L, containing 1 μ L of template DNA (50–200 ng μ L⁻¹), 3 μ L of 10 \times buffer, 2 μ L of dNTPs (2.5 mM), 1.2 μ L of each primer (10 μ M), 0.13 μ L of Pro-Taq Plus polymerase (Protech, Taipei) and 16.47 μ L of deionized water. PCR cycling conditions included an initial denaturation at 94 °C for 5 min, followed by 36 cycles of denaturing at 94 °C for 30 sec, annealing at 50 °C for 30 sec, and extension at 70 °C for 1 min, and a final extension at 72 °C for 8 min. After checking qualities by electrophoresis, PCR products were purified using the SAP-Exo purification kit (Jena Bioscience, Jena) according to the manufacturer's protocols. Sequencing was conducted by an ABI 3730 automated sequencer. Newly generated sequences were edited manually using MEGA version X (Kumar et al. 2018) and translated into amino acids to ensure absence of insertions, deletions, or stop codons. All sequences used in this study were submitted to the GenBank online database (Accession numbers MN187015–MN187034).

The genetic diversity indexes of haplotype diversity (*h*) and nucleotide diversity (π) were calculated in DnaSP version 6 (Rozas et al. 2017). A minimum spanning network of haplotypes was reconstructed by PopART version 1.7 (Leigh and Bryant 2015) to infer the interrelationships among the haplotypes.

Measurement of otolith Sr:Ca ratios and growth increments

Sagittal otoliths were extracted from eight and five specimens from the FR and MLC populations, respectively. The otoliths were cleaned and embedded in Epofix resin (Struers, Denmark) before repeated grinding and polishing along the sagittal plane until the core was revealed on the surface. The otoliths were coated with a layer of carbon (Q150TE, Quorum Technologies Ltd., UK) to increase the electron conductance when the otoliths were analyzed by the electron probe microanalyzer (EPMA, JEOL JXA-8900R, JEOL, Japan). Quantitative analyses of Sr and Ca were conducted along a transect from the otolith core to the edge at 10 μm intervals. Electron beam conditions were 15 kV for the acceleration voltage and 3 nA for the current, with a $5 \times 4 \mu\text{m}$ rectangular scanning beam size. The wavelength dispersive spectrum at the Sr $L\alpha$ peak position was measured for 80 s and each of the upper and lower baselines for 20 s. The peak concentration of Ca $K\alpha$ was measured for 20 s and each of the upper and lower baselines for 10 s. Synthesized strontianite [(Sr_{0.95}Ca_{0.05})CO₃; NMNH R10065] and aragonite (CaCO₃) were used as standards to calibrate the concentration of Ca and Sr, respectively, in the otoliths. The Sr:Ca ratios were calculated after a correction using the PRZ (phi-rho-z) method (Goldstein et al. 1992). The detection limits were better than 500 ppm for Ca and Sr and the analytical errors were smaller than 0.05 wt% in Sr (Iizuka 2012). The otolith Sr:Ca ratios $< 4 \times 10^{-3}$ and $> 5 \times 10^{-3}$ were regarded as freshwater and marine residences, respectively. The values between 4×10^{-3} and 5×10^{-3} represent the transition between river and marine habitats.

After the analysis of otolith Sr:Ca ratios, the otoliths were polished to remove the carbon coating and etched with 0.1 M HCl for 10–15 s to enhance the contrast of growth increment observed under a compound light microscope (Olympus BX 51, Japan). Two experienced researchers counted the otolith growth increments from the core to a high-contrast growth increment (an otolith check), or to a structural transition from clear concentric rings to ambiguous growth increments. This otolith check, appearing at the transition of high-to-low otolith Sr:Ca ratios, represented the ontogenetic change from pelagic larvae to demersal juvenile living in the river. If the two counts differed, the otolith was examined once more and final age was determined after discussion. The maximal distance from the core to the otolith check, or to a structural transition was also measured, which was further divided by the number of the growth increments to estimate the mean otolith growth rate during the pelagic larval stage of the gobies. One-way ANOVA was used to compare the otolith Sr:Ca ratios representing marine and freshwater life stages. The student's t-test was used to compare the PLD and otolith growth increment width between the landlocked and amphidromous gobies. Statistical significance was set at $\alpha = 0.05$.

Results

Molecular analyses

A fragment of mtDNA *COI* (555 bp) from 20 specimens obtained from two localities (Fig. 2) was analyzed. In total, six haplotypes were identified with two collected in FR

and five in MLC. Among the six haplotypes, only one was shared by both populations and the rest were unique to either population. Both haplotype (π) and nucleotide (h) diversities of FR were lower than those of MLC (mean \pm SD; h : 0.200 ± 0.154 and π : 0.00036 ± 0.00028 vs. h : 0.800 ± 0.100 and π : 0.00244 ± 0.00064). Total haplotype and nucleotide diversity were 0.574 ± 0.122 and 0.00161 ± 0.00046 , respectively (Table 1).

The haplotype network showed that all *COI* sequences obtained from the two populations were mixed. Monophyly of either population was not recovered, with the shared haplotype comprising 13 individuals and the rest of the five haplotypes each consisting of not more than three fish (Fig. 3).

Otolith Sr:Ca ratios and pelagic larval durations of the gobies

For the gobies collected in MLC, five individuals showed high Sr:Ca ratios (approximately $5\text{--}10 \times 10^{-3}$) from the otolith core to around 200 to 300 μm , followed by low otolith Sr:Ca ratios (approximately $0\text{--}5 \times 10^{-3}$) to the edge (Fig. 4a–e). The high-to-low variations of otolith Sr:Ca ratios suggested that the fish had a planktonic stage in the sea followed by a freshwater residence as found in other species (e.g., Shen et al. 1998; Shiao et al. 2015). A high-contrast growth increment, namely an otolith check, appeared at the transition of high-to-low otolith Sr:Ca ratios (Fig. 5a). The mean (\pm standard deviation) otolith Sr:Ca ratios before the otolith check varied between $5.1 \pm 2.4 \times 10^{-3}$ and $6.6 \pm 2.0 \times 10^{-3}$ among the fish, which were significantly larger than the values ($2.0 \pm 1.3 \times 10^{-3}$ to $2.5 \pm 1.2 \times 10^{-3}$) beyond the otolith check (one-way ANOVA, $F = 389.9$, $P < 0.01$). It is likely that the otolith check was formed when the gobies migrated from the sea into the river during the post-larval or early juvenile stages as found in other amphidromous goby species (Shen and Tzeng 2002). Therefore, the growth increments before the otolith check were defined as the marine PLD, which varied from 38 to 89 rings with the mean value of 58.8 ± 18.7 rings (Table 2; $N = 5$).

A different pattern of consistently low Sr:Ca ratios from the otolith core to the edge was found in all the gobies collected in the Jingualiao Creek although some fish showed one or two relatively higher Sr:Ca ratios (Fig. 6). In addition, the high-contrast growth increment otolith check was not observed in the early life stage of these gobies (Fig. 5b). These results suggested that these gobies did not migrate to the sea and spent their whole life in the creeks. The gobies examined showed clear and concentric growth increments in the inner part of the otolith then the growth increments became inconspicuous in the outer area. The transition from clear to ambiguous growth increments were regarded as the end of PLD, as observed in many species (e.g., Victor 1986; Raventós and Macpherson 2001). The otolith growth increments from the core to the structural transition varied between 24 and 46 rings with a mean of 38.8 ± 7.1 rings. These results suggested that the landlocked gobies might have a PLD between 24 and 46 days (Table 2; $N = 8$), which was significantly shorter than the PLD of the amphidromous gobies (student's t -test, $t = 2.79$, $P = 0.018$). However, the mean otolith growth rate before the settlement was similar between FR ($5.5 \pm 1.1 \mu\text{m d}^{-1}$) and MLC ($5.3 \pm 1.3 \mu\text{m d}^{-1}$) populations and not statistically significant (student's t -test, $t = 0.26$, $P = 0.80$).

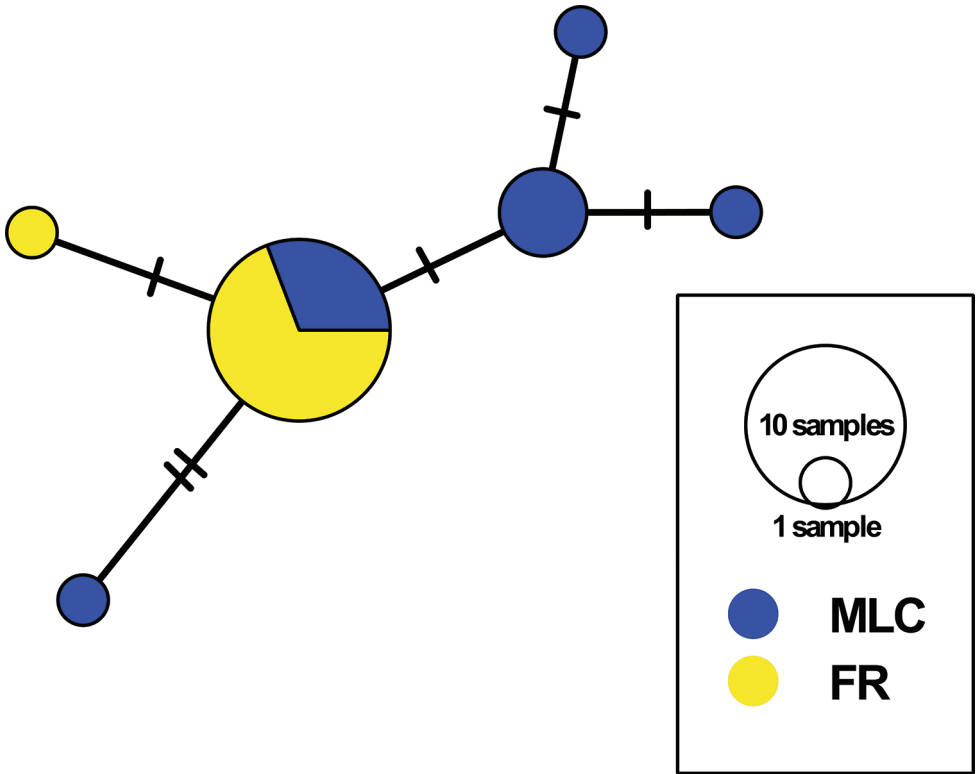


Figure 3. Minimum spanning network built from 20 *COI* sequences of *Rhinogobius formosanus* with six haplotypes. Colors represent correspondent sampling sites; pie chart sizes are proportional to the number of individuals; short bars represent haplotypes not collected in this study. FR, Feitsui Reservoir, representing a landlocked population; MLC, Malian Creek, representing an amphidromous population.

Table 2. Otolith growth increments (days) and growth rate ($\mu\text{m d}^{-1}$) corresponding to the pelagic larval duration of *Rhinogobius formosanus*. FR, Feitsui Reservoir, MLC, Malian Creek. SL for standard length in mm. na for data not available due to damage of specimens.

Locality	Catalog number	SL	Otolith growth increments	Otolith growth rates
FR	DOS03534-11	31.0	44	4.3
	DOS03534-14	na	46	3.9
	DOS03534-15	na	45	5.2
	DOS03534-16	32.6	36	6.3
	DOS03534-19	na	39	5.9
	DOS03534-33	na	24	7.4
	DOS03534-35	31.0	40	5.5
	DOS03534-37	31.5	36	5.3
	average \pm SD	31.5 \pm 0.8	38.8 \pm 7.1	5.5 \pm 1.1
MLC	DOS02416-6	31.3	57	4.8
	DOS02416-7	33.5	89	3.4
	DOS02416-12	29.4	58	5.6
	DOS02416-13	30.2	52	6.1
	DOS02416-15	na	38	6.7
	average \pm SD	31.1 \pm 1.8	58.8 \pm 18.7	5.3 \pm 1.3

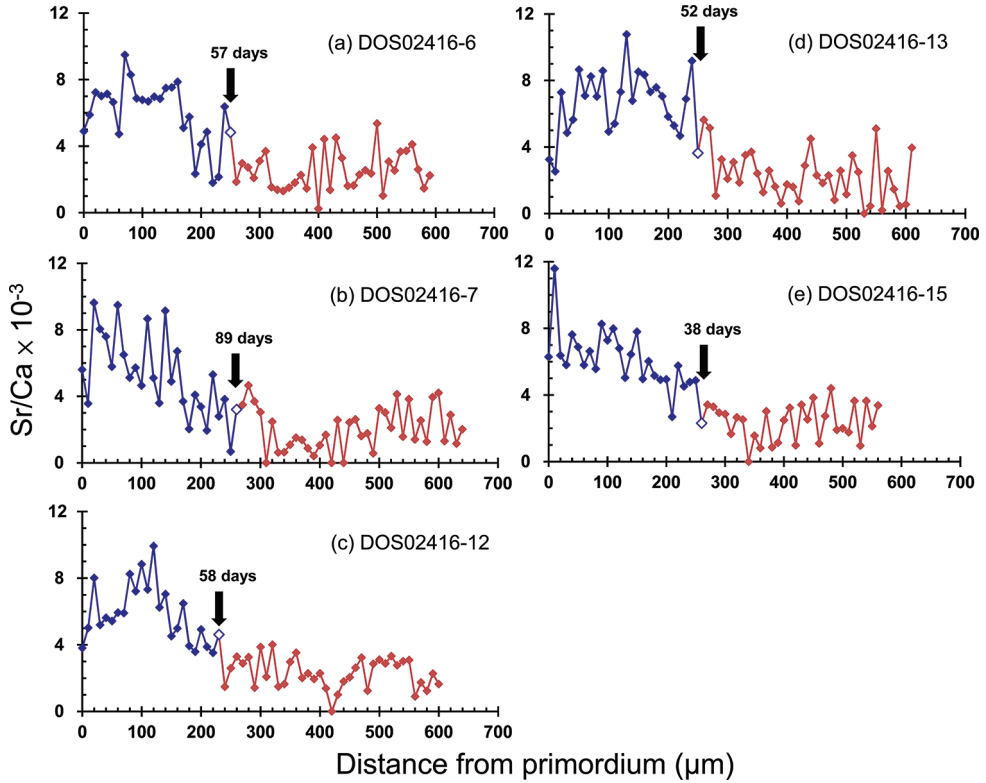


Figure 4. Analyzed transects of otolith Sr:Ca ratios from the core to the edge of sagittal otoliths of *Rhinogobius formosanus* collected in the Malian Creek of northern Taiwan. The arrows represent the formation days of the otolith check mark counted from the core. a-e represent their catalog numbers.

Discussion

Molecular analyses show haplotypes of FR and MLC populations are mixed without reciprocal monophyly (Fig. 3), implying that gobies of these two populations are conspecific and the observed otolith differences can be considered intraspecific variations. Results of the present study support our first hypothesis that the population of *R. formosanus* in the creek discharging into the reservoir is landlocked based on the data of consistently low otolith Sr:Ca ratios throughout life (Fig. 6; Tsunagawa and Arai 2008), rather than artificially released founders with an amphidromous signature. Otolith Sr:Ca ratios were mainly related to the water Sr concentration or salinity (Tran et al. 2019). However, physiological and water temperature might also affect otolith Sr:Ca ratios (Elsdon and Gillanders 2002). Therefore, one or two analyzed spots with Sr:Ca ratios $> 5 \times 10^{-3}$ in the otoliths of FR goby were not regarded as a marine signal but might be an analytical artifact due to the microstructure defects such as cracks, an unsmooth otolith surface or being influenced by the organic composition (Goldstein et al. 1992; McFadden et al. 2015). This result is in line with expectations since the dam of the FR is too high to be ascended by the fish. Various kinds of dam construc-

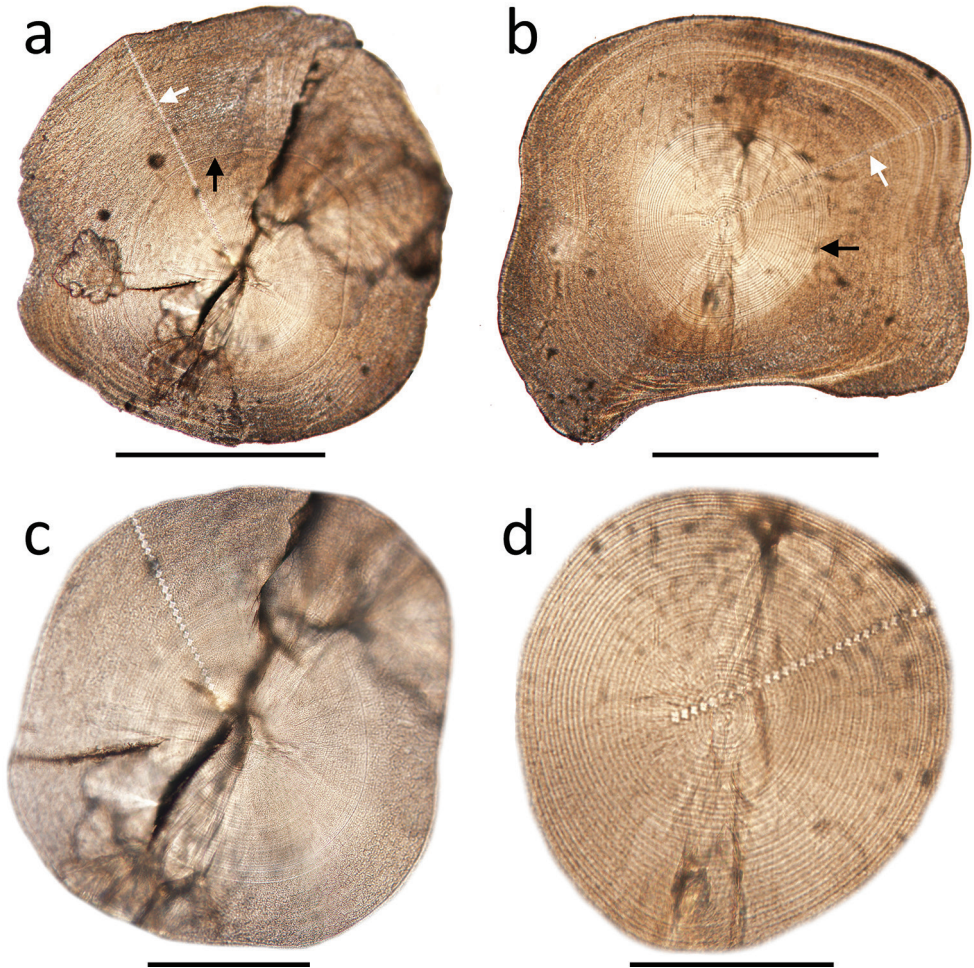


Figure 5. Otolith microstructure of an amphidromous goby (DOS02416-7, panel **a** and **c**) and a land-locked goby (DOS03534-19, panel **b** and **d**). Panel **c** and **d** illustrate the clear growth increments during the pelagic larval duration of the goby. The white arrows in panel **a** and **b** indicate the transect of otolith Sr:Ca ratio analysis. The black arrows indicate the otolith check mark where otolith Sr:Ca ratios drop from marine to freshwater signatures (panel **a**) and structural transition from clear concentric ring to ambiguous rings (panel **b**), respectively. Scale bars: 500 µm for panel **a**, **b**; 100 µm for panel **c**, **d**.⁷

tions have become major impediments to freshwater fish for the upstream migration in the rivers of Taiwan (Chang et al. 1999). In contrast, the gobies collected in MLC were all amphidromous (Fig. 4). These results imply that *R. formosanus*, like other goby species namely, *Rhinogobius* spp., the cross-band type, the large-dark type, the dark type, the cobalt type, the orange type (Sakai et al. 2004; Tsunagawa and Arai 2008), is a facultatively amphidromous goby, which can develop normally, grow, and complete their life cycle in freshwater environments.

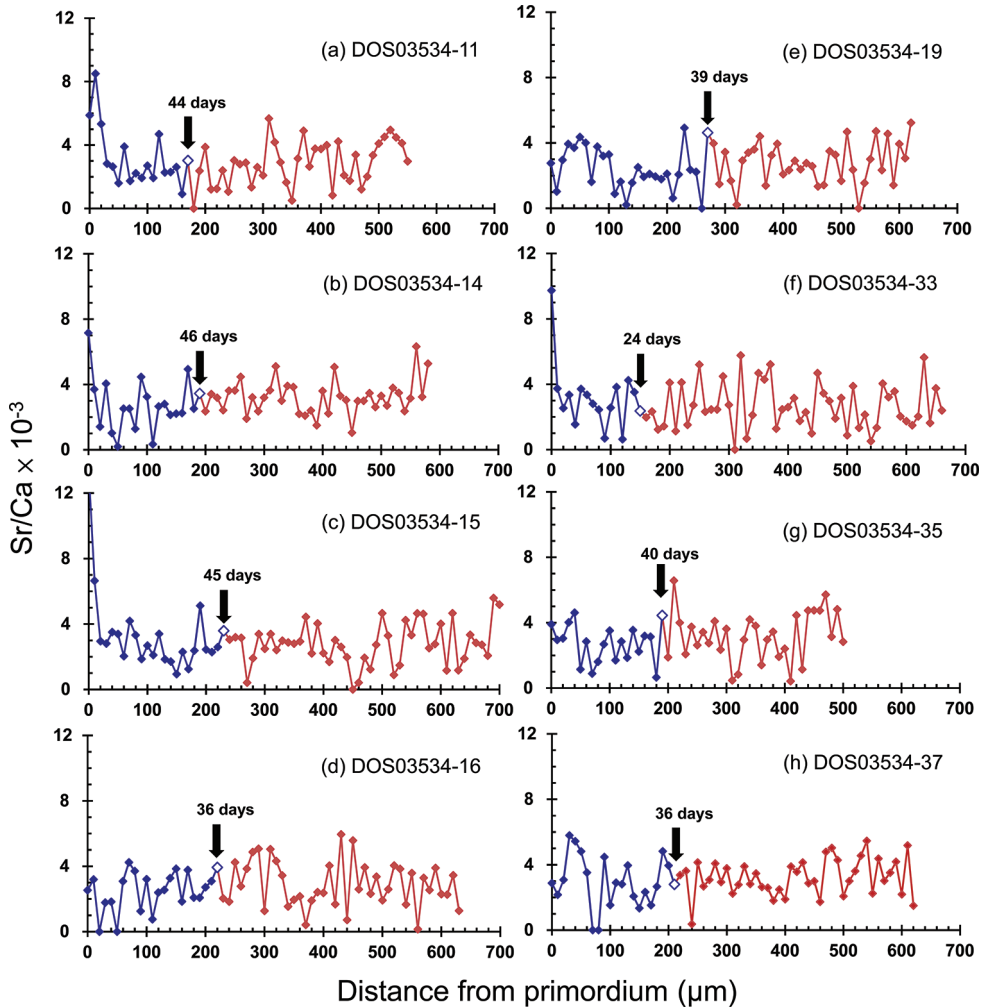


Figure 6. Sr:Ca ratios along transects from the core to the edge of sagittal otolith of *Rhinogobius formosanus* collected in the Feitsui Reservoir. a-h represent their catalog numbers.

To the best of our knowledge, very little comparative data, if any, between the amphidromous and landlocked gobies has been reported. The present study found that the PLD of *R. formosanus* were on average 20 days longer in the amphidromous population compared with the landlocked population based on the assumption that the otolith growth increments were deposited in a daily cycle as found in many goby species (e.g., Hoareau et al. 2007; Maeda et al. 2007; Taillebois et al. 2012; Shiao et al. 2015). Our results are different from previous studies that found prolonged exposure to freshwater may postpone development of goby larvae (Lindstrom and Brown 1994; Yokoi and Hosoya 2005). Variations of PLD between populations have been found and the mechanisms examined in many fish species (Sponaugle and Cowen 1994;

Sponaugle et al. 2002; Huang et al. 2018). The timing of larval metamorphosis may be either size-, age-, or habitat-dependent (Benoît and Pepin 1999; Shen and Tzeng 2008). In the case of amphidromous *R. formosanus*, there are large variations in PLD of 38–89 days while the landlocked *R. formosanus* has shorter and less variable PLD of 24–46 days. Therefore, the triggering of metamorphosis of this species is probably not age-dependent. The size of larvae, freshwater discharge and suitable benthic habitats may be the vital factors triggering metamorphosis. However, all our specimens are either adult or juvenile, and it is not possible to evaluate size at metamorphosis. Nevertheless, otolith growth was usually closely related to somatic growth (Campana and Neilson 1985). The otolith growth rate was very similar between the FR and MLC populations, suggesting a similar somatic growth rate of the larval gobies either in the sea or in the river discharging into the reservoir. This implies that size may not be a concern since gobies of FR and MLC undergo metamorphosis at different PLDs and therefore supposed to be of different sizes. The habitats or environments experienced by *R. formosanus* larvae may explain the different PLD between the amphidromous and landlocked populations. The longer PLD of amphidromous gobies is likely due to the time needed for hatched larvae to drift downstream from the creek to the sea, the feeding and growth to post-larvae in the sea, and the time for actively searching and swimming to the estuary (Keith 2003). Although amphidromous larval gobies tend to stay in coastal areas (Sorensen and Hobson 2005), larval transportation into the open ocean may occur in extreme situations. It is likely that the gobies experiencing longer dispersion will need more time to come back to the estuaries in the original or nearby areas. However, long dispersion may also lead to the death of the larval gobies if a suitable benthic habitat is not encountered when the maximal plasticity of the PLD is reached. Therefore, a longer and more variable PLD (38–89 days) is likely due to the complex amphidromous life history of *R. formosanus*. On the other hand, the stable environment in the creek or in the reservoir (Kolding and Zwieter 2012) may facilitate the larval development in a shorter and less variable time for the landlocked population. Furthermore, a shorter PLD can facilitate an earlier habitat change of larval fish from the upper water column to settlement in benthic habitats where shelter is more abundant. Therefore, a shorter PLD may enhance the survival rate of a pelagic larval goby living in a creek connecting to the reservoir.

Pelagic larval duration, usually considered a measure of dispersal potential, has been shown to be positively correlated to range size and negatively correlated to species richness, implying that PLD may regulate speciation rate as an evolutionary mechanism (Lester and Ruttenberg 2005). Selkoe and Toonen (2011) provide new insight at the molecular level and conclude that PLD is negatively correlated to isolation by distance, further supporting the concept of an evolutionary mechanism. *Rhinogobius formosanus* may have a PLD as long as three months as observed in this study, which may allow the larvae to disperse over hundreds of kilometers, depending on the current speed and ocean hydrodynamics, and explain the wide distribution of this species in the southeastern coast of China and the northern coast of Taiwan. Due to lack of genetic differentiation between FR and MLC populations, the variation in the PLD of *R. formosanus* is probably a consequence of acclimatization rather than adaptation.

Molecular analyses show haplotypes of FR and MLC populations are mixed without reciprocal monophyly and the genetic diversity of the former is much lower than the latter (Table 1). Lower genetic diversity might be a consequence of a founder effect and imply an artificial released population in FR (Tzeng et al. 2005; Hamner et al. 2007). On the other hand, a small native population isolated after the construction of the dam may also result in the same genetic pattern. However, the present data is not able to answer the origin of the FR population and range wide population genetic study on this species may be needed to provide more information.

Acknowledgements

We are grateful to Brian Jessop, Harald Ahnelt and an anonymous referee for their constructive comments. We thank Zen-Wei Lin for his assistance in sampling and Yu Hsieh for the preparation of otolith samples. This study was supported by grants from the Ministry of Science and Technology to T.Y.L. (105-2611-M-110-008-) and J.C.S. (108-2611-M-002-007).

References

- Aonuma Y, Chen IS (1996) Two new species of *Rhinogobius* (Pisces, Gobiidae) from Taiwan. *Journal of Taiwan Museum* 49: 7–16.
- Benoît HP, Pepin P (1999) Individual variability in growth rate and the timing of metamorphosis in yellowtail flounder *Pleuronectes ferrugineus*. *Marine Ecology Progress Series* 184: 231–244. <https://doi.org/10.3354/meps184231>
- Brown RJ, Severin KP (2009) Otolith chemistry analyses indicate that water Sr:Ca is the primary factor influencing otolith Sr:Ca for freshwater and diadromous fish but not for marine fish. *Canadian Journal of Fisheries and Aquatic Sciences* 66: 1790–1808. <https://doi.org/10.1139/F09-112>
- Campana SE (1999) Chemistry and composition of fish otoliths: pathways, mechanisms and applications. *Marine Ecology Progress Series* 188: 263–297. <https://doi.org/10.3354/meps188263>
- Campana SE, Neilson JD (1985) Microstructure of fish otoliths *Canadian Journal of Fisheries and Aquatic Sciences* 42: 1014–1032. <https://doi.org/10.1139/f85-127>
- Chen IS, Fang LS (1999) The freshwater and estuaries fishes of Taiwan. National Museum of Marine Biology and Aquarium, Pingtung, 287 pp. [in Chinese]
- Chang MH, Lin YS, Chung LC (1999) Effect of dams on fish assemblages of the Tachia River, Taiwan. *Acta Zoologica Taiwanica* 10(2): 77–90.
- Elsdon TS, Gillanders BM (2002) Interactive effects of temperature and salinity on otolith chemistry: Challenges for determining environmental histories of fish. *Canadian Journal of Fisheries and Aquatic Sciences* 59(11): 1796–1808. <https://doi.org/10.1139/f02-154>
- Gill TN (1859) Notes on a collection of Japanese fishes, made by Dr. J. Morrow. *Proceedings of the Academy of Natural Sciences of Philadelphia* 11: 144–150.

- Goldstein JI, Newbury DE, Echlin P, Joy DC, Fiori C (1992) Scanning Electron Microscopy and X-ray Microanalysis – A Text for Biologists, Materials Scientists, and Geologists. Plenum Press, New York, 840 pp. <https://doi.org/10.1007/978-1-4613-0491-3>
- Hamner RM, Freshwater DW, Whitfield PE (2007) Mitochondrial cytochrome b analysis reveals two invasive lionfish species with strong founder effects in the western Atlantic. *Journal of Fish Biology* 71: 214–222. <https://doi.org/10.1111/j.1095-8649.2007.01575.x>
- Hoareau T, Lecomte-Finiger R, Grondin HP, Conand C, Berrebi P (2007) Oceanic larval life of La Réunion ‘bichiques’, amphidromous gobiid post-larvae. *Marine Ecology Progress Series* 333: 303–308. <https://doi.org/10.3354/meps333303>
- Huang WC, Chang JT, Liao C, Tawa A, Iizuka Y, Liao TY, Shiao JC (2018) Pelagic larval duration, growth rate, and population genetic structure of the tidepool snake moray *Uropterygius micropterus* around the southern Ryukyu Islands, Taiwan, and the central Philippines. *PeerJ* 6: e4741. <https://doi.org/10.7717/peerj.4741>
- Iizuka Y (2012) Electron microprobe study of otolith: Migratory behavior and habitat of three major temperate species of eels. *JEOL News* 47: 33–50.
- Ju YM, Hsu CH, Fang LS, Lin HD, Wu JH, Han CC, Chen IS, Chiang TY (2013) Population structure and demographic history of *Sicyopterus japonicus* (Perciformes; Gobiidae) in Taiwan inferred from mitochondrial control region sequences. *Genetic and Molecular Research* 12: 4046–4059. <https://doi.org/10.4238/2013.September.27.6>
- Keith P (2003) Biology and ecology of amphidromous Gobiidae of the Indo-Pacific and the Caribbean regions. *Journal of Fish Biology* 63: 831–847. <https://doi.org/10.1046/j.1095-8649.2003.00197.x>
- Keith P, Watson RE, Marquet G (2004) *Sicyopterus aiensis*, a new species of freshwater goby (Gobioidei) from Vanuatu, South Pacific. *Cybium* 28: 111–118.
- Kolding J, van Zwieten PAM (2012) Relative lake level fluctuations and their influence on productivity and resilience in tropical lakes and reservoirs. *Fisheries Research* 115: 99–109. <https://doi.org/10.1016/j.fishres.2011.11.008>
- Kumar S, Stecher G, Li M, Knyaz C, Tamura K (2018) MEGA X: molecular evolutionary genetics analysis across computing platforms. *Molecular Biology and Evolution* 35: 1547–1549. <https://doi.org/10.1093/molbev/msy096>
- Leigh JW, Bryant D (2015) popart: full-feature software for haplotype network construction. *Methods in Ecology and Evolution* 6(9): 1110–1116. <https://doi.org/10.1111/2041-210X.12410>
- Lester SE, Ruttenberg BI (2005) The relationship between pelagic larval duration and range size in tropical reef fishes: a synthetic analysis. *Proceedings of the Royal Society B: Biological Sciences* 272: 585–591. <https://doi.org/10.1098/rspb.2004.2985>
- Lindstrom DP, Brown CL (1994) Early development and biology of the amphidromous Hawaiian stream goby *Lentipes concolor*. *Systematics and Evolution of Indo-Pacific Fishes, Proceedings of the Fourth Indo-Pacific Fish Conference*. Faculty of Fisheries, Bangkok, 397–409.
- Lord C, Brun C, Hautecoeur M, Keith P (2010) Insights on endemism: comparison of the duration of the marine larval phase estimated by otolith microstructural analysis of three amphidromous *Sicyopterus* species (Gobiidae: Sicydiinae) from Vanuatu and New Caledonia. *Ecology of Freshwater Fish* 19: 26–38. <https://doi.org/10.1111/j.1600-0633.2009.00386.x>
- Lord C, Lorion J, Dettai A, Watanabe S, Tsukamoto K, Cruaud C, Keith P (2012) From endemism to widespread distribution: phylogeography of three amphidromous *Sicyopterus*

- species (Teleostei: Gobioidae: Sicydiinae). *Marine Ecology Progress Series* 455: 269–285. <https://doi.org/10.3354/meps09617>
- Lozys L, Shiao JC, Iizuka Y, Minde A, Putys Z, Jakubaviciute E, Dainys J, Gorfine H, Tzeng WN (2017) Habitat use and migratory behaviour of pikeperch *Sander lucioperca* in Lithuanian and Latvian waters as inferred from otolith Sr:Ca ratios. *Estuarine, Coastal and Shelf Science* 198: 43–52. <https://doi.org/10.1016/j.ecss.2017.08.020>
- Maeda K, Yamasaki N, Tachihara K (2007) Size and age at recruitment and spawning season of sleeper, genus *Eleotris* (teleostei: Eleotridae) on Okinawa island, southern Japan. *Raffles Bulletin of Zoology* 14: 199–207.
- McDowall RM (2007) On amphidromy, a distinct form of diadromy in aquatic organisms. *Fish and fisheries* 8: 1–13. <https://doi.org/10.1111/j.1467-2979.2007.00232.x>
- McFadden A, Wade B, Izzo C, Gillanders BM, Lenehan CE, Pring A (2015) Quantitative electron microprobe mapping of otoliths suggests elemental incorporation is affected by organic matrices: implications for the interpretation of otolith chemistry. *Marine and Freshwater Research* 67(7): 889–898. <https://doi.org/10.1071/MF15074>
- Oshima M (1919) Contributions to the study of the fresh water fishes of the island of Formosa. *Annals of the Carnegie Museum* 12: 169–328.
- Pallas PS (1770) *Spicilegia zoologica quibus novae imprimis et obscurae animalium species iconibus, descriptionibus atque commentariis illustrantur. Fasciculus Octavus*. Lange, Berlin, 54 pp.
- Raventós N, Macpherson E (2001) Planktonic larval duration and settlement marks on the otoliths of Mediterranean littoral fishes. *Marine Biology* 138: 1115–1120. <https://doi.org/10.1007/s002270000535>
- Regan CT (1908) XXIV.—Descriptions of new freshwater fishes from China and Japan. *Annals and Magazine of Natural History* 1: 149–153. <https://doi.org/10.1080/00222930808692377>
- Rogers TA, Fowler AJ, Steer MA, Gillander BM (2019) Resolving the early life history of King George whiting (*Sillaginodes punctatus*: Perciformes) using otolith microstructure and trace element chemistry. *Marine and Freshwater Research* 70: 1659–1674. <https://doi.org/10.1071/MF18280>
- Rozas J, Ferrer-Mata A, Sánchez-DelBarrio JC, Guirao-Rico S, Librado P, Ramos-Onsins SE, Sánchez-Gracia A (2017) DnaSP 6: DNA sequence polymorphism analysis of large data sets. *Molecular Biology and Evolution* 34: 3299–3302. <https://doi.org/10.1093/molbev/msx248>
- Sakai H, Arai T, Imai C, Sugiyama H, Sato H, Jeon SR (2004) Landlocked populations of an amphidromous goby, *Rhinogobius* sp. CO. *Japanese Journal of Ichthyology* 51(2): 175–180.
- Selkoe KA, Toonen RJ (2011) Marine connectivity: a new look at pelagic larval duration and genetic metrics of dispersal. *Marine Ecology Progress Series* 436: 291–305. <https://doi.org/10.3354/meps09238>
- Shen KN, Lee YC, Tzeng WN (1998) Use of otolith microchemistry to investigate the life history pattern of gobies in a Taiwanese stream. *Zoological Studies* 37: 322–329.
- Shen KN, Tzeng WN (2008) Reproductive strategy and recruitment dynamics of amphidromous goby *Sicyopterus japonicus* as revealed by otolith microstructure. *Journal of Fish Biology* 73: 2497–2512. <https://doi.org/10.1111/j.1095-8649.2008.02102.x>
- Shen KN, Tzeng WN (2002) Formation of a metamorphosis check in otoliths of the amphidromous goby *Sicyopterus japonicus*. *Marine Ecology Progress Series* 228: 205–211. <https://doi.org/10.3354/meps228205>

- Shiao JC, Chen CY, Zhang J, Iizuka Y (2016) Habitat use and migratory life history of salangid icefish (Salangidae) revealed by otolith Sr/Ca ratios. *Zoological Studies* 55: 1–3. <https://doi.org/10.6620/ZS.2016.55-03>
- Shiao JC, Tzeng CS, Li PC, Bell KNI (2015) Upstream migration and marine early life history of amphidromous gobies inferred from otolith increments and microchemistry. *Environmental Biology of Fishes* 98: 933–950. <https://doi.org/10.1007/s10641-014-0329-5>
- Sorensen PW, Hobson KA (2005) Stable isotope analysis of amphidromous Hawaiian gobies suggests their larvae spend a substantial period of time in freshwater river plumes. *Environmental Biology of Fish* 74: 31–42. <https://doi.org/10.1007/s10641-005-3212-6>
- Sponaugle S, Cowen RK (1994) Larval durations and recruitment patterns of two Caribbean gobies (Gobiidae): contrasting early life histories in demersal spawners. *Marine Biology* 120: 133–143.
- Sponaugle S, Cowen RK, Shanks AL, Morgan SG, Leis J, Pineda J, Boehlert G, Kingsford MJ, Lindeman K, Grimes C, Munro JL (2002) Predicting self-recruitment in marine populations: Biophysical correlates and mechanisms. *Bulletin of Marine Science* 70: 341–375.
- Taillebois L, Maeda K, Vigne S, Keith P (2012) Pelagic larval duration of three amphidromous Sicydiinae gobies (Teleostei: Gobioidae) including widespread and endemic species. *Ecology of Freshwater Fish* 21: 552–559. <https://doi.org/10.1111/j.1600-0633.2012.00575.x>
- Tanaka S (1909) Descriptions of one new genus and ten new species of Japanese fishes. *Journal of the College of Science, Imperial University of Tokyo* 27: 1–27.
- Tran NT, Labonne M, Hoang HD, Panfili J (2019) Changes in environmental salinity during the life of *Pangasius krempfi* in the Mekong Delta (Vietnam) estimated from otolith Sr : Ca ratios. *Marine and Freshwater Research* 70: 1734–1746. <https://doi.org/10.1071/MF18269>
- Tsunagawa T, Arai T (2008) Flexible migration of Japanese freshwater gobies *Rhinogobius* spp. as revealed by otolith Sr-Ca ratios. *Journal of Fish Biology* 73: 2421–2433. <https://doi.org/10.1111/j.1095-8649.2008.02089.x>
- Tzeng CS, Lin YS, Lin SM, Wang TY, Wang FY (2005) The Phylogeography and Population Demographics of Selected Freshwater Fishes in Taiwan. *Zoological Studies* 45: 285–297.
- Tzeng WN, Shiao JC, Iizuka Y (2002) Use of otolith Sr:Ca ratios to study the riverine migratory behaviors of Japanese eel *Anguilla japonica*. *Marine Ecology Progress Series* 245: 213–221. <https://doi.org/10.3354/meps245213>
- Victor BC (1986) Duration of the planktonic larval stage of one hundred species of Pacific and Atlantic wrasses (family Labridae). *Marine Biology* 90(3): 317–326. <https://doi.org/10.1007/BF00428555>
- Ward RD, Zemlak TS, Innes BH, Last PR, Hebert PD (2005) DNA barcoding Australia's fish species. *Philosophical Transactions of the Royal Society of London B: Biological Sciences* 360: 1847–1857. <https://doi.org/10.1098/rstb.2005.1716>
- Watanabe S, Iida M, Kimura Y, Feunteun E (2006) Genetic diversity of *Sicyopterus japonicus* as revealed by mitochondrial DNA sequencing. *Coastal Marine Science* 30: 473–479.
- Weber M, de Beaufort LF (1915) Les poissons d'eau douce de la Nouvelle-Calédonie. In: Sarsin F, Roux J (Eds) *Nova Caledonia. Recherches scientifiques en Nouvelle-Calédonie et aux Iles Loyalty*. Zoology A, Paris, 2: 17–41.

- Yamasaki YY, Nishida M, Suzuki T, Mukai T, Watanabe K (2015) Phylogeny, hybridization, and life history evolution of *Rhinogobius* gobies in Japan, inferred from multiple nuclear gene sequences. *Molecular Phylogenetics and Evolution* 90: 20–33. <https://doi.org/10.1016/j.ympev.2015.04.012>
- Yokoi K, Hosoya K (2005) Larval salinity tolerance in the endangered goby *Rhinogobius* sp. BI (Gobiidae) from the Bonin Islands. *Japanese Journal of Ichthyology* 52: 31–34. <https://doi.org/10.11369/jji1950.52.31>
- Yuan LY, Zhou ZC, Zhou JJ, Fang YF, Yang J (2012) Preliminary Investigation of Fish Resources in the Tongshan River. *Sichuan Journal of Zoology* 31: 961–964. [in Chinese with English abstract] <https://doi.org/10.4155/cli.12.106>

A conservation checklist of the amphibians and reptiles of Mexico City, with comparisons with adjoining states

Julio A. Lemos-Espinal¹, Geoffrey R. Smith²

1 *Laboratorio de Ecología-UBIPRO, FES Iztacala UNAM, Avenida los Barrios 1, Los Reyes Iztacala, Tlalnepantla, edo. de México, 54090, México* **2** *Department of Biology, Denison University, Granville, Ohio 43023, USA*

Corresponding author: Julio A. Lemos-Espinal (lemos@unam.mx)

Academic editor: Annemarie Ohler | Received 26 March 2020 | Accepted 5 June 2020 | Published 22 July 2020

<http://zoobank.org/F9DE6895-7032-41AA-A38B-4B1281EB7E4C>

Citation: Lemos-Espinal JA, Smith GR (2020) A conservation checklist of the amphibians and reptiles of Mexico City, with comparisons with adjoining states. ZooKeys 951: 109–131. <https://doi.org/10.3897/zookeys.951.52578>

Abstract

Mexico City houses one of the most populous urban areas of the world, and the modification of its natural habitat likely influences the biological diversity found there. In particular, amphibians and reptiles are likely affected by these modifications. Herein, we present an updated list of the species of amphibians and reptiles that inhabit Mexico City. Mexico City harbors 65 species of amphibians and reptiles, which represent 21 families and 33 genera. These include 18 species of amphibians (nine anurans and nine salamanders) and 47 species of reptiles (14 lizards, 30 snakes [one introduced], and three turtles [one introduced]). Forty-eight of the amphibian and reptile species in Mexico City are endemic to Mexico, with two endemic to Mexico City. The most diverse region of Mexico City is the Forests and Ravines region, which is home to 43 species. Eleven species of amphibians and reptiles in Mexico City are IUCN listed, 16 are placed in a protected category by SEMARNAT (Secretaría del Medio Ambiente y Recursos Naturales), and 27 species are categorized as high risk by the EVS (Environmental Viability Score). Mexico City shares almost 94% of its species with the State of Mexico.

Keywords

amphibians, frogs, herpetofauna, lizards, reptiles, salamanders, snakes, turtles

Introduction

Since pre-Hispanic times the Basin of Mexico, upon which Mexico City (formerly Mexico, Distrito Federal) sits, caught the attention of the inhabitants of central Mexico. This large lake surrounded by fertile land was the location of important human settlements that, at the arrival of the Spaniards, were represented mainly by Tenochtitlan, which along with a large number of villages located around the basin reached over a million inhabitants (Wikipedia: https://es.wikipedia.org/wiki/Ciudad_de_M%C3%A9xico – accessed 27 December 2019). At the arrival of the Spaniards, in 1519, the basin was occupied by a well-developed civilization whose economy revolved around the Chinampas that surrounded the lake (Fig. 1). With the Spanish conquest of Mexico, cattle were introduced to the basin and a radical transformation began, including the drying of the Basin and the felling of the forests that surrounded it. The population around the Basin began to decline to such extent that at the end of the 18th century the number of inhabitants in Mexico City was only 120,000. It was not until the middle of the 20th century that the population explosion began creating diverse and complex problems that today overwhelm Mexico City (Imaz 1989). Currently the population of Mexico City is approximately 8.9 million inhabitants; however, including the metropolitan area of the Valley of Mexico, which extends over the Basin of Mexico, the population totals 22 million inhabitants, the ninth most populated urban area in the world, and the largest in the Americas (Wikipedia: https://es.wikipedia.org/wiki/Ciudad_de_M%C3%A9xico – accessed 27 December 2019).

The urban area of Mexico City covers almost the whole northern half of Mexico City *sensu lato* (previously Distrito Federal) and is rapidly expanding (e.g., Hernández-Flores et al. 2017), including through illegal development (Rodríguez López et al. 2017). The southern half of Mexico City *sensu lato* is occupied by mountains and ravines covered by extensive forests and grasslands, some of them highly fragmented by housing developments and cultivated fields. The air pollution is such that the governments of Mexico City and the State of Mexico created a program at the end of 1989 that limits motor vehicle use in the city. However, air pollution continued to increase despite the initial restrictions, and currently there are increased limitations on vehicle use. Spaces for new residential development within the city are fewer and the population continues to grow and demand more resources, increasing the production of waste, the emission of greenhouse gases, the number of fires, the illegal occupation of protected areas, and the depletion of available natural resources (Santibáñez-Andrade et al. 2015; SEMARNAT 2016; Heider et al. 2018). Increased urbanization around Mexico City proper has also affected rivers and streams (Caro-Borrero et al. 2016). This considerable modification of the natural habitat exerts a constant pressure on the biological diversity of Mexico City. Amphibians and reptiles are strongly affected by these changes, and there are species whose presence in Mexico City is known only from their original records (e.g., *Geophis bicolor* and *G. petersi*), or whose conservation status is quite tenuous (e.g., *Eleutherodactylus grandis*, *Rana tlaloci*, *Ambystoma mexicanum*, and *Crotalus transversus*).

Herein, we present an updated list of amphibians and reptiles that inhabit Mexico City in an effort to disseminate important information about its herpetofauna to help



Figure 1. Basin of Mexico, circa 1519. Source: https://upload.wikimedia.org/wikipedia/commons/9/99/Basin_of_Mexico_1519_map-en.svg

in their conservation. Previous recent efforts to catalog the herpetofauna of Mexico City reported a list of 18 species of amphibians and 39 species (one of them introduced) of reptiles from Mexico City (García-Vázquez and Méndez-de la Cruz 2016; García-Vázquez et al. 2016).

Physiographic characteristics

Mexico City is one of 32 federal entities in Mexico. It is the capital of the country. It is located between 19°35'34"N and 19°2'54"N, and 98°56'25"W and 99°21'54"W. It is bordered by the State of Mexico to the north, east, and west, and by Morelos to the south (Fig. 2). It covers 1,485 km², which represents 0.1% of the total area of Mexico. The urban area of Mexico City is in the Valley of Mexico, a large valley in the high plateaus in the center of Mexico, at an altitude of 2,240 m (Figs 2, 3; INEGI 2017; https://en.wikipedia.org/wiki/Mexico_City – accessed 17 December 2019).

The topography of Mexico City is highly variable, including an extensive high plateau in the northern half of the city, where the urban area sits, and mountains and volcanoes that reach up to 3,930 m of altitude (Volcán Ajusco) that surround the urban area mainly on its southern and western sides (Fig. 3). Mexico City is located in the physiographic province of the Neovolcanic Axis, sub-province of Lagos and Volcanes of Anahuac. Mexico City is divided into an urban development area, usually referred to as urban land (41% of the territory, mostly on the northern half of the city), and an ecological conservation area, referred to as conservation land (59% of the territory, mostly on the southern half of the city). Urban land primarily consists of the urbanized plain area of the city, whereas conservation land includes areas with natural ecosystems (Reygadas-Prado 2016). Natural vegetation is primarily distributed in the conservation land, and in general terms it is represented by forests (55.6%), ag-

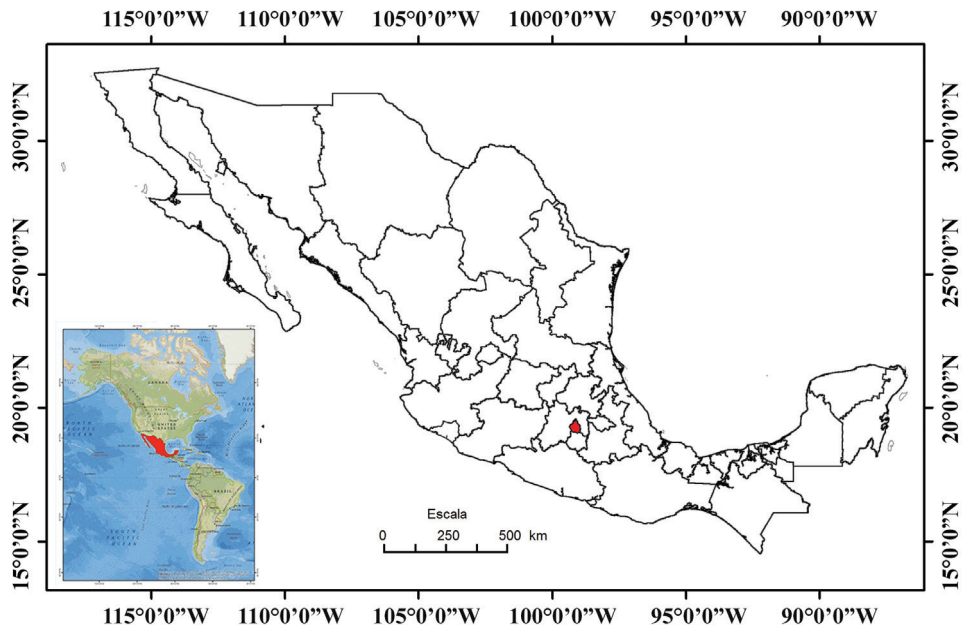


Figure 2. Map of Mexico with Mexico City shown in red (modified from INEGI 2018).

gricultural areas (35.8%), grasslands (7.17%), and scrublands (1.43%) (Fig. 4; INEGI 2017). According to the Köppen climate classification modified by García (1998), the climate of Mexico City is broadly divided into Subhumid Temperate with summer rains, covering much of the city (Fig. 5). A Semicold Subhumid climate with summer rains is present in the highest parts of the mountains that surround the city, from the west-central part running diagonally to the southeastern end on the border with Morelos; and Semiarid Temperate with summer rains present in the east-northeast end of the city, including the Sierra de Santa Catarina in the eastern part of the city and a considerable portion of the northeastern end of the city in the boroughs of Gustavo A. Madero, Venustiano Carranza, and Iztacalco (Fig. 5).

Reygadas-Prado (2016) provided a regionalization of Mexico City based on biophysical characteristics that consists of six regions. The Forests and Ravines region is made up of the largest and best-preserved forest massifs and ravines found in the south and southwest of the city, occupying an area of 532.4 km². The principal forests in this region are oak, pine-oak, and pine forests, with some cloud forest relics in the vicinity of the Dínamos de Contreras. The Wetlands of Xochimilco and Tláhuac region is found

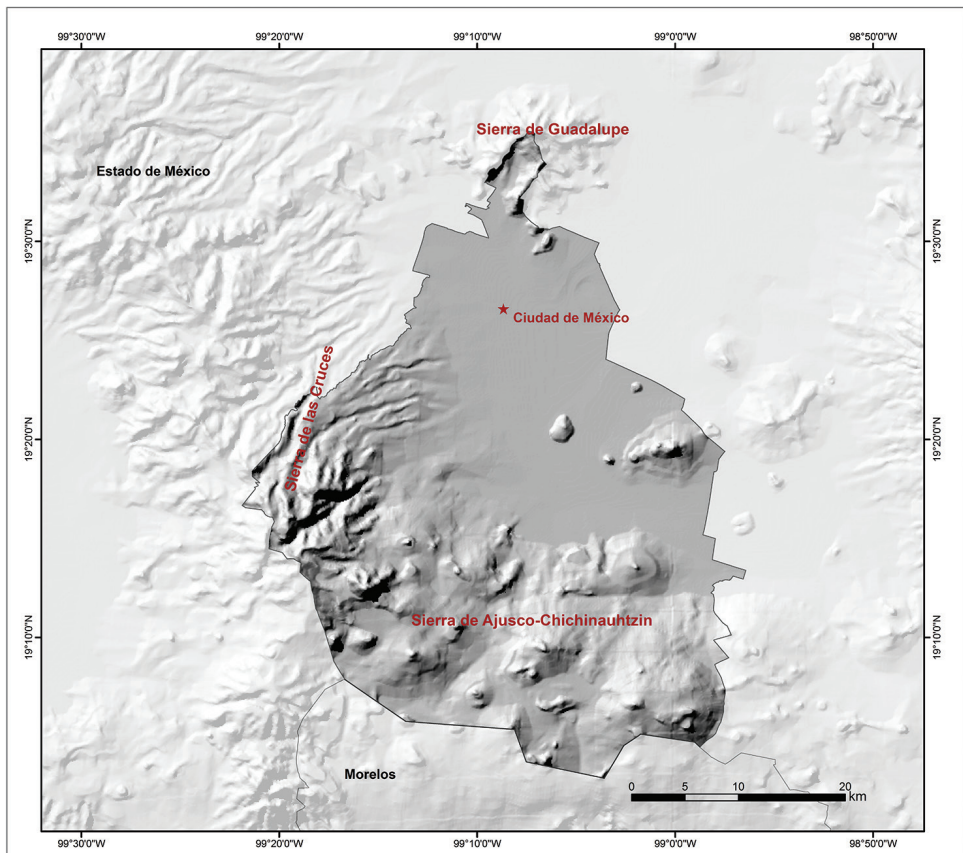


Figure 3. Topographical map of Mexico City, Mexico (Source: CONABIO 1997).

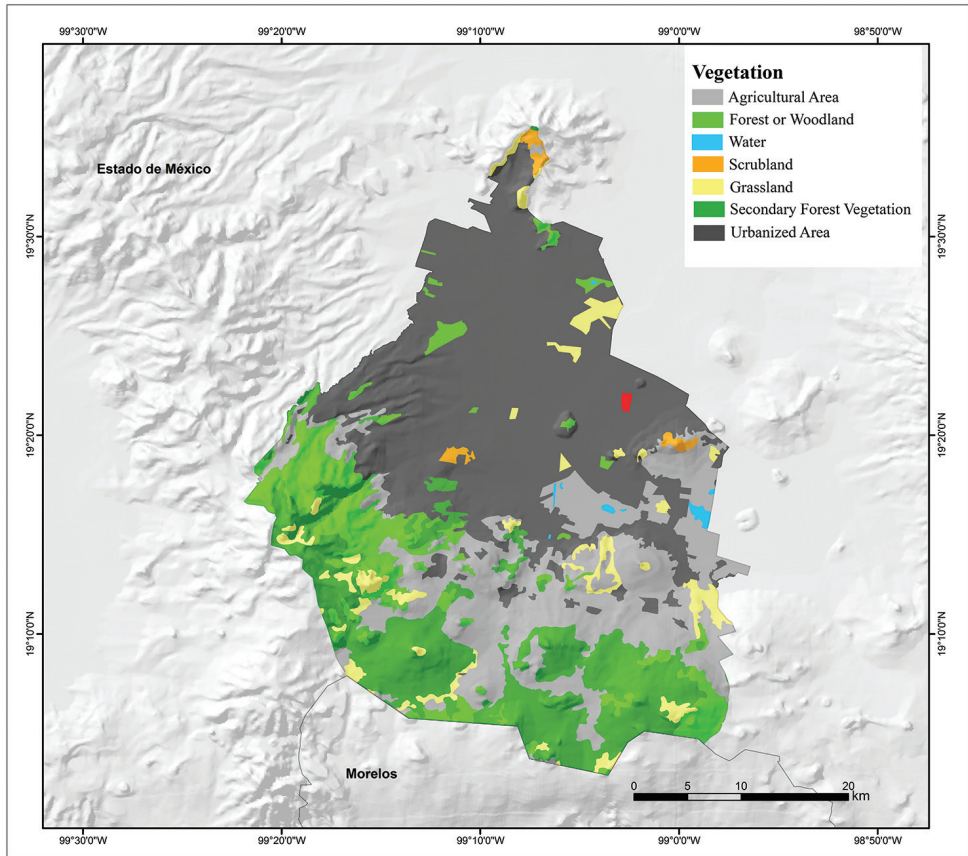


Figure 4. Vegetation map of Mexico City, Mexico (modified from Dirección General de Geografía; INEGI 2016).

in the Chinampas area of Xochimilco, San Gregorio, San Luis Tlaxialtemanco, Tláhuac and the lowlands of Tláhuac, occupying an area of 60.3 km². This region is located in the east-central parts of the city. The Urban Parks and Gardens region includes parks, gardens, forests, protected natural areas, and areas of environmental value located on urban land, and occupies an area of 607.3 km². It is found in the northern half of the city, except for the Sierra de Guadalupe, and two areas in the central and eastern parts of the city that represent the Sierra de Santa Catarina region. This region includes the urbanized area of Mexico City. The Mountains of Xochimilco and Milpa Alta region is found between the Urban Parks and Gardens and the Forests and Ravines regions, and it occupies an area of 237.5 km². It runs from west-central to eastern Mexico City. It consists of an area of forests fragmented by housing developments; however, important areas of oak, pine-oak, and pine forests are located in this region. The Sierra de Guadalupe region is located in northern Mexico City and includes the protected natural areas of Sierra de Guadalupe, La Armella, and Tepeyac National Park and occupies an area of 12.9 km². Its characteristic vegetation is xerophilous scrub. The Sierra de Santa Catarina

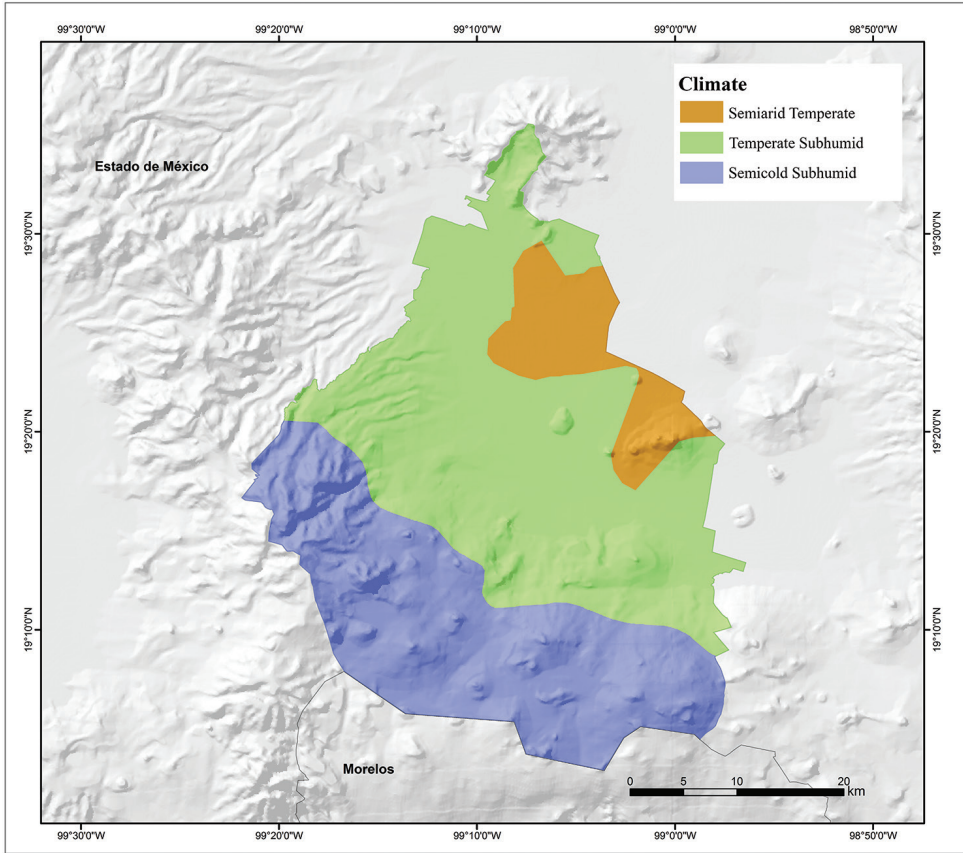


Figure 5. Climate map of Mexico City, Mexico (modified from García and Comisión Nacional para el Conocimiento y Uso de la Biodiversidad 1998).

region, located in eastern and central Mexico City, occupies an area of 31.4 km². The vegetation here is similar to the Sierra de Guadalupe, with an important area of grassland and a greater number of tree species for reforestation (Fig. 6; Reygadas-Prado 2016).

Materials and methods

We compiled our list of amphibians and reptiles for Mexico City using our field-work, a thorough examination of the literature, records from VertNet.org and Servicio de Descarga de Ejemplares del Sistema Nacional de Información sobre Biodiversidad (SNIB-CONABIO): Amphibians Ciudad de México and Reptiles Ciudad de México data bases. We included species in the list if they had confirmed records, either by direct observation, literature report, or through documented museum records or vouchers. We follow Frost (2020) and AmphibiaWeb (2020) for amphibian names and Uetz and Hošek (2019) for reptile names.

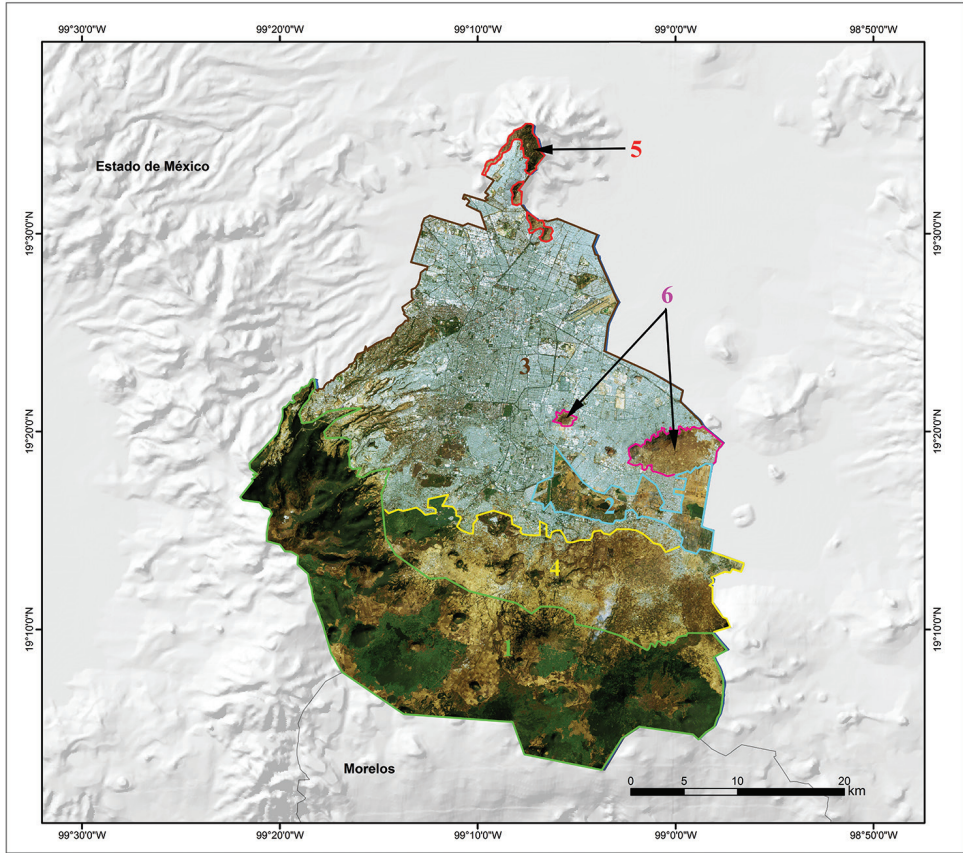


Figure 6. Satellite map showing the topographic features of Mexico City (source: Comisión Nacional para el Conocimiento y Uso de la Biodiversidad 2003) and Regions of Mexico City according to Reygadas-Prado (2016): 1) Forests and Ravines; 2) Wetlands of Xochimilco and Tláhuac; 3) Urban Parks and Gardens; 4) Mountains of Xochimilco and Milpa Alta; 5) Sierra de Guadalupe; 6) Sierra de Santa Catarina.

We did not include some of the species in the Rütthling collection (AMNH) for Mexico City, as that collection includes specimens from a German School Collection, from Mexico City. These were donated to Rütthling, namely *Sonora michoacanensis mutabilis* Stickel, 1943 (paratypes: AMNH R-19714-6), *Trimorphodon tau tau* (Cope, 1870) (AMNH R-19718), *Micrurus elegans elegans* (Jan, 1858) (AMNH R-19720), and *Thamnophis proximus* (Say, 1823) (AMNH R-19809-10), but do not occur in Mexico City. In addition, some of the specimens in the German School Collection obtained by Rütthling were most likely not collected in Mexico City (Zweifel 1959). However, some of the specimens in the German School Collection donated to Rütthling could have been collected in Mexico City (e.g., *Senticolis triaspis* (Cope, 1866) [AMNH R-19838]), as there are two more records of this species in other collections: BMNH 1868.4.7.16 collected by Doorman and reported by Günther (1894: 115) and

ENCB-IPN 7398 from San Gregorio, Xochimilco). Other specimens from the Rütling collection donated by the German School are likely to occur in Mexico City (e.g., *Tantilla bocourti* (Günther, 1895) [AMNH R-19735]), but as no other records of the species are available, we decided not to include this species in our list.

We created species accumulation curves for the total herpetofauna, as well as amphibians and reptiles separately, using the year of the first recorded observation for each species. Such species accumulation curves likely provide a good estimate of potential herpetofaunal richness (see Raxworthy et al. 2012). In addition, we recorded the conservation status of each species based on the IUCN Red List 2019-2 (IUCN 2019), SEMARNAT (2019), and Environmental Vulnerability Scores from Wilson et al. (2013a, b) and Johnson et al. (2015). We determined the number of overlapping species with the two states that neighbor Mexico City using recent state lists (State of Mexico, Lemos-Espinal and Smith in press; Morelos, Lemos-Espinal and Smith in 2020).

Results and discussion

Mexico City harbors 65 species of amphibians and reptiles, which represent 21 families (two introduced: Typhlopidae Merrem, 1820 and Emydidae [Rafinesque, 1815]) and 33 genera (two introduced: *Indotyphlops* Hedges, Marion, Lipp, Marin & Vidal, 2014 and *Trachemys* Agassiz, 1857) (Tables 1, 2). These include 18 species of amphibians (nine anurans and nine salamanders) and 47 reptiles (14 lizards, 30 snakes [one introduced], and three turtles [one introduced]). It appears that this list of amphibian and reptile species is likely fairly complete given the shape of the species accumulation curves (Fig. 7). The species accumulation curves indicate a rapid accumulation of species in the late 1800s, followed by a slow gradual increase in species throughout the 20th and early 21st centuries, with a leveling off in recent years.

The two introduced species are Brahminy Blindsnake, *Indotyphlops braminus* (Daudin, 1803), and Huastecan Slider, *Trachemys venusta* (Gray, 1855). Two of the 63 native species are endemic to Mexico City: Great Piping Frog, *Eleutherodactylus grandis* (Dixon, 1957), and Axolotl, *Ambystoma mexicanum* (Shaw & Nodder, 1798). The latter species originally inhabited lakes in the State of Mexico and Mexico City but is currently only known from the remnants of Lake Xochimilco (Frost 2020). The most species-rich amphibian family is Plethodontidae Gray, 1850, and the most species-rich reptile family is Phrynosomatidae Fitzinger, 1843 (Table 1).

We compiled a list of eight species (six amphibians, two reptiles: Table 3) that potentially occur in Mexico City based on their distribution along the border with Morelos and the State of Mexico. We used distributional records in Vertnet.org and the Sistema Nacional de Información sobre Biodiversidad (SNIB-CONABIO) for the two neighboring states and Mexico City to generate this list. As more herpetological work is done near the borders with the neighboring states, we believe that these “likely to occur” species will be recorded for Mexico City.

General distribution

Fifteen of the 18 species of amphibians found in Mexico City are endemic to Mexico. Two species are endemic to Mexico City (*Eleutherodactylus grandis* and *Ambystoma mexicanum*), one species has a spotty distribution in Mexico City and the State of Mexico, seven are distributed in central Mexico (*Dryophytes plicatus* [Brocchi, 1877], *Ambystoma altamirani* Dugès, 1895, *Aquiloerycea cephalica* [Cope, 1865], *Chiropterotrion orculus* [Cope, 1865], *Pseudoerycea altamontana* [Taylor, 1939], *P. leprosa* [Cope, 1869], and *P. tlilicxitl* Lara-Góngora, 2003), two are distributed in central Mexico and the Mexican Altiplano (*Rana montezumae* Baird, 1854, and *Anaxyrus compactilis* [Wiegmann, 1833]), one occurs in central Mexico, the Mexican Altiplano, the Sierra Madre Occidental, and the Sierra Madre Oriental (*Dryophytes eximius* [Baird, 1854]), and one occurs along the Neovolcanic Axis, the Sierra Madre Occidental, the Sierra Madre Oriental, and the Sierra Madre del Sur of Guerrero (*Isthmura belli* [Gray, 1850]). The three amphibian species not endemic to Mexico that inhabit Mexico City are species found in the United States and Mexico (Table 1). Twelve of the 14 species of lizards that occur in Mexico City are endemic to Mexico, six of the endemic species are restricted to a small area in the State of Mexico and Morelos and Mexico City, and in some cases the states of Puebla or Oaxaca (*Sceloporus aeneus* Wiegmann, 1828, *S. anahuacus* Lara-Góngora, 1983, *S. mucronatus* Cope, 1885, *S. palaciosi* Lara-Góngora, 1983, *S. sugillatus* Smith, 1942, and *Plestiodon copei* [Taylor, 1933]), and the other six endemics are widely distributed in the Neovolcanic Axis, including parts of the Sierra Madre Occidental, the Sierra Madre Oriental, and in some cases the Mexican Altiplano (*Barisia imbricata* [Wiegmann, 1828], *Phrynosoma orbiculare* [Linnaeus, 1758], *Sceloporus scalaris* Wiegmann, 1828, *S. spinosus* Wiegmann, 1828, *S. torquatus* Wiegmann, 1828, and *Plestiodon brevirostris* [Günther, 1860]). One of the non-endemic species ranges widely from southeastern United States, south through most of Mexico to southern Oaxaca (*Sceloporus grammicus* Wiegmann, 1828), and the other species ranges from central United States to Central America (*Aspidoscelis gularis* [Baird & Girard, 1852]) (Table 1). Twenty-one of the 29 species of snakes that inhabit Mexico City are endemic to Mexico. Of the eight snake species not endemic to Mexico that inhabit Mexico City, five are found in Canada and/or the United States and Mexico (*Diadophis punctatus* [Linnaeus, 1766], *Micrurus tener* Baird & Girard, 1853, *Rena dulcis* Baird & Girard, 1853, *Thamnophis eques* (Reuss, 1834), and *Crotalus molossus* Baird & Girard, 1853), one is found from Mexico to Central America (*Pituophis lineaticollis* [Cope, 1861]), and two range from the southern United States to Central America (*Senticolis triaspis* [Cope, 1866] and *Thamnophis cyrtopsis* [Kennicott, 1860]).

Habitat types

The most diverse region of the city is the Forests and Ravines region, which is home to 43 species (13 amphibians, 30 reptiles), which represents 70.5% of the species

Table 1. Amphibians and reptiles of Mexico City with distributional and conservation status. Region: (1 = Forests and Ravines; 2 = Wetlands of Xochimilco and Tláhuac; 3 = Urban Parks and Gardens; 4 = Mountains of Xochimilco and Milpa Alta; 5 = Sierra de Guadalupe; 6 = Sierra de Santa Catarina) according to Reygadas-Prado (2016). Species with asterisk (*Geophis bicolor* and *G. petersii*), are records without a specific locality, assigned to a region that we consider the best fit, and species with a question mark (*Lampropeltis polyzona* and *Micrurus tener*) are records without a specific locality representing species with a wide range of habitat use, such that is not possible to assign them to a specific region. IUCN Status: (DD = Data Deficient; LC = Least Concern, VU = Vulnerable, NT = Near Threatened; EN = Endangered; CR = Critically Endangered; NE = not Evaluated) according to the IUCN Red List (The IUCN Red List of Threatened Species, Version 2019-2 (www.iucnredlist.org; accessed 29 November 2019); conservation status in Mexico according to SEMARNAT (2019): (P = in danger of extinction, A = threatened, Pr = subject to special protection, NL = not listed); Environmental Vulnerability Score: (EVS – the higher the score the greater the vulnerability: low (L) vulnerability species (EVS of 3–9); medium (M) vulnerability species (EVS of 10–13); and high (H) vulnerability species (EVS of 14–20) from Wilson et al. (2013a,b) and Johnson et al. (2015); Global Distribution: 0 = Endemic to Mexico City; 1 = Endemic to Mexico; 2 = Shared between the US and Mexico; 3 = widely distributed from Mexico to Central or South America; 4 = widely distributed from the US to Central or South America; IN = introduced to Mexico City. Date in which the first record appeared; and Source of the first record.

	Region	IUCN	SEMARNAT	EVS	Global	Year	Source
Class Amphibia							
Order Anura							
Family Bufonidae Gray, 1825							
<i>Anaxyrus compactilis</i> (Wiegmann, 1833)	1, 2, 3, 4, 5	LC	NL	H (14)	1	1890	Herrera 1890
Family Craugastoridae Hedges, Duellman, & Heinecker, 2008							
<i>Craugastor augusti</i> (Dugès, 1879)	5	LC	NL	L (8)	2	1981	Méndez de la Cruz et al. 1992
Family Eleutherodactylidae Lutz, 1954							
<i>Eleutherodactylus grandis</i> (Dixon, 1957)	3	CR	Pr	H (18)	0	1957	Dixon 1957
Family Hylidae Rafinesque, 1815							
<i>Dryophytes arenicolor</i> (Cope, 1886)	1, 3	LC	NL	L (7)	2	1919	AMNH A-13254
<i>Dryophytes eximius</i> (Baird, 1854)	1, 2, 3, 4, 5	LC	NL	M (10)	1	1853	USNM 3248
<i>Dryophytes plicatus</i> (Brocchi, 1877)	1, 3	LC	A	M (11)	1	1917	MCZ-A 17702
Family Ranidae Batsch, 1796							
<i>Rana montezumae</i> Baird, 1854	2, 3, 4, 5	LC	Pr	M (13)	1	1854	Baird 1854
<i>Rana tlaloci</i> Hillis & Frost, 1985	1, 2, 3, 5	CR	P	H (15)	1	1919	AMNH A-12214
Family Scaphiopodidae Cope, 1865							
<i>Spea multiplicata</i> (Cope, 1863)	1, 2, 3, 4	LC	NL	L (3)	2	1890	Herrera 1890
Order Caudata							
Family Ambystomatidae Gray, 1850							
<i>Ambystoma altamirani</i> Dugès, 1895	1, 3	EN	A	M (13)	1	1908	Gadow 1908
<i>Ambystoma mexicanum</i> (Shaw & Nodder, 1798)	2	CR	P	H (15)	0	1798	Shaw and Nodder 1798
<i>Ambystoma velasci</i> Dugès, 1888	5	LC	Pr	M (10)	1	1882	USNM 12721
Family Plethodontidae Gray, 1850							
<i>Aquiloerycea cephalica</i> (Cope, 1865)	1, 3	NT	A	H (14)	1	1941	AMNH A-52026
<i>Chiropterotriton orculus</i> (Cope, 1865)	1, 3, 4	VU	NL	H (18)	1	1890	Herrera 1890
<i>Isthmura belli</i> (Gray, 1850)	1, 3	VU	A	M (12)	1	1868	BMNH 1868.4.7.37-38

	Region	IUCN	SEMARNAT	EVS	Global	Year	Source
<i>Pseudoeurycea altamontana</i> (Taylor, 1939)	1	EN	Pr	H (17)	1	2004	MZFC 23438
<i>Pseudoeurycea leprosa</i> (Cope, 1869)	1, 3, 4	LC	A	H (16)	1	1890	Herrera 1890
<i>Pseudoeurycea tilixci</i> Lara-Góngora, 2003	1	EN	NL	H (17)	1	1979	CNAR 3682
Class Reptilia							
Suborder Lacertilia							
Family Anguillidae Gray, 1825							
<i>Barisia imbricata</i> (Wiegmann, 1828)	1, 2, 3, 4, 5, 6	LC	Pr	H (14)	1	1868	BMNH 1868.4.7.45–47
Family Phrynosomatidae Fitzinger, 1843							
<i>Phrynosoma orbiculare</i> (Linnaeus, 1758)	1, 3, 4, 5, 6	LC	A	M (12)	1	1818	MVZ 43510
<i>Sceloporus aeneus</i> Wiegmann, 1828	1	LC	NL	M (13)	1	1918	AMNH R-15492
<i>Sceloporus anahuacus</i> Lara-Góngora, 1983	1	LC	NL	H (15)	1	1976	Lara-Góngora 1983
<i>Sceloporus grammicus</i> Wiegmann, 1828	1, 2, 3, 4, 5, 6	LC	Pr	L (9)	2	1892	USNM 18994
<i>Sceloporus mucronatus</i> Cope, 1885	1	LC	NL	M (13)	1	1944	AMNH R-65701
<i>Sceloporus palaciosi</i> Lara-Góngora, 1983	1, 4	LC	NL	H (15)	1	1979	MZFC 790
<i>Sceloporus scalaris</i> Wiegmann, 1828	2, 3, 5, 6	LC	NL	M (12)	1	1896	USNM 46877
<i>Sceloporus spinosus</i> Wiegmann, 1828	5, 6	LC	NL	M (12)	1	1882	USNM 12720
<i>Sceloporus sugillatus</i> Smith, 1942	1	LC	NL	H (16)	1	2008	Mendoza-Hernández et al. 2008
<i>Sceloporus torquatus</i> Wiegmann, 1828	1, 2, 3, 4, 5, 6	LC	NL	M (11)	1	1882	USNM 12719
Family Scincidae Gray, 1825							
<i>Plestiodon brevirostris</i> (Günther, 1860)	1	LC	NL	M (11)	1	?	FMNH w/o number
<i>Plestiodon copei</i> (Taylor, 1933)	1	LC	Pr	H (14)	1	1958	ENCB 810
Family Teiidae Gray, 1827							
<i>Aspidozelis gularis</i> (Baird & Girard, 1852)	4, 5, 6	LC	NL	L (9)	4	1919	AMNH R-14221
Suborder Serpentes							
Family Colubridae Oppel, 1811							
<i>Conopsis biserialis</i> (Taylor & Smith, 1942)	3	LC	A	M (13)	1	1960	ENCB 124
<i>Conopsis lineata</i> (Kennicott, 1859)	1, 3, 4	LC	NL	M (13)	1	1890	Herrera 1890
<i>Conopsis nasus</i> (Günther, 1858)	3, 5	LC	NL	M (11)	1	1903	BMNH 1903.9.30.200
<i>Lampropeltis polyzona</i> Cope, 1860	?	LC	NL	L (7)	1	1868	BMNH 1868.4.7.4
<i>Pituophis deppei</i> (Dumeril, 1853)	1, 2, 3, 4, 5, 6	LC	A	H (14)	1	1868	BMNH 1868.4.7.38
<i>Pituophis lineaticollis</i> (Cope, 1861)	1	LC	NL	L (8)	3	1932	FMNH 106582
<i>Salvadora bairdi</i> Jan & Sordelli, 1860	1, 3, 5, 6	LC	Pr	H (15)	1	1919	AMNH R-19528
<i>Senticolis triaspis</i> (Cope, 1866)	2	LC	NL	L (6)	4	1868	BMNH 1868.4.7.16
<i>Tantilla calamarina</i> Cope, 1866	1	LC	Pr	M (12)	1	1919	AMNH R-19750
Family Dipsadidae Bonaparte, 1838							
<i>Diadophis punctatus</i> (Linnaeus, 1766)	1, 2, 3, 5	LC	NL	L (4)	2	1868	Günther 1868
<i>Geophis bicolor</i> Günther, 1868	1*	DD	Pr	H (15)	1	1868	Günther 1868

	Region	IUCN	SEMARNAT	EVS	Global	Year	Source
<i>Geophis petersii</i> Boulenger, 1894	1*	DD	Pr	H (15)	1	1894	Boulenger 1894
<i>Rhadinaea laureata</i> (Günther, 1868)	1,3,6	LC	NL	M (12)	1	1868	Günther 1868
<i>Rhadinaea taeniata</i> (Peters, 1863)	1	LC	NL	M (13)	1	1868	BMNH 1868.4.7.13-14
Family Elapidae Boie, 1827							
<i>Micrurus tener</i> Baird & Girard, 1853	?	LC	NL	M (11)	2	1868	BMNH 1868.4.7.5
Family Leptotyphlopidae Stejneger, 1892							
<i>Rena dulcis</i> Baird & Girard, 1853	3	LC	NL	M (13)	2	2009	Méndez de la Cruz et al. 2009
Family Natricidae Bonaparte, 1838							
<i>Storeria storerioides</i> (Cope, 1866)	1, 3, 4	LC	NL	M (11)	1	1868	BMNH 1868.4.7.15
<i>Thamnophis cyrtopsis</i> (Kennicott, 1860)	1	LC	A	L (7)	4	1890	Herrera 1890
<i>Thamnophis eques</i> (Reuss, 1834)	1, 3, 5, 6	LC	A	L (8)	2	1860	Kennicott 1860
<i>Thamnophis melanogaster</i> (Wiegmann, 1830)	2, 3	EN	A	H (15)	1	1882	USNM 12726
<i>Thamnophis pulchrilatus</i> (Cope, 1885)	1	LC	NL	H (15)	1	1890	Herrera 1890
<i>Thamnophis scalaris</i> Cope, 1861	1, 3, 5	LC	A	H (14)	1	1890	Herrera 1890
<i>Thamnophis scaliger</i> (Jan, 1863)	1, 2, 3, 4	VU	A	H (15)	1	1868	BMNH 1868.4.7.10
Family Typhlopidae Merrem, 1820							
<i>Indotyphlops braminus</i> (Daudin, 1803)	3	IN	NA	NA	NA	1995	CNAR 11281
Family Viperidae Opperl, 1811							
<i>Crotalus aquilus</i> Klauber, 1952	5	LC	Pr	H (16)	1	2016	García-Vázquez and Méndez de la Cruz 2016
<i>Crotalus molossus</i> Baird & Girard, 1853	3, 4, 5, 6	LC	Pr	L (8)	2	1868	BMNH 1868.4.7.2
<i>Crotalus polystictus</i> (Cope, 1865)	2	LC	Pr	H (16)	1	1890	Herrera 1890
<i>Crotalus ravus</i> Cope, 1865	1, 2, 3, 4, 5, 6	LC	A	H (14)	1	1944	UMMZ 99847
<i>Crotalus transversus</i> Taylor, 1944	1	LC	P	H (17)	1	?	ROM 47094
<i>Crotalus triseriatus</i> (Wagler, 1830)	1, 2, 3, 4	LC	NL	H (16)	1	1868	BMNH 1946.1.17.70
Order Testudines							
Family Emydidae (Rafinesque, 1815)							
<i>Trachemys venusta</i> (Gray, 1855)	3	IN	NA	NA	NA	2009	Méndez de la Cruz et al. 2009
Family Kinosternidae Agassiz, 1857							
<i>Kinosternon hirtipes</i> (Wagler, 1830)	2,5	LC	Pr	M (10)	2	1888	Dugès 1888
<i>Kinosternon integrum</i> LeConte, 1854	2	LC	Pr	M (11)	1	1888	Dugès 1888

pool for the city. This region occupies the second place in the territorial area of the city with 534.4 km² (36.0% of the surface of Mexico City). This region is in the best conservation state and is where there is the possibility of rediscovering species known only from historical records such as *Geophis bicolor* Günther, 1868, *Geophis petersii* Boulenger, 1894, and *Rhadinaea taeniata* (Peters, 1863), or finding new species records such as for *Eleutherodactylus nitidus* (Peters, 1870), *Exerodonta smaragdina* (Tay-

lor, 1940), and *Tantilla bocourti* (Günther, 1895). This region also has a high number of species listed in an IUCN protected category (7 amphibians, 1 reptile), listed in a SEMARNAT protected category (6 amphibians, 7 reptiles), and categorized as high risk by the EVS (7 amphibians, 15 reptiles). The second most diverse region of Mexico City is the Urban Parks and Gardens that hosts 34 species (13 amphibians, 21 reptiles). This region occupies the largest area of the city with 607.3 km² (40.9% of the surface of Mexico City). It is also the most populated region and is dominated by urban habitats, which are generally not suitable for most amphibians and reptiles. However, it has two important urban parks, the Pedregal de San Angel Ecological Reserve (REPSA) and the Chapultepec Forest, where the largest number of species has been recorded for this region. The number of species in this region listed in an IUCN protected category (6 amphibians, 2 reptiles), listed as protected by SEMARNAT (6 amphibians, 7 reptiles), and categorized as high risk by the EVS (6 amphibians, 8 reptiles) is also high. The Wetlands of Xochimilco and Tláhuac and the Mountains of Xochimilco and Milpa Alta, and the Sierra de Guadalupe host similar numbers of amphibian and reptile species and also have similar numbers of species included in the IUCN and SEMARNAT lists or categorized as high risk by the EVS. In the Wetlands of Xochimilco and Tláhuac, 20 species (6 amphibians, 14 reptiles) are present, of which four are listed by the IUCN, five by SEMARNAT, and 10 are categorized as high risk by the EVS. In the Mountains of Xochimilco and Milpa Alta, 19 species (6 amphibians, 13 reptiles) are found, of which two are listed by the IUCN, four by SEMARNAT, and nine are categorized as high risk by the EVS. In the Sierra de Guadalupe, 23 species (6 amphibians, 17 reptiles) occur, of which one is listed by the IUCN, five by SEMARNAT, and eight are categorized as high risk by the EVS. The Sierra de Santa Catarina region is like an island, a mountain with disturbed vegetation surrounded by urban habitats. It has an area of only 31.4 km² (2.1% of the area of Mexico City; Fig. 7) and harbors 13 species of reptiles. However, the government of Mexico City mentioned the presence of two amphibians and 14 reptiles, with only eight reptile species included in the SEMARNAT list (Gobierno del Distrito Federal [= Mexico City] 2005). None of the reptile species in this region are included in the IUCN list, three are in the SEMARNAT list, and four are categorized as high risk by the EVS. Our observations of the distribution of amphibians and reptiles in Mexico City are broadly consistent with the findings of García Vázquez and Méndez de la Cruz (2016) and García Vázquez et al. (2016).

Conservation status

Eleven of the 63 species (17.5%) of amphibians and reptiles in Mexico City are included in the IUCN Red List (i.e., Vulnerable, Near Threatened, or Endangered), 17 (27.0%) are placed in a protected category (excluding NL and Pr, this last category is equivalent to the LC category of IUCN) by SEMARNAT, and 27 species (42.9%) are categorized as high risk by the EVS (Fig. 8; Table 2). For amphibians, 38.9% (7 of 18 species) are included in the IUCN Red List and are protected by SEMARNAT, and

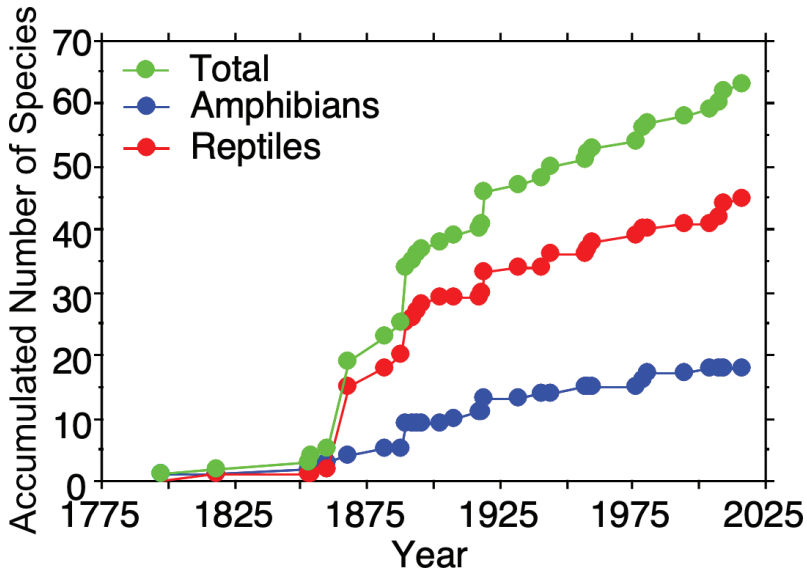
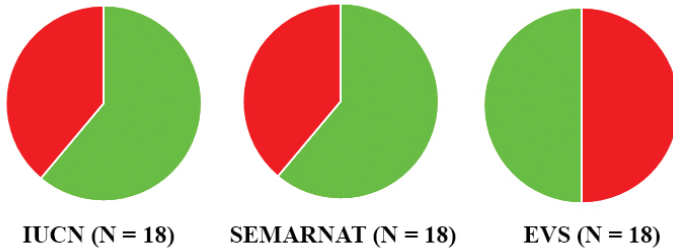


Figure 7. Species accumulation curves for total herpetofauna of Mexico City, Mexico, as well as separately for amphibians and reptiles.

A) Amphibians



B) Reptiles

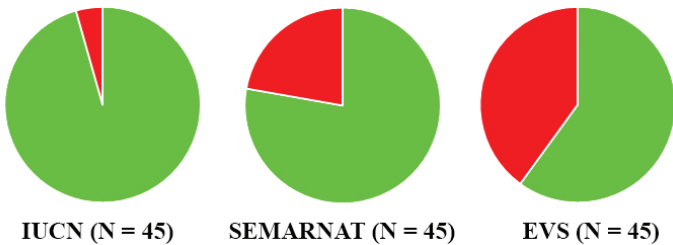


Figure 8. Percentage of species included in the IUCN Red List or listed by SEMARNAT, and the Environmental Vulnerability Score (EVS). **A** Amphibians **B** reptiles. Green is percentage in Data Deficient and Least Concern (IUCN); Not Listed and Subject to Special Protection (we regarded the category of Subject to Special Protection in SEMARNAT equivalent to IUCN's Least Concern) (SEMARNAT); low and medium EVS. Red is percentage in protected categories or high EVS. *N* is the number of species assessed by each agency.

Table 2. Summary of native species present in Mexico City by class, family, order, and suborder. Status summary indicates the number of species found in each IUCN conservation status in the order DD, LC, VU, NT, EN, CR (see Table 1 for abbreviations). For mean EVS (Environmental Vulnerability Score), scores ≥ 14 are considered to have high vulnerability (Wilson et al. 2013a, b). Conservation status in Mexico are number of species in each category (NL, Pr, A, P; see Table 1 for abbreviations) according to SEMARNAT (2019).

Scientific name	genera	species	IUCN	\bar{x} EVS	SEMARNAT
			DD, LC, VU, NT, EN, CR		NL, Pr, A, P
Class Amphibia					
Order Anura	6	9	0, 7, 0, 0, 0, 2	11	5, 2, 1, 1
Bufonidae	1	1	0, 1, 0, 0, 0, 0	14	1, 0, 0, 0
Craugastoridae	1	1	0, 1, 0, 0, 0, 0	8	1, 0, 0, 0
Eleutherodactylidae	1	1	0, 0, 0, 0, 0, 1	18	0, 1, 0, 0
Hylidae	1	3	0, 3, 0, 0, 0, 0	9.3	2, 0, 1, 0
Ranidae	1	2	0, 1, 0, 0, 0, 1	14	0, 1, 0, 1
Scaphiropodidae	1	1	0, 1, 0, 0, 0, 0	3	1, 0, 0, 0
Order Caudata	5	9	0, 2, 2, 1, 3, 1	14.7	2, 2, 4, 1
Ambystomatidae	1	3	0, 1, 0, 0, 1, 1	12.7	0, 1, 1, 1
Plethodontidae	4	6	0, 1, 2, 1, 2, 0	15.7	2, 1, 3, 0
Subtotal	11	18	0, 9, 2, 1, 3, 3	12.8	7, 4, 5, 2
Class Reptilia					
Order Squamata	19	43	2, 39, 1, 0, 1, 0	12.3	23, 10, 9, 1
Suborder Lacertilia	5	14	0, 14, 0, 0, 0, 0	12.6	10, 3, 1, 0
Anguidae	1	1	0, 1, 0, 0, 0, 0	14	0, 1, 0, 0
Phrynosomatidae	2	10	0, 10, 0, 0, 0, 0	12.8	8, 1, 1, 0
Scincidae	1	2	0, 2, 0, 0, 0, 0	12.5	1, 1, 0, 0
Teiidae	1	1	0, 1, 0, 0, 0, 0	9	1, 0, 0, 0
Suborder Serpentes	14	29	2, 25, 1, 0, 1, 0	12.2	13, 7, 8, 1
Colubridae	6	9	0, 9, 0, 0, 0, 0	11	5, 2, 2, 0
Dipsadidae	3	5	2, 3, 0, 0, 0, 0	11.8	3, 2, 0, 0
Elapidae	1	1	0, 1, 0, 0, 0, 0	11	1, 0, 0, 0
Leptotyphlopidae	1	1	0, 1, 0, 0, 0, 0	13	1, 0, 0, 0
Natricidae	2	7	0, 5, 1, 0, 1, 0	12.1	2, 0, 5, 0
Viperidae	1	6	0, 6, 0, 0, 0, 0	14.5	1, 3, 1, 1
Order Testudines	1	2	0, 2, 0, 0, 0, 0	10.5	0, 2, 0, 0
Kinosternidae	1	2	0, 2, 0, 0, 0, 0	10.5	0, 2, 0, 0
Subtotal	20	45	2, 41, 1, 0, 1, 0	12.2	23, 12, 9, 1
Total	31	63	2, 50, 3, 1, 4, 3	12.4	30, 16, 14, 3

50.0% (9 species) are at high risk according to the EVS (Fig. 8; Table 2). For reptiles, 4.4% (2 of 45 species) are listed by the IUCN, 22.2% (10 species) are protected by SEMARNAT, and 40.0% (18 species) are at high risk according to the EVS (Fig. 8; Table 2). These results suggest that the amphibians of Mexico City are considered to be of relatively high conservation concern at a global and national scale (IUCN and SEMARNAT lists), but there are even greater conservation concerns based on the EVS. The limited distribution of half of the amphibian species that inhabit Mexico City, coupled with the loss of available habitat, places them in a delicate conservation status. For example, the Axolotl, *Ambystoma mexicanum*, which is listed as Critically Endangered by the IUCN and In Danger of Extinction by SEMARNAT, currently appears to be limited to Lake Xochimilco and faces threats such as introduced predators, illegal

Table 3. List of amphibian and reptile species that potentially occur in Mexico City.

Taxon	Likely to occur in:
Class Amphibia	
Order Anura	
Family Bufonidae	
<i>Incilius marmoreus</i> (Wiegmann, 1833)	southern Mexico City
<i>Incilius occidentalis</i> (Camerano, 1879)	southern Mexico City
Family Eleutherodactylidae	
<i>Eleutherodactylus nitidus</i> (Peters, 1870)	southern Mexico City
Family Hylidae	
<i>Exerodonta smaragdina</i> (Taylor, 1940)	southern Mexico City
<i>Tlalocohyla smithii</i> (Boulenger, 1902)	southern Mexico City
Family Ranidae	
<i>Rana spectabilis</i> Hillis & Frost, 1985	southern Mexico City
Class Reptilia	
Order Squamata	
Suborder Lacertilia	
Family Scincidae	
<i>Plestiodon indubitatus</i> (Taylor, 1933)	southern Mexico City
Suborder Serpentes	
Family Colubridae	
<i>Tantilla bocourti</i> (Günther, 1895)	southern Mexico City

collection, and pollution (Griffiths et al. 2004; Contreras et al. 2009; Recuero et al. 2010). On the other hand, reptiles are of lesser conservation concern than amphibians according to the IUCN and SEMARNAT lists, but not the EVS list (Fig. 8), which is a reflection that EVS uses more variables in determining country-level conservation status than either the IUCN or SEMARNAT (see Wilson et al. 2013a, 2013b).

Comparison with neighboring states

Mexico City shares more than 90% of its species (59 of 63 species = 93.7%, Table 4), with the State of Mexico, such that the herpetofauna of Mexico City is practically contained in that of the State of Mexico. Both the city and state are in the Basin of Mexico, which is included in the physiographic province of the Neovolcanic Axis, and all of Mexico City belongs to the sub-province of Lagos y Volcanes de Anáhuac, which also forms a part of the State of Mexico. Thus, the topographic and physiographic characteristics shared by these two entities result in a great similarity of their biological diversity, including their herpetofaunas. Additionally, the State of Mexico surrounds Mexico City on three sides (west, north, and east), and this, coupled with the small territorial area of Mexico City, results in a nesting of the species richness of Mexico City in the species richness of the State of Mexico. There are four species that Mexico City does not share with the State of Mexico. These include *Eleutherodactylus grandis*, which is limited to the Pedregal de San Angel in the Urban Parks and Gardens region; *Ambystoma mexicanum*, currently limited to two wild populations, one in the channels

Table 4. Summary of the numbers of species shared between Mexico City and neighboring Mexican states (not including introduced species). The percent of Mexico City species shared by a neighboring state are given in parentheses. Total refers to the total number of species found in Mexico City and two neighboring states (i.e., regional species pool) and the number in parentheses in this column is the percent of the regional species pool found in Mexico City. – indicates either Mexico City or the neighboring state has no species in the taxonomic group, or none of that specific taxon is shared between the states, thus no value for shared species is provided.

Taxon	Mexico City	State of Mexico	Morelos	Total
Class Amphibia	18	16 (88.9)	14 (77.8)	55 (32.7)
Order Anura	9	8 (88.9)	7 (77.8)	39 (23.1)
Bufonidae	1	1 (100)	1 (100)	5 (20.0)
Centrolenidae	–	–	–	1 (0)
Craugastoridae	1	1 (100)	1 (100)	5 (20.0)
Eleutherodactylidae	1	–	–	5 (20.0)
Hylidae	3	3 (100)	3 (100)	10 (30.0)
Leptodactylidae	–	–	–	1 (0)
Microhylidae	–	–	–	3 (0)
Phyllomedusidae	–	–	–	1 (0)
Ranidae	2	2 (100)	1 (50)	7 (28.6)
Scaphiopodidae	1	1 (100)	1 (100)	1 (100)
Order Caudata	9	8 (88.9)	7 (77.8)	16 (56.3)
Ambystomatidae	3	2 (66.7)	1 (33.3)	8 (37.5)
Plethodontidae	6	6 (100)	6 (100)	8 (75.0)
Class Reptilia	45	43 (95.6)	35 (77.8)	125 (36.0)
Order Squamata	43	41 (95.3)	33 (76.7)	120 (35.8)
Suborder Lacertilia	14	14 (100)	12 (85.7)	49 (28.6)
Anguidae	1	1 (100)	1 (100)	5 (20.0)
Dactyloidae	–	–	–	1 (0)
Eublepharidae	–	–	–	1 (0)
Helodermatidae	–	–	–	1 (0)
Iguanidae	–	–	–	1 (0)
Phrynosomatidae	10	10 (100)	9 (90.0)	23 (43.5)
Phyllodactylidae	–	–	–	3 (0)
Scincidae	2	2 (100)	2 (100)	6 (33.3)
Teiidae	1	1 (100)	–	8 (12.5)
Suborder Serpentes	29	27 (93.1)	21 (72.4)	71 (40.8)
Boidae	–	–	–	1 (0)
Colubridae	9	9 (100)	9 (100)	24 (37.5)
Dipsadidae	5	4 (80.0)	2 (40.0)	18 (27.8)
Elapidae	1	1 (100)	1 (100)	3 (33.3)
Leptotyphlopidae	1	–	–	3 (33.3)
Loxocemidae	–	–	–	1 (0)
Natricidae	7	7 (100)	4 (57.1)	10 (70.0)
Viperidae	6	6 (100)	5 (83.3)	11 (54.5)
Order Testudines	2	2 (100)	2 (100)	5 (40.0)
Emydidae	–	–	–	1 (0)
Geoemydidae	–	–	–	1 (0)
Kinosternidae	2	2 (100)	2 (100)	3 (66.7)
Total	63	59 (93.7)	49 (77.8)	180 (35.0)

of Lake Xochimilco and a second in the remnants of Lake Chalco, both in southern Mexico City, where it faces serious conservation problems (Zambrano González et al. 2003; Recuero et al. 2010); *Geophis petersi*, a snake with secretive habits, which is difficult to find and known only from the type series; and *Rena dulcis*, reported by Méndez de la Cruz et al. (2007, 2009) in the Pedregal de San Angel.

Geophis petersi was collected by H. Doorman in 1868 and its type locality at Mexico City was questioned and restricted to Pátzcuaro, Michoacán by Smith and Taylor (1950); however, Downs (1967) pointed out that this restriction was unjustified and that the presence of *G. petersi* at the southern tip of the Mexican Altiplano seems reasonable. Due to the secretive habits and presence of similar habitats in the State of Mexico, it is possible that *G. petersi* also inhabits the State of Mexico but not yet recorded from there. A similar situation occurs for *R. dulcis*, the other species not yet recorded in the State of Mexico, but due to its secretive habits and tiny size, this snake might also likely occur in the State of Mexico.

Mexico City shares 49 of its amphibians and reptiles with Morelos (77.8%; Table 4). The lower percentage of shared species compared to the State of Mexico is partly due to the fact that Morelos is not within the Basin of Mexico; however, part of it is included in the physiographic province of the Neovolcanic Axis, subprovince of Lagos y Volcanes de Anáhuac. In addition, less temperate forest is present in Morelos, and Morelos is smaller compared to the State of Mexico (Lemos-Espinal and Smith 2020). These characteristics result in fewer species shared with Morelos than with the State of Mexico. Seven of the 14 species that Mexico City does not share with Morelos probably inhabit this latter state, but they have not been recorded yet (*Ambystoma velasci*, *Sceloporus anahuacus*, *Diadophis punctatus*, *Geophis bicolor*, *G. petersi*, *Thamnophis melanogaster*, and *T. pulchrilatus*) (Lemos-Espinal and Smith 2020).

Acknowledgements

We thank Jesús Sigala for very helpful comments that greatly improved the manuscript. Support for this study was provided by Dirección General de Asuntos del Personal Académico, Programa de Apoyo a Proyectos de Investigación e Innovación Tecnológica (DGAPA-PAPIIT) through the Project IN215418. We are grateful to A. Núñez Merchand from the National Commission for the Understanding and Use of Biodiversity (CONABIO) for kindly creating and providing the municipality, topographic, physiographic, climate, and vegetation maps used in this publication, and to I. Cruz, also from CONABIO, for providing the satellite images of Mexico City. We are grateful to A. Resetar and J. Mata from the Field Museum of Natural History, Chicago, Illinois; E.M. Braker from the University of Colorado Museum, University of Colorado at Boulder, Colorado; J. McGuire, C. Spencer, and D. Wake from the Museum of Vertebrate Zoology at Berkeley, University of California at Berkeley, California; and D. Dickey and D.A. Kizirian from the American Museum of Natural History, New York.

References

- AmphibiaWeb (2020) AmphibiaWeb University of California, Berkeley, CA, USA. <https://amphibiaweb.org> [Accessed on: 2020-1-10]
- Baird SF (1854) Descriptions of new genera and species of North American frogs. *Proceedings of the Academy of Natural Sciences of Philadelphia* 7: 59–62.
- Boulenger GA (1894) Catalogue of the snakes in the British Museum (Natural History). Volume II., Containing the Conclusion of the Colubridae Aglyphae. British Museum of Natural History, London, xi, 382 pp.
- Caro-Borrero A, Carmona Jiménez J, Mazari Hiriart M (2016) Evaluation of ecological quality in peri-urban rivers in Mexico City: a proposal for identifying and validating reference sites using benthic macroinvertebrates as indicators. *Journal of Limnology* 75: 1–16. <https://doi.org/10.4081/jlimnol.2015.1304>
- CONABIO [Comisión Nacional para el Conocimiento y Uso de la Biodiversidad] (1997) “Modelo Digital del Terreno”. Escala 1:250 000. Mexico.
- Contreras V, Martínez-Meyer E, Valiente E, Zambrano L (2009) Recent decline and potential distribution in the last remnant area of the microendemic Mexican axolotl (*Ambystoma mexicanum*). *Biological Conservation* 142: 2881–2885. <https://doi.org/10.1016/j.biocon.2009.07.008>
- Cope ED (1885) Twelfth contribution to the herpetology of tropical America. *Proceedings of the American Philosophical Society* 22: 167–194.
- Dixon JR (1957) Geographic variation and distribution of the genus *Tomodactylus* in Mexico. *Texas Journal of Science* 9: 379–409.
- Downs FL (1967) Intrageneric relations among colubrid snakes of the genus *Geophis* Wagler. *Miscellaneous Publications Museum of Zoology, University of Michigan* 131: 1–193.
- Dugès AAD (1888) *Erpetología del Valle de Mexico*. La Naturaleza. Serie 2. México 1: 97–146.
- Frost DR (2020) *Amphibian Species of the World: an Online Reference*. Version 6.1 (10 January 2020). American Museum of Natural History, New York. <https://doi.org/10.5531/db.vz.0001>
- Gadow H (1908) *Through Southern Mexico: Being an Account of the Travels of a Naturalist*. Witherby & Co., London, 527 pp.
- García E, Comisión Nacional para el Conocimiento y Uso de la Biodiversidad (CONABIO) (1998). *Climas (Clasificación de Köppen, modificado por García)*. Escala 1:1 000 000. Mexico.
- García-Vázquez UO, Méndez de la Cruz F (2016) Reptiles. In: *La Biodiversidad de la Ciudad de México*, Vol. 2. CONABIO/SEDEMA, México, 390–397.
- García-Vázquez UO, Trujano-Ortega M, Casas-Andreu G (2016) Anfibios. In: *La Biodiversidad de la Ciudad de México*, Vol. 2. CONABIO/SEDEMA, México, 383–389.
- Gobierno del Distrito Federal (2005) Acuerdo por el que se aprueba el programa de manejo del Área Natural Protegida con carácter de Zona de Conservación Ecológica “Sierra de Santa Catarina”. *Gaceta Oficial del Distrito Federal* 98. <http://paot.org.mx/centro/programas/manejo/santacatarina.pdf>
- Griffiths RA, Bride IG, Meléndez A, Álvarez-Romero JG, Arana F, Arroyo IA, Benítez H, Buley K, Bustamante E, Chaparro D, Chávez JM, Contreras AV, Díaz M, Gual F, Ibáñez

- R, Leyaz A, Marín AI, Martínez S, McKay J, Millán E, Mistry E, Molina A, Morales O, Mosig P, Núñez J, Olivera C, Ortiz Y, Pérez-Gil R, Ramos P, Reséndiz J, Reyes O, Rivas M, Romero AP, Rosas I, Sandoval, Sarina N, Servín E, Sherezada E, Solzoor A, Steck A, Stephan-Otto E, Valiente E, Vanegas C, Wilkinson R (2004) The conservation of the axolotl (*Ambystoma mexicanum*) in Xochimilco, Mexico City: a species/habitat action plan. Produced by the Darwin Initiative International Seminar-Workshop held at UAMXCI-BAC, Dec. 6–9, Mexico City. Durrell Institute of Conservation and Ecology (DICE), University of Kent, Canterbury.
- Günther ACLG (1868) Sixth account of new species of snakes in the collection of the British Museum. *Annals and Magazine of Natural History (Series 4)* 1: 413–429. <https://doi.org/10.1080/00222936808695725>
- Heider K, López JMR, Scheffran J (2018) The potential of volunteered geographic information to investigate peri-urbanization in the conservation zone of Mexico City. *Environmental Monitoring and Assessment* 190: 219. <https://doi.org/10.1007/s10661-018-6597-3>
- Hernández-Flores M de la L, Otazo-Sánchez EM, Galeana-Pizaña M, Roldán-Cruz EI, Razo-Zárate R, González-Ramírez CA, Galindo-Castillo E, Grodillo-Martínez AI (2017) Urban driving forces and megacity expansion threats. Study case in the Mexico City periphery. *Habitat International* 64: 109–122. <https://doi.org/10.1016/j.habitatint.2017.04.004>
- Herrera AL (1890) Notas acerca de los vertebrados del Valle de México. *La Naturaleza (2ª Ser.)* 1: 299–342.
- Imaz M (1989) Historia natural del Valle de México. *Revista Ciencias* 15: 15–21.
- INEGI (2016) Conjunto de Datos Vectoriales de Uso de Suelo y Vegetación. Escala 1:250 000. Serie VI (Capa Unión), escala: 1:250 000. Edición: 1. Instituto Nacional de Estadística y Geografía, Aguascalientes, México.
- INEGI (2017) Anuario estadístico y geográfico de la Ciudad de México 2017. Instituto Nacional de Estadística y Geografía, México.
- INEGI (2018) 'Áreas Geoestadísticas Estatales', escala: 1:250000. edición: 1. Instituto Nacional de Estadística y Geografía, Aguascalientes, México.
- IUCN (2019) IUCN Red List of Threatened Species, Version 2019.2. <https://www.iucnredlist.org> [Accessed on: 2019-11-19]
- Johnson JD, Mata-Silva V, Wilson LD (2015) A conservation reassessment of the Central American herpetofauna based on the EVS measure. *Amphibian & Reptile Conservation* 9: 1–94.
- Kennicott R (1860) Descriptions of new species of North American serpents in the museum of the Smithsonian Institution, Washington. *Proceedings of the Academy of Natural Science of Philadelphia* 12: 328–338. <https://doi.org/10.5735/086.047.0401>
- Lara-Góngora G (1983) Two new species of the lizard genus *Sceloporus* (Reptilia, Sauria, Iguanidae) from the Ajusco and Ocuilan Sierras, Mexico. *Bulletin of the Maryland Herpetological Society* 19: 1–14.
- Lemos-Espinal JA, Smith GR (in press) A conservation checklist of the amphibians and reptiles of the State of Mexico, Mexico with comparisons with adjoining states. *ZooKeys*.
- Lemos-Espinal JA, Smith GR (2020) A conservation checklist of the herpetofauna of Morelos, with comparisons with adjoining states. *ZooKeys* 941: 121–144. <https://doi.org/10.3897/zookeys.941.52011>

- Méndez de la Cruz FR, Camarillo-Rangel JL, Villagrán-Santa Cruz M, Aguilar-Cortéz R (1992) Observaciones sobre el estatus de los anfibios y reptiles de la Sierra de Guadalupe (Distrito Federal – Estado de México). *Anales del Instituto de Biología, Universidad Nacional Autónoma de México, Serie Zoológica* 63: 246–256.
- Méndez de la Cruz FR, Díaz de la Vega Pérez AH, Jiménez-Arcos VH (2009) Herpetofauna. In: Lot A, Cano-Santana Z (Eds) *Biodiversidad del Pedregal de San Ángel*. UNAM, Reserva Ecológica del Pedregal de San Ángel y Coordinación de la Investigación Científica, D.F. México, 243–260.
- Méndez de la Cruz FR, Zúñiga-Vega JJ, Díaz de la Vega Pérez AH, Lara-Reséndiz RA, Martínez-Méndez N (2007) Anfibios y reptiles. In: Lot A (Ed.) *Guía ilustrada de la Cantera Oriente. Caracterización ambiental e inventario biológico*. Reserva Ecológica del Pedregal de San Ángel. Coordinación de la Investigación Científica, UNAM., D.F. México, 203–219.
- Mendoza-Hernández AA, García-Vázquez UO, Nieto-Montes de Oca A (2008) *Sceloporus sugillatus*. *Herpetological Review* 39: 483–484.
- Raxworthy CJ, Ananjeva N, Orlov NC (2012) Complete species inventories. In: McDiarmid RW, Foster MS, Guyer C, Gibbons JW, Chernoff N (Eds) *Reptile Biodiversity: Standard Methods for Inventory and Monitoring*. University of California Press, Berkeley, 209–215.
- Recuero E, Cruzado-Cortés J, Parra-Olea G, Zamudio KR (2010) Urban aquatic habitats and conservation of highly endangered species: the case of *Ambystoma mexicanum* (Caudata, Ambystomatidae). *Annales Zoologici Fennici* 47: 223–238. <https://doi.org/10.5735/086.047.0401>
- Reygadas-Prado DD (2016) Delimitación del área de estudio y regionalización. *La Biodiversidad de la Ciudad de México*, Vol. 1. CONABIO/SEDEMA, México, 30–35.
- Rodríguez López JM, Heider K, Scheffran J (2017) Frontiers of urbanization: identifying and explaining urbanization hot spots in the south of Mexico City using human and remote sensing. *Applied Geography* 79: 1–10. <https://doi.org/10.1016/j.apgeog.2016.12.001>
- Santibáñez-Andrade G, Castillo-Argüero S, Vega-Peña EV, Lindig-Cisneros R, Zavala-Hurtado JA (2015) Structural equation modeling as a tool to develop conservation strategies using environmental indicators: the case of the forests of the Magdalena river basin in Mexico City. *Ecological Indicators* 54: 124–136. <https://doi.org/10.1016/j.ecolind.2015.02.022>
- SEMARNAT (2016) Informe de la situación del medio ambiente en México 2015. Compendio de estadísticas ambientales, indicadores clave, de desempeño ambiental y de crecimiento verde. Secretaría de Medio Ambiente y Recursos Naturales, México. https://apps1.semarnat.gob.mx:8443/dgeia/informe15/tema/pdf/Informe15_completo.pdf
- SEMARNAT (2019) Modificación al anexo normativo III, lista de especies en riesgo de la Norma Oficial Mexicana NOM-059-SEMARNAT-2010. Protección ambiental-Especies nativas de México de flora y fauna silvestres-Categorías de riesgo y especificaciones para su inclusión, exclusión o cambio-Lista de especies en riesgo, publicada el 30 de diciembre del 2010 (14 noviembre 2019). Secretaría de Medio Ambiente y Recursos Naturales, México. https://www.dof.gob.mx/nota_detalle.php?codigo=5578808&fecha=14/11/2019
- Smith HM (1943) Summary of the collections of snakes and crocodilians made in Mexico under the Walter Rathbone Bacon Traveling Scholarship. *Proceedings of the United States National Museum* 93 (3169): 393–504.

- Smith HM, Taylor EH (1950) Type localities of Mexican reptiles and amphibians. University of Kansas Science Bulletin 33: 313–380.
- Shaw G, Nodder FP (1798) The Naturalist's Miscellany; or Coloured Figures of Natural Objects Drawn and Described Immediately from Nature. Volume 9. Nodder and Company, London, 287 pp.
- Uetz P, Hošek J (2019) The Reptile Database. <http://www.reptile-database.org> [Accessed on: 2019-12-17]
- Wilson LD, Johnson JD, Mata-Silva V (2013a) A conservation reassessment of the amphibians of Mexico based on the EVS measure. *Amphibian & Reptile Conservation* 7: 97–127.
- Wilson LD, Mata-Silva V, Johnson JD (2013b) A conservation reassessment of the reptiles of Mexico based on the EVS measure. *Amphibian & Reptile Conservation* 7: 1–47.
- Zambrano González L, Reynoso VH, Herrera G (2003) Abundancia y estructura poblacional del axolotl (*Ambystoma mexicanum*) en los sistemas dulceacuicolas de Xochimilco y Chalco. Universidad Nacional Autónoma de México. Instituto de Biología. Informe final SNIB-CONABIO proyecto No. AS004. México, D.F.
- Zweifel RG (1959) Additions to the herpetofauna of Nayarit, Mexico. *American Museum Novitates* 1953: 1–13.

Appendix I

Museum collections included in the VertNet.org database records of Mexico City amphibians and reptiles that house specimens of the first record of a species in Mexico City.

- AMNH** Collection of Herpetology, Herpetology Department, American Museum of Natural History
- BMNH** Zoological Collection, Natural History Museum (London)
- CNAR** Colección Nacional de Anfibios y Reptiles, Instituto de Biología, Universidad Nacional Autónoma de México
- ENCB** Escuela Nacional de Ciencias Biológicas, Instituto Politécnico Nacional
- FMNH** Division of Amphibians and Reptiles, Field Museum of Natural History
- MCZ** Collection of Herpetology, Museum of Comparative Zoology, Harvard University Cambridge
- MVZ** Museum of Vertebrate Zoology at Berkeley, Herpetological Collection
- MZFC** Colección Herpetológica, Museo de Zoología Alfonso L. Herrera, Facultad de Ciencias, UNAM
- ROM** Herpetology Collection, Royal Ontario Museum
- UMMZ** Collection of Herpetology, Museum of Zoology, University of Michigan Ann Arbor
- USNM** Collection of Herpetology, Department of Vertebrate Zoology, National Museum of Natural History, Smithsonian Institution

Resolving a taxonomic and nomenclatural puzzle in mantellid frogs: synonymization of *Gephyromantis azzurrae* with *G. corvus*, and description of *Gephyromantis kintana* sp. nov. from the Isalo Massif, western Madagascar

Walter Cocca¹, Franco Andreone², Francesco Belluardo¹, Gonçalo M. Rosa^{3,4},
Jasmin E. Randrianirina⁵, Frank Glaw⁶, Angelica Crottini^{1,7}

1 CIBIO, Research Centre in Biodiversity and Genetic Resources, InBIO, Universidade do Porto, Campus Agrário de Vairão, Rua Padre Armando Quintas, No 7, 4485-661 Vairão, Portugal **2** Sezione di Zoologia, Museo Regionale di Scienze Naturali, Via G. Giolitti, 36, 10123 Torino, Italy **3** Institute of Zoology, Zoological Society of London, Regent's Park, NW1 4RY London, UK **4** Centre for Ecology, Evolution and Environmental Changes (cE3c), Faculdade de Ciências da Universidade de Lisboa, Bloco C2, Campo Grande, 1749-016 Lisboa, Portugal **5** Parc Botanique et Zoologique de Tsimbazaza, BP 4096, Antananarivo 101, Madagascar **6** Zoologische Staatssammlung München (ZSM-SNSB), Münchhausenstraße 21, 81247 München, Germany **7** Departamento de Biologia, Faculdade de Ciências da Universidade do Porto, R. Campo Alegre, s/n, 4169-007, Porto, Portugal

Corresponding author: Angelica Crottini (tiliquait@yahoo.it)

Academic editor: A. Ohler | Received 14 February 2020 | Accepted 9 May 2020 | Published 22 July 2020

<http://zoobank.org/5C3EE5E1-84D5-46FE-8E38-42EA3C04E942>

Citation: Cocca W, Andreone F, Belluardo F, Rosa GM, Randrianirina JE, Glaw F, Crottini A (2020) Resolving a taxonomic and nomenclatural puzzle in mantellid frogs: synonymization of *Gephyromantis azzurrae* with *G. corvus*, and description of *Gephyromantis kintana* sp. nov. from the Isalo Massif, western Madagascar. ZooKeys 951: 133–157. <https://doi.org/10.3897/zookeys.951.51129>

Abstract

The genus *Gephyromantis* belongs to the species-rich family Mantellidae and is currently divided in six subgenera. Among these is the subgenus *Phylacomantis*, which currently includes four described species: *Gephyromantis pseudoasper*, *G. corvus*, *G. azzurrae*, and *G. atsingy*. The latter three species are distributed in western Madagascar, and two of them (*G. azzurrae* and *G. corvus*) occur in the Isalo Massif. Based on the analysis of molecular data (a fragment of the 16S rRNA gene), morphological inspection of museum specimens, and photographic comparisons, *G. azzurrae* is synonymised with *G. corvus* and the second

Phylacomantis lineage of Isalo is described as *G. kintana* **sp. nov.** This medium-sized frog species (adult snout-vent length 35–44 mm) is assigned to this subgenus according to genetic and morphological similarities to the other known species of *Phylacomantis*. *Gephyromantis kintana* **sp. nov.** is known only from the Isalo Massif, while new records for *G. corvus* extend its range to ca. 200 km off its currently known distribution. These two taxa seem to occur in syntopy in at least one locality in Isalo, and the easiest way to distinguish them is the inspection of the ventral colouration, dark in *G. corvus* and dirty white in *G. kintana*.

Keywords

Amphibia, Mantellidae, Mantellinae, *Phylacomantis*, integrative taxonomy

Introduction

The biodiversity hotspot of Madagascar hosts a unique, diverse, and imperilled ecosystem (Myers et al. 2000; Goodman and Benstead 2003, 2005). The island's amphibians contribute significantly to its rich biodiversity with 100% of the autochthonous species being endemic to the country (Glaw and Vences 2007; Perl et al. 2014; Zimkus et al. 2017). All native amphibians of Madagascar are anurans and belong to four distinct families: Mantellidae Laurent, 1946, Microhylidae Günther, 1858, Hyperoliidae Laurent, 1943 and Ptychadenidae Dubois, 1987 (Glaw and Vences 2007; Crottini et al. 2012). The family Mantellidae is the most species rich clade with ca. 230 currently described species (AmphibiaWeb 2020) and several new species are awaiting formal description (Vicites et al. 2009; Perl et al. 2014). Mantellids are divided in three subfamilies, the Boophinae Vences & Glaw, 2001 (with 79 described species), the Laliostominae Vences & Glaw, 2001 (with seven described species), and the Mantellinae Laurent, 1946 (with 143 described species) (AmphibiaWeb 2020). Based on significant genetic differentiation, habitat requirement and morphology mantellin frogs are classified in nine recognised genera: *Blommersia* Dubois, 1992, *Boehmantis* Glaw & Vences, 2006, *Gephyromantis* Methuen, 1920, *Guibemantis* Dubois, 1992, *Mantella* Boulenger, 1882, *Mantidactylus* Boulenger, 1895, *Spinomantis* Dubois, 1992, *Tsingymantis* Glaw, Hoegg and Vences 2006 and *Wakea* Glaw & Vences, 2006 (Glaw and Vences 2006, 2007).

The genus *Gephyromantis* is currently divided in six subgenera: *Gephyromantis* Methuen, 1920, *Laurentomantis* Dubois, 1980, *Vatomantis* Glaw & Vences, 2006, *Phylacomantis* Glaw & Vences, 1994, *Duboimantis* Glaw & Vences, 2006 and *Asperomantis* Vences, Köhler, Pabijan, Bletz, Gehring, Hawlitschek, Rakotoarison, Ratsoavina, Andreone, Crottini & Glaw, 2017.

Gephyromantis are mostly small to medium-sized frogs that, for a long time, most of them were thought to be direct developers (not depending on water bodies for their larval development). However, and despite development being unknown for the majority of the species, free-swimming, exotrophic tadpoles have been recorded in some of them (Glaw and Vences 2007; Randrianiaina et al. 2011). In addition, endotrophic

(non-feeding) nidicolous tadpoles, genetically identified as belonging to the subgenus *Duboisimantis*, were recently identified (Randrianiaina et al. 2011). Eggs of these species are most probably laid into the leaf-litter and washed into streams where they complete the larval development and metamorphosis (Randrianiaina et al. 2011). The majority of the *Gephyromantis* species can be found in the low and mid-altitude rainforest of the north and east of Madagascar, with the exception of most species of the subgenus *Phylacomantis*, which primarily occupy western Madagascar (Glaw and Vences 2007; Mercurio and Andreone 2007; Crottini et al. 2011a; Andreone et al. 2014; Cocca et al. 2018).

The subgenus *Phylacomantis* currently contains four described species distributed in the north, west and south-west of Madagascar: *G. pseudoasper* (Guibé, 1974), *G. corvus* (Glaw & Vences, 1994), *G. azzurrae* Mercurio & Andreone, 2007, and *G. atsingy* Crottini, Glaw, Casiraghi, Jenkins, Mercurio, Randrianantoandro, Randrianirina & Andreone, 2011. These medium-sized frogs are mostly terrestrial, being active mainly in crepuscular and night hours (Glaw and Vences 1994, 2006). With the exception of *G. pseudoasper*, which can be found far from water bodies, all the species are typically encountered in rocky habitats along small streams in dry deciduous forest (Glaw and Vences 2006, 2007). Males are often heard calling from the ground, from bushes or trees at relatively low perch. Some species of the subgenus *Phylacomantis* are known to have exotrophic carnivorous tadpoles capable of emitting sounds, possibly as an aggressive signal towards conspecific tadpoles during prey capture (Reeve et al. 2011).

In this paper we combined available evidence (morphological and genetic data, photographic material) on the two *Phylacomantis* species inhabiting the Isalo Massif (currently referred to as *G. azzurrae* and *G. corvus*) and compared it with recently collected material. The results of this analysis point to the need to synonymise the name *Gephyromantis azzurrae* with *G. corvus* and describe a new taxon that had for long time remained hidden in plain sight (i.e., under the name *G. corvus*).

Materials and methods

Study sites

The Isalo Massif is situated in the southwestern corner of the Ihorombe region. A large portion of the massif is included within the Parc National de l'Isalo, one of the largest protected areas in Madagascar (81,540 ha). It consists of a low to mid-altitude mountain range (altitudinal range from 500 to 1,300 m a.s.l.), characterised by the occurrence of numerous canyons and valleys, varying in size, depth and in the level of humidity and water availability. This area hosts numerous patches of dry deciduous forest, which are generally associated to streams within the canyon system (Fig. 1; Table 1; Mercurio and Andreone 2007; Mercurio et al. 2008; Cocca et al. 2018).

In addition to Isalo, we surveyed an area close to the Andringitra Massif (in the south-east): we found individuals of *Phylacomantis* in Tsaranoro forest, Anja Reserve

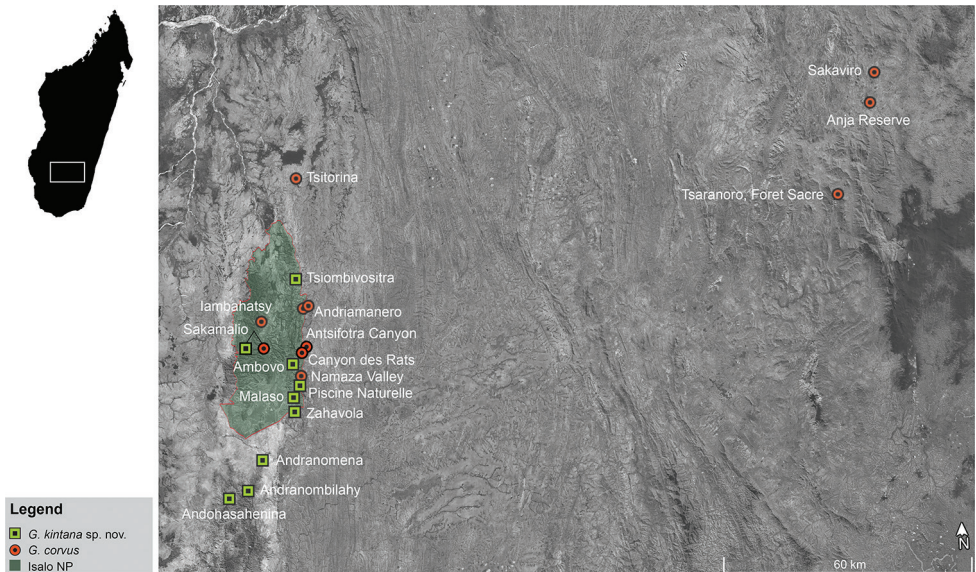


Figure 1. Distribution of *Gephyromantis corvus* and *G. kintana* sp. nov. Note that in Sakamalio the two species are found in syntopy.

and Sakaviro Community Reserve, all within the administrative region of Haute Matsiatra (Fig. 1). Tsaranoro forest is a small fragment of ca. 46 ha, ca. 4 km away from the western entrance of the Parc National d’Andringitra and it is characterised by a semi-deciduous dry forest surrounded by villages and rice fields (Fig. 1; Gould and Andrianomena 2015). Anja Reserve is located ca. 13 km south of Ambalavao, and is characterised by the presence of forest fragments at the base of some large granitic boulders known to host several microendemic species (Crottini et al. 2011b, 2012, 2015). Sakaviro Community Reserve is a small (ca. 14 ha) remaining fragment of semi-deciduous dry forest at the base of a granitic dome, which is located ca. 8 km north of Anja Reserve (Fig. 1; Table 1).

Voucher collection

Frogs were searched during the day and night (using headlamps and torches). The position of each site was recorded with a GPS device. Special efforts have been invested in collecting specimens at Namazaha (or Namaza) Valley, the type locality of *G. corvus* within the Isalo N.P. Twenty individuals (collected over several years) were euthanised by immersion in a solution of MS-222, fixed in 96% ethanol and stored in 70% ethanol. From each voucher specimen we collected a tissue sample, which was preserved separately in 96% ethanol for genetic analyses. Vouchers were deposited in the herpetological collection of the Zoologische Staatssammlung München, Germany (ZSM), and of the Mention “Zoologie et Biodiversité Animale” of the University of

Table 1. List of toponyms and corresponding GPS coordinates and altitudes.

Locality	Latitude / Longitude	Altitude [m a.s.l.]
Ambovo	-22.50800000S, 45.35250000E	999
Andohasahenina	-22.83333300S, 45.18800000E	876
Andranombilahy	-22.55000000S, 45.41670000E	920
Andranomena	-22.74016700S, 45.27500000E	740
Andriamanero 1	-22.36716700S, 45.39200000E	663
Andriamanero 2	-22.37333333S, 45.37850000E	792
Anja	-21.85962000S, 46.85827000E	970
Antsifotra Canyon	-22.42120000S, 45.27450000E	743
Canyon des Rats	-22.47987500S, 45.37663200E	841
Iambahatsy	-22.40583300S, 45.26883300E	742
Malaso	-22.58850000S, 45.35533333E	966
Namazaha Valley	-22.55000000S, 45.41670000E	820
Piscine Naturelle	-22.55966700S, 45.37183300E	841
Sakamalio	-22.43483300S, 45.25516700E	726
Sakaviro	-22.42120000S, 45.27450000E	1018
Tsaranoro	-22.08473000S, 46.77515000E	946
Tsiombivositra	-22.30250000S, 45.35833300E	900
Tsitorina	-22.05816700S, 45.35616700E	465
Zahavola	-22.62153610S, 45.35866700E	881

Antananarivo, Madagascar (**UADBA-A**) (for detailed information on the collections material please refer to Fig. 2). The eight vouchers hosted in the UADBA-A collection were analysed genetically but have not been measured. Other institutional abbreviations used herein are

MRSN Museo Regionale di Scienze Naturali di Torino, Italy
ZFMK Zoologisches Forschungsmuseum Alexander Koenig, Bonn, Germany
SMF Senckenberg Museum Frankfurt, Germany.

Codes ACZC and ACZCV refer to field numbers of A. Crottini and the code FAZC refers to field numbers of F. Andreone.

Morphological measurements

Morphological measurements (in mm) were taken with a digital calliper to the nearest 0.1 mm by W. Cocca (Table 2):

ED horizontal eye diameter,
END eye-nostril distance, measured from the anterior corner of eye to the centre of the nostril,
FORL forelimb length, measured from the axilla to the tip of the longest (third) finger with the forelimb extended,
FOTL foot length including tarsus, measured from the tibio-tarsal articulation to the tip of the longest (fourth) toe,

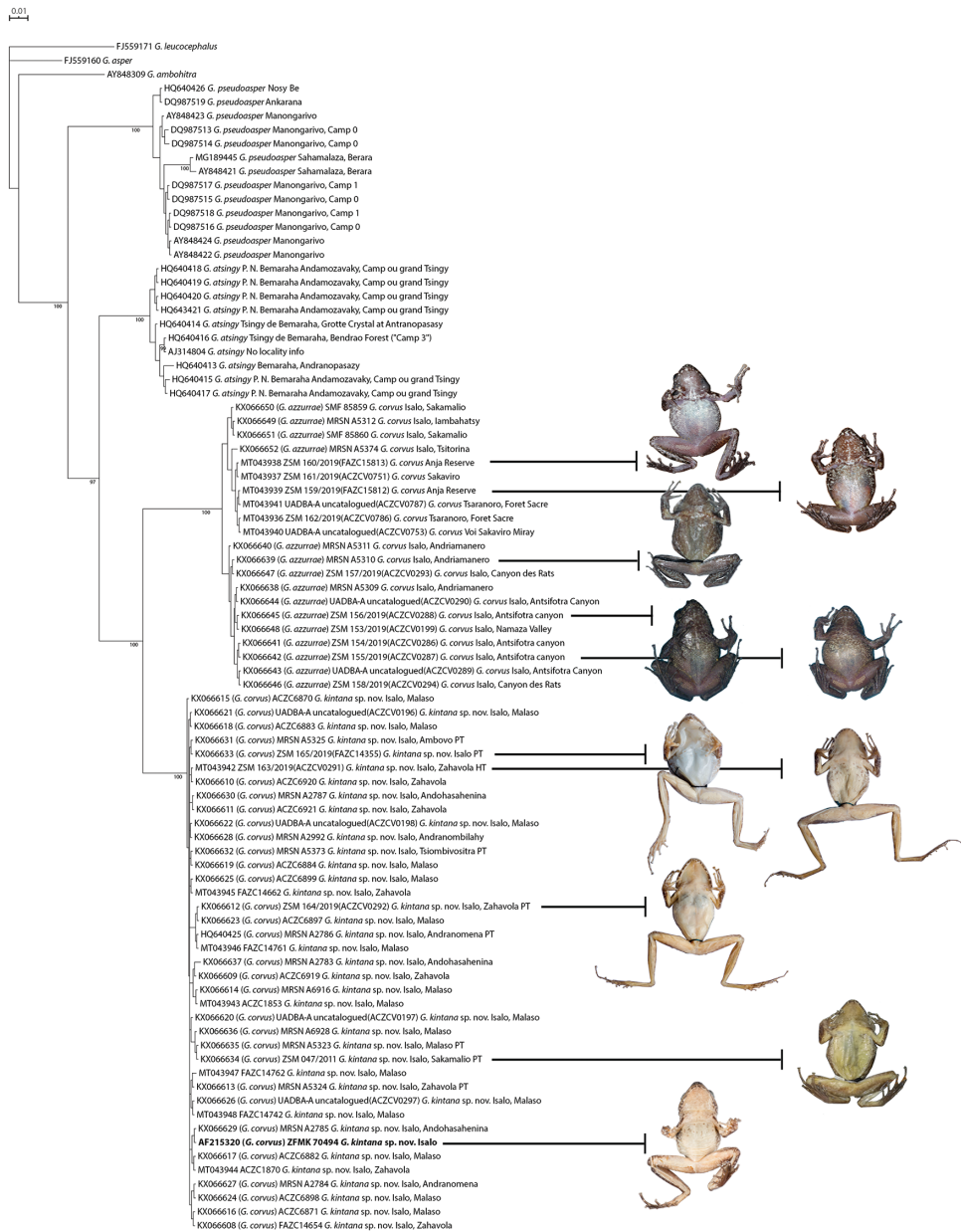


Figure 2. Phylogenetic consensus tree of the subgenus *Phylacomantis*. Bayesian majority rule consensus tree based on a fragment of the mitochondrial 16S rRNA gene. Numbers at nodes are Posterior Probability (PP) values. In bold is highlighted the sequence (AF215320) of the adult male (ZFMK 70494) that was used as genetic reference for *G. corvus* in Vences (2000) and following contributions. Each sequence is reported with the following information: GenBank accession number, GenBank taxon identification (given in parenthesis when taxon ID does not match with the currently proposed definition), institutional catalogue number and/or field number (when specimen was not collected), species ID, locality. *G. leucocephalus*, *G. asper*, and *G. ambohitra* were used as outgroups.

HAL	hand length, measured from the base of the hand to the tip of the longest (third) finger,
HIL	hind-limb length, measured from the cloaca to the tip of the longest (fourth) toe with the foot extended laterally outward from the body,
HIL/SVL	ratio between hind-limb length and snout-vent length,
HL	head length, measured as the diagonal from the maxillary commissure to the snout tip (Note: this is measured along the jaw, and not parallel to the longitudinal axis of the animal),
HW	head width at widest point,
IMTL	length of inner metatarsal tubercle,
NND	nostril-nostril distance, measured from the centre of the nostrils,
NSD	nostril-snout tip distance, measured from the centre of the nostril,
SVL	snout-vent length,
TD	horizontal tympanum diameter,
TD/ED	ratio between horizontal tympanum diameter and horizontal eye diameter,
TIBL	point reached by tibio-tarsal articulation when hindlimbs are adpressed along body).

For adult male individuals we also collected measurements for the femoral macro-gland cluster:

FGL	length of the femoral macrogland cluster,
FGW	width of femoral macrogland cluster,
GD	mean diameter of granules composing the right femoral gland,
NG	number of granules composing the right femoral gland.

Granules were counted after having opened and flipped the skin where the gland is located. Webbing formula follows Blommers-Schlösser (1979), and femoral glands definition follows Glaw et al. (2000). Terminology and description scheme follow Mercurio and Andreone (2007). Description of colour in life is based on the holotype, with some reference to variation as observed in paratypes.

Molecular analysis

Total genomic DNA was extracted from tissue samples using proteinase K digestion (10 mg/ml concentration) followed by a standard high-salt extraction method (Bruford et al. 1992). We amplified a fragment of ca. 550 bp of the 3' terminus of the mitochondrial 16S rRNA gene (hereafter 16S) proven to be suitable for amphibian identification (Vences et al. 2005; Vieites et al. 2009). We used the primers 16S-AR 5'-CGCCTGTTTATCAAAAACAT-3' and 16S-BR 5'-CCGGTYTGAACCTCA-GATCAYGT-3', modified from Palumbi et al. (1991), as described in Crottini et al. (2011a). Standard polymerase chain reactions (PCR) were performed in a final volume of 25 µL and using 0.75 µL each of 10 pmol primer, 0.4 µL of total dNTP 10 mM

Table 2. Morphometric measurements of specimens of *Gephyromantis corvus* and *G. kintana* sp. nov. All measurements are in mm. Numbers in TIBL indicate different states: 1, eye, 2, nostril, 3, snout, 4, beyond the snout. HT (holotype), PT (paratype), M (male), F (female), * (subadult), Juv (juvenile), NA (not available), ♀ (type specimens of *G. azzurrae*).

Species	GenBank	Locality	Voucher	Fieldnumber	Type	Sex	SVL	HW	HL	ED	END	NSD	NND	TD	TD/ED	HAL	FORL	FOTL	IMTL	HIL	HIL/SVL	TIBL	NG	FGL	FGW	GD
<i>G. corvus</i>	Unavailable	Namaza Valley	ZFMK 574/30		HT	M	37.8	14.0	14.2	5.5	NA	NA	NA	2.7	0.5	11.5	38.4	25.0	1.1	56.0	1.5	1	38	8.1	2.7	0.2
<i>G. corvus</i>	Unavailable	Namaza Valley	ZSM 574/1999 (ZFMK57431)		PT	M	37.0	13.5	13.8	4.2	NA	NA	NA	3.1	0.7	11.9	23.3	27.7	0.9	60.3	1.6	3	32	6.4	2.5	0.4
<i>G. corvus</i>	KX066639, EF222301	Andriamanero	MRSN A5310	FAZCI2568	HT♀	M	41.1	16.9	13.4	6.1	3.9	2.5	4.0	4.0	0.7	12.1	20.0	30.0	1.1	41.1	1.0	1	45	6.3	2.0	0.5
<i>G. corvus</i>	KX066638, EF222300	Andriamanero	MRSN A5309	FAZCI2567	PT♀	M	38.5	15.3	12.8	5.2	4.3	2.2	3.7	3.7	0.7	11.1	19.9	26.7	1.3	41.1	1.1	1	38	6.5	2.7	0.5
<i>G. corvus</i>	KX066640, EF222302	Andriamanero	MRSN A5311	FAZCI2569	PT♀	M	40.2	15.8	14.1	6.0	4.0	2.7	4.0	4.1	0.7	11.2	19.9	27.7	1.1	41.0	1.0	1	40	6.7	2.7	0.6
<i>G. corvus</i>	KX066650, EF222305	Sakamallo	SMF 85859 (MRSN A5314)	FAZC 12979	PT♀	M	42.7	16.4	14.3	5.4	3.7	2.6	3.9	3.5	0.6	13.4	21.0	29.9	1.1	41.1	1.0	1	42	7.0	3.0	0.6
<i>G. corvus</i>	KX066651, EF222303	Sakamallo	SMF 85860 (MRSN A5315)	FAZC 12980	PT♀	M	43.7	16.4	13.5	5.7	4.0	2.5	3.8	4.0	0.7	12.2	21.1	27.7	1.0	42.3	1.0	1	42	7.5	2.7	0.5
<i>G. corvus</i>	KX066642	Antsifotra Canyon	ZSM 155/2019	ACZCV_287		M	39.6	14.7	15.4	4.7	3.8	2.0	3.9	3.6	0.8	11.3	27.1	26.9	0.5	66.4	1.7	2	29	8.2	2.9	0.8
<i>G. corvus</i>	KX066645	Antsifotra Canyon	ZSM 156/2019	ACZCV_288		M	41.1	16.0	18.5	5.4	3.9	2.6	3.6	3.6	0.7	11.1	25.1	29.8	0.8	70.4	1.7	1	58	9.2	2.7	0.5
<i>G. corvus</i>	KX066648	Namaza Valley	ZSM 153/2019	ACZCV_199		M	39.2	15.4	14.1	4.2	3.9	2.0	3.4	3.4	0.8	12.7	26.6	27.5	0.9	65.5	1.7	1	NA	NA	NA	NA
<i>G. corvus</i>	MT043936	Tsaranoro	ZSM 162/2019	ACZCV_786		M	41.8	14.6	14.0	4.2	3.9	2.9	3.4	3.0	0.7	12.2	27.4	28.3	0.8	62.6	1.5	1	43	7.4	2.6	0.3
<i>G. corvus</i>	MT043937	Sakavito	ZSM 161/2019	ACZCV_751		M	39.3	15.4	14.4	4.1	4.0	2.2	3.9	1.8	0.4	11.6	24.0	27.8	0.7	62.1	1.6	2	43	7.6	2.8	0.4
<i>G. corvus</i>	MT043938	Anja	ZSM 160/2019	FAZCI5813		M	41.1	14.4	14.3	4.7	4.3	1.9	3.3	3.3	0.7	12.5	25.5	30.2	0.9	70.3	1.7	3	45	7.9	2.5	0.4
<i>G. corvus</i>	MT043939	Anja	ZSM 159/2019	FAZCI5812		F	42.0	14.3	15.1	5.2	3.8	2.5	3.3	3.0	0.6	11.3	24.4	28.4	0.5	64.1	1.5	2	NA	NA	NA	NA
<i>G. corvus</i>	KX066641	Antsifotra Canyon	ZSM 154/2019	ACZCV_286		F	37.2	13.8	14.2	4.9	4.4	2.9	3.5	3.3	0.7	10.3	24.3	27.0	0.4	60.5	1.6	1	NA	NA	NA	NA
<i>G. corvus</i>	KX066649, JN664352, EF222304	Iambahasy	MRSN A5312	FAZCI2910	PTE	M*	23.3	8.8	8.8	4.1	2.8	1.4	2.2	2.5	0.6	8.8	11.1	17.7	0.5	24.5	1.1	1	NA	NA	NA	NA

Species	GenBank	Locality	Voucher	Fieldnumber	Type	Sex	SVL	HW	HL	ED	END	NSD	NND	TD	TD/ED	HAL	FORL	FOTL	IMTL	HIL	HIL/SVL	TIBL	NG	FGL	FGW	GD
<i>G. corvus</i>	KX066647	Canyon des Rats	ZSM 157/2019	ACZCV_293		M*	27.4	11.3	11.2	3.2	2.8	1.5	2.4	2.0	0.6	9.0	18.5	21.2	0.4	44.8	1.6	3	35	4.8	2.0	0.1
<i>G. corvus</i>	KX066646	Canyon des Rats	ZSM 158/2019	ACZCV_294		Juv	21.4	8.1	8.5	3.6	2.0	1.4	2.2	1.7	0.5	5.8	13.0	15.4	0.1	35.2	1.6	4	NA	NA	NA	NA
<i>G. kintana</i>	MT043942	Zahavola	ZSM 163/2019	ACZCV_291	HT	M	38.2	15.6	14.6	4.0	4.1	2.5	3.4	3.0	0.8	11.5	25.1	30.4	0.8	67.5	1.8	4	71	9.4	3.6	0.3
<i>G. kintana</i>	KX066634, JN664348	Sakamaito	ZSM 0047/2011 (MRSN A5313)	FAZCI2951	PT	M	37.2	14.9	12.3	5.5	4.1	2.3	3.5	3.3	0.6	11.1	15.6	26.6	0.9	40.0	1.1	1	29	8.2	2.2	0.6
<i>G. kintana</i>	Unavailable	Malaso	MRSN A5322	FAZCI2627	PT	M	43.6	15.2	16.5	5.5	NA	NA	NA	3.6	0.7	11.9	26.7	30.2	0.7	69.0	1.6	3	24	7.5	3.3	0.6
<i>G. kintana</i>	KX066632, HQ640423	Tsiombivositra	MRSN A5373	FAZCI2859	PT	M	39.8	16.1	15.3	5.8	4.8	2.9	4.3	3.7	0.6	11.8	16.3	28.6	1.4	38.7	1.0	2	96	9.1	4.1	0.6
<i>G. kintana</i>	Unavailable	Piscine Naturelle	ZSM 1553/2009	NA	PT	M	35.7	13.8	15.0	4.9	NA	NA	NA	2.5	0.5	11.6	20.2	26.8	0.8	59.6	1.7	1	35	8.9	3.0	0.4
<i>G. kintana</i>	KX066633	Malaso	ZSM 165/2019	FAZCI4355	PT	M	41.9	15.9	15.9	4.7	4.5	2.2	3.5	3.2	0.7	12.8	25.6	31.1	0.8	70.1	1.7	2	75	10.5	4.3	0.6
<i>G. kintana</i>	KX066612	Zahavola	ZSM 164/2019	ACZCV_292	PT	F	38.0	14.1	15.1	4.6	3.9	2.6	3.0	2.9	0.6	11.0	22.9	28.5	0.7	64.3	1.7	1	NA	NA	NA	NA
<i>G. kintana</i>	KX066613, HQ640424	Zahavola	MRSN A5324	FAZCI2758	PT	F	40.1	15.0	16.3	6.1	4.4	2.8	4.2	3.3	0.5	10.8	16.9	28.0	0.7	37.2	0.9	2	NA	NA	NA	NA
<i>G. kintana</i>	KX066631	Ambovo	MRSN A5325	FAZCI3000	PT	F	40.0	15.2	16.2	6.4	4.3	2.6	4.1	3.2	0.5	10.7	18.2	30.1	0.6	40.3	1.0	2	NA	NA	NA	NA
<i>G. kintana</i>	Unavailable	Ambovo	MRSN A5326	FAZCI3001	PT	F	38.0	13.0	14.9	4.6	NA	NA	NA	2.9	0.6	9.6	23.1	27.9	0.7	62.6	1.6	3	NA	NA	NA	NA
<i>G. kintana</i>	HQ640425	Andranomena	MRSN A2786	FAZCI1964	PT	F	40.8	15.0	15.8	6.3	4.7	2.7	4.3	3.6	0.6	11.1	17.7	30.2	0.7	40.5	1.0	2	NA	NA	NA	NA
<i>G. kintana</i>	KX066635, HQ640422	Malaso	MRSN A5323	FAZCI2661	PT	F	39.0	15.0	15.7	6.1	4.4	2.8	4.2	3.6	0.6	11.9	17.6	29.7	0.8	39.3	1.0	2	NA	NA	NA	NA

(Promega), 0.1 μL of 5 U/mL GoTaq, 5 μL 5X Green GoTaq Reaction Buffer (Promega) and 4 μL of MgCl_2 25mM (Promega). Successfully amplified and purified fragments were sequenced using dye-labelled dideoxy terminator cycle sequencing on an ABI 3730XL automated sequencer at Macrogen Inc. Chromatograms were checked and sequences were manually edited, where necessary, using the sequence alignment editor of BIOEDIT (v.7.2.0; Hall 1999). All new sequences have been deposited in GenBank (MT043936–MT043948; Table 2).

We aligned the newly generated 16S sequences with all available homologous sequences of the species of the subgenus *Phylacomantis* (see Fig. 2 for details of GenBank accession numbers), and one sequence each of *G. ambobitra* (AY848309), *G. asper* (FJ559160) and *G. leucocephalus* (FJ559171), belonging to different subgenera, for outgroup rooting. This alignment contained 86 sequences. We computed matrices of average genetic distance (uncorrected p-distance values transformed into percent, using the pairwise deletion option) within and between individuals belonging to the four *Phylacomantis* taxa. Distances were computed using MEGA, v. 7.0.21 (Kumar et al. 2016) (Table 3).

We conducted Bayesian inference (BI) searches based on 511 bp of the 16S fragment (Fig. 2). The determination of the best-fitting substitution model based on the corrected Akaike information criterion (AICc) was determined in jModelTest2 (Darriba et al. 2012). Phylogenetic analyses were conducted in MRBAYES v. 3.2.6 (Ronquist et al. 2012) on CIPRES Science Gateway v. 3.3 (Miller et al. 2010). The Markov chain Monte Carlo sampling included two runs of four chains each (three heated, one cold) sampled every 10^3 generations for a total of 10^7 generations. The first 25% of generations were discarded as burn-in, and 7.5 million trees were retained post burn-in and summed to generate a 50% majority rule consensus tree (Fig. 2).

Results

Justification for the synonymisation of *G. azzurrae* with *G. corvus*

The 16S sequence deposited in GenBank with the number AF215320 was obtained from the amplification of a tissue sample of the specimen ZFMK 70494 (Figs 2, 3; Vences 2000). This specimen was collected in Isalo in 1999 when only one *Phylacomantis* species was recognised in the area, and therefore this sequence was associated with the specific name “*corvus*”. No precise locality data are available for the collection of this specimen, but after morphological study of this specimen, and of the type series of *G. corvus* and *G. azzurrae* (Table 2; Figs 2, 3) we conclude that: 1) *G. corvus* and *G. azzurrae* are conspecific (we did not detect any relevant morphological difference between the two holotypes; see following sections for the list of diagnostic characters between the two sympatric *Phylacomantis* taxa from Isalo; see Fig. 3); 2) specimen ZFMK 70494 is different from the holotypes of *G. corvus* and *G. azzurrae* (see below; Fig. 3) and since no name is available for this taxon, it needs to be formally described. ZFMK 70494 and its sequence should no longer be associated with the specific name “*corvus*”.

Mercurio and Andreone (2007) already identified clear morphological differences between the two sympatric species of *Phylacomantis* they found in Isalo (see “Morphological comparison with other species” section in Mercurio and Andreone 2007). Unfortunately, at the time, the authors did not inspect the type specimens of *G. corvus*. The authors detected morphological differences, deep genetic differentiation ($> 7.5\%$ p-distance between the two mitochondrial lineages), and bioacoustic differences (based on the comparative analysis of the call of one male from Ambovo and the call of *G. azzurrae* paratype specimen MRSN A5313, now ZSM 0047/2011). Based on these differences they described the taxon *G. azzurrae*. The only *Phylacomantis* sequence available from Isalo at that time was the one obtained from the analysis of the specimen ZFMK 70494. The deep genetic difference they observed between the analysed sequences of the type series of *G. azzurrae* and the sequence of the ZFMK 70494 specimen convinced Mercurio and Andreone (2007) that the lineage they collected in Andriamanero, Iambahatsy, and Sakamalio was different from *G. corvus* and belonged to a different, and still undescribed, species. Although Mercurio and Andreone (2007) were correct in identifying differences in their comparative analyses, their taxonomic conclusions were erroneous. Moreover, the *G. azzurrae* paratype MRSN A5313 (now ZSM 0047/2011) from Sakamalio (KX066634) was not sequenced at the time of the species description. This was done by Cocca et al. (2018), who found it to be conspecific with ZFMK 70494, but not conspecific with the holotype of *G. azzurrae* (MRSN A5310). Cocca et al. (2018) therefore assigned this specimen to *G. corvus* because at this time it was not yet evident that ZFMK 70494 represented an undescribed species.

Based on these observations, we consider *G. azzurrae* as a junior synonym of *G. corvus*. We confirm the existence of two *Phylacomantis* lineages in the Isalo Massif, and we provide the formal description of the unnamed taxon. We follow the integration by the congruence approach proposed by Padial et al. (2010) and define species as independent evolutionary lineages if two or more independent lines of evidence support their distinctness. This new species forms a monophyletic group based on mitochondrial data and differs by an uncorrected pairwise sequence divergence (p-distance) $> 7.5\%$ in the analysed 16S fragment from its sister species (Table 3). This value is much higher than the standard value used as threshold for species-level units in amphibians (Fouquet et al. 2007).

We confirmed the distinctness of the two lineages by mitochondrial DNA sequences and morphology, and interpret the concordance between these independent lines of evidence as a strong support their specific distinctness (Avice and Ball 1990).

Molecular variation and differentiation

The majority rule consensus tree confirms the occurrence of two *Phylacomantis* taxa in Isalo (Fig. 2) and provides evidence for the first unambiguous record of one of these two lineages outside of Isalo (Figs 1, 2). These two lineages are sister taxa (Posterior probability = 100), and together they are the sister group of *G. atsingy* (Posterior probability = 97), which is currently known only from Tsingy de Bemaraha, in western Madagascar. Together, these three *Phylacomantis* species are the sister group of *G. pseudoasper*

Table 3. Genetic distances. Uncorrected p-distance (transformed into percent) matrix between and within (on the diagonal and in bold) species of the subgenus *Phylacomantis*, for the analysed 16S fragment.

	<i>G. corvus</i>	<i>G. kintana</i>	<i>G. atsingy</i>	<i>G. pseudoasper</i>
<i>G. corvus</i>	0.38%			
<i>G. kintana</i>	9.90%	0.06%		
<i>G. atsingy</i>	12.45%	10.68%	0.76%	
<i>G. pseudoasper</i>	14.89%	13.42%	12.40%	1.36%

(Posterior probability = 100), which is the only *Phylacomantis* species found in rainforest habitat and distributed in the north of Madagascar.

The analysed specimens of the two *Phylacomantis* lineages were genetically uniform and showed limited intraspecific divergence (Table 3). All the samples of *Phylacomantis* collected at Anja Reserve, Sakaviro and Tsaranoro cluster together with samples from Sakamalio, Iambahatsy and Tsitorina, and show evidences of slight genetic differentiation with the samples collected at Andriamanero, Canyon des Rats and Namazaha Valley. The second *Phylacomantis* lineage present in Isalo seems to be microendemic to this sandstone massif. The genetic distance observed between the different *Phylacomantis* taxa ranges between 9.9% (comparison between the two *Phylacomantis* taxa occurring in Isalo), and 14.9% (comparison between *G. corvus* and *G. pseudoasper*). More details on 16S genetic distances between species of the *Phylacomantis* subgenus are provided in Table 3.

Taxonomy

Gephyromantis (Phylacomantis) kintana sp. nov.

<http://zoobank.org/7E684B14-3C30-48E0-8911-2A3D4501EE94>

Figures 3D, 4D

Etymology. Mercurio and Andreone (2007) dedicated *G. azzurrae* to F. Andreone's second daughter, Kintana Azzurra Andreone. Since this name turned out to be a junior synonym of *G. corvus*, F. Andreone and the other authors of this paper wish to dedicate the new species to honour her with the new name. The Malagasy word "*kintana*" means "star" and is used as a noun in apposition.

Remarks. DNA sequences of this species have been wrongly referred to as *Gephyromantis corvus* by Vences (2000; AF215320), Vieites et al. (2009; AF215320), Crottini et al. (2011a; HQ640422–HQ640425), Kaffenberger et al. (2012; JN664348), Cocca et al. (2018; KX066608–KX066637) and all other studies where these accession numbers have been used.

Holotype. ZSM 163/2019 (ACZCV_0291; Figs 3D, 4D; tissue sample taken for genetic analysis: MT043942), adult male from Zahavola (Isalo, Ihorombe region, Ranohira Fivondronona, southwestern Madagascar), -22.6215361S, 45.358667E, ca. 881 m a.s.l., canyon with a narrow gallery forest laying on the edge of the border of Isalo National Park, collected on 26 November 2014 by F. Andreone, A. Crottini, and G. M. Rosa.

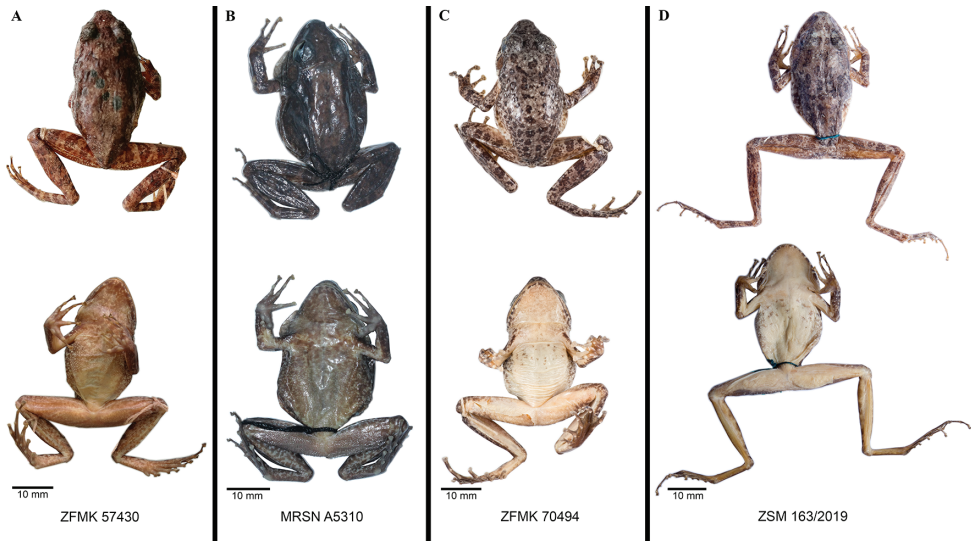


Figure 3. Images of preserved specimens of *Gephyromantis corvus* and *G. kintana* sp. nov. Comparison of dorsal and ventral views of preserved specimens of the two sister species *G. corvus* and *G. kintana* sp. nov. from Isalo, with particular emphasis on the diagnostic ventral colouration. **A** holotype of *G. corvus* (ZFMK 57430), adult male from Namazaha Valley; **B** holotype of *G. azzurrae* (MRSN A5310), adult male from Andriamanero; **C** adult male (ZFMK 70494) used as genetic reference (AF215320) for *G. corvus* in Vences (2000), from an unknown locality of the Isalo Massif (photographs made available by Dennis Rödder and Morris Flecks); **D** holotype of *G. kintana* sp. nov. (ZSM 163/2019, ACZCV_0291), adult male from Zahavola.

Paratypes. ZSM 164/2019 (ACZCV_0292; tissue sample taken for genetical analysis: KX066612), adult female, collected at the same locality and date and by the same collectors of the holotype; MRSN A5324 (FAZC 12758; tissue sample taken for genetical analysis: KX066613 and HQ640424), adult male collected at the same locality as the holotype on 17 November 2004 by F. Andreone; ZSM 1553/2009, adult male collected in an imprecise locality within Isalo National Park (original collection data: “Isalo, zwischen Canyons und Piscine” probably referring to a locality close to Piscine Naturelle; Isalo, Ihorombe region, Ranohira Fivondronona, southwestern Madagascar), -22.559667S, 45.371833E, ca. 890 m a.s.l., on 5 June 2003 by N. Lutzmann; ZSM 165/2019 (FAZC 14355; tissue sample taken for genetical analysis: KX066633), adult male, collected at Malaso (Isalo, Ihorombe region, Ranohira Fivondronona, southwestern Madagascar), -22.5885S, 45.35533333E, ca. 966 m a.s.l., a shallow canyon with almost no gallery forest and included within Isalo National Park, on 30 November 2009 by F. Andreone, A. Crottini and G. M. Rosa; MRSN A5322 (FAZC 12627), adult male, collected at Malaso (Isalo, Ihorombe region, Ranohira Fivondronona, southwestern Madagascar), -22.5885S, 45.35533333E, ca. 966 m a.s.l., on 22 November 2004 by F. Andreone; MRSN A5323 (FAZC 12661; tissue sample taken for genetical analysis: KX066635, HQ640422), adult female collected at Malaso (Isalo, Ihorombe region, Ranohira Fivondronona, southwestern Madagascar),

-22.5885S, 45.35533333E, ca. 966 m a.s.l., on 24 November 2004 by F. Andreone; MRSN A5373 (FAZC 12859; tissue sample taken for genetical analysis: KX066632, HQ640423), adult male collected at Tsiombivositra (Isalo, Ihorombe region, Ranohira Fivondronona, southwestern Madagascar), -22.3025000S, 45.3583330E, ca. 900 m a.s.l., a locality close to the border but included within Isalo National Park, on 11 December 2004 by F. Andreone; MRSN A5325 (FAZC 13000; tissue sample taken for genetical analysis: KX066631) and MRSN A5326 (FAZC 13001), adult females collected at Ambovo (Isalo, Ihorombe region, Ranohira Fivondronona, southwestern Madagascar), -22.508S, 45.3525E, ca. 999 m a.s.l., within the borders of Isalo National Park, on 18 December 2004 by F. Andreone; MRSN A2786 (FAZC 11964; tissue sample taken for genetical analysis: HQ640425), adult female collected at Andranomena (Isalo, Ihorombe region, Ranohira Fivondronona, southwestern Madagascar), -22.740167S, 45.275E, ca. 740 m a.s.l.), a locality close to Ilakaka and situated outside of the borders of Isalo National Park, on 25 January 2004 by V. Mercurio and J. E. Randrianirina.

Diagnosis. A species assigned to the genus *Gephyromantis* (*sensu* Glaw and Vences 2006), subgenus *Phylacomantis*, based on genetic and morphological similarities to the other known species (*G. atsingy*, *G. corvus*, and *G. pseudoasper*), and recognisable by the presence of the following morphological characters and natural history traits: (1) medium size (adult male SVL 36–44 mm), (2) webbing between toes present, (3) lateral metatarsalia partly connected, (4) inner and outer metatarsal tubercles present, (5) presence of femoral glands of “Type 2” (*sensu* Glaw et al. 2000), (6) presence of a paired subgular vocal sac, (7) tongue bifid, (8) enlarged triangular finger tips; (9) dirty white throat, belly and thighs, (10) males with white vocal sacs; (11) brownish to olive-grey dorsal colouration with multiple and irregular brown-olive patches, (12) occurrence in young (shallow) canyons with limited (to almost no) vegetation, (13) mostly crepuscular/nocturnal activity, (14) advertisement call (see Mercurio and Andreone 2007 for the description of the advertisement call of specimen MRSN A5313 (ZSM 0047/2011), now genetically assigned to *G. kintana* sp. nov.).

The new species differs from the three other species of *Phylacomantis* by high genetic differentiation (pairwise 16S distance ranging from 9.9% to 13.4%), as well as from a combination of morphological and natural history traits.

Gephyromantis kintana sp. nov. is overall similar to the other three species of the subgenus *Phylacomantis*. Distinguished from *G. pseudoasper* by: (a) dirty white throat (vs. darker colouration); (b) ventrally dirty white thighs (vs. orange colouration); (c) presence of white vocal sacs (vs. blackish vocal sacs); (d) less granular dorsal skin; (e) larger size (maximum SVL in males 43.6 vs. 37.4 mm), (f) higher maximum number of granules in the femoral glands (96 vs. 43), (g) occurrence in young (shallow) canyons with limited vegetation (vs. mostly rainforest), (h) advertisement call (15–21 vs. 3 notes per call and lower dominant frequency, 3,000–3,200 Hz vs. 3,400–5,000 Hz).

Distinguished from the sympatric *G. corvus* by: (a) brownish to olive grey dorsal colouration with multiple and irregular brown-olive patches (vs. darker brown dorsal colouration, often with a broad vertebral stripe), (b) dirty white throat (vs. dark brown throat), (c) dirty white belly (vs. brown belly), (d) dirty white thighs (vs. brown

thighs); (e) presence of white vocal sacs (vs. brown-blackish vocal sacs), (f) higher maximum number of granules in the femoral glands (96 vs. 58), (g) occurrence in young (shallow) canyons with limited vegetation (vs. dry deciduous gallery forest in deep canyons), (g) advertisement call (15–21 vs. 10–14 notes per call and higher dominant frequency, 3,000–3,200 Hz vs. 2,400–2,700 Hz).

Distinguished from *G. atsingy* by: (a) brownish to olive grey dorsal colouration with multiple and irregular brown-olive patches (vs. light brown-beige with a greenish shading), (b) less granular dorsal skin; (c) larger size (maximum SVL in males 43.6 vs. 36.6 mm), (d) higher maximum number of granules in the femoral glands (96 vs. 70), (e) occurrence in young (shallow) canyons with limited/missing vegetation (vs. “*tsingy*” geological formations).

Description of the holotype (Figs 3D, 4D). Adult male in good state of preservation, distal phalanx of the 5th toe of the left foot removed as tissue sample and part of the ventral surface of thighs cut and opened to count the number of the granules of the femoral gland. SVL 38.2 mm; for other measurements see Table 2. Body slender; head slightly wider than long; snout slightly pointed in dorsal view, rather rounded in lateral view; nostrils directed laterally much nearer to tip of snout than to eye; canthus rostralis moderately defined; tympanum distinct, rounded, its horizontal diameter 0.8 of eye diameter; supratympanic fold well distinct, regularly curved; tongue distinctly bifid posteriorly. Arms slender; subarticular tubercles single; outer metacarpal tubercle poorly developed, inner metacarpal tubercle relatively well developed; fingers without webbing; finger disks triangular and distinctly enlarged; nuptial pads absent. Hind limbs slender; tibiotarsal articulation reaching beyond the snout tip when hindlimbs are depressed along body; lateral metatarsalia partly connected; inner metatarsal tubercle distinct, outer metatarsal tubercle small but recognisable; webbing of foot 1(1), 2i(1.75), 2e(0.75), 3i(2), 3e(1), 4i(2), 4e(2), 5(0.5). Skin slightly granular on dorsum and belly, ventral skin smooth on throat and chest. Femoral glands are distinctly recognisable from external view and are arranged in a typical glandular cluster (“Type 2”, according to Glaw et al. 2000), including 71 single whitish granular glands of ca. 0.3 mm diameter. The vocal sacs in the male holotype are white and distinct.

Colouration of the holotype (Fig. 3D). After almost six years in 70% ethanol the holotype conserves the original colour patterns, although it showed a slightly faded dorsal colour (Fig. 3D). Overall grey-brown colouration with distinct darker brown markings. Forelimbs dorsally grey-brown with one distinct darker brown cross-band on upper arm and three brown cross-bands on lower arm and hand, hands speckled. Finger and toe tips are grey-cream and first and second toes are lighter in colour than the other toes. Flanks with the same colour of the dorsum but with less distinct darker patches. Overall the darker dorsal colour fades into the whitish ventral colour. Nostril distinctly surrounded by a cream thin line; lateral head same colour as dorsum. Ventral colouration in the preserved specimen is more contrasted than in the living specimen. Throat, belly and thighs dirty white, ventral shanks slightly darker than thighs, chest flecked with a few distinct and scattered grey-brownish markings; sole of foot brown. Colouration of limbs is overall similar to the dorsum, although it has less defined markings. Hindlimbs with five dark brown cross-bands on femur, four on tibia, four

on tarsus and foot; dorsal foot grey-brown with four slightly defined perpendicular darker brown crossbands.

Colouration of the holotype in life (Fig. 4D). The live dorsal colouration, based upon photographs, is olive grey with multiple and irregular brown-olive patches with some greenish and orangish shades in dorsal surface. These markings are more contrasted than in the preserved specimen (Figs 3D vs. 4D). The tympanum is cream with multiple small light brown markings. Slightly defined interocular bar. Flanks with multiple brown-olive flecks that become increasingly smaller ventrally. Brown-olive irregular markings present also in lateral head. Hindlimbs dorsally olive grey with brown-olive crossbands and markings and some greenish and orangish shades. Ventral skin colouration in life unknown. The iris of the holotype is golden with a thin black vertical line in the lower portion of the eye, and a mid-horizontal metallic reddish brown broad band.

Variations. Individuals of *G. kintana* sp. nov. have small variations in colouration if compared with the holotype (see Fig. 4B, C, E–G). In life, dorsal colouration can have a very variable number of irregular brown-olive patches. The female paratype ZSM 164/2019 has a lighter dorsum and the dark spots are more contrasted and more visible than in the holotype. The female paratype MRSN A5326 has darker markings on the chest. Two juveniles of *G. kintana* (specimens not collected) showed multiple copper markings on dorsum and on forelimbs and hindlimbs (Fig. 4B, E).

The number of granules composing the femoral glands varies among the analysed specimens. The holotype has 71 granules while specimens MRSN A5322, ZSM 1553/2009, ZSM 0047/2011 (former MRSN A5313) and ZSM 165/2019 have respectively 24, 35, 29 and 75 granules. Paratype MRSN A5373 has the highest number of granules (96; Table 2).

We observed minor variation in the webbing formula in two paratypes, with specimen ZSM 164/2019 with 1(1), 2i(1.75), 2e(0.5), 3i(2), 3e(1), 4i(2), 4e(2.25), 5(0.5); and ZSM 165/2019 with 1(1), 2i(1.5), 2e(0.5), 3i(2), 3e(0.75), 4i(2), 4e(2.25), 5(0.5).

Distribution. *Gephyromantis kintana* sp. nov. is currently known from localities inside (Piscine Naturelle, Zahavola, Sakamalio, Malaso, Tsiombivositra, and Ambovo) and outside (Andranomena, Andranombilahy, Andohasahenina, and possibly Ilakaka) the borders of Isalo National Park (Fig. 1). However, this known distributional area remains restricted to the southern and western portion of the Isalo Massif. Now that we provided a straightforward way to distinguish this species from its sympatric sister species *G. corvus* more field surveys should be conducted to characterise its distribution in detail. The range encompasses elevations from 726–999 m a.s.l. The population densities are not known but it can be locally abundant, with several individuals grouping together close to remaining water bodies forming ponds in shallow (young) canyons (see Fig. 5C).

Natural history. *Gephyromantis kintana* can be found in relatively undisturbed areas in shallow (young) canyons in the Isalo Massif (Fig. 5A–C). Different from the individuals of *G. corvus* in Isalo, that are generally found calling from low vegetation on the lower branches of the trees laying over canyon streams (Fig. 5D), males of *G. kintana* generally call from rocks within the canyon (see Figs 4G, 5C). Most of the sampled individuals were found on the walls of the canyons, and most of the times far from the trees. Different from old (deeper) canyons, which are characterised by the oc-

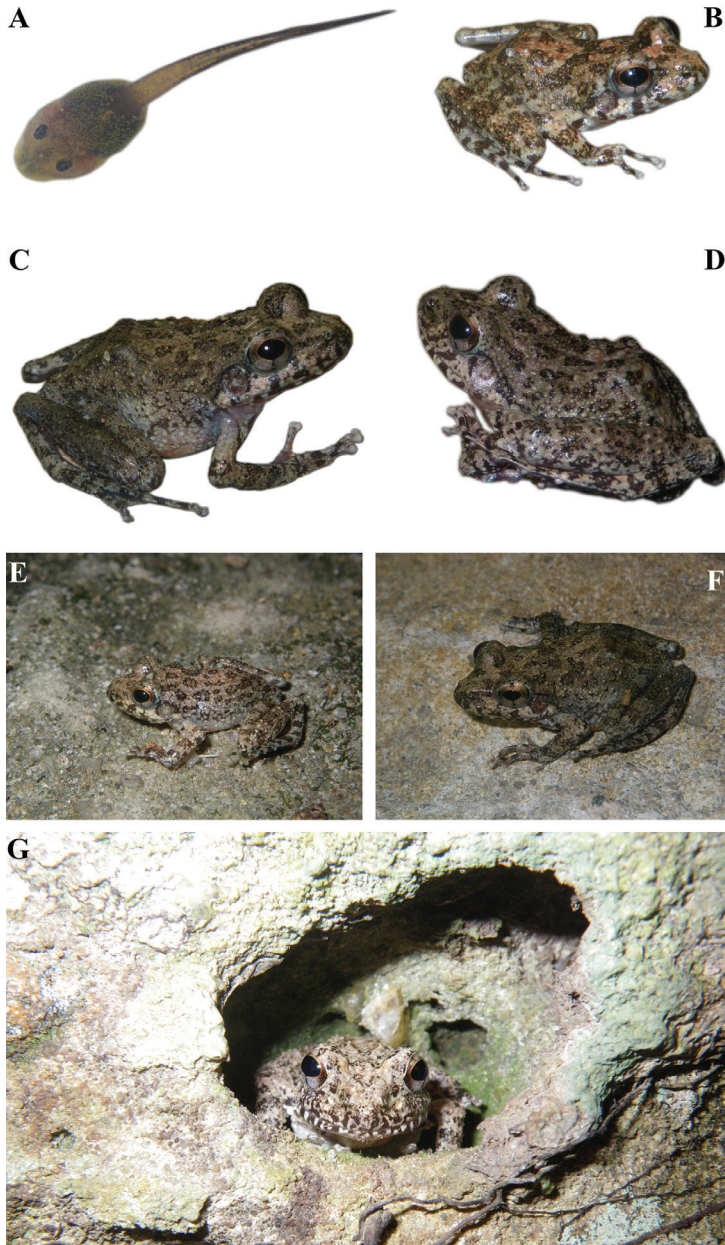


Figure 4. Images of living individuals of *Gephyromantis kintana* sp. nov. Living individuals of *G. kintana* sp. nov. showing the main developmental stages of the newly described species and its natural environment. **A** UADBA-A uncatalogued (ACZCV_0297), tadpole from Malaso, dorsal view; **B** ACZC 6920 (individual not collected), juvenile from Zahavola, dorsolateral view; **C** ACZC 6919 (individual not collected), adult female from Zahavola, dorsolateral view; **D** ZSM 163/2019 (ACZCV_0291), adult male holotype from Zahavola, dorsolateral view; **E** ACZC 6921 (individual not collected), juvenile from Zahavola found on rocks, dorsolateral view; **F** ACZC 6919 (individual not collected), adult female from Zahavola on rocky substrate, dorsolateral view; **G** ACZC 1853 (individual not collected), adult from Malaso hiding in a hole in the wall of the canyon. Photographs by Angelica Crottini.

currence of a dense gallery forest (Fig. 5D), younger canyons are generally surrounded by sparse vegetation (Fig. 5A). In Malaso, *G. kintana* was often observed sitting on the walls, approximately 1 m above the water (Fig. 5C), while in Zahavola the species was observed using holes on the sandstone walls as shelters (Figs 4G, 5B). Active individuals were found during the day and at dusk, when males start calling quite loudly, but also at night.. The tadpoles of *G. kintana* found at Malaso have a dark fin (Fig. 4A). *Phylacomantis* tadpoles with a reddish fin are also known, but there is no molecular taxonomic identification for this material, and it is therefore not yet possible to conclude if this colour variation (black vs. red) is a diagnostic character between the two *Phylacomantis* species inhabiting the Isalo Massif. Acoustic communication in tadpoles of *G. kintana* has yet to be recorded, which would not be surprising considering the sound repertoire described in *G. corvus* larvae (see Reeve et al. 2011).

Conservation status. If suitable habitat is considered to encompass all areas within the polygon drawn among the known localities (likely an over-estimate), then the EOO (extent of occurrence) totals 563 km². If plots with a scale of 2 km² are used to estimate AOO (area of occupancy), then this species occurs within 36 km² of habitat. Based on IUCN Red List guidelines (IUCN Standards and Petitions Subcommittee

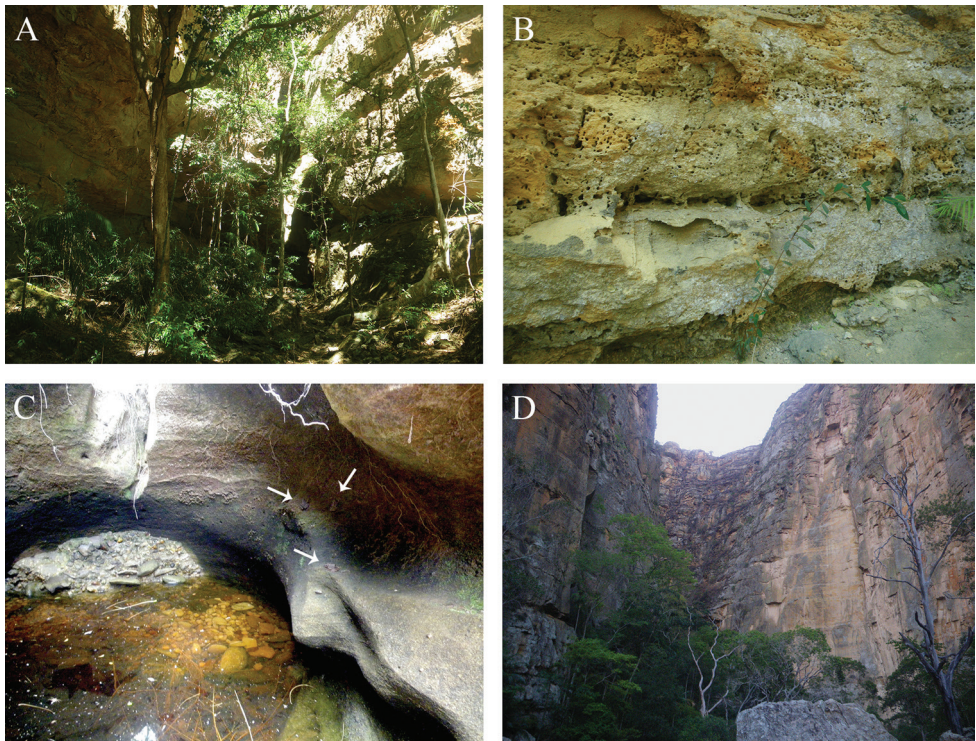


Figure 5. Habitats of *Gephyromantis corvus* and *G. kintana* sp. nov. **A** vegetation within Zahavola Canyon, type locality of *G. kintana* sp. nov.; **B** vertical walls at Zahavola with multiple holes, which are used as shelters by *G. kintana*; **C** lentic water at Malaso Canyon. Multiple *G. kintana* sp. nov. individuals are sitting on the wall of the canyon ca. 1 m above the water (arrows point to the three specimens); **D** Canyon des Rats with its typical dry deciduous gallery forest, habitat of *G. corvus*. Photographs by Angelica Crottini.

2019) we propose that *G. kintana* should be considered as Endangered (under criterium B1ab(iii)+2ab(iii)). This suggestion considers the species' narrow distribution and apparent restriction to inhabit young canyons as well as the fact that the area of the Isalo Massif not included in the borders of the National Park is under severe exploitation by various anthropogenic activities (Mercurio et al. 2008). In these areas the main threats are: 1) the use of periodic, and often uncontrolled fires to maintain the savannahs (Mercurio et al. 2008); 2) excavations for sapphire mines (Duffy 2006); and 3) unsustainable logging of remaining gallery forests (Mercurio et al. 2008). Despite very limited information on this species, the ongoing pressure on the extent and quality of the habitat is expected to impact the populations likely leading to their declines. Rakotondravony and Goodman (2011) listed *G. corvus* for the Makay Massif region (also discussed in Cocca et al. 2018). We do not consider this record here because we did not have access to any voucher material from this area at this time, and from the available photographs it was not possible to unequivocally assign this geographic record to either *G. corvus* or *G. kintana*.

Discussion

In this study we synonymised *G. azzurrae* with *G. corvus* based on molecular and morphological evidence, and described *G. kintana* sp. nov., which, as far as we know, represents a new microendemic species of the Isalo Massif. The most recent species account for the area reported the occurrence of 47 reptile taxa and 24 amphibians (Cocca et al. 2018). In this recent paper, five amphibian taxa were considered Isalo endemics: *Gephyromantis azzurrae*, *Mantella expectata*, *Scaphiophryne gottlebei*, *Mantidactylus noralottae*, and *M. sp. aff. multiplicatus* Ca65 "Isalo" (Cocca et al. 2018). Now, despite the synonymisation of *G. azzurrae* with *G. corvus*, the number of endemic amphibian taxa of the Isalo Massif remains the same since we could add *G. kintana* to this list.

The inspection of the ventral colouration is the clearest morphological difference between this pair of sympatric sister species and represents the most straightforward way to discriminate these taxa in the field. This morphological variation has been known for several years, but for a long time it was thought to reflect individual variation within the same species. Disentangling this situation was possible only after the inspection of all photographic records, of specimen ZFMK 70494 (the individual from which the first *Phylacomantis* sequence from Isalo has become available) and of all specimens formerly assigned to *G. corvus* and *G. azzurrae* in the herpetological collections of MRSN and ZSM, in combination with the compilation of all genetic data. This approach enabled us to conclude that specimen ZFMK 70494 was different from the holotypes of both *G. corvus* and *G. azzurrae*, that ventral colouration represented a diagnostic character and that the second *Phylacomantis* species still needed to be formally described (Fig. 2). Based on these findings, we also clarify that the tadpoles studied in Reeve et al. (2011) and assigned to *G. azzurrae* actually belong to *G. corvus* and, so far, the sound emission has not been observed in the tadpoles of *G. kintana* sp. nov.

This study provides evidence for the occurrence of *G. corvus* ca. 200 km away from the Isalo Massif (Figs 1, 6). This finding, together with the synonymisation of *G. azzurrae*

with *G. corvus*, may likely require the modification of the IUCN Red List assessment of *G. corvus*, highlighting how important it is to combine the efforts of performing herpetological surveys with the molecular characterisation of the collected material. Although demanding, this combined method is proving to be an excellent way to increase our knowledge on species distribution and is boosting our capacity to discover candidate

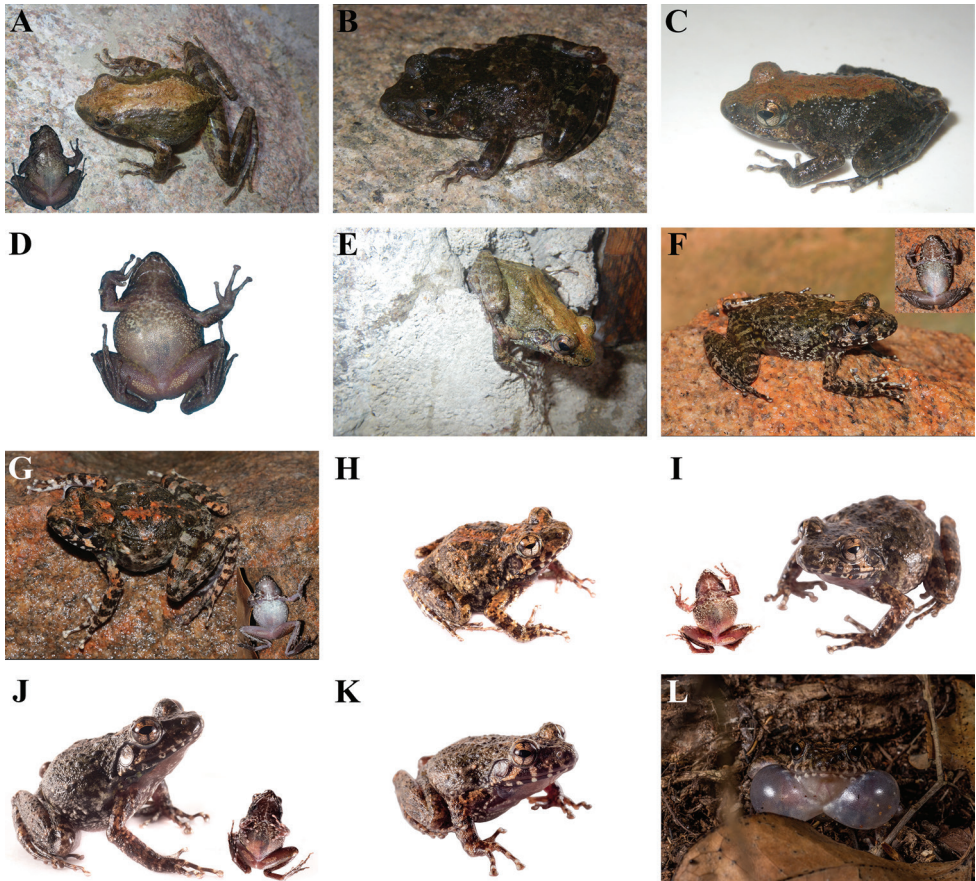


Figure 6. Images of living individuals of *G. corvus*. Photographs showing dorsal and ventral colour variability and habitats of *G. corvus*. When both ventral and dorsal picture of one individual are available, ventral colouration is given in inset. **A** ZSM 156/2019 (ACZCV_0288) adult male from Antsifotra Canyon; **B** ZSM 154/2019 (ACZCV_0286) adult female from Antsifotra Canyon; **C** ACZCV_0290 (UADBA-A uncatagued) adult female from Antsifotra Canyon; **D** ZSM 155/2019 (ACZCV_0287) ventral view of an adult male from Antsifotra Canyon; **E** ACZCV_0289 (UADBA-A Uncatalogued) adult male from Antsifotra Canyon; **F** ZSM 159/2019 (FAZC 15812) adult female from Anja Reserve; **G** ZSM 160/2019 (FAZC 15813) adult male from Anja Reserve; **H** ACZC 10901 (individual not collected) adult male from Sakaviro; **I** ACZC 10904 (UADBA-A uncatagued) adult male from Sakaviro; **J** ACZC 10957 (individual not collected) adult male from Tsaranoro; **K** ACZC 10958 (UADBA-A uncatagued) adult male from Tsaranoro; **L** ACZC 10964 (individual not collected) adult male from Tsaranoro calling from the leaf litter. Photographs **A–E** by Angelica Crottini, **F–G** by Franco Andreone, **H–L** by Javier Lobón-Rovira.

species and update our reference molecular databases. Since 2004, 140 new species of amphibians have been described from Madagascar (AmphibiaWeb 2020), but the number of candidate species is still very high (Vieites et al. 2009; Perl et al. 2014; but see also Glaw et al. 2019 for a more updated estimate of the candidate species and their formal description). In the last 15 years ten major taxonomic revisions on the amphibians of Madagascar have been published (Glaw and Vences 2006; Glaw et al. 2010; Vences et al. 2010; Köhler et al. 2010, 2015; Wollenberg et al. 2012; Rakotoarison et al. 2015, 2017; Scherz et al. 2017, 2019), all of which represented crucial steps in unveiling the biodiversity value of this irreplaceable hotspot of biodiversity. The currently discussed case demonstrated how vouchering continues to be an extremely valuable tool that enable specimen direct comparison and facilitate the identification, and taxonomic revision of collected material and name bearing types (Funk et al. 2005; Rocha et al. 2014).

Acknowledgements

We are grateful to the Ministère de l'Environnement et du Développement Durable for providing research and export permits (305/14/MEEF/DGF/DCB.SAP/SCB and 240N-EA11/MG14, 222/18/MEEF/SG/DGF/DSAP/SCB.Re, 008N-EA01/MG19 and 389N-EA12/MG18), and MICET for logistical help. Special thanks go to Dennis Rödder and Morris Flecks for providing photographic material of specimen ZFMK 57430 hosted under their care in the herpetological collection of the Zoological Research Museum Alexander Koenig in Bonn (Germany). We also thank Yuri Simone for his assistance in taking images of preserved material. We thank Malalâtiana Rasoazananay for her help in the surveys in the Haute Matsiatra region, and Javier Lobón-Rovira for his help in the field and for providing photos of *G. corvus* from Tsaranoro forest and Sakaviro. Gennaro Aprea, Paolo Eusebio Bergò, Fabio Mattioli, Vincenzo Mercurio, Nirhy H. Rabibisoa, Tokihery J. Razafindrabe, our MNP guides Anicet, Haza, Emile Rajeriarison, and Bonne Année, were of companionship in the Isalo field surveys and we thank them all for their valuable help. This work was financially supported by Portuguese National Funds through FCT – Foundation for Science and Technology under the research project PTDC/BIA-EVL/31254/2017. FCT also supports the PhD fellowship of WC (SFRH/BD/102495/2014), FB (PD/BD/128493/2017) and the Investigador FCT (IF) grant to AC (IF/00209/2014).

References

- AmphibiaWeb (2020) University of California, Berkeley, CA, USA. <https://amphibiaweb.org> [Accessed 7 February 2020]
- Andreone F, Rosa GM, Raselimanana AP (2014) Les amphibiens des zones arides de l'Ouest et du Sud de Madagascar. Guides sur la diversité biologique de Madagascar. Association Vahatra, Antananarivo, 386 pp.

- Avise JC, Ball RM (1990) Principles of genealogical concordance in species concepts and biological taxonomy. In: Futuyma D, Antonovics J (Eds) *Surveys in Evolutionary Biology*. Oxford University Press, New York, 45–67. <https://api.semanticscholar.org/> [CorpusID:83179200]
- Blommers-Schlösser RMA (1979) Biosystematics of the Malagasy frogs. I. Mantellinae (Ranidae). *Beaufortia* 352: 1–77. <https://www.repository.naturalis.nl/document/548811>
- Bruford MW, Hanotte O, Brookfield JFY, Burke T (1992) Single-locus and multilocus DNA fingerprinting. In: Hoelzel R (Ed.) *Molecular Genetic Analysis Of Populations: A Practical Approach*. IRL Press, Oxford, 225–269.
- Cocca W, Rosa GM, Andreone F, Aprea G, Bergò PE, Mattioli F, Mercurio V, Randrianirina JE, Rosado D, Vences M, Crottini A (2018) The herpetofauna (Amphibia, Crocodylia, Squamata, Testudines) of the Isalo Massif, Southwest Madagascar: combining morphological, molecular and museum data. *Salamandra* 54: 178–200. <http://www.salamandra-journal.com/index.php/home/contents/2018-vol-54/1909-cocca-w-g-m-rosa-f-andreone-g-aprea-p-e-bergo-f-mattioli-v-mercurio-j-e-randrianirina-d-rosado-m-vences-a-crottini>
- Crottini A, Glaw F, Casiraghi M, Jenkins RKB, Mercurio V, Randrianantoandro C, Randrianirina JE, Andreone F (2011a) A new *Gephyromantis* (*Phylacomantis*) frog species from the pinnacle karst of Bemaraha, western Madagascar. *Zookeys* 81: 51–71. <https://doi.org/10.3897/zookeys.81.1111>
- Crottini A, Gehring P, Glaw F, Harris DJ, Lima A, Vences M (2011b) Deciphering the cryptic species diversity of dull-coloured day geckos *Phelsuma* (Squamata: Gekkonidae) from Madagascar, with description of a new species. *Zootaxa* 2982: 40–48.
- Crottini A, Miralles A, Glaw F, Harris DJ, Lima A, Vences M (2012) Description of a new pygmy chameleon (Chamaeleonidae: *Brookesia*) from central Madagascar. *Zootaxa* 3490: 63–74. <https://doi.org/10.11646/zootaxa.3490.1.5>
- Crottini A, Harris DJ, Miralles A, Glaw F, Jenkins RKB, Randrianantoandro JC, Bauer AM, Vences M (2015) Morphology and molecules reveal two new species of the poorly studied gecko genus *Paragehyra* (Squamata: Gekkonidae) from Madagascar. *Organisms Diversity & Evolution* 15: 175–198. <https://doi.org/10.1007/s13127-014-0191-5>
- Crottini A, Madsen O, Poux C, Strauß A, Vieites DR, Vences M (2012) Vertebrate time-tree elucidates the biogeographic pattern of a major biotic change around the K-T boundary in Madagascar. *Proceedings of the National Academy of Sciences of the United States of America* 109: 5358–5363. <https://doi.org/10.1073/pnas.1112487109>
- Darriba D, Taboada GL, Doallo R, Posada D (2012) jModelTest 2: more models, new heuristics and parallel computing. *Nature Methods* 9: 772. <https://doi.org/10.1038/nmeth.2109>
- Duffy R (2006) Global environmental governance and the challenge of shadow states: the impact of illicit sapphire mining in Madagascar. *Development and Change* 36: 825–843. <https://doi.org/10.1111/j.0012-155X.2005.00437.x>
- Fouquet A, Gilles A, Vences M, Marty C, Blanc M, Gemmell NJ (2007) Underestimation of species richness in neotropical frogs revealed by mtDNA analyses. *PLoS One* 2(10): e1109. <https://doi.org/10.1371/journal.pone.0001109>
- Funk VA, Hoch PC, Prather LA, Wagner WL (2005) The importance of vouchers. *Taxon* 54: 127–129. <https://doi.org/10.2307/25065309>

- Glaw F, Vences M (1994) A Field Guide to the Amphibians and Reptiles of Madagascar. Second Edition. Vences & Glaw Verlags GbR, Köln, 335 pp.
- Glaw F, Vences M (2006) Phylogeny and genus-level classification of mantellid frogs (Amphibia, Anura). *Organisms, Diversity and Evolution* 6: 236–253. <https://doi.org/10.1016/j.ode.2005.12.001>
- Glaw F, Vences M (2007) A Field Guide to the Amphibians and Reptiles of Madagascar. Third Edition. Vences & Glaw Verlags GbR, Köln, 496 pp.
- Glaw F, Vences M, Gossmann V (2000) A new species of *Mantidactylus* (subgenus *Guibemantis*) from Madagascar, with a comparative survey of internal femoral gland structure in the genus (Amphibia: Ranidae: Mantellinae). *Journal of Natural History* 34: 1135–1154. <https://doi.org/10.1080/00222930050020140>
- Glaw F, Köhler J, de la Riva I, Vieites DR, Vences M (2010) Integrative taxonomy of Malagasy treefrogs: combination of molecular genetics, bioacoustics and comparative morphology reveals twelve additional species of *Boophis*. *Zootaxa* 2382:1–82. <https://doi.org/10.11646/zootaxa.2383.1.1>
- Glaw F, Hawlitschek O, Glaw K, Vences M (2019) Integrative evidence confirms new endemic island frogs and transmarine dispersal of amphibians between Madagascar and Mayotte (Comoros archipelago). *The Science of Nature* 106: 19. <https://doi.org/10.1007/s00114-019-1618-9>
- Goodman SM, Benstead JP (2003) *The Natural History of Madagascar*. The University of Chicago Press, 1728 pp.
- Goodman SM, Benstead JP (2005) Updated estimates of biotic diversity and endemism for Madagascar. *Oryx* 39: 73–77. <https://doi.org/10.1017/S0030605305000128>
- Gould L, Andrianomena P (2015) Ring-tailed lemurs (*Lemur catta*), forest fragments, and community-level conservation in South-Central Madagascar. *Primate Conservation*, 29: 67–73. <https://doi.org/10.1896/052.029.0108>
- Hall TA (1999) BioEdit: a user-friendly biological sequence alignment editor and analysis program for Windows 95/98/NT. *Nucleic Acids Symposium Series* 41: 95–98.
- IUCN (2019) *The IUCN Red List of Threatened Species*. Version 2019-1. <http://www.iucn-redlist.org> [Downloaded on 2 July 2019]
- Kaffenberger N, Wollenberg KC, Köhler J, Glaw F, Vieites DR, Vences M (2012) Molecular phylogeny and biogeography of Malagasy frogs of the genus *Gephyromantis*. *Molecular Phylogenetics and Evolution* 62: 555–560. <https://doi.org/10.1016/j.ympev.2011.09.023>
- Köhler J, Vences M, D’Cruze N, Glaw F (2010) Giant dwarfs: discovery of a radiation of large-bodied ‘stump-toed frogs’ from karstic cave environments of northern Madagascar. *Journal of Zoology* 282: 21–38. <https://doi.org/10.1111/j.1469-7998.2010.00708.x>
- Köhler J, Glaw F, Pabijan M, Vences M (2015) Integrative taxonomic revision of mantellid frogs of the genus *Aghyptodactylus* (Anura: Mantellidae). *Zootaxa* 4006: 401–438. <https://doi.org/10.11646/zootaxa.4006.3.1>
- Kumar S, Stecher G, Tamura K (2016) MEGA7: Molecular Evolutionary Genetics Analysis Version 7.0 for bigger datasets. *Molecular Biology and Evolution* 33: 1870–1874. <https://doi.org/10.1093/molbev/msw054>

- Mercurio V, Andreone F (2007) Two new canyon-dwelling frogs from the arid sandstone Isalo Massif, central-southern Madagascar (Mantellidae, Mantellinae). *Zootaxa* 1574: 31–47. <https://doi.org/10.11646/zootaxa.1574.1.2>
- Mercurio V, Aprea G, Crottini A, Mattioli F, Randrianirina JE, Razafindrabe TJ, Andreone, F (2008) The amphibians of Isalo Massif, southern-central Madagascar: high frog diversity in an apparently hostile dry habitat. In: Andreone F (Eds) *A Conservation Strategy for the Amphibians of Madagascar*. Monografie del Museo Regionale di Scienze Naturali di Torino 45: 143–196. https://www.academia.edu/22428469/The_amphibians_of_Isalo_Massif_southern-central_Madagascar_high_frog_diversity_in_an_apparently_hostile_dry_habitat
- Miller MA, Pfeiffer W, Schwartz T (2010) Creating the CIPRES Science Gateway for inference of large phylogenetic trees. In: *Proceedings of the Gateway Computing Environments Workshop (GCE)*, New Orleans, LA, November 2010: 1–8. <https://doi.org/10.1109/GCE.2010.5676129>
- Myers N, Mittermeier RA, Mittermeier CG, da Fonseca GAB, Kent J (2000) Biodiversity hotspots for conservation priorities. *Nature* 403: 853–858. <https://doi.org/10.1038/35002501>
- Palumbi S, Martin A, Romano S, McMillan WO, Stice L, Grabowski G (1991) *The Simple Fools Guide to PCR*. Version 2.0, Department of Zoology and Kewalo Marine Laboratory, University of Hawai'i at Manoa, USA, 47 pp. <https://discover.libraryhub.jisc.ac.uk/search?ti=The%20simple%20fool%E2%80%99s%20guide%20to%20PCR&rn=1>
- Perl RGB, Nagy ZT, Sonet G, Glaw F, Wollenberg KC, Vences M (2014) DNA barcoding Madagascar's amphibian fauna. *Amphibia-Reptilia* 35: 197–206. <https://doi.org/10.1163/15685381-00002942>
- Rakotoarison A, Crottini A, Müller J, Rödel MO, Glaw F, Vences M (2015) Revision and phylogeny of narrow-mouthed treefrogs (*Cophyla*) from northern Madagascar: integration of molecular, osteological, and bioacoustic data reveals three new species. *Zootaxa* 3937: 61–89. <https://doi.org/10.11646/zootaxa.3937.1.3>
- Rakotoarison A, Scherz MD, Glaw F, Köhler J, Andreone F, Franzen M, Glos J, Hawlitschek O, Jono T, Mori A, Ndriantsoa SH, Raminosa NR, Riemann JC, Rödel MO, Rosa GM, Vieites DR, Crottini A, Vences M (2017) Describing the smaller majority: integrative taxonomy reveals twenty-six new species of tiny microhylid frogs (genus *Stumpffia*) from Madagascar. *Vertebrate Zoology* 67: 271–398. <https://www.senckenberg.de/de/wissenschaft/publikationen/wissenschaftliche-zeitschriften/vertebrate-zoology/archiv/2017-2/>
- Randrianiaina RD, Wollenberg KC, Rasolonjatovo Hiobiarilanto T, Strauß A, Glos J, Vences M (2011) Nidicolous tadpoles rather than direct development in Malagasy frogs of the genus *Gephyromantis*. *Journal of Natural History* 45: 2871–2900. <https://doi.org/10.1080/00222933.2011.596952>
- Rakotondravony HA, Goodman SM (2011) Rapid herpetofaunal surveys within five isolated forests on sedimentary rock in western Madagascar. *Herpetological Conservation and Biology* 6: 297–311. http://www.herpconbio.org/contents_vol6_issue2.html
- Reeve E, Ndriantsoa SH, Strauß A, Randrianiaina R-D, Hiobiarilanto TR, Glaw F, Glos J, Vences M (2011) Acoustic underwater signals with a probable function during competitive feeding in a tadpole. *Naturwissenschaften* 98: 135. <https://doi.org/10.1007/s00114-010-0752-1>

- Rocha LA, Aleixo A, Allen G, Almeda F, et al. (2014) Specimen collection: an essential tool. *Science* 344: 814–815. <https://doi.org/10.1126/science.344.6186.814>
- Ronquist F, Teslenko M, van der Mark P, Ayres DL, Darling A, Höhna S, Larget B, Liu L, Suchard MA, Huelsenbeck JP (2012) MrBayes 3.2: efficient Bayesian phylogenetic inference and model choice across a large model space. *Systematic Biology* 61: 539–542. <https://doi.org/10.1093/sysbio/sys029>
- Scherz MD, Hawlitschek O, Andreone F, Rakotoarison A, Vences M, Glaw F (2017) A review of the taxonomy and osteology of the *Rhombophryne serratopalpebrosa* species group (Anura: Microhylidae) from Madagascar, with comments on the value of volume rendering of micro-CT data to taxonomists. *Zootaxa* 4273: 301–340. <https://doi.org/10.11646/zootaxa.4273.3.1>
- Scherz MD, Hutter CR, Rakotoarison A, Riemann JC, Rödel MO, Ndriantsoa SH, Glos J, Roberts SH, Crottini A, Vences M, Glaw F (2019) Morphological and ecological convergence at the lower size limit for vertebrates highlighted by five new miniaturised microhylid frog species from three different Madagascan genera. *PLoS One* 14: e0213314. <https://doi.org/10.1371/journal.pone.0213314>
- Vences M (2000) Phylogenetic studies of ranoid frogs (Amphibia: Anura), with a discussion of the origin and evolution of the vertebrate clades of Madagascar. Doctoral dissertation, Universität Bonn.
- Vences M, Thomas M, Bonett RM, Vieites DR (2005) Deciphering amphibian diversity through DNA barcoding: chances and challenges. *Philosophical Transactions of the Royal Society London, Series B* 360: 1859–1868. <https://doi.org/10.1098/rstb.2005.1717>
- Vences M, Glaw F, Köhler J, Wollenberg KC (2010) Molecular phylogeny, morphology and bioacoustics reveal five additional species of arboreal microhylid frogs of the genus *Anodonthyla* from Madagascar. *Contributions to Zoology* 79: 1–32. <https://doi.org/10.1163/18759866-07901001>
- Vieites DR, Wollenberg KC, Andreone F, Köhler J, Glaw F, Vences M (2009) Vast underestimation of Madagascar's biodiversity evidenced by an integrative amphibian inventory. *Proceedings of the National Academy of Sciences of the United States of America* 106: 8267–8272. <https://doi.org/10.1073/pnas.0810821106>
- Wollenberg KC, Glaw F, Vences M (2012) Revision of the little brown frogs in the *Gephyromantis decaryi* complex, with description of a new species. *Zootaxa* 3421: 32–60. <https://doi.org/10.11646/zootaxa.3421.1.2>
- Zimkus BM, Lawson LP, Barej MF, Barratt CD, Channing A, Dash KM, Dehling JM, Preez LD, Gehring PS, Greenbaum E, Gvoždík V, Harvey J, Kielgast J, Kusamba C, Nagy ZT, Pabijan M, Penner J, Rödel MO, Vences M, Lötters S (2017) Leapfrogging into new territory: How Mascarene ridged frogs diversified across Africa and Madagascar to maintain their ecological niche. *Molecular Phylogenetics and Evolution* 106: 254–269. <https://doi.org/10.1016/j.ympev.2016.09.018>

